Thesis submitted for the degree of PhD in Systems Biology

Circadian clock and light input system in the sea urchin larva

Libero Petrone

Department of Genetics Evolution and Environment

University College London

London, December 2015

I, Libero Petrone, confirm that the work presented in this thesis is my own. Where information has been derived from other sources, I confirm that this has been indicated in the thesis.

Abstract

A circadian clock is an endogenous time-keeping mechanism that synchronizes several biological processes with local environment. In metazoans the circadian system is driven by a regulatory network of so called “clock” genes interconnected in transcriptional-translational feedback loops that generate rhythmicity at mRNA and protein level. Sea urchin and its molecular tools can facilitate the comprehension of the evolution of the time-keeping mechanism in bilaterians. For this purpose we identified and analysed the expression of orthologous clock genes in the sea urchin larvae. Genome survey identifies almost all canonical clock genes known in protostomes and deuterostomes, with exception of *period*, indicating that the last common ancestor of all bilaterians already had a complex clock toolkit. Quantitative gene expression data reveal that the circadian clock begins to oscillate consistently in the free-living larva. *Sp_vcry* and *sp_tim* mRNA cycle in both light/dark (LD) and free running (DD) conditions; several other genes consistently show oscillation in LD condition only; while, neither *sp_clock*, nor *sp_bmal* have rhythmic expression. Interestingly, *in-situ* hybridization of key sea urchin clock genes together with cell markers (*e.g.* serotonin) suggest the presence of two types of light perceiving cells in the apical region of the larva: serotoninergic cells expressing *sp_dcry* and no-serotoninergic cells expressing *sp_opsin3.2*. Furthermore, functional analysis was performed to discern linkages in the regulatory network of clock genes. In larvae entrained to light/dark cycles, knockdown of *sp_dcry* induces arrythmicity in the expression of itself, reduction of amplitude of oscillation in *sp_vcry*, and reduction of amplitude of oscillation and lower levels of expression in *sp_tim*. Knockdown of *sp_opsin3.2* reduces levels of expression of *sp_hlf*; and *sp_vcry* knockdown induces arrythmicity in *sp_tim.*

Importantly, our study highlights differences in the architecture and gene regulation of the sea urchin larval circadian clock compared to other metazoan clocks.

Acknowledgments

I am thankful to my supervisor Paola Oliveri for having given me the opportunity to participate in this PhD project, for the supervision, the performing of the microinjections and the reading and correction of this thesis.

I would like to thank my second supervisors David Whitmore and Nicholas Luscombe for helpful discussion held at the upgrade viva. In particular, I thank the Whitmore lab for having been always available for explanations, use of reagents and the use of the Packard TopCount NXT Microplate Scintillation & Luminiscence counter.

I am thankful to my thesis examiners Ralph Stanewsky and Pedro Martinez for having read the thesis and given valuable comments to improve it. Thanks to Ina Arnone for having hosted me in her laboratory in Stazione Zoologica for the sampling of the sea urchin larvae and Margherita Perillo for her availability in helping me during my time in Stazione Zoologica and everytime I have contacted her.

The realization of this thesis has been supported by the contribution of people that, before me, started to work on the circadian clock in the sea urchin. For this reason I would like to thank Thomas Muller, Avi Lerner, Teresa Mattiello, Agnieska Chomka and Edmondo Iovine.

My PhD has been enriched by the opportunity to be tutor to Claile Louise and Harriett Stephenson. They have helped me in the execution of some experiments and have given to me the opportunity to have a role as tutor. I would also like to thank Patrick Toolan-Kerr for valuable comments on the manuscript.

I would like to thank also Wendy Hart for having helped me in the execution of some experiments.

In this adventure I have been accompanied by two great lab mates David Dylus and Anna Czarkwiani. I am grateful for their help in everything (and if I start to write about it I would never finish this session), for having built up together an unique atmosphere in the lab and, especially, for having shared our life also outside the lab.

For the same reason I am thankful to members of Telford lab and Roberto Mayor lab at the board game sessions and the refreshing lunch times. I thank all people met in London that contributed to this amazing experience.

I am grateful to Luca and Massimo that have kept strong our friendship for far away and have always encouraged me for arriving at this exact moment where I am writing these lines. Finally I am grateful to my parents and sister for being always present.

Table of contents

List of figures

List of tables

Abbreviations

LD	Light/Dark
DD	Dark/Dark
PCR	Polymerase Chain Reaction
RACE	Rapid Amplification of cDNA Ends
qPCR	quantitative Polymerase Chain Reaction
WMISH	Whole Mount *in-situ* Hybridization
DIC	Differential Interference Contrast
MO	Morpholino Oligonucleotide
FASW	Filtered Artificial Sea Water
ASW	Artificial Sea Water
TTFL	Transcriptional-Translational Feedback Loop
CPF	Cryptochrome/Photolyase Family
PRC	Photo-Receptor Cell
wpf	week post fertilization
dpf	days post fertilization
ZT	Zeitgeber Time
ccgs	clock controlled genes
PAS	Per-Arnt-Sim
LN	Lateral Neurons
DN	Dorsal Neurons
SCN	Superchiasmatic Nucleus
PHR	Photolyase Homology Region
FAD	Flavin Adenin Dinucleotide
GRN	Gene Regulatory Network
Sp	*Strongylocentrotus purpuratus*
NLS	Nuclear Localization Signal
NES	Nuclear Export Signal
RE	Restriction Sites
LB	Luria Broth
ppt	parts per trillion
DAPI	4',6-diamidino-2-phenylindole
DEPC	Diethyl Pyrocarbonate

Ct	Cycle of threshold
ML	Maximum Likelihood
CT	Circadian Time
hpf	hours post fertilization
b-HLH	basic Helix-Loop-Helix
TF	Transcription Factor
BMAL	Brain and Muscle ARNT-Like
CLOCK	Circadian Locomotor Output Cycles Kaput
HLF	Hepatic Leukemia Factor
ROR	RAR-related Orphan Receptor

Chapter1

Introduction

1.1 Circadian clock synchronizes several biological processes with the local environment.

The circadian clock is an endogenous time-keeping mechanism with a period of about 24h that synchronizes several daily biological processes such as cell cycle, metabolism, locomotor activity, sleeping/wakefulness periods with the local environment (Young and Kay, 2001). It is present in all organisms so far investigated (as diverse as bacteria, plants, fungi, insects and mammals) conferring an evolutionary advantage to anticipate predictable environmental changes, such as the day-night transition, and, thus to allow a more efficient use of energy (Hut and Beersma, 2011). The circadian clock has evolved as a result of combined evolutionary pressures comprising of abiotic and biotic cycles of the environment. In particular, since the dawn of life first living organisms have been under influence of the rhythmic presence of light caused by Earth's rotation around its axis. Light is both a source of energy and a DNA damaging agent, and first living beings had to adapt to such evolutionary pressure. Indeed the main hypothesis that explains evolution of the circadian clock is related to the minimization of UV damage to DNA (Pittendrigh, 1960; Gehring and Rosbash, 2003). A theory, regarding evolution of the time-keeping system in cyanobacteria, has proposed that the protein KaiC, a component of their circadian system, forms hexamers involved in the process of compaction of DNA during the light phase of the day to protect it against UV damage (Simons, 2009). Similarly, a theory of "escape from light" has been hypothesized for first metazoans that were marine organisms. They might have possessed a time-keeping mechanism to regulate diel vertical migration in water and thus to sink in lower levels of the water column to avoid intense light irradiation (Hut and Beersma, 2011).

The circadian clock can be described as a system formed by three major parts (Fig.1.1): a pacemaker, or core clock, that generates circadian rhythmicity; input pathways that allow the pacemaker to be synchronized with the local environment and output pathways through which the core clock regulates daily physiological and behavioural functions. The input pathways respond to environmental cues, known as Zeitgebers (German for "time giver"). Light is the principal and more investigated Zeitgeber, other examples are temperature, food availability and social contacts (Ben-Shlomo and Kyriacou, 2002; Mrosovsky et al, 1989). Furthermore, this system can be characterized

by auto-regulatory loops in which input pathways can be under the circadian control and output pathways can feedback on the core clock (Millar, 1999; Mrosovsky, 1996).

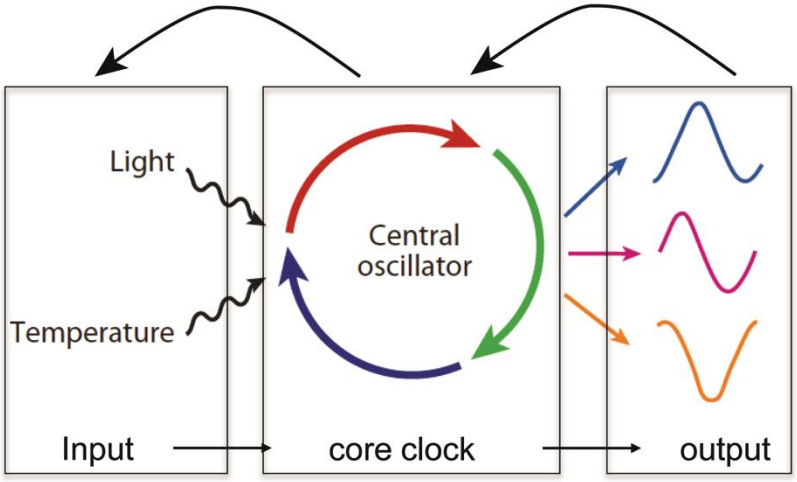

Fig.1.1 Schematic representation of the circadian time-keeping system. Input pathways, regulated by different Zeitgebers such as light and temperature, entrain the pacemaker, or core clock, to the local environment. The core clock is a self-sustained time-keeping mechanism with a period of roughly 24 hours that regulates behavioural and/or physiological outputs.

In eukaryotes, the core clock consists of a regulatory network of so called clock genes interconnected in transcriptional-translational feedback loops (TTFLs) that generate rhythmicity at RNA and protein level. In addition to TTFLs, several molecular and cellular mechanisms jointly operate to synchronize multiple cellular pacemakers of an organism (Cermakian and Sassone-Corsi, 2000). These are post-transcriptional regulation, epigenetic changes, post-translational modification, intercellular interactions and cellular translocations. Molecular components differ completely between fungi, plants and animals suggesting independent evolution in the different eukaryotic lineages (Brown et al, 2012; Rosbash et al, 2009).

1.2 Circadian clock in Metazoa.

In Metazoa, behavioural, physiological and molecular studies that describe circadian rhythmicity have been mainly carried out in insects and chordates with *Drosophila* and mouse as the major model systems. They have been used as potent model systems for the understanding of molecular and cellular mechanisms underlying the circadian clock thanks to the combined use of experimental tools that allow the execution of behavioural, genetic and molecular analysis. So far, these model systems have

promoted the comprehension of how a circadian TTFL is assembled and entrained to environmental cues, how output processes are regulated (paragraph 1.2.1), how a circadian system can be organized at an organismal (paragraph 1.2.2) level etc.
Furthermore, studies performed in other organisms such as non-drosophilid insects (paragraph 1.2.3), zebrafish (paragraph 1.2.4), and marine organisms (paragraph 1.2.5) gave a significant insight into understanding the diversity and complexity of the circadian clock in animals. Almost all clock genes are conserved within Eumetazoa suggesting that this molecular clock dates at least to the cnidarian-bilaterian ancestor (Reitzel, 2013).

1.2.1 Core clock in *Drosophila* and mouse.

The regulation of the core clock responsible for generating 24h rhythmicity has been dissected in the fruit fly and mouse at different levels: transcriptional, post-transcriptional and post-translational (for review see Peschel and Helfrich-Förster, 2011; Lowrey and Takahashi, 2011; Partch et al., 2014; Hardin, 2011). The two TTFL models (Fig.1.2; 1.3) have a similar structure and can be divided in a core loop that generate 24h rhythmic expression of clock genes and secondary interlocked loops that confer stability and robustness to the core loop ensuring that the mechanism requires 24 hours to complete a cycle.
In *Drosophila*, positive elements of the core loop are the bHLH-PAS transcription factors Clock (Clk) and Cycle (Cyc) that form a heterodimer binding E-boxes elements in the regulatory regions of the clock genes *period* (*per*), *timeless* (*tim*), *vrille* (*vri*), *pdp1*. (Fig.1.2). Clock and Cycle are characterized by basic a helix-loop-helix (bHLH) domain, a PER-ARNT-SIM homology (PAS) domain devided in two structural motifs (PAS-A and PAS-B) which facilitates protein-protein interactions (Darlington et al., 1998; Allada et al., 1998; Rutila et al., 1998; Huang et al., 1993) and a region downstream of PAS-B called PAC that are likely to contribute to the PAS structural domain (Ponting and Aravind, 1997). Further, dCLK possesses a glutamine-rich region at the C-terminus that acts as transactivation domain functioning in transcriptional activation (Darlington et al., 1998; Allada et al., 1998).
The negative feedback of the core loop is achieved by Tim/Per heterodimers that translocate back to the nucleus to repress their own transcription by acting on the Clock/Cycle complex.

In the early night, *per* and *tim* mRNA levels reach their maximum levels, while their protein products accumulate in the cytoplasm with a delay of 4-6 hours, reaching peak levels late in the night. Per is a member of the PAS (Per-Arnt-Sim) protein family and contains two dimerization domains (PAS-A, PAS-B) and a 30-residue segment that directs phosphorylation by Double time (DBT) and casein kinase 2 (CK2) (Yildiz et al., 2005). The former induces Per ubiquitination by the F-Box protein Slimb and its degradation in the proteasome (Grima et al., 2002); the latter mediates the transport of Per in the nucleus (Akten et al. 2003).

Tim is a helical-repeat protein characterized by two armadillo (ARM) repeats and Per binding sites. The binding to Per is responsible of the stabilization of the complex Per-DBT (Shafer et al., 2002). Tim is phosphorilated by Shaggy (SGG) accelerating heterodimerization and promoting nuclear translocation of PER-DBT/TIM (Martinek et al., 2001). Thus phosphorylation of Per by CK2 and Tim by SGG induces nuclear localization of the complex Per-Tim-DBT. Once in the nucleus, Per interacts with Clock inducing its phosphorylation by DBT and consequently the hyper-phosphorylated transcription factor reduces its affinity for E-box elements of clock genes. In this way transcription of clock genes is inhibited. Whereas, in presence of light, Tim interacts with a UV-A/blue-light responsive protein, the *Drosophila*-like cryptochrome (dCry or Cry1), that targets Tim for ubiquitin-mediated degradation through action of the E3 ubiquitin ligase Jetlag (Jet). Jet induces also degradation of dCRY through action of BRWD3 E3 ubiquitin ligase. In absence of Tim, Per is phosphorylated by DBT becoming target of ubiquitination. Consequently, hypo-phosphorylated Clk accumulates again to form dimers with Cyc and initiate a new cycle of transcription.

Fig.1.2 (Following page). Schematic representation of the circadian TTFL model in *Drosophila.* The core loop is driven by Clock and Cycle to generate 24 hour rhythmicity at mRNA and protein level. The secondary loop is driven by Pdp1 and Vrille to confer stability and robustness to the core loop. See text for details. Adapted from Tomioka and Matsumoto (2010). Rhythmic gene expression is indicated by oscillatory coloured curves, positive and negative inputs are indicated by arrows and barred lines respectively.

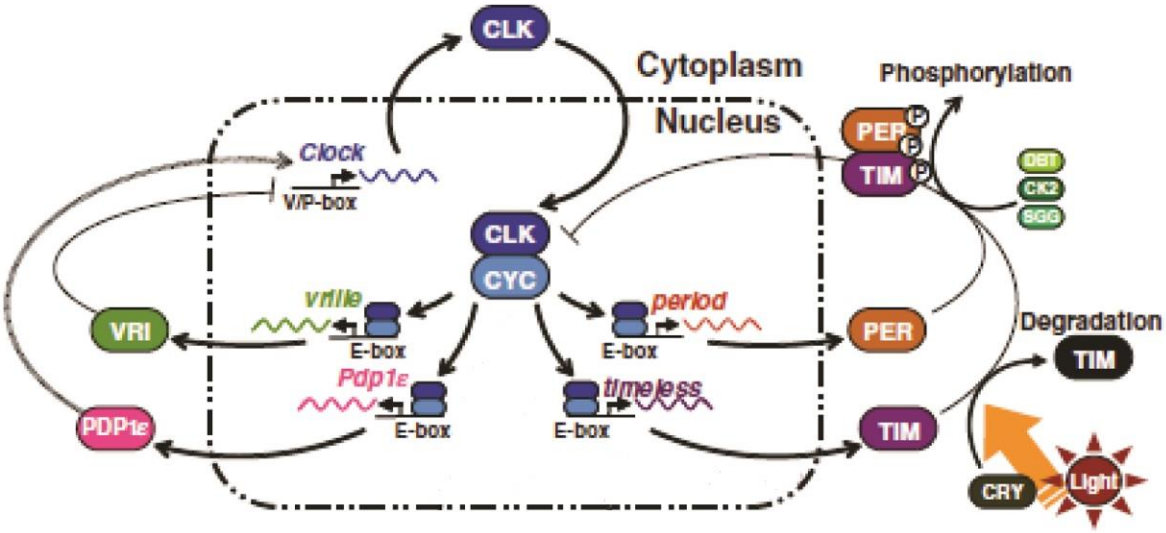

The secondary loop is formed by the bZIP (Basic Leucine Zipper) transcription factors Vri and Pdp1 that regulate rhythmic expression of *clk,* while *cyc* is constitutively expressed. The two bZIP transcription factors compete for the same binding sites, so called, Vri/Pdp1 boxes (V/P-boxes) in the regulatory region of *clk* inducing its rhythmic expression. In the early night Vri expression is higher than Pdp1 and inhibits *clk* expression; while in the early morning Pdp1 dominates on Vri levels and activates *clk* expression. Similarly, *dcry* expression is likely regulated by the same mechanism that drives rhythmicity in *clock* transcription (Zheng et al., 2008). Whereas dCry protein levels are regulated by light and are low in the light phase, they accumulate after light is off and remain constant in the dark phase (Emery et al., 1998).

In addition to the core loop and secondary loop described above, there are other components that have been showed to contribute to the overall oscillatory activities of the clock genes suggesting that the complete understanding of the circadian TTFL may be still incomplete in *Drosophila*. Examples are given by Cwo (Clock work orange) and Creb2 (cAMP response element-binding protein). *Cwo* encodes a bHLH orange-domain putative transcription factor that modulates clock gene expression through both repressor and activator transcriptional functions (Richier B. et al., 2008). The gene *creb2*, although not rhythmically expressed, encodes a transcription factor whose activity is regulated in a rhythmic way and binds into *per* and *tim* regulatory regions (Belvin, 1999).

Besides dCry, *Drosophila* uses other light input pathways for the entrainment of the circadian system to the local environment that involve three different photoreceptive organs: the compound eyes, the ocelli, and the Hofbauer-Buchner eyelet (H-B eyelet),

which are internal structures located underneath the compound eye (Helfrich-Förster et al., 2001; Rieger et al., 2003; Veleri et al., 2007). These are structures that express rhodopsin-based photopigments and in particular rhodopsin 1, 6 and 5 have been found involved in the circadian entrainment (Hanai et al., 2008; Szular et al., 2012). Finally another light-responsive molecule, Quasimodo, characterized by a membrane-anchored Zona Pellucida domain, is involved in a dCry–indipendent light input pathway that triggers degradation of Tim (Chen et al., 2011). It has been suggested that rhodopsins may be involved in its activation and in turn Quasimodo interacts with other membrane proteins, for example ion channels, to alter electrical properties of clock neurons in a light-dependent way.

In mammals, the core clock (Fig. 1.3) also depends on the b-HLH transcription factors Clock and Bmal1 (homolog to Cycle). Differently from *Drosophila*, the *bmal1* gene is rhythmically expressed whereas *clock* is constitutively transcribed. Indeed, the *bmal1* gene is characterized by the presence of RevErbA/ROR-binding elements (ROREs) in its regulatory regions. Thus, the secondary loop involves members of the nuclear receptor family: the activators RORα (retinoic acid receptor-related orphan receptor α), Rorβ, or Rorγ and the repressors Rev-Erbα (reverse orientation c-erbA α) or Rev-Erbβ. Furthermore, differently from *Drosophila* where *Clock* plays an essential role in the rhythmic control of E-box-mediated circadian transcription, in mammals BMAL1 has been found to be involved in such role with the presence of a transactivation domain at the C-terminal (Kiyohara et al., 2006).

Vertebrates do not possess orthologs of *dcry* and *tim*, and the repression of Clk/Bmal1 is determined by the dimer mPer/mCry where Per prevents Cry ubiquitination and aids its nuclear import (Czarna et al., 2013; Hirano et al., 2013; Yoo et al., 2013). Mammals are characterized by the presence of three *mper* (*per1*, *per2*, *per3*) and two *mcry* (*cry1*, *cry2*) genes.

mPer1 and 2 proteins are involved in the core loop and are partners of mCry proteins, while mPer3 is not part of the core loop and seems to be involved in the regulation of output processes (Bae et al., 2001). mCry1 and mCry2 are cryptochromes that belong to the class of vertebrate-type Crys (or Cry2) characterized by transcriptional repressor activity. Rui Ye et al. (2014) have proposed a model according to which the complex mCry1/mPer inhibits Clk/Bmal1 in a dual mechanism. In the early morning, mCry1 levels are high and it interacts with Clk/Bmal1 inducing repression of clock gene transcription with the two transcription factors blocked on E-box elements (blocking-type

mechanism). During the day, mCry1 levels decrease and Clk/Bmal1 are active. Whereas late at night, both mCry1 and Per2 levels are high, resulting in the dissociation of Clk/Bmal1 from the E-box elements mediated by the mCry1/mPer complex (displacement-type mechanism).

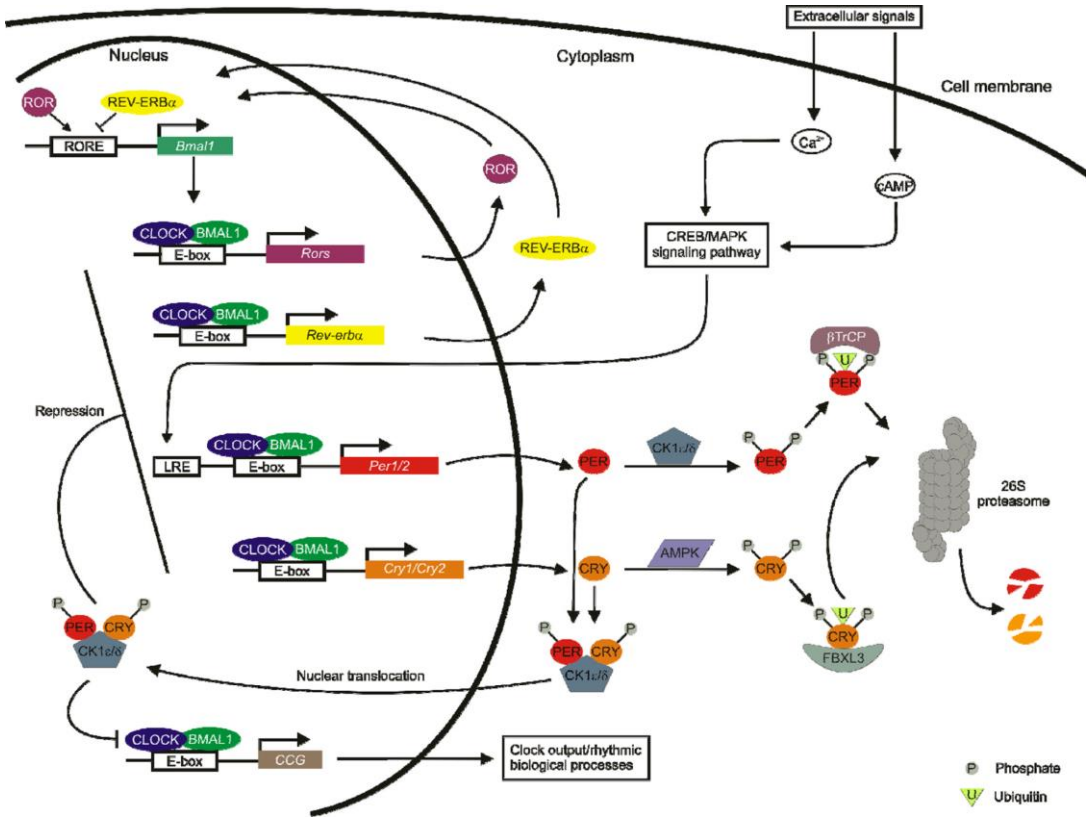

Fig.1.3 Schematic representation of the circadian TTFL model of mouse.
See text for details. Adapted from Lowrey and Takahashi (2011).

Similarly to *Drosophila*, kinases carry out a role in regulating clock proteins activity. In particular, CK1ε/δ mediates phosphorylation of mPer proteins to trigger their ubiquitination by βTrCP (β-Transducing repeat Containing Protein); while mCry1 and mCry2 are target, respectively, of Ampk1 (5' Adenosine Monophosphate-activated Protein Kinase) and GSK-3β (Glycogen Synthase Kinase). Interestingly, PAR bZIP transcription factors orthologous to the *Drosophila* Vrille and Pdp1 are output regulators rather than components of the secondary loop. These are the activators Dbp (D-box binding protein), Tef (thyrotroph embryonic factor), Hlf (hepatic leukemia factor), and the repressor E4BP4 (E4 promoter-binding protein 4) that act via D-box elements in target clock controlled genes (ccgs) (Mitsui et al., 2001).

In mammals, light entrainment of the circadian system relies on three types of photoreceptive cells: rods, cones and the intrinsically photosensitive retinal ganglion cells (ipRGCs, see paragraph 1.2.2 for details). Rods and cones, located in the retina, express ciliary opsins and are not only responsible for vision but they also provide light information to the clock (Lucas et al., 2012).

ipRGCs express the photopigment melanopsin (Foster et al., 1991; Berson et al., 2002) that mediate light entrainment throughout the action of Creb homodimers which activate transcription of mPer1 and mPer2 (Travnickova-Bendova et al., 2002);

In both organisms the core clock drives the oscillations of numerous clock-controlled genes (ccgs) that are characterized by E-box, V/P-box, D-box and RORE elements in their regulatory regions (Jin et al., 1999; Yamaguchi et al., 2000b; Mitsui et al., 2001). The ccgs encode factors that are involved in generating circadian oscillations in several molecular, physiological and behavioural mechanisms. For istance, in the *Drosophila* head, chromatin immunoprecipitation (ChIP) tiling array assays (ChIP–chip) identified 800 Clk direct target genes, among them 60 transcription factors involved in diverse biological functions such as nucleic acid metabolism, synaptic and sensory functions, signal transduction, metabolism, detoxification, transport and protein cleavage (Abruzzi et al., 2011).

1.2.2 Cellular organization of circadian system in *Drosophila* and mouse.

Circadian clock genes are ubiquitously expressed in the nervous system and in most of peripheral tissues of the organisms so far investigated (Nagoshi et al., 2004; Welsh et al., 2004; Giebultowicz, 2001; Glossop and Hardin, 2002; Schibler and Sassone-Corsi, 2002; Whitmore et al., 1998).

Cellular oscillators must be synchronized with one another and with the environment to produce coherent output signals. For some organisms such as *Drosophila* and zebrafish, light can directly entrain the rhythm of cellular oscillators and allow such synchronization (Plautz et al., 1997a; Whitmore et al., 2000). On the contrary, in mammals the circadian system has a hierarchical organization, consisting of a master clock located in the brain that is entrained to the local environment and synchronizes peripheral clocks dispersed in the organism (Reppert and Weaver, 2002).

In *Drosophila* several pacemaker clocks have been identified in the head and body that are able to respond independently to the local environment indicating the lack of a master clock in the nervous system (Plautz et al., 1997; Emery et al., 1997;

Giebultowicz and Hege, 1997). The circadian system is organized autonomously in a network of central clock neurons that control a number of physiological and behavioural rhythms such as the locomotor activity (Glossop and Hardin; 2002) and peripheral clocks present in most of the organs so far investigated that mediate other physiological and behavioural rhythms such as the olfactory response controlled by antennal neurons (Tanoue et al., 2004), and the eclosion by the prothoracic gland (Myers et al., 2003).

The central clock of the fruit fly (Fig. 1.4) is organized in roughly 150 neurons divided into three groups: lateral neurons (LN) located in the anterior-lateral cortex of the central brain, the dorsal neurons (DN) in the dorsal cortex and the lateral-posterior neurons (LPN) in the lateral-posterior side of the brain. LNs are further divided into small and large ventral-lateral neurons (sLNv and lLNv respectively) and the dorsal-lateral neurons (LNd). DN are also divided in three groups of dorsal neurons (DN1, DN2, and DN3) (Helfrich-Forster, 2005). Clock neurons establishes an oscillatory cellular network. This coupling function is mediated by the neuropeptide pigment dispersing factor (PDF) that is expressed in the small and large ventral lateral neurons (Renn et al., 1999; Lear et al., 2005).

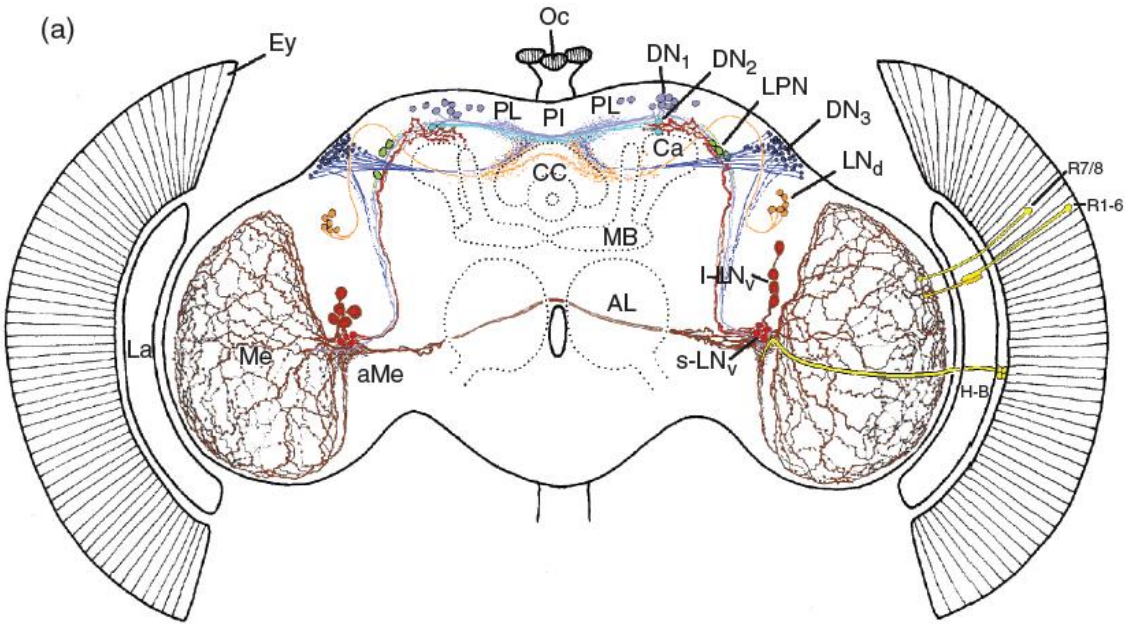

Fig.1.4 Network of clock neurons in *Drosophila*. The neuronal network that forms the central clock of *Drosophila* is composed of the lateral neurons (LNd, l-LNv, s-LNv; in red/orange), the dorsal neurons (DN1, DN2, DN3; in blue), and the posterior lateral neurons (LPN; in green). These neurons send processes to different parts of the brain overlapping each other. The s-LNv processes terminate close to the Calyces (Ca) of the

(continue caption of Fig. 1.4) mushroom Bodies (MB) and overlap with processes from the DN1 and DN2 cells. LNd and DN3 processes terminate close to the central complex (CC) and seem to contact the DN1 and DN2 processes. In the right hemisphere the light input pathways from photoreceptor cells R1-6, R7/8 of the compound eye and from the H-B eyelet cells are shown. The R1-6 and R7/8 cells appear to contact the fiber network derived from the l-LNv cells on the surface of the medulla (Me) and the H-B eyelet cells contact putative dendritic terminals from the s-LNv and l-LNv in the accessory medulla (aMe). AL: antennal lobe; Ey: compound eye; La: lamina; bodies; Oc: ocelli; PI, PL: pars intercerebralis/lateralis. Modified from Helfrich-Forster (2005).

The clock neurons send also processes to the dorsal part of the brain that contains most of the fly neuro-secretory cells (Kaneko and Hall, 2000; Helfrich-Forster et al., 2003). Thus, circadian signals arising from the clock neurons is transferred electrically or/and via humoral pathways to effector organs (Kaneko and Hall, 2000). This implies that, although circadian oscillators are autonomous and light-entrainable, communication between clock neurons and peripheral oscillators is necessary to maintain their synchrony. This is the case for instance of the the interaction between the prothoracic gland and lateral neurons necessary for rhythms in eclosion (Morioka et al., 2011).

Cell-autonomous light entrainment is achieved because dCry operates as a photoreceptor both in central and peripheral oscillators (Emery et al., 2000b). In addition, it has been shown that dCry has a photoreceptor-independent role as transcriptional repressor in the peripheral TTFL implying differences between the molecular architecture of central and peripheral core clocks (Krishnan et al., 2001; Collins et al., 2006).

Differently from *Drosophila*, the mouse circadian system has a hierarchical organization with a master clock located in the brain that is necessary for the synchronization of all peripheral clocks dispersed in the organism (Fig 1.5). A master clock consists of a group of specialized clock cells organized bilaterally in a region of the hypothalamus forming the superchiasmatic nuclei (SCN) (Reppert and Weaver, 2002). These cells respond to light inputs perceived by photoreceptor cells located within the eye.

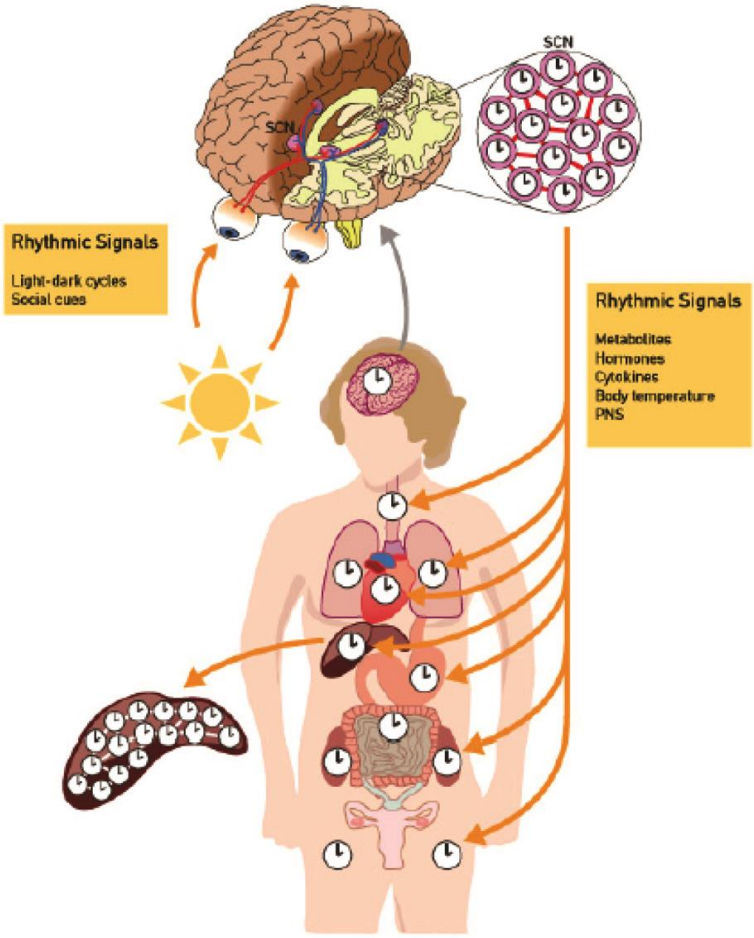

Fig.1.5 Cellular organization of the circadian system in mammals. Light information is perceived through the eyes to entrain cellular clocks of the SCN. The master clock synchronizes peripheral clocks to the local environment via the release of rhythmic signals such as hormones. Each peripheral clock is cell-autonomous but the master clock is essential for their synchronization. Adapted from Bollinger and Schibler (2014).

In the retina, rods, cones and intrinsically-photosensitive retinal ganglion cells (ipRGCs) contribute cooperatively to the circadian light response (Fig. 1.6) (Lucas et al., 2012). ipRGCs are the principal route that provides light information to the SCN and integrates synaptic inputs from rods and cones via bipolar and amacrine cells. ipRGCs express melanopsin and are linked to the SCN through axonal projections known as the retinohypothalamic tract (RHT) (Gooley et al., 2001). Light absorption by melanopsin activates a G-protein signalling cascade, which causes ipRGCs axon terminals to release glutamate and pituitary adenylate cyclase-activating polypeptide (PACAP) onto clock neurons (Ebling et al. 1996; Hannibal et al., 1997; Morin and Allen, 2005).

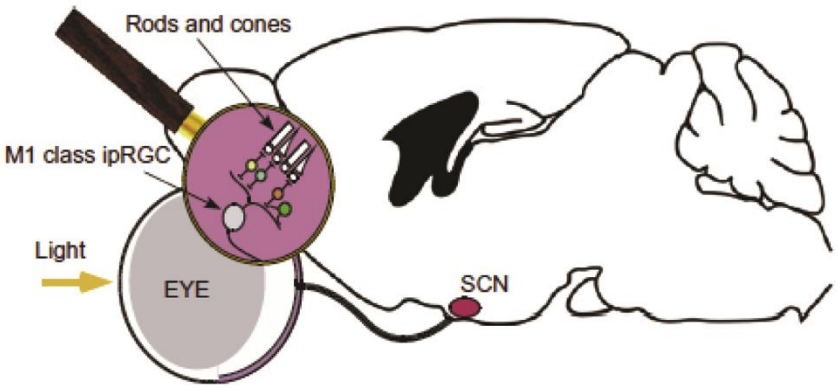

Fig. 1.6 Schematic illustration of the mammalian light input pathway. The SCN receives light information via the RHT. The RHT is connected to the photosensitive retinal ganglion cells ipRGCs that also receives input signals for circadian entrainment from rod and cone photoreceptors, components of the visual pathway. Adapted from Lucas et al. (2012).

The SCN of the mouse contains approximately 20,000 neurons (Abrahamson and Moore, 2001) connected in an oscillatory network through the action of neurotransmitters, neuropeptides, gap junctions, and chemical synaptic mechanisms (Welsh et al., 2010). A well-characterized neuropeptide is the vasoactive intestinal polypeptide (VIP) involved in the synchronization between clock neurons within the SCN. The loss of this neuropeptide results in isolation of SCN neurons from each other (Vosko et al., 2007).

The SCN communicate temporal information to peripheral clocks through both autonomic neural connections (Ueyama et al., 1999; Vujovic et al., 2008), and release of hormones (Kaneko et al., 1980; Kaneko et al., 1981; Oster et al., 2006). An example of a behavioural output under hormonal control is the locomotor activity in mouse, regulated by diffusible signals released from the SCN such as the transforming growth factor α (TGFα), cardiotrophin-like cytokine and prokineticin 2 (PK2) (Kramer et al., 2001; Kramer et al., 2005).

1.2.4 Circadian clock in non-drosophilid insects.

Analysis of the circadian system in other insects has showed diversity of the molecular oscillatory mechanism within this group of animals. In particular, a second *cry* gene homolog to the vertebrate-like cryptochrome is present in all non-drosophilid species so far investigated indicating that this gene was lost in the drosophilid lineage (Yuan et al., 2007). The vCry expressed in insects acts as transcriptional repressor of Clk/Cyc and is

not light sensitive (Zhu et al., 2005). Thus several insects, like mosquitos and butterflies, express both a dCry and a vCry, whereas honeybee *Apis millifera* and the beetle *Tribolium castaneum* express only a vertebrate-like Cry (Zhu et al., 2005; Rubin et al., 2006). In addition to the loss of a *dcry* gene, no homolog to *timeless* was found in *Apis millifera* suggesting that its core clock may be similar to the mammalian one (Rubin et al., 2006). Based on the presence/absence of the cryptochromes, three models that describe the diversity of the clockwork in insects have been proposed (for details see Fig. 1.7).

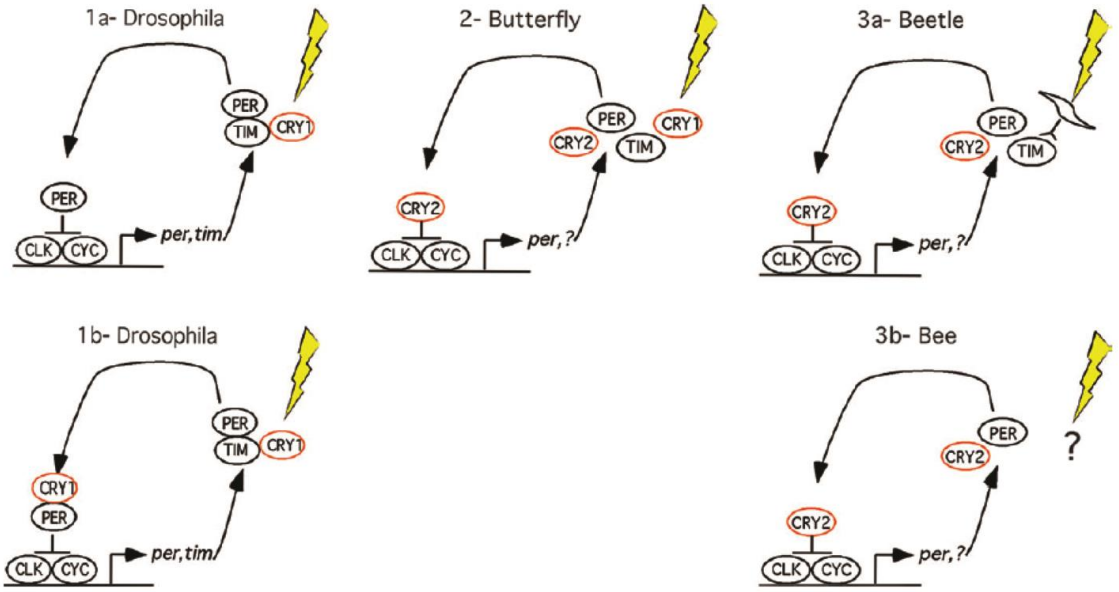

Fig.1.7 Diversity of TTFL model in insects. Aside from the *Drosophila* model, other two models have been suggested for non-drosophilid insects based on the presence of cryptochromes dCry (Cry1) and vCry (Cry2). In 1, the *Drosophila* model is illustrated with dCry, which functions only as photoreceptor in clock neurons (1a) and as photoreceptor and transcriptional repressor in peripheral clocks (1b). The monarch butterfly (2) is characterized by the presence of both cryptochromes that act as photoreceptor (dCry) and transcriptional repressor (vCry). Finally, beetles (3a) and bees (3b) lost the *dcry* gene and express only vCry that maintains the role as transcriptional repressor. In beetles, that express a homolog to Tim, the light input pathway may be mediated by opsins through a Tim-dependent pathway. Whereas bees lack a homolog to Tim and a novel input pathway may be involved in the entrainment. Adapted from Yuan et al., 2007.

Interestingly, the loss of a *dcry* gene in beetle and honeybee indicates that other input pathways, based likely on opsins, are used to synchronize the circadian clock (Gilbert 1994; Velarde et al., 2005).

Finally, another difference that distinguishes *Drosophila* from other insects regards the role of transcriptional activation of the heterodimer Clk/Cyc. In the fruit fly this function is executed by polyQ repeats present at the C-terminal of Clk; while in other insects a transactivation domain at the C-terminal of Cyc is involved in this function (Rubin et al., 2006).

1.2.5 Circadian clock in zebrafish.

The analysis of the zebrafish *Danio rerio* circadian system has revealed differences in the organization of the circadian clock mechanism within vertebrates. The TTFL is similar to that represented in mammals, but it is characterized by extra copies of clock genes compared to the mouse because of the genome duplication event that occurred during the evolution of the teleost lineage (Toloza-Villalobos et al., 2015). This teleost-specific genome duplication is likely the cause of several biological innovations that generated high degree of diversity in this group (Meyer and Van de Peer, 2005). In *Danio rerio*, the set of core clock genes is composed of 3 *clock* genes (*clock 1a*, *1b* and *2*), 3 *bmal* genes (*bmal1a*, *1b* and *2*), 4 *per* genes (*per1a*, *1b*, *per2* and *per3*) and six *cry* genes: *cry1a*, *1b*, *2a*, *2b*, *3* and *4*.

Duplicated gene copies can maintain redundant functions or diverge into more specialized functions. An example is given by *cry* genes. Cry1a, 1b, 2a and 2b share most sequence similarities with the mammalian mCry (vCry) and have the ability to repress Clk/Bmal activity. On the other side, Cry3 and Cry4 have been shown to not repress the heterodimer Clk/Bmal (Kobayashi et al. 2000). Interestingly Cry4 sequence resembles a *Drosophila*-type Cry leading to the speculation that this zebrafish cryptochrome might function as a photoreceptor (Kobayashi et al. 2000; Vatine et al., 2011). As in the fruit fly, the organization of the circadian system in zebrafish relies on the presence of cell autonomous and light-entrainable circadian oscillators dispersed throughout the organism (Tamai et al., 2005). The pineal gland contains all the elements required to be the central clock: it is photoreceptive and regulates locomotor activity (Korf et al., 1998; Falcon et al., 2010). This central clock contains cells that have specialized photoreceptor function sharing various structural and functional properties with retinal photoreceptors and neurons that innervate a variety of brain regions (Yáñez et al., 2009).

However, the identity of the circadian photoreceptors still remains unclear. Candidates for mediating the resetting of clock genes by light are melanopsin, the most plausible

photoreceptor (Ramos et al., 2014), teleost multiple tissue opsin (TMT), detected in the central nervous system and most peripheral tissues (Cavallari et al., 2011), a vertebrate ancient opsin and a phototransducing flavin-containing oxidase. This latter may trigger cellular accumulation of H_2O_2 that activates the MAPK signalling pathway that in turn drives light-dependent activation of genes such as *cry1a* and *per2* (Hirayama et al., 2007).

1.2.6 Circadian clock in marine metazoans.

The marine environment is characterized by dramatically different environmental cues with respect to the terrestrial ones. In addition to daily variations in light intensity and temperature, geophysical cycles that affect marine life are also represented by tidal cycles, caused by the gravitational forces of the sun and moon on the earth's water masses. Tidal cycles have a rhythm of 12 hours and 25 minutes and cause rhythmic variations in temperature, hydrostatic pressure, salinity and wave action.

Physiological and behavioural processes that exhibit not only circadian but also circa-tidal and circa-lunar (29,5 days) rhythmicity have been documented in marine organisms (Naylor, 2001; Naylor, 2002). Circa-lunar cycles are linked to changing levels of moonlight that depend on the phases of the moon. Physiological and behavioural processes related to a tidal and lunar rhythm, such as gametes spawning and breeding, have been extensively described in marine organisms (Naylor, 2010) giving examples of the presence of other types of molecular clocks. In addition, light reduces its intensity, varying its spectral quality over the depth and, for this reason it is a selective force that generates different habitats at different depths (Herring, 2003). Most of ultraviolet and infrared light is absorbed in the first few meters; red, orange, yellow, and green light is absorbed more rapidly than blue light with depth. Light is thought to have been the selective force that has induced most plankton species to adopt diel vertical migrations to avoid the damaging action of UV-light. They undergo vertical migration rhythms of daily periodicity descending in the column of water during light or dark phase (Nybakken, 2001).

Molecular studies of circadian clock in marine metazoans have been carried out in teleosts, annelids, crustaceans and cnidarians, confirming the high degree of diversity of this molecular mechanism among different species likely related to adaptation to various environmental conditions.

In particular, the presence of almost all core clock components in *Cnidaria* suggests early origins of the circadian clock mechanism at least in the common ancestor of cnidarians and bilaterians (Fig. 1.8).

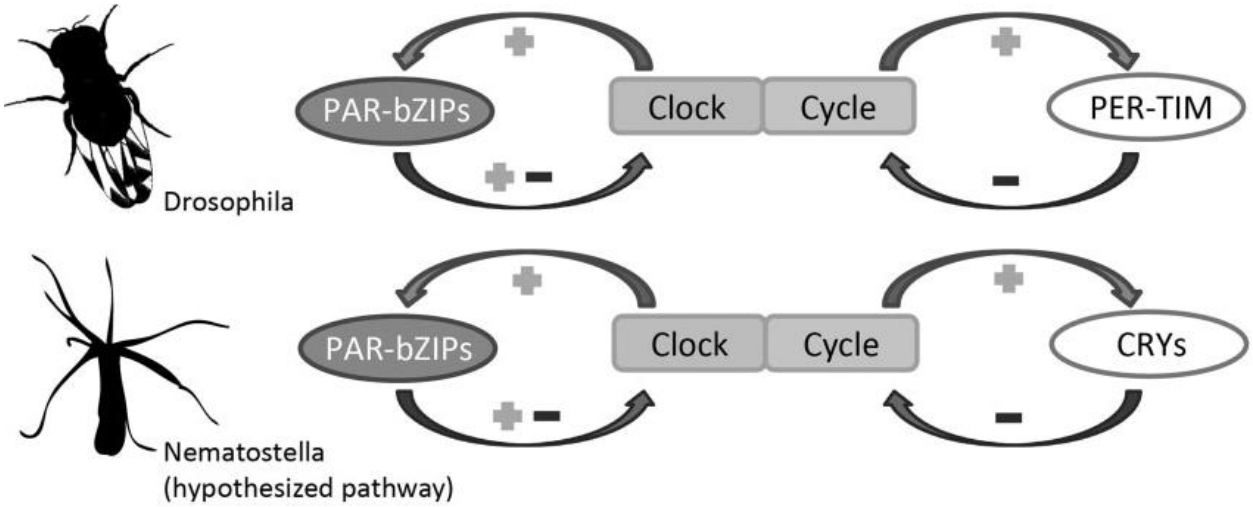

Fig.1.8 Hypothetical model of circadian TTFL in *Nematostella* based on presence/absence of canonical clock components. The core clock mechanism may be conserved in *Cnidaria* with respect to the *Drosophila* one. *Nematostella vectensis* expresses homologs to *cycle* and *clock* and bzip transcription factors. Moreover, the *Nematostella* genome lacks homologs to *per* and *tim* suggesting that only cryptochromes may be involved in the core loop. Modified from Reitzel et al. (2013).

This analysis has been performed in the anthozoans *Nematostella vectensis, Favia fragum, Acropora millepora* and *Acropora digitifera.* All of them encode homologs to *clock* and *cycle* with detection of rhythmic expression for the first gene in *N. vectensis* and *F. fragum* (Reitzel et al. 2010; Brady et al. 2011; Hoadley et al. 2011). In these species the presence of two types of cryptochromes has been described as well; phylogenetic analysis show that one type is sister group to *Drosophila-like* cryptochromes, and the other belongs to the vertebrate-like cryptochromes (Levy et al., 2007; Shoguchi et al., 2013; Oliveri et al., 2014). Interestingly, several copies of the two types of cryptochromes have been found in *Nematostella vectensis* and *Acropora* spp. as a result of duplication events within the cnidarian lineage (Reitzel et al. 2010; Shoguchi et al. 2013).

Cnidarians so far investigated lack *period* and *timeless,* as well as homologs of *rev-erb* and *ror* (Reitzel et al. 2010; Shoguchi et al. 2013; Reitzel and Tarrant 2009; Reitzel et al. 2012). On the other hand, phylogenetic analyses of the bZIP superfamily of

transcription factors identified cnidarian genes that group in the PAR-bZIP family with two of them showing light-dependent expression in *Nematostella vectensis* (Amoutzias et al. 2007; Reitzel et al., 2013).

Other studies carried out in the adults of the anellid *Platinereis dumerilii* and the crustacean *Eurydice pulchra* have focused on characterizing the relationship between the molecular circa-lunar and circa-tidal clock mechanisms, respectively, with the circadian clock (Zantke et al., 2013; Zhang et al., 2013). *Platynereis* is characterized by locomotor activity under circadian clock control and possesses the full complement of *Drosophila* and mouse clock genes: *bmal, clock, timeless, period, vertebrate-like cry, Drosophila-like cry, pdp1, vrille*. In addition *bmal*, *period*, *clock*, *v-cry*, *vrille* and *pdp1* exhibit robust circadian cycles at mRNA levels. Functional experiments using S2 cells suggest that Bmal, Clock, and the vertebrate-like Cry likely function in the core circadian clock of *Platynereis* similarly to their orthologs in other species. As well, *Pdu-l-cry* (the ortholog of D*rosophila*-like Cry) may function as a circadian light receptor. In addition to a circadian clock mechanism, *Platynereis dumerilii* is characterized by a circalunar timekeeping mechanism that has been shown to drive spawning cycles. The molecular mechanism and components that drive this oscillatory mechanism are distinct from the ones described in the circadian clock. Interestingly the circalunar clock has an influence on the circadian clock by modulating directly or indirectly transcript levels of *clock*, *period*, *pdp1*, and *timeless* and, at behavioural level, the period length and strength of the circadian locomotor activity (Zantke et al., 2013).

Eurydice pulchra is an intertidal isopod crustacean that shows circadian rhythmicity in the pigment dispersion of the dorsal chromatophores. This organism shows a complement of canonical circadian genes comparable to those of fly and mouse. So far homologs to *period*, *timeless*, *clock*, *bmal1*, *vertebrate-like cry* have been found in its genome, but any homolog to the *Drosophila-like cry* has been found. Interestingly, *tim* is the only canonical clock gene found with circadian mRNA oscillation. Functional tests in S2 cells have confirmed the respective transactivational roles of CLK and BMAL1 at E-boxes and the negative regulatory properties of EpCRY2, EpPER, and EpTIM. *Eurydice pulchra* exhibits also robust circatidal swimming rhythms driven by a circatidal clock. In Zhang et al. (2013) have shown that the circatidal clock is an independent timekeeping mechanism, distinct and separable from the circadian clock. They also suggest that the kinase CK1ε might play a role in both tidal and circadian timekeeping providing phosphorylation to very different substrates.

1.3 Components of circadian photoreception.

Light emitted by the sun is the most important zeitgeber that provides information about the time of day. Its spectrum changes during the day because of the Earth's rotation, scattering and absorption by the atmosphere and variable weather conditions. At noon, light emits in the blue-green region (400-500 nm), while at sunset, long wavelengths of orange-red (600-700 nm) prevail over blue light (Ugolini, 2007). These daily changes in light quality induced the evolution of photoreceptors sensitive to different wavelengths, capable of providing distinct light information for the clock, in particular for its resetting. Indeed, entrainment of the circadian clock to light/dark cycles requires the cooperative contribution of at least three photoreceptor systems: visual, nonvisual opsins, and cryptochromes. In *Drosophila* rhodopsins 1, 5 and 6 contribute to the synchronization to green, yellow and red light (Hanai and Ishida, 2009; Hanai et al., 2008) while the *Drosophila*-like cryptochrome is sensitive to light in the ultraviolet-A/blue range (Ozturk et al., 2011). Similarly in mouse, rods, cones, and melanopsin contribute differently to the dynamic light environment. Rods and melanopsin respond to gradual changes in light intensity, while cones respond to its rapid changes (Lucas et al., 2012).

1.3.1 The opsin family.

Animal opsins are membrane proteins coupled to G-proteins formed by seven transmembrane α-helices with the N- and C-terminal facing outside and inside of the cell, respectively (Spudich et al., 2000). They are one of the biggest gene families among the Metazoa: more than 1000 sequences of opsins are available from jellyfish to humans (Santillo et al., 2006). They are involved in several mechanisms that range from visual and nonvisual phototransduction to entrainment of the circadian clock and photoisomerization (Spudich et al., 2000; Palczewski et al., 2006; Shichida et al., 2009). Light response is achieved because of the binding to the chromophore retinal, a vitamin A-based retinaldehyde. Upon light absorption isomerization of the chromophore induces structural changes in opsins allowing activation of a G protein and, thus, transducing light stimuli into chemical signal (Kroeze et al. 2003). According to the type of G-protein, a different chemical signal can be produced. Gt opsin activates a phosphodiesterase (PDE) that changes the concentration of cyclic guanosine monophosphate (cGMP) in the cell (Arshavsky et al., 2002), while Gq opsin involves activation of phospholipase C (PLC) and the inositol phosphate (IP3) pathway (Nasi et al., 2000).

Based on sequence similarities, the opsin family can be categorized into seven subfamilies (Fig. 1.9): vertebrate and invertebrate Gq opsins, encephalopsin and teleost multiple tissue (tmt) opsin, Gt opsins and pinopsin, Go opsins, peropsin, neuropsins, photoisomerases (Terakita, 2005).

In most vertebrates, the photoreceptor cells that mediate vision, rods and cones, contain visual opsins that activate a phototransduction cascade involving a type of Gt protein, the transducin. This, in turn, stimulates cyclic GMP (cGMP) phosphodiesterase, which hydrolyzes cGMP to GMP, causing the closure of a cGMP-gated cation channel and leading to hyperpolarization of the visual cell (Shichida and Imai, 1998). On the other hand, protostomes such as cephalopods and arthropods have a different type of visual opsin where the phototransduction cascade is mediated by a Gq protein that stimulates phospholipase C, resulting in the depolarization of the photoreceptor cells (Nasi et al., 2000). To highlight is the close relationship of melanopsins, that drives a Gq/phosphoinositide-mediated transduction cascade, with the protostome Gq visual opsin family (Koyanagi and Terakita, 2008). Melanopsin genes have been found in a wide variety of vertebrates and also in the invertebrate deuterostome amphioxus and sea urchin, whereas protostomes possess only visual Gq opsin genes (Koyanagi and Terakita, 2008). Interestingly, photoreceptor cells diverge in terms of morphology and cellular light response in relation to the type of opsin expressed. Vertebrate opsins, encephalopsins and Go opsins are expressed in ciliary-type photoreceptor cells; while Gq opsins are expressed in rhabdomeric-type photoreceptor cells. The former is characterized by an extended cilium from which membrane vesicles are formed and localize the opsin; the latter by microvilli formed by evaginations of the plasma membrane (Arendt et al., 2004).

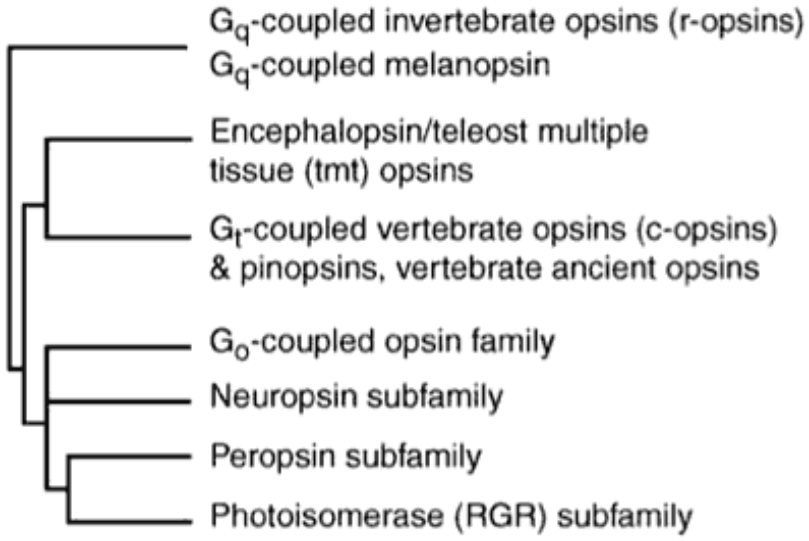

Fig.1.9 Schematic molecular phylogenetic tree showing the seven known opsin subfamilies. Three opsin subfamilies transduce light using G protein-coupled mechanisms: G_q or r-opsins (rhabdomeric opsins) found in invertebrate photoreceptors, melanopsin and G_t or c-opsins (ciliary opsins) found in vertebrate photoreceptors. Encephalopsin and tmt opsins are found in different tissues of several vertebtrates with unknown function. Pinopsins, closely related to c-opsins, are expressed in the pineal organ of several vertebrates, and vertebrate ancient opsins are expressed in non-photoreceptor retinal cells, including amacrine and horizontal neurons in teleost fish retinas. Similarly, neuropsins are found in eye, brain, testes, and spinal cord in mouse and human, but little is known about them. Peropsins and the photoisomerase family of opsins bind *all-trans*-retinal, and light isomerizes it to the 11-*cis* form, which suggests a role in photopigment renewal. RGR, retinal G protein-coupled receptor. Adapted from Fernald, (2006)

Ciliary and rhabdomeric photoreceptor cells are present in both protostomes and deuterostomes, strongly suggesting that the common ancestor of Eumetazoa already used these two types of photoreceptor cells to mediate the two functions induced by light: circadian rhythmicity and photo-taxis (Fig.1.10) (Arendt et al., 2009). While in protostomes rhabdomeric photoreceptor cells are involved in visual and non-visual functions; in the chordate lineage, rhabdomeric photoreceptor cells must have been relegated only to a nonvisual function and must have lost their rhabdomeric morphology to evolve in photosensitive retinal ganglion cells characterized by the expression of melanopsin and involved in circadian entrainment (Aredent, 2003).

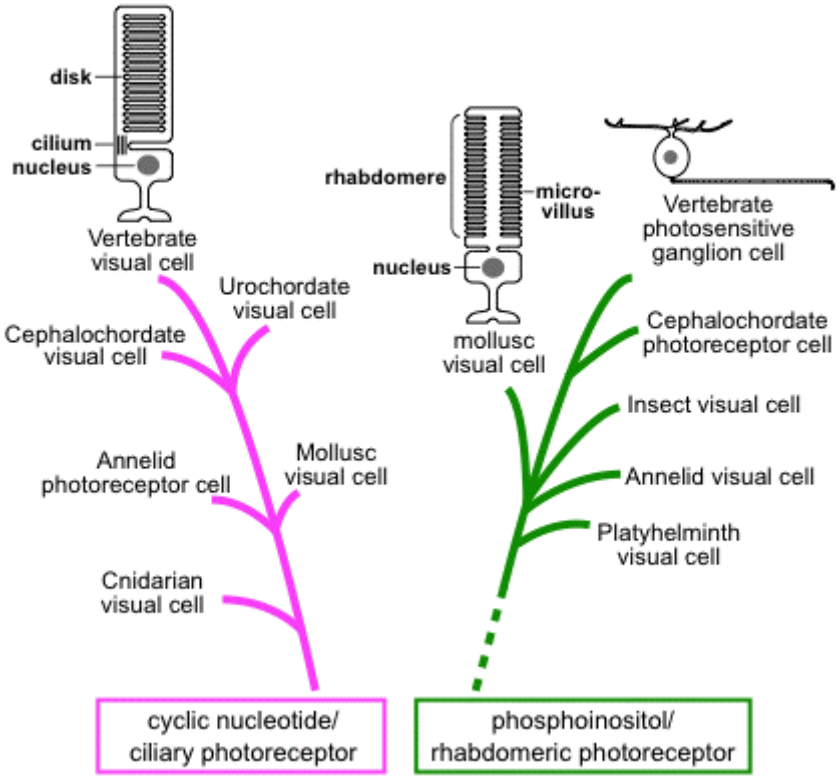

Fig. 1.10 Phylogenetic scheme showing the evolution of animal photoreceptor cells. Adapted from http://www.photobiology.info/Terakita.html.

1.3.2 The Cryptochrome/Photolyase family.

The family of photolyases/cryptochromes (CPF) includes UV-A/blue-light responsive proteins present in many organisms ranging from cyanobacteria to mammals (Chaves et al., 2011). All the components of this family have a similar structure with a chromophore binding photolyase homology region (PHR) that can bind to two chromophores, and a pterin and a flavin adenin dinucleotide (FAD). The photolyases group consists of the cyclobutane pyrimidine dimer (Cpd) photolyases and the (6–4) pyrimidine-pyrimidone photoproduct photolyases (6-4 photolyase). These enzymes utilize light energy for repairing UV-damaged DNA and can be distinguished from each other by the capacity to fix different DNA damages, cyclobutane pyrimidine dimers and (6–4) photoproducts respectively. Contrarily, cryptochromes, in addition to the PHR have a C-terminal regulatory tail region of variable length and sequence (Cashmore, 2003). They can be divided into three classes: Cry-DASH, plant Cry and animal Cry. Cry-DASH cryptochromes have structural and photochemical properties similar to

photolyases and retain DNA repair activity (Pokorny et al., 2008) with high affinity for ssDNA.

On the other hand, plant and animal cryptochromes have generally lost the DNA repair activity and acquired novel specialized functions involved in photoperiodic photoreception and growth in plants (Moglich et al., 2010; Liu et al., 2011; Harmer, 2009), and circadian photoreception and transcriptional regulation in animals (dCry and vCry) (see paragraph 1.2 for details). The C-terminal region is necessary to regulate cryptochromes activities. In *Drosophila*-like Cry, in darkness, the C-terminal tail has a conformation that prevents interactions with Tim and Jet (Busza et al., 2004; Peschel et al., 2009), while, in presence of light, conformational change of the tail allows dCry-Tim-Jet interactions (Ozturk et al., 2011) and subsequent proteasomal degradation of dCry and Tim (Peschel et al., 2009). In mammalian Crys, the C-terminus tail and coiled-coil helix of the PHR interact with the C-terminal of mBmal1 to repress the transcriptional activity of Bmal1/Clock (Sato et al., 2006).

One of the last phylogenetic analyses of the CPF components summarizes the main evolutionary events that gave rise to animals, plants and diatoms photolyases and cryptochromes (Oliveri et al., 2014). This study has highlighted the presence of the phylogenetic group Crys/6–4 photolyases suggesting that the last common eukaryotic ancestor might have possessed a precursor gene which later gave rise to animal 6–4 Photolyase, vCry and dCry classes, as well as the diatoms double function Cpf class. These latter possess both photoreceptor and 6–4 photolyase activities (Coesel et al., 2009) suggesting, furthermore, that the precursor gene might have possessed this double function and subsequently, this function might have been retained in animals photolyases/Crys.

In the same study, the presence of a novel class of cryptochromes has been identified in several metazoans, diatoms and plants belonging to the group of plant-type cryptochrome. The identified cryptochromes have been named plant-like Cry (pCry-like). They differ from the plant Cry due to a lack of a key aspartate essential for plant Cry biophysical properties and possess an N-terminal extension that normally is not present in other CPFs.

Finally, the last common eukaryotic ancestor might have possessed a component of each superclass, and lately, events of duplication and deletion and adaptability to different environmental conditions have generated the diversity of CPF components observable in Eukaryota (Fig.1.11).

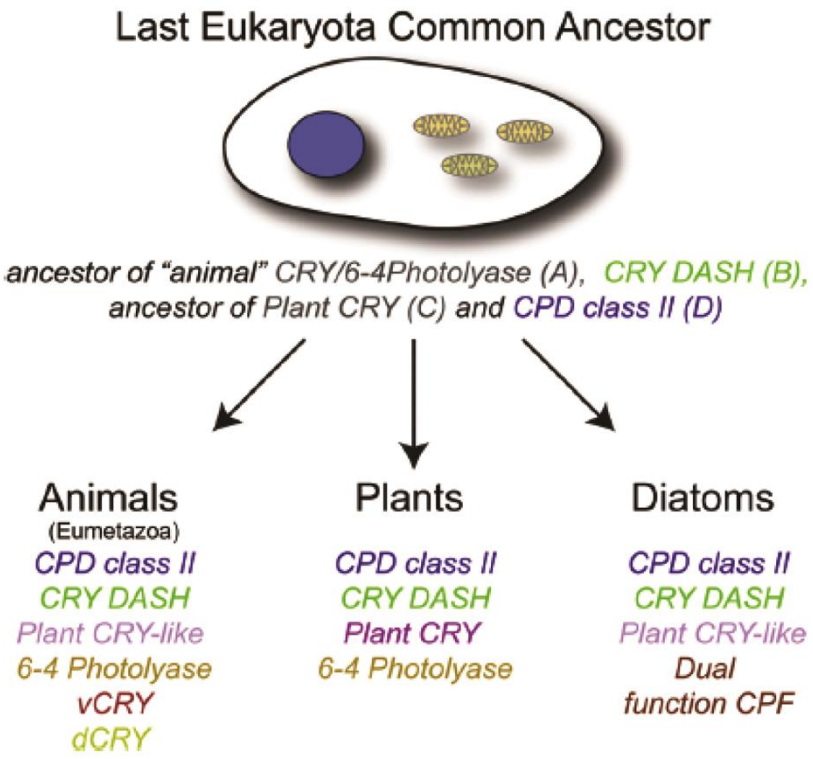

Fig.1.11 Illustration that summarizes the evolution of Cpf genes in Eukaryota. The last common ancestor of eukaryotes likely possessed precursor genes for each CPF superclass. Later in evolution, gene duplication, functional diversification and/or gene losses led to the diversity of CPF genes observed, nowadays, in each eukaryotic lineage. Adapted from Oliveri et al., 2014.

1.4 The sea urchin *Strongylocentrotus purpuratus* as a model system.

S. purpuratus (Fig. 1.12) is a marine invertebrate organism that belongs to the Echinodermata *phylum* that includes five extant classes: Asteroidea (sea stars), Echinoidea (sea urchins, sand dollars and sea biscuits), Holothuroidea (sea cucumbers), Ophiuroidea (brittle stars and basket star) and Crinoidea (sea lilies and feather stars). The characteristics that specify this group of animals are: adults with pentameric symmetry, embryos and larvae with bilateral symmetry, presence of endoskeleton and a water vascular system.

Fig. 1.12 *S. purpuratus* adult.

Based on molecular data, morphological analysis and sequencing of genomes, the Echinodermata are clearly deuterostomes and together with hemichordates form the Ambulacraria group, the sister group of Chordates (Fig. 1.13) (Sodergren et al., 2006; Delsuc et al. 2006, Swalla and Smith, 2008). Thus, sea urchins and other echinoderms are phylogenetically close to chordates providing an excellent basis for evolutionary and comparative studies in evaluating chordate specific features and protostome/deuterostome homologies. In addition, echinoderms diverged from chordates prior to gene duplication events that occurred in the evolution of vertebrates, indeed many of the genes that are found in multiple copies in vertebrates have only a single homolog in echinoderms. In comparative studies, this feature allows to avoid problems related to the functional redundancy between multiple paralogs often observed in vertebrates (see above about cryptochromes in teleosts). Therefore the use of echinoderms in comparative studies allows assessing the degree of functional conservation of genes and regulatory linkages of genes between different metazoans genomes. The sea urchin has been used as an excellent model organism to study embryology, developmental biology, and to elucidate gene regulatory networks involved in cell specification and differentiation (Ernst, 2011). Nowadays, these kinds of studies are facilitated by the availability of genome and transcriptome sequences (Sodergren et al., 2006; Tu et al., 2012). In addition, their experimental success stems from their easily obtainable gametes (millions can be obtained almost instantly in the lab), ease of *in vitro* fertilisation and culture of embryos, and rapid, synchronous development of transparent embryos and larvae, making them ideal for microscopy. Embryos are also robust to manipulation, such as microinjection, and have easy gene transfer and reporter gene expression. All this facilitates studies involved in analysing and perturbing gene expression and function.

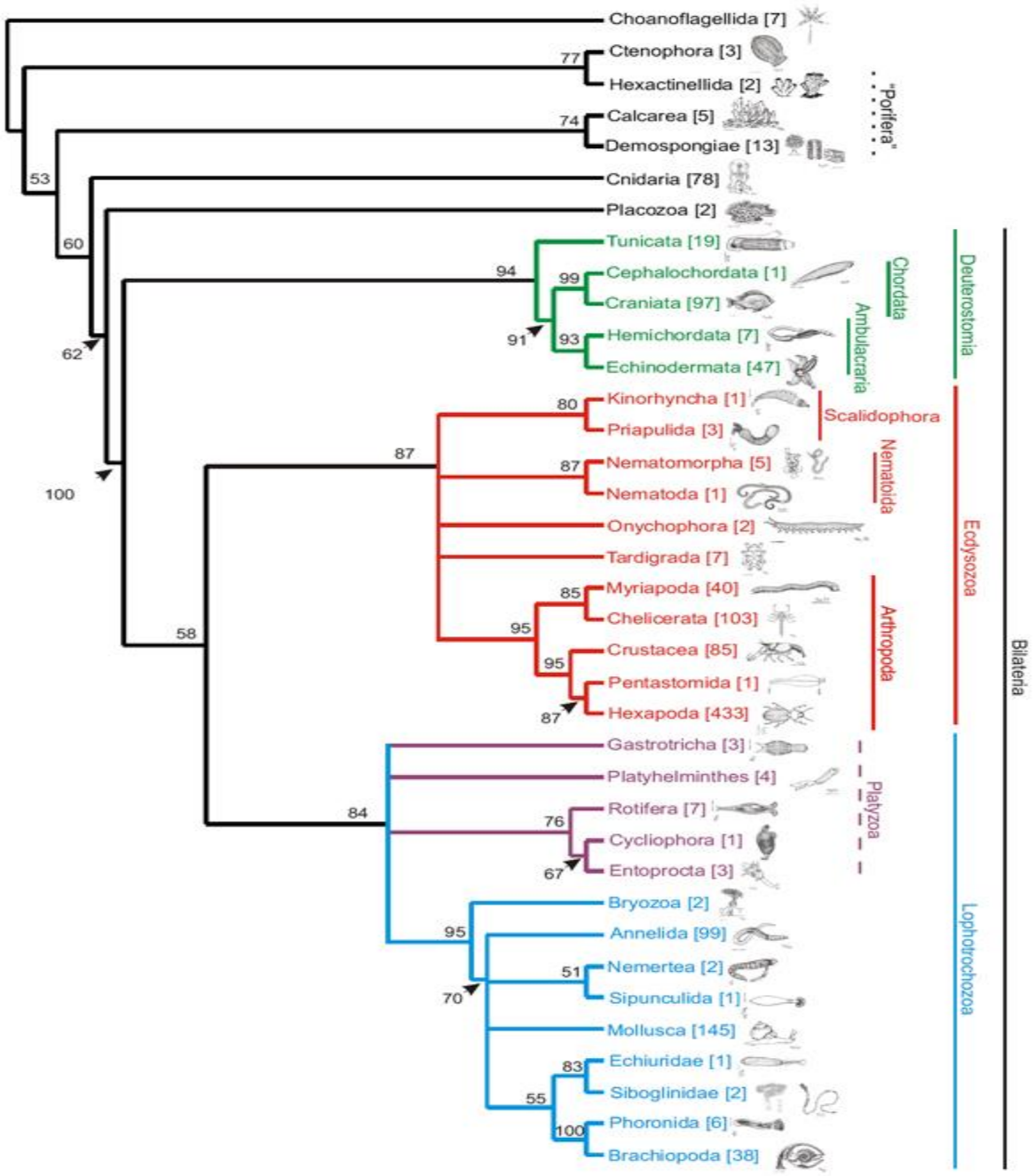

Fig. 1.13 Phylogenetic tree of the Metazoa (Gerlach et al. 2007). The phylogenetic tree was calculated with ProfDist. Numbers at nodes indicate bootstrap values greater than 50%; numbers in brackets indicate the number of sequences in the respective subtree. Colour code: green for Deuterostomia; red for Ecdysozoa; blue for Lophotrochozoa**.**

1.4.1 Sea urchin development.

Most sea urchin species undergo a maximally indirect development with embryogenesis that occurs over a short period, for example three days in the species of the Californian purple sea urchin *Strongylocentrotus purpuratus*. In this species eggs are oligolecithal containing low reserve of uniformly distributed yolk and they have completed meiosis before they are released from the ovary. Embryonic development proceeds through a series of radial and holoblastic cleavages that culminate in the formation of a 120-cell blastula. At 60-cell stage embryos comprise various specified cellular territories (Fig.1.14). These are conceived as groups of blastomeres, characterised by a unique regulatory state that will give rise to one or multiple cell types (Oliveri et al., 2008). At this stage there are five major embryonic territories: the small micromere (deep purple), the skeletogenic large micromere (red), the endo-mesoderm (blue), the oral ectoderm (yellow) and the aboral ectoderm (green).

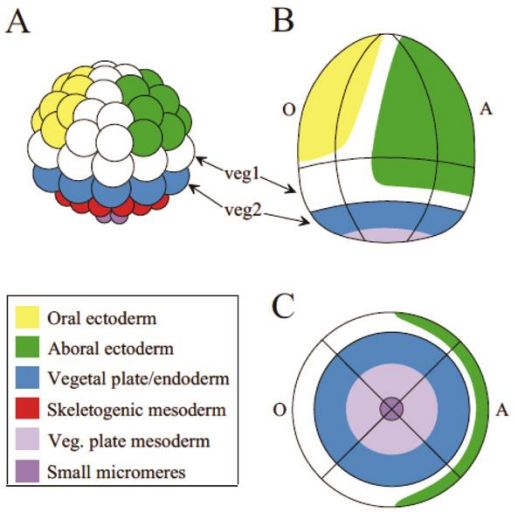

Figure 1.14 Fate map of sea urchin embryo. In A, lateral view of a 60-cell stage embryo characterized by eight skeletogenic large micromeres (shown in red), the four small micromeres (shown in deep purple) and the eight blastomeres of the veg2 ring specified in the endo-mesoderm territory (blue). The veg1 domain, here shown in white, is not yet specified. In B and C, external lateral view and vegetal view, respectively, of a mesenchyme blastula (about 500 cells). Endoderm (blue) and mesoderm (light purple) are now specified as two different territories. Colour codes are reported in the figure key; in white, domains not yet specified. Veg1 and Veg 2 are tiers of macromeres that arise at 5th cleavage; O: oral; A: aboral. Modified from Davidson et al. (1998).

At blastula stage, cells are of equal size and form a ciliated sphere surrounding a central cavity. After hatching from the fertilization membrane, swimming embryos continue development through to the mesenchyme blastula stage (Fig. 1.15). At this stage, cells descendent from the large micromeres undergo epithelial to mesenchymal transition (EMT) and ingress into the blastocoel to become the skeletogenic mesoderm (SM) also called primary mesenchyme cells (PMCs). SM cells migrate in two ventro-lateral clusters, eventually producing the skeleton that will give shape and sustain the sea urchin larva. Following SM cells ingression, the vegetal plate begins to buckle inwards, invaginating itself to form the early archenteron and blastopore (site of the anus). During gastrulation, from the tip of the archenteron the non-skeletogenic mesoderm (NSM), also known as the secondary mesenchyme cells (SMCs), extend long and thin filopodia toward the animal pole, while remaining attached to the archenteron and pulling it upwards towards the animal pole. In the late stages of development the cells of the archenteron undergo convergent extension to form a tube-like structure. In addition, NSM cells disperse in the blastocoel, differentiate mesodermal structures and finally the archenteron fuses with the oral ectoderm forming a mouth and a tripartite digestive tube (foregut, midgut and hingut) (reviewed by Wolpert, 2007; Gilbert, 2010; McClay, 2011).

Prior to mouth formation, two pouches of cells outpocket from the tip of the archenteron, one on each side, forming the left and right coelomic pouches that will contribute to form the adult rudiment during larval development. The final product of embryonic development is a fully differentiated free-swimming larva that possesses a differentiated nervous system to monitor and interact with its environment as well as immune system, gut, muscles, pigment cells and other structures. It has an elongated shape, a flattened aboral side and an oral side characterized by a concavity sustained by four arms elongated by the skeleton (fig. 1.15). The larva is able to swim and feed thanks to the movements of cilia, which form along the edges of the four arms and around the mouth. The free-living larva spends several weeks (from six to eight) in the plankton floating with currents and feeding on phytoplankton. During this time, larvae increase in cell numbers, in nervous system complexity and in number of arms (from four to eight) (Smith et al., 2008). At the same time, adult tissues are formed in the rudiment, and when competent to metamorphose, the bilaterally symmetrical larva settles down on a substrate to give rise to the radially symmetrical juvenile (Smith et al., 2008).

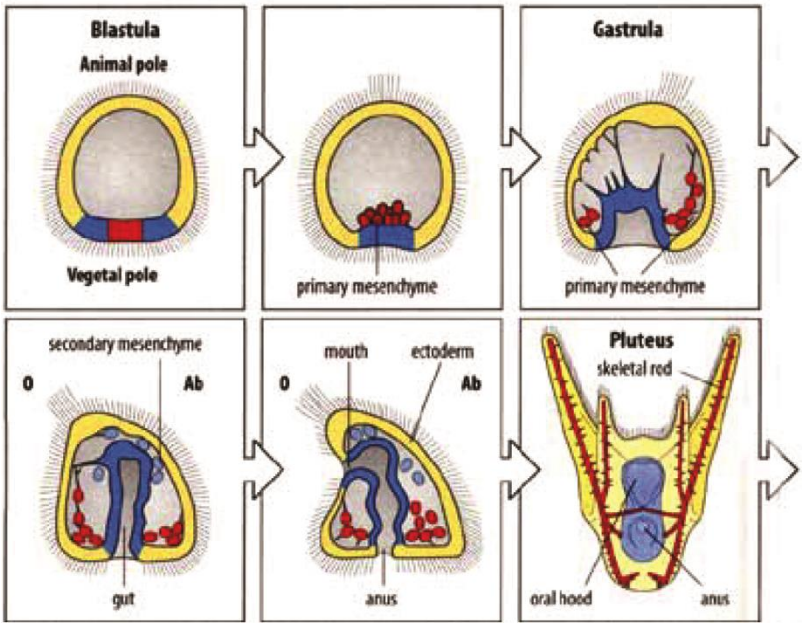

Figure 1.15 Sea urchin development from blastula stage. From left to right, hatched blastula (18 hours post fertilization (hpf)), mesenchyme blastula (24 hpf), early gastrula (30 hpf), late gastrula (48 hpf) in lateral view, pluteus (72 hpf) in lateral (bottom panel) and oral view (top panel). The endoderm territory is depicted in blue; secondary mesenchyme cells in light blue; the skeletogenic mesoderm in red; the ectoderm territory in yellow. O: oral; Ab: aboral.

1.4.2 Nervous system of the sea urchin larva.

The sea urchin larva possesses a fully differentiated nervous system that allows the regulation and coordination of vital functions such as swimming and feeding (Strathmann, 1975; Yaguchi and Katow, 2003). Indeed principal effectors of the nervous system are the ciliated cells of the ciliary band and the musculature of the oesophagus and mouth (Strathmann, 1971; 1975). The nervous system is organised into three main territories (Fig.1.16): the apical organ, the ciliary band and the pharingeal neurons and two lateral ganglia that project axons throughout the posterior end of the larva (Nakajima et al., 2004b; Wei et al., 2011).

The apical organ is formed by a bilaterally symmetrical group of neurons, clustered as ganglia, positioned between the pre-oral arms of the larva. It comprises 4-6 serotonergic neurons, 10-12 non-serotonergic neurons and several non-neural support cells (Bisgrove and Burke, 1987; Beer et al., 2001; Burke et al., 2006). The apical organ is likely involved in mediating sensory responses during larval development. Serotoninergic neurons seem to have a role in regulating direction of swimming (Byrne et al., 2007; Yaguchi and Katow, 2003).

The ciliary band is predominantly composed of specialized ciliated cells and neurons, whose axons form a ganglion that lies beneath ciliated cells. In addition, at the left and right side of the ciliary band, lateral ganglia project axons throughout the posterior end of the larva (Nakajima et al., 2004b).

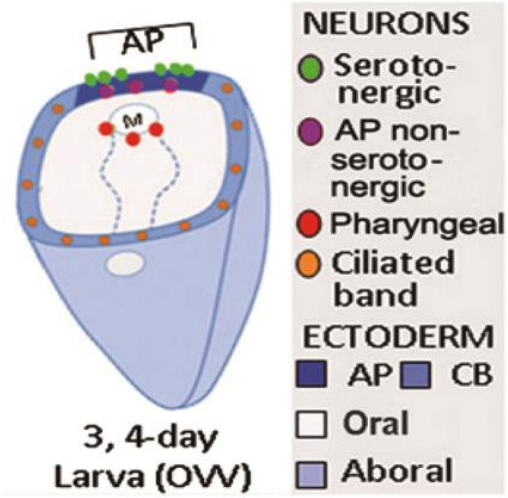

1.16 Schematic drawing of a sea urchin pluteus showing the nervous system organization. See key and text for details. OVV: oral vegetal view; AP: apical organ; M: mouth; CB: ciliary band. Adapted from Wei et al., 2011.

Neuronal topology has been investigated in *S. droebachiensis* larvae by Burke and Bisgrove (1987) (Fig. 1.17). Using immunofluorescence experiments with antibodies against dopamine, GABA and serotonin they have showed how the number and diversity of neurons increases with larval development (Bisgrove and Burke, 1987). Sea urchins larval nervous system arises during gastrulation with the presence of serotonin in a single cell of the apical domain. In the four-arm larva, serotoninergic neurons increase in number and extend their axons to form a ganglion in the apical organ. Late in development they appear in the lower lip of the larva and extend their axons along the base of the epidermis to innervate the antero-lateral arms, the ciliary band, the oesophagus and the rudiment (Byrne et al., 2007).

Dopaminergic neurons differentiate in the early pluteus and are localized in the lower lip of the mouth and at the bases of the post-oral arms to innervate the ciliary band. As well as dopaminergic neurons, GABAergic ones appear at the four-arm stage in the dorsal surface of the oesophagus and, later, in the upper lip of the mouth.

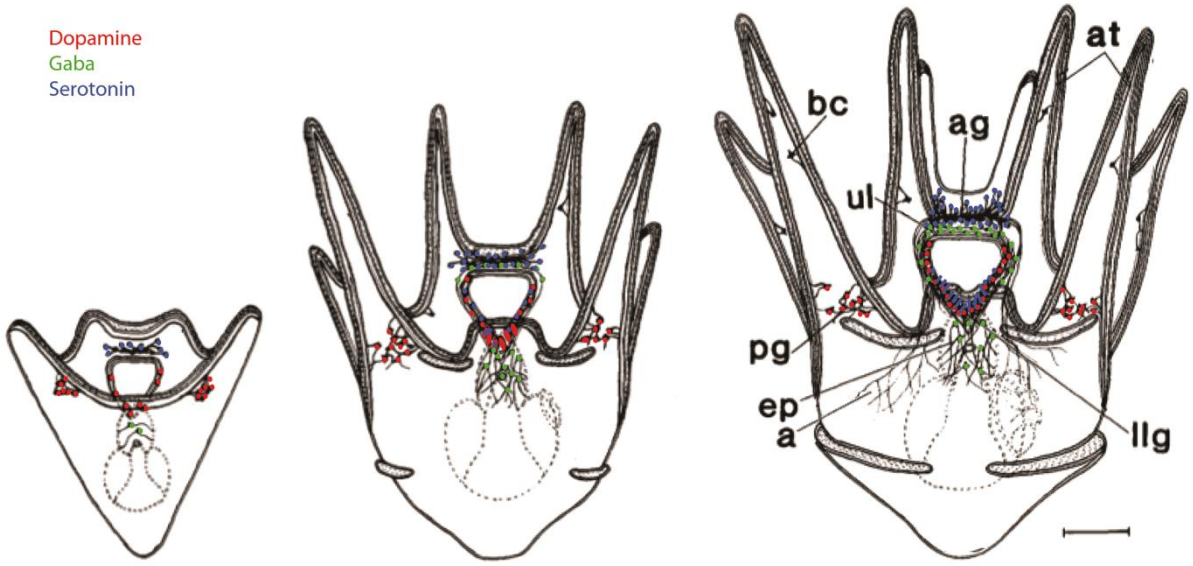

Fig. 1.17 Distribution of dopaminergic (red), GABAergic (green) and serotoninergic (blue) neurons during larval development of *S. droebachiensis*. From left to right, four-arms larva, six-arms larva, eight-arms larva. Modified from Bisgrove and Burke (1987).

1.4.3 Photoreception and photoperiod in sea urchin.

Sea urchins display several light-induced behavioural and physiological responses such as: colour change, spine movements, tube foot reactions, covering, phototaxis photoperiod and spatial vision (Yoshida, 1966; Millott 1975; Yerramilli and Johnsen; 2010). Phototaxis has been documented both in adults and larvae. Adult sea urchins have generally phototactic responses by reacting to illumination by intensifying tube feet and spines activity (Yoshida, 1966). The response can be positive or negative, depending on the species: adults of *S. purpuratus* have negative phototaxis (Ullrich-Lüter et al., 2011), instead *Lytechinus variegatus* show a positive phototaxis (Sharp and Gray, 1962).

Regarding phototactic response in echinoderm larvae, there is only a single study by Pennington and Emlet (1986) where diel vertical migration was investigated in the pluteus of the sand dollar *Dendraster excentricus.* They showed that plutei undergo diel vertical migration sinking down in presence of light and swimming towards the surface at night. In particular this behaviour was detected when larvae were exposed only to unfiltered sunlight or irradiated with UV-B suggesting a vertical migratory response for UV avoidance. Despite this diversity of processes that respond to light intensity, the molecular mechanism that integrates light stimuli has not yet been thoroughly studied.

Opsins have been analysed as molecular components involved in photoreception in *S. purpuratus* (Raible et al., 2006; Lesser et al., 2011; Ullrich-Lüter et al., 2011; Agca et al., 2011; Ullrich-Lüter et al., 2013). The sea urchin genome encodes for 9 opsins belonging to different opsin classes (Delroisse et al., 2014; D'Aniello et al., 2015; table 1.1).

Table 1.1 Description of the opsin family in sea urchin. The table lists, from left to right, opsin genes identified in *S. purpuratus*; type of opsin; the accession number for the sea urchin genome version 3.1; accession number for the transcriptome database. Modified from Delroisse et al., 2014.

Gene name in Sp	Opsin class	Gene Model(s)	Transcriptome
sp_opsin 1	Pinopsin (ciliary opsin)	XP_783302.2	-
sp_opsin 2	Echinopsin A	SPU_003451	WHL22.272775
sp_opsin 3.1	Rhodopsin G0 coupled-like	XP_003723700.1	-
sp_opsin 3.2	Rhodopsin G0 coupled-like	SPU_027633	WHL22.338995
sp_opsin 4	Rhabdomeric opsin	XP_003730546.1	-
sp_opsin 5	Echinopsin B	XP_784559.2	-
sp_opsin 6	peropsin-like	XP_784266.2	-
sp_opsin 7	RPE retinal G protein coupled receptor like	XP_003727813.1	-
sp_opsin 8	Neuropsin (opsin 5 like)	XP_001199309.1	-

Importantly, some studies focused on the identification of photoreceptor systems (Fig. 1.18) in the sea urchin adult using *sp_opsin4* (rhabdomeric opsin) and *sp_opsin1* (ciliary opsin) as molecular markers to identify photoreceptor cells (PRCs; Ullrich-Lüter et al., 2011; Ullrich-Lüter et al., 2013). *Sp_opsin4* expression pattern defines two arrays of PRCs in the tube feet: within the rim of the tube foot disk and in the basal portion of the tube foot stalk in a groove where the nerve enters the body cavity. Dispersed *sp_opsin4*

expressing PRCs have also been localized along the basal portion of the tube foot nerve, the lateral nerve and within the spine nerves. These PRCs have been suggested to be involved in the phototaxis response (Ullrich-Lüter et al., 2011).

In contrast, *sp_opsin1* is expressed throughout the entire body surface in many different types of tissues (spines, pedicellarieae, tube feet and some portions of epidermis) (Ullrich-Lüter et al., 2013). Likely *sp_opsin_1* expressing cells are not involved in the phototaxis response but their dispersion over the body may suggest that they might mediate dermal sensing of light, that is the sensitiveness of sea urchin epidermis to changes in light intensity (Yoshida, 1966; Millot, 1975; Ullrich-Lüter et al., 2013).

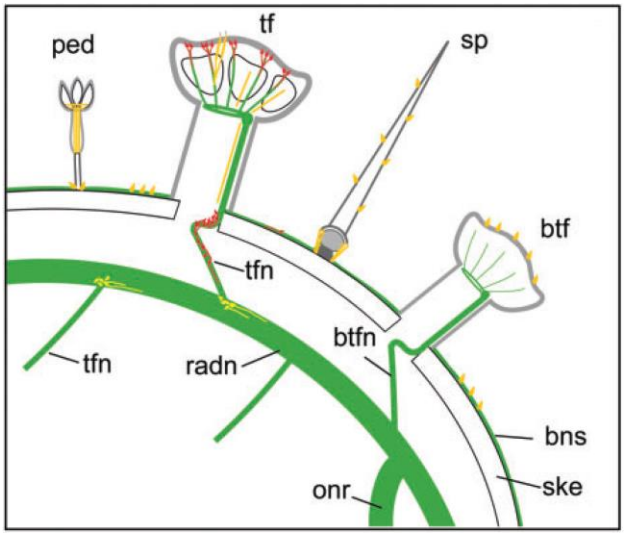

Fig. 1.18 Scheme displaying the spatial distribution of PRCs expressing *sp_opsin1* (yellow) and *sp_opsin4* (red) relative to the nervous system (green). Bns, basiepithelial nervous system; btf, buccal tube foot; btfn, btf nerve; onr, oral nerve ring; ped, pedicellaria; radn, radial nerve; ske, skeleton; sp, spine; tf, tube foot; tfn, tube-foot nerve. Modified from Ullrich-Lüter et al., 2013.

In addition, circadian rhythmic behaviours or physiological processes have not been analysed in sea urchin so far, neither has the mechanism of circadian clock been studied at molecular level. Some studies highlight the presence of physiological processes in sea urchin adults that have a rhythm matching the lunar phase (Morgan, 2001; Kennedy and Pearse, 1975). Several sea urchin species are characterized by a monthly spawning rhythm that fit in with the period of the lunar phase. *Diadema Setosum* (Morgan, 2001) and *Centrostephanus coronatus* (Kennedy and Pearse, 1975) are examples of those species.

1.5 Aim of the thesis.

So far an extensive research on the molecular and cellular characterization of circadian clock has been mainly performed in terrestrial animals with the exception of zebrafish. Studies on marine animals have primarily focused on the identification of canonical clock components and their possible rhythmic expression. Only in the marine annelid *P. dumerilii* and in the marine crustacean *Eurydice pulchra* the role of the respective vCrys has been investigated using heterologous systems confirming that it conserves its function as a transcriptional repressor (Zhang et al., 2013; Zantke et al., 2013). These studies gave a significant insight into understanding the diversity and complexity of the circadian clock in animals likely caused by evolutionary pressures exercised by different environmental cues. Rhythmic geophysical cues characterized Earth's environment long before the dawn of life and it seems evident that the evolution of internal molecular clocks passed through the adaptation to such rhythms. In particular the sea is influenced by environmental cues in a different way with respect to the mainland, and additionally, life evolved in the sea. Thus, investigating circadian clock in marine organisms appears crucial to understand how a genome encodes a mechanism that responds to the marine environment and which contributes significantly to the evolutionary history of circadian clocks in Metazoa.

The circadian function is encoded by a network of clock genes and the analysis of functional linkages between these genes can be applied to dissect such a network (Yan et al., 2008; Li et al., 2013).

Sea urchin, as potent model system used to study gene regulation and gene regulatory networks (GRNs), provides tools to analyse the circadian system of a marine organism and, as basal deuterostome, can facilitate the comprehension of the evolution of the circadian clock in Metazoa. In particular, the circadian clock and light input system have been analysed in the sea urchin larva mostly at the stage of 1wpf (week post fertilization). Although there is an absence of studies that highlight the presence of circadian behaviours, there are many indications suggesting that the sea urchin larva may possess a time keeping mechanism: they possess a nervous system with potential neurosensory activities that may integrate environmental stimuli to optimize vital functions such as swimming and feeding.

Therefore my PhD project focused on:

1) identifying canonical clock genes in the sea urchin genome;

2) assessing daily expression profiles of candidate genes that may have a role in the circadian system of the sea urchin larva;

3) analysing the cellular and molecular organization of the light perceiving system of sea urchin larva;

4) analysing the functional linkages between key clock genes to compile a provisional model of the sea urchin circadian network.

A further clarification useful for understanding the organization of experiments and interpretation of results, which I describe in the following chapters, consists in defining the properties of a circadian rhythm. According to the current research (Sehgal, 2004), a rhythm, at any level of analysis (changes of mRNA, protein expression, locomotor activity etc.) to be considered circadian has to respect the following criteria:

- The clock is an endogenous mechanism, thus a rhythm is circadian if it shows a period of approximately 24 hours under constant environmental conditions (free running, e.g. constant dark, constant temperature). Conversely, if a rhythm persists only in presence of light/dark cycles (L/D) it implies that oscillations are light dependent but not under circadian control.
- A rhythm is entrained to the local environment by rhythmic environmental cues, thus, in the case of light, the period of a rhythm will match to that of the imposed light/dark cycles.
- The remaining key property is temperature compensation, meaning that over a range of physiological temperatures, the frequency/cycle of a rhythm does not change.

Chapter 2 describes materials and techniques used to analyse the circadian clock in sea urchin larvae in terms of GRN and transcriptional regulation. In chapter 3, I describe the identification of canonical clock genes in the sea urchin genome and, for some of them, the characterization of their putative functional protein domains. Additionally, I list other candidate genes, previously identified in sea urchin, that have been considered in this project for their potential involvement in the circadian system. In chapter 4, I show results relating to the gene expression analysis performed in sea urchin larvae to measure daily expression profiles of the candidate genes and thus to assess their eventual belonging to the circadian network. Furthermore, spatial expression patterns of

key genes are reported to describe the cellular organization of the circadian clock and light input pathways. In chapter 5, results of functional experiments are described to compile a provisional circadian network of the sea urchin larva. Functional analysis was performed by generating a knockdown of key genes via microinjections of morpholino antisense oligonucleotides (MO). Subsequently, daily expression profiles of candidate genes were monitored in perturbed samples and compared with unperturbed ones to assess the presence of functional linkages. Finally, in chapter 6, the results described in chapter 3, 4 and 5 are discussed together providing for the first time indications about the functioning of the circadian clock in the sea urchin larva.

Chapter2

Materials and methods

The following chapter describes materials and techniques used to analyse the circadian clock in sea urchin larvae in terms of GRN and transcriptional regulation. The chapter has been organized in 4 sections according the aim of a specific experimental design: bioinformatics tools, methods for molecular cloning, techniques of embryology, methods of gene expression analysis.

2.1 Bioinformatics tools

2.1.1 Identification of "clock" and light responsive genes in the sea urchin genome.

The identification of sea urchin genes encoding for canonical components of circadian clock, cryptochromes, photolyases and related proteins was accomplished using a reciprocal BLAST strategy. Genes of *Drosophila* and mouse, involved in the core clock and input mechanisms, were used to run TBLASTX against both the Sp Gene and Sp Genome 3.1 databases (http://www.echinobase.org/Echinobase/; Cameron et al., 2009). Sea urchin sequences with the 5 highest hits (applied a cut off at E value = $9.00E^{-32}$) were chosen and used to run a BLASTX and a TBLASTX against the no redundant (NR) nucleotide database from NCBI (http://blast.ncbi.nlm.nih.gov/Blast.cgi). Sea urchin sequences that identified the initial metazoan sequences were defined as putative homolog genes (sea urchin genes identified in this work have been listed in table 3.1).

2.1.2 Analysis of conserved functional domains and motifs in sea urchin "clock" proteins.

The survey of conserved motifs and domains in a protein may provide insights into its function. For this reason the identified "clock" and cryptochrome/photolyase protein sequences have been analysed for the presence of conserved domains and motifs and compared to homolog proteins in other organisms. Protein domains were identified either using SMART server (Shultz et al. 1998; Letunic et al. 2012) or by comparing manually sea urchin aminoacidic sequences with sequences of proteins domains previously described in different Metazoa (see Results to have information about sources of metazoan sequences). Such manual comparison was performed using either pairwise sequence alignments (EMBOSS Needle, pairwise sequence alignment

(http://www.ebi.ac.uk/Tools/psa/emboss_needle/) or multiple sequence alignments (CLUSTALOmega, EBI multiple sequence alignment; Goujon et al., 2010) with default settings.

Nucpred (Brameier et al., 2007), NLS mapper (Kosugi et al., 2009) and NLStradamus (Nguyen et al., 2009) tools were used to search for putative nuclear localization signals (NLS). NLS motifs were considered valid if predicted by two out of 3 of these independent computational tools. NetNES 1.1 tool (la Cour et al., 2004) was used to search for putative nuclear export signals. The protein structure prediction server Phyre2 (Kelley et al., 2015) was used to search for Armadillo repeats in *sp_tim*.

2.1.3 Identification of E-box motifs in the *Sp_vcry* genomic locus.

Manual searching and use of ConSite, a transcription factor binding site search tool (http://asp.ii.uib.no:8090/cgi-bin/CONSITE/consite/), were used to identify canonical (CACGTG) and non-canonical E-box elements within a region of ~37kb upstream of the start codon of the *Sp_vcry* gene (SPU_007204). The software was used with default settings.

2.1.4 Primer design.

Cloning PCR primers were designed using the Pimer3 software (Rozen and Skaletsky, 2000, http://frodo.wi.mit.edu/primer3/) with default settings for all the fields. DNA sequences were obtained from the annotated genome of *Strongylocentrotus purpuratus* (Sodergren et al., 2006) or the transcriptome database (http://www.spbase.org/SpBase/rnaseq/; Tu et al., 2012).

QPCR primers were designed with Pimer3 as well. Default settings were changed as follow: “max 3’ end stability” and “max poly-X” were amended to 8 and 3 respectively, and “product size” was changed to 120-180 nucleotides. Primers sequences were searched back in the sea urchin genome using BLASTN in SpBase to check for aberrant binding to any other part of the genome and/or transcriptome. Primers were ordered from MWG Eurofins (http://www.eurofinsgenomics.eu) and 100 µM stock solutions were prepared from lyophilized products. Lists of all primers used in this work are reported in Appendix A, table A1 and A2.

2.2 Methods of molecular cloning

2.2.1 Polymerase Chain Reaction (PCR).

In order to amplify a fragment of a specific gene, PCRs were performed using Expand High Fidelity PCR system (Roche) or KAPA HIFI PCR kit (Kapa Biosystems). When the aim of the experiment was to amplify the coding region of a gene, cDNA was used as template in the PCR reaction. cDNAs were previously synthesized using total RNA extracted from *S. purpuratus* embryos at different developmental stages, 1 Wpf (week post fertilization) larvae or tube feet, using Qiagen RNeasy Micro kit and Bio-Rad iScript cDNA synthesis kit (see below for details). Appropriate stages were chosen for cloning of each gene using temporal expression data obtained either from the developmental transcriptome of *S.purpuratus* (http://www.spbase.org:3838/quantdev/) or from our qPCR data.

When the aim of PCR was to amplify regulatory regions upstream the start of transcription of a gene, 1 μl of genomic DNA (50 ng/μl) of *S. purpuratus* extracted previously from male sperm was used as template and PCR reactions were set up in a final volume of 25 μl. Table 2.1 illustrates the protocols used for each kit. Amplification was carried out using a Bio-Rad C1000 thermal cycler using the cycle conditions listed in table 2.2.

Additionally, in order to add restriction enzymes (RE) sites to PCR fragments, initial PCR products were used as initial template and amplified using primers with RE sites sequences in presence of gradients of the annealing temperature (table 2.3). PCR reactions were analysed on agarose gel (see below).

Reagents (Roche High Fidelity)	Final concentration/amount
10x Buffer+$MgCl_2$	1X
dNTP mix (10mM)	0.2Mm
Forward primer (10µM)	0.3 µM
Reverse primer (10µM)	0.3 µM
cDNA/gDNA/PCR product	10 ng/1 µl/ 1 ng
Taq DNA Polymerase (3.5U/ µl)	1.75 or 2.6
N-free H_2O	Up to 25 µl

Reagents (KAPA HIFI PCR kit)	Final concentration/amount
5x Buffer+$MgCl_2$	1X
dNTP mix (10mM)	0.3 mM
Forward primer (10µM)	0.3 µM
Reverse primer (10µM)	0.3 µM
cDNA/gDNA	10 ng/50 ng
Taq DNA Polymerase (1U/ µl)	0.5 U
N-free H_2O	Up to 25 µl

Table 2.1 Reaction mix for PCR amplification using Roche High Fidelity kit or Kapa Biosystems HIFI PCR kit**.**

PCR steps	Temperature (°C)/ Time (Roche High Fidelity)	Temperature (°C)/ Time(KAPA HIFI PCR kit)	Nr of cycles
Initial denaturation	95/3’	95/5’	1
Denaturation	95/30”	98/20”	30 – 35
Annealing	Depending on Tm of primers/30“	Depending on Tm of primers/15”	
Elongation	72/Depending on the length of the fragment (based on 1 min. per kb of fragment size)	72/Depending on the length of the fragment (based on 30 sec. per kb of fragment size)	
Final elongation	72/7’	72/2’	1

Table 2.2 Temperatures and time conditions used for PCR amplifications using Roche High Fidelity kit or Kapa Biosystems HIFI PCR kit. (‘) indicates minutes and (“) seconds.

PCR steps	Temperature (°C)/ Time	Nr of cycles
Initial denaturation	94/3’	1
Denaturation	94/30”	5
Annealing	56 - 58 - 60/30”	
Elongation	72/ Depending on the length of the fragment (based on 1 min. per kb of fragment size)	
Denaturation	94/30“	20-25
Annealing	72/30”	
Elongation	95/ Depending on the length of the fragment (based on 1 min. per kb of fragment size)	
Final elongation	72/7‘	1

Table 2.3 Temperatures and time conditions used for PCR amplifications using Roche High Fidelity kit when a PCR product was used as template.

2.2.2 Rapid Amplification of cDNA ends (3’ RACE PCR).

3’ RACE-PCR was performed to amplify, clone and sequence the 3’ end coding region of *sp_dcry* (SPU_000282). RNA was previously extracted from *S. purpuratus* embryos at the stage of 33 hours. 1 µg of total RNA was used to synthesize cDNA using the polyA 3’ RACE adapter (FirstChoise® RLM-RACE kit; Ambion) according the manufacturer’s instructions. The outer and inner 3’ RACE PCR reactions were set up as described in the manufacturers instructions. In the outer PCR, 1 µl of cDNA was used as template; dNTP and 3’ RACE outer primer were provided by the RLM-RACE kit, 10X buffer and DNA taq polymerase were provided by the High Fidelity kit (Roche). Amplification was carried out using a Bio-Rad C1000 thermal cycler using the cycle conditions described in the manufacturer’s instructions with a temperature of annealing of 60 °C and an extension time of 1 minute and 30 seconds. The inner 3’ RACE PCR reaction was performed as described in the manufacturers instructions by using the same PCR cycling profile as in the outer 3' RACE PCR.

2.2.3 Gel electrophoresis.

Gel electrophoresis of DNA or RNA samples were performed to check the outcome of a PCR reaction, DNA enzymatic digestion (paragraph 2.2.8) or probe synthesis (paragraph 2.5.5). DNA or RNA samples (suitable amount) mixed with 1x Loading Buffer (6X; 0,25% (w/v) Bromophenol Blue, 15% (v/v) Ficoll 400, 120 mM EDTA, 0.25% (w/v) Xylene Cyanol FF) were run in agarose gel (0.8 – 2 % in 0.5X TBE (10X, Sigma)) containing 0.5 µg/ml of ethidium bromide (Sigma). In order to determine the molecular weight of a nucleic acid, all DNA solutions were run in comparison with a solution containing a 5-7 µg of DNA ladder. Recipe of DNA ladder solution is: 67 µg of 1 Kb plus DNA ladder (1 µg/µl, Invitorgen), 1 x TE (10X, Tris-EDTA), 2X loading buffer (6X), N-free H2O up to 670 µl.

2.2.4 PCR clean up and gel extraction.

PCR fragments were cleaned from undesired reagents (primer dimers, polymerase and unincorporated reagents) or, in case of undesired bands, appropriate band was cut from the agarose gel and extracted using the NucleoSpin® Extract II kit (Macherey-Nagel) following the manufacturers instructions. NanoDrop 2000c Spectophotometer was used to measure DNA concentration.

2.2.5 Ligation and bacterial transformation.

To create a stable clone containing the desired fragment of DNA PCR products were ligated into pGEM®-T Easy Vector (Promega) or pCRblunt II TOPO (Invitrogen) following the manufacturers instructions: 5X or 2X Ligation buffer, 25 ng of pGEM-T Easy Vector, T4 ligase (3 Weiss units), DNA fragment and N-free H_2O (Nuclease free) up to a final volume of 10 µl. The amount of fragment required for ligation was calculated in order to have an insert:vector molar ratio of 3:1 or 6:1. The reactions were incubated at 12 °C overnight or over the weekend.

All recombinant clones used in this project were transformed into bacterial chemical competent cells One Shot® Top10 *E. coli* or DH5α *E. coli* (Invitrogen). 5 µl of ligated DNA were added to a 50 µl aliquot of competent cells and the obtained mixture was incubated on ice for 30 min. Then, the mixture was heat shocked at 42 °C for 20 sec. and cooled on ice for 2 min. 950 µl of Luria Broth (LB; Tryptone (pancreatic digest of casein) 10 g/L, Yeast extract 5 g/L and NaCL 5 g/L (Sigma)) was added to the mixture and incubated at 37 °C for 1 hour at 225 rotations per minute (RPM). 100 µl and 900 µl of the transformed bacteria were plated on two separate LB plates containing or

ampicillin (100 µg/ml) or kanamycin (50 µg/ml) (depending by the antibiotic resistance expressed by the plasmid) and X-gal (50 µg/ml) for blue/white screening of colonies.

2.2.6 Colony PCR.

PCR were used as methodology to screen for the desired recombinant a large number of transformed bacterial colonies by amplifying the fragment inserted in the cloning site of the vector, using universal primers. Single white colonies were inoculated into 20 µl of LB broth containing a specific antibiotic and incubated for 2 hours at 37 °C. PCR reactions were set up with Taq DNA Polymerase (Invitrogen) as follows: 2 µl of PCR Buffer (10X), 0.6 µl of $MgCl_2$ (50 mM), 0.1 µl Taq DNA Polymerase (5 Units/µl), 0.8 µl each of T7 and SP6 primers (10 mM), 0.4 µl of 10 mM dNTP mixture (2.5 mM each), 1 µl of LB containing the picked colony and N-free H_2O up to 20 µl. Colony PCR reactions were carried out using BioRad C1000 thermal cycler using the following cycle conditions: initial denaturation at 98 °C for 5 minutes; 25 cycles of denaturation at 94 °C for 30 sec., annealing at 55 °C for 30 sec., elongation at 72 °C at X time (depending by the length of the fragment); and a final extension step of 72 °C for 5 min. At PCR completion, samples were run on agarose gel to visualize the presence and the size of the amplified DNA band.

2.2.7 DNA miniprep.

To prepare recombinant clones sufficient to further applications, bacterial colonies positive to the transformation were grown in 3 ml of LB in presence of the appropriate antibiotic and incubated overnight at 37 °C shaking at 225 rpm. Recombinant plasmids were extracted using NucleoSpin® Plasmid Mini-Prep kit (Macherey-Nagel) following the manufacturers instructions. Purified plasmids were eluted into 50 µl Elution Buffer AE (5 mMTris/HCl, pH 8.5) and final concentration of DNA was determined using NanoDrop 2000c Spectophotometer.

2.2.8 DNA digestion.

DNA digestion was used as experimental tool to confirm the presence of the expected DNA fragment inserted in a vector, delete specific DNA fragments from a clone, generate empty vectors ready for cloning DNA fragments, linearize a vector for cloning or linearize a reporter vector for microinjection.

All the digestion reactions were set up using Promega reagents following the manufacturer's instructions (see Table 2.4 for details).

Exceptions to the manufacturer's protocol were the digestion reactions performed with the restriction enzymes *SacI* (Promega) and *MluI* (Roche): due to different buffer requirements double digestions were performed in 2 steps. The first digestion with *SacI* was performed according to manufacturer's guidelines, scaling up the digestion to use a total volume of 100 µl and using 5 µg of substrate DNA. After 2 hours this reaction was heat inactivated (65°C, 15 min.) and 4µl *MluI* enzyme plus the appropriate buffer H (Roche) were added. The reaction was left for a further 4 hours to allow complete digestion.

Electrophoretic gel analysis was used to confirm the completion of digestion.

Linearized vectors used for microinjection were purified using the PCR purification protocol NucleoSpin® Gel and PCR Clean-Up Kit (Macherey-Nagel) according to manufacturer's guidelines and eluted in 35µl NE Buffer (pH 8.5) (Macherey-Nagel).

Table 2.4 The table lists the different digestion reactions performed in this work. In each row is reported the vector and the amount used, the type of enzyme, the total volume of the reaction, time of incubation and the aim of the experiment.

Name of empty vector or cloned plasmid (amount used)	**Enzyme used (10 units/µl)**	**Volume of reaction**	**Time of incubation**	**Aim of digestion**
pGEM-T Easy vector + inserted fragment (2 µl)	*EcoRI*	20 µl	1 h	diagnostic
EpGFPII and *smp::gfp* (5 µg)	*HindIII* and *XbaI*	100 µl	2 h	Release of the GFP cassette
per1::luc2 (5 µg)	HindIII and XbaI	100 µl	2 h	Release of the Luc2 cassette
Ep-luc2 and *smp::luc* (2 µl)	Hind III and XbaI	20 µl	1 h	diagnostic
sp_vcry-1.6reg (5 µg)	EcoRI	100 µl	2 h	Deletion of a non-coding region at the 3'
Ep-luc2 and EpGFPII (5 µg)	*EcoRI and SacI*	100 µl	2 h	Make the vectors competent for further ligation
sp_vcry::gfp-s, sp_vcry::luc-s, sp_vcry::gfp-l, sp_vcry::luc-l (2 µl)	*SacI, Mlu1 and EcoRI*	20 µl	1 h	Diagnostic
sp_vcry::gfp-l, sp_vcry::luc-l (10µg)	*HindIII and SmaI*	200 µl	4 h	Deletion of Endo16 promoter
sp_vcry::gfp-l, sp_vcry::luc-l (2 µl)	*HindIII and SmaI*	20 µl	1 h	Diagnostic digestion

Continue Table 2.4

sp_vcry::gfp-s, sp_vcry::gfp-l, sp_vcry::gfp-l-ep(-), sp_vcry::luc-s, sp_vcry::luc-l and sp_vcry::luc-ep(-) (2.5 µg)	*SacI*	50 µl	2 h	Linearization of reporter construct
smp::luc (2.5 µg)	*BamHI*	50 µl	2 h	Linearization of reporter construct
smp::gfp and sp_he_gfp (2.5 µg)	*KpnI*	50 µl	2 h	Linearization of reporter construct

2.2.9 Klenow polymerase reaction.

Because *HindIII* restriction enzyme causes the formation of sticky ends in a DNA fragment not suitable for ligation, vectors digested with Hind*III* were incubated with a Klenow polymerase (Promega) to allow the fill in of the *HindIII* sites. The reaction was performed according the manufacturers guidelines in a final volume of 50µl using 4µg of DNA substrate.

2.2.10 DNA sequencing.

Recombinant clones (100 ng/µl) were prepared for sequencing to confirm the correct fragment had been cloned using T7, SP6 or custom primers (see appendix for details). Sequencing reactions were performed by the Scientific Support Services at the Wolfson Institute for Biomedical Research and the UCL Cancer Institute.

2.3 Techniques of embryology.

In order to perform experiments of gene expression and perturbation analysis so as to investigate light-response and circadian rhythmicity in sea urchin larvae, cultures of embryos were set up to allow the sampling of larvae exposed to light/dark cycles (L/D) of 12 hours of light and 12 hours of dark and constant dark (D/D) over 1 or 2 days (explanations for the set up of this experiment are reported in chapter3).

Larvae were processed for total RNA extractions, Nanostring nCounter reactions, fixed for whole mount *in-situ* hybridization (WMISH) or collected to monitor *in-vivo* expression of reporter constructs.

2.3.1 Animals maintenance.

Sea urchin larvae processed to analyse gene expression in normal conditions were cultured in Stazione Zoologica “Anton Dohrn” Naples, Italy; while larvae injected with GFP, luciferase reporter constructs and MOs (morpholino oligonucleotides) were cultured at UCL (see paragraph 2.3.4 for microinjection experiment). In both cases, adult *S. purpuratus* were obtained from Pat Leahy (Kerchoff Marine Laboratory, California Institute of Technology, USA), and fed regularly with seaweed (*Ulva lactuca*).

At the Stazione Zoologica, animals were kept in tanks filled with Mediterranean Sea water at a temperature of 15 °C, while at UCL they were kept in tanks filled with artificial seawater (36 ppt, pH 8; Instant Ocean, Aquarium System) at a temperature of 12 °C.

2.3.2 Collection of gametes.

There are not external morphological differences between males and females, thus the sex can be determined after the release of gametes. Sea urchins were vigorously shaken to collect gametes from the gonopores situated on the aboral part of the animal (Fig. 2.1). If shaking was not sufficient, intracoelomic injection of ~1 ml of 0.5M KCl was given to induce spawning of gametes. Sperm was collected using a pipette and kept dried in a 1.5 ml eppendorf tube on ice until used for fertilization or stored at 4 °C a maximum of 15 days. Female sea urchins were placed upside down on a beaker filled with filtered seawater (FSW, formula in Appendix C) to allow eggs to settle down by gravity. Eggs were washed through a 100 µm filter mesh to remove debris.

To proceed with the fertilization, 5-10 µl of dry sperm was diluted in 10 ml FSW and mixed with eggs.

The event of fertilization was monitored using a dissecting scope to observe the elevation of the fertilization membrane. After that, embryos were washed three times with FSW to remove the excess of sperm and diluted in a concentration of ~1000 embryos/ml.

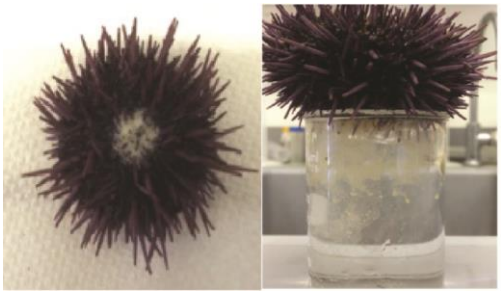

Fig. 2.1 On the left, a male sea urchin is releasing sperm (white colour); on the right a female sea urchin is releasing eggs (orange colour). The female sea urchin is placed upside down on a beaker filled with sea water to allow eggs to settle down by gravity. The picture has been taken and modified from the website http://thenode.biologists.com/a-day-in-the-life-of-a-sea-urchin lab/lablife/.

2.3.3 Set up of larval cultures and sampling.

At the Stazione Zoologica, embryos were cultured at 15 °C in thermostatic rooms illuminated with white neon light of total intensity of 1000-2000 lux and exposed to 12 hours:12 hours L/D cycles with zeitgeber time 0 (ZT0) at 7am (light on) and ZT12 at 7pm (light off). Mediterranean Seawater has a value of salinity of 38 ppt, thus it was diluted 9:1 with deionized H_2O to reach the optimum value of salinity for *S. purpuratus* embryos (36 ppt). A mix of antibiotics, penicillin and streptomycin, at a final concentration of 20 U/ml and 50 µg/ml respectively, were added to the seawater to prevent bacterial growth.

After 72 hours post fertilization, larvae were diluted at the concentration of 10-30 larvae/ml and fed every two days with 1:10 dilution of *Isochrisis galbana* (10.000/ml) and *Rhodomonas cryptophyta* (3000/ml) algae. The day before the sampling, cultures were split in two fractions: one exposed to the same L/D cycles, the second one moved in a thermostatic chamber where light was constantly off (D/D). The following day, ~1000 larvae were collected per each time point every four hours over 36 hours and 44 hours, in L/D and D/D respectively. Larvae were either lysed in 1 ml of RLT buffer (Quiagen) and stored at -80 ^{o}C or fixed for WMISH. For experiments performed at UCL, embryos were cultured as described above using filtered artificial seawater (FASW, for formula see Appendix C). Embryos injected with GFP and luciferase reporter constructs were cultured at 13 °C in a thermostatic room exposed 12h/12h L/D cycles using a light box (Kenro lightbox). On the other hand, larvae injected MOs were cultured at 13 °C in two lightproof tents (Fig. 2.2) (Black Orchid hydrobox light tent, Fantronix) equipped with a daylight bulb of total intensity of 1750 lumens (1750 lux/m2).

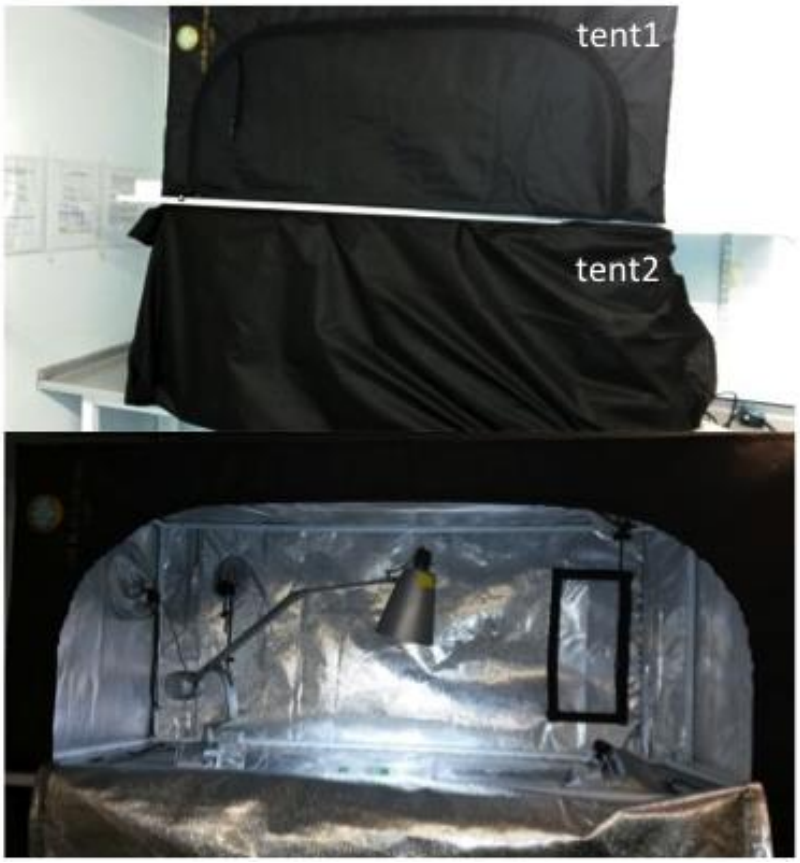

Fig. 2.2 Pictures of the tents used for culture sea urchin larvae exposed to light/dark cycles. In tent1 light/dark cycles had a regime 7am light on, 7pm light off; in tent2 the cycles were inverted with ZT0 at 7pm and ZT12 at 7am. The picture underneath depicts the inside of the tents with the presence of a lamp. Tent 2 was covered with a black cloth to eliminate completely the chances of light penetration during subjective night.

A tent (tent 1) was characterized by a 12:12 light/dark cycle (ZT0 at 7 am (light on), ZT12 at 7 pm (light off)) and the other (tent 2) characterized by an inverted cycle 12:12 dark/light (ZT0 at 7 pm (light on), ZT12 at 7am (light on)). After microinjection, embryos were cultured in tent 1 for 20-24 hours; after transfer of embryos in new plates with fresh ASFW, cultures were split in the two tents. At the desired larval stage, about 50-100 larvae were collected per each time point every six hours in a period of 12 hours for one or two consecutive days. Larvae, fed with the alga *Dunaliella salina,* were lysed in 10 µl of lysis buffer and stored at -80 °C. In all the experiments, larvae sampled in dark were exposed to red light from a LED headlamp.

2.3.4 Microinjection experiment in sea urchin fertilized eggs.

Microinjection technique consists in injecting DNA constructs, mRNAs, MOs etc. in cells or embryos. In sea urchin, microinjection is a well-established tool that offers high efficiency and reproducibility allowing the execution of several functional experiments. In the present work, fertilized eggs have been microinjected: to deliver GFP and luciferase cassettes recombined with *sp_vcry* regulatory regions to monitor "circadian" expression in sea urchin larvae; and MASOs to inhibit the translation of specific proteins, and therefore, to analyse the expression of key genes in knockdown conditions.

Gamete preparation.

Gametes were obtained as described in paragraph 2.3.2 and handled for microinjection experiments as follows:

Eggs were de-jellied to dissolve their jelly coat, allowing them to stick to plates coated with protamine sulphate. De-jellying was performed mechanically by pouring the eggs through a 70 µm filter mesh. Protamine plates were prepared using a solution of 1% protamine sulphate in dH_2O (SIGMA), incubated on 60 mm plastic Petri-dish lids (Falcon) for 1 minute at room temperature, washed off with dH_2O and air-dried. Eggs were rowed, using a pulled Pasteur pipette, on protamine plates filled with AFSW containing 2mM para-aminobenzoic acid (PABA). The presence of PABA in FASW prevents the hardening of the fertilization membrane.

Microinjection solutions.

Microinjection solutions for DNA reporter constructs were prepared with ~1000 molecules of linearized plasmid DNA in a total volume of 5µl. The other constituents of the solution were: 0.2µl Carrier DNA (500ng/µl), 0.6µl KCl (1M), 0.5µl Rhodamine dextran (10mg/µl; MW 10,000) and Nuclease free water up to 5µl. In this case, carrier DNA is made of *S. purpuratus* genomic DNA purified from sperm and totally digested with *KpnI* (*Promega*).

Microinjection solutions containing MOs were prepared as following: 150 – 300 µM of MO (500 or 1000 µM), 1.2 µl KCl (1M), 1 µl Rhodamine dextran (10mg/µl; MW 10,000) and N-free H_2O up to 10 µl. Translation blocker MOs sequences were designed and manufactured by Gene Tools (http://www.gene-tools.com/) using gene sequences from the sea urchin transcriptome database. Lyophilized MO were resuspended in N-free H_2O to a concentration of 500 or 1000 µM and stored indefinitely at -20 °C. To prepare

microinjection solutions, concentrated MO solutions were incubated at 50 °C for 10 min. to allow complete dissolution of the oligonucleotides. All microinjection solutions were centrifuged for 5 min. in order to collect any debris at the bottom of tubes and avoid clogging of the needles. In Appendix A, table A5, sequences and characteristics for each MO are reported.

Microinjection and embryos culture.

A few microliters of dried sperm were diluted in PABA-FASW in order to be activated and some drops of such solution were transferred in the protamine coated plate containing eggs. Fertilized eggs were microinjected using a Picospritzer®III, (Intracel) and incubated in FASW+Penicillin/Streptomycin (PS) antibiotic at 12 or 15°C for 20-24hours They were then transferred to fresh plates filled with fresh FASW+PS and kept to grow until the reaching of the desired larval stage.

When MO solutions were injected, a solution containing a standard control MO (provided by Gene-Tools and prepared at the same concentration of a specific MO) was used as negative control to assess that the presence of a possible phenotype was not caused by the toxicity of morpholino oligonucleotides.

Needles for the microinjection were prepared using borosilicate glasses with filament (1 mm outside diameter and 0.75 mm inside diameter; Sutter Instrument). These glasses were pulled on a Sutter P-97 micropipette puller with the following parameters: P=500, H=496, Pu=160, V=60, T=210.

2.4 Analysis of gene expression.

The quantification of mRNA levels of specific genes at different zeitgeber times, circadian times or in perturbed conditions was carried out using two different strategies:

- qPCR quantifies the abundance of PCR products at each cycle by measuring the amount of fluorescence that is emitted by a not specific fluorescent dye (SYBR Green) that intercalates in double-strand DNA;
- NanoString nCounter (NanoString nCounter Technologies) directly uses total RNA (10-100 ng) in a hybridization reaction with antisense mRNA colour-coded probes. After removal of the excess of probes, tagged mRNA molecules are counted by a Digital Analyzer (Nanostring Technologies), composed of an epi-fluorescent microscope and a CCD camera that collect image data and convert them to digital signals.

Samples collected as described in paragraph 2.3.3 were processed either for extraction of total RNA or used directly for Nanostring nCounter analysis. In the former case, total RNA was then used for cDNA synthesis.

2.4.1 RNA extraction and cDNA synthesis.

50 or 100 µl of lysate (corresponding to ~ 50 or 100 larvae) were mixed with an equal volume of lysis buffer (RNaqueous Micro Kit, Ambion) and total RNA was extracted and treated with DNase I using RNaqueous Micro kit (Ambion) accordingly to manufacturer's instructions. Concentration and quality of total RNA was measured with NanoDrop 2000c Spectrophotometer (Termo Scientific) or 2100 Bioanalyzer Instruments (Agilent Technologies).

qPCR uses cDNA as template, thus 15 µl of total RNA (out of 20 µl) of total RNA corresponding to the equivalent of 37-75 larvae was used to synthesize a first strand cDNA using iScript cDNA synthesis kit (Biorad). Reactions were set up as follows: 4 µl of iScript Reaction mix (5X), 15 µl of total RNA, 1 µl of iScript Reverse Transcriptase. Reactions were incubated in a BioRad thermal cycler using the following conditions: 25 °C for 5 min., 42 °C for 30 min, 85 °C for 5 min. cDNA was diluted to the concentration equivalent of 1 or 2 larvae/µl using DEPC H_2O and stored at -20° C.

2.4.2 Quantitative Polymerase Chain Reaction (qPCR).

qPCR reactions were set up in quadruplicate (for each combination of cDNA and primers) in 384-wells plates (Applied Byosystems) as follows: 0.5 µl of cDNA, 1.1 µl of forward and reverse primers mix (2,5 pmol/µl each), 5 µl of 2X Power SYBR Green PCR Master Mix (Applied Biosystems) and 3 µl of nuclease-free H_2O. Reactions were run in the 7900 HT Fast Real-Time PCR System (Applied Biosystems) with the following thermal cycling parameters in 9600 emulation mode:

- Stage 1: 95° C for 30 sec.;
- Stage 2: 95° C for 10 min.;
- Stage 3: 15 sec. at 95° C and 1 min. at 60° C, 40 cycles
- Stage 4: dissociation step to verify the presence of a single PCR product (15 sec. at 95° C and 1 min. at 60°).

During the reaction fluorescent signal is measured in each well because of the presence of the SYBR Green, which binds double-stranded DNA. Thereby the amount of detected fluorescent is related to the amount of amplified PCR products. The higher is initial number of molecules of cDNA target in a sample, the faster the fluorescence increases during the PCR cycles. The cycle in which fluorescence signal is detected above the background is termed cycle of threshold (Ct) and is chosen to fall within the exponential phase of the PCR reaction where theoretically doubling of PCR products accumulates at each cycle (the reaction is at its maximum of efficiency). Thus, Ct values of different reactions are proportional to initial input of cDNA molecules and can be compared in different samples.

For sea urchin embryos and larvae, *ubiquitin* is used as internal standard because its levels of expression have been measured and shown to be constant at least during the first 72 hours of development (Nemer et al., 1991). Moreover *ubiquitin* is used as positive control to assess the quality of each qPCR experiment, while, to assess potential contaminations, reactions characterized just by the presence of primers and H_2O are used as negative controls.

In qPCR experiments performed in this study, to verify technical reproducibility, the Cts of four replicas were averaged and standard deviation was calculated. In presence of standard deviation higher than 1, experimental points were discarded. Raw data were used to calculate the absolute number of transcripts of a specific gene expressed in one larva as follows. Averaged Ct for a specific gene was normalized to the averaged Ct of ubiquitin (ΔCT= Ct gene – Ct *ubiquitin*); the cycles difference ΔCT was converted in folds of change ($1{,}92^{\Delta CT}$) where 1,92 stands for the efficiency of amplification of primers (Materna and Oliveri, 2008). The absolute number of transcripts was calculated using the following formula: nr of transcripts = $50000 \cdot 1{,}92^{\Delta CT}$; where 50000 is the number of ubiquitin domain copies per embryo (Materna et al., 2010).

2.4.3 Nanostring nCounter.

Nanostring nCounter utilizes a 3-step procedure to counts number of transcripts of hundreds of different genes in a single RNA sample. The first step consists in a hybridization reaction. Two 50-base probes are designed per each target transcript: a reporter probe that carries an unique fluorescent barcode for detection; and a capture probe characterized by the presence of a biotin molecule used to immobilize the tagged transcript to a streptavidin-coated well. The reaction of hybridization occurs in PCR

tubes at 65° C for at least 12 hours. The second step is carried out by a liquid handling robot (Prep Station, Nanostring Technologies) that removes the excess of probes and aligned electrophoretically the complexes probe-transcript in a 12-lanes cartridge (Nanostring Technologies) where each lane is streptavidin-coated. Cartridges are placed in the Digital Analyzer that counts the different colour barcodes and tabulates them for each target transcript. Thus, the data output is a comma- separated text (.csv) file that lists gene names and number of times that their transcripts have been counted in one sample. The probe set used in this project included 53 genes and was synthesized by NanoString Technology (see appendix A, table 4, for a full list of genes, accession numbers and probe sequence). Probes were designed using sequences present in the sea urchin transcriptome database (Tu et al., 2012), in Sp Genome 3.1 database (http://www.spbase.org/SpBase; Cameron et al., 2009) or using probe sequences already designed in other code-sets (Davidson laboratory, see Appendix A table 4 for details). Hybridization reactions were set up in the following steps:

- Preparation of a master mix for 12 reactions: 130 µl of hybridization buffer (NanoString Technologies) were added to a tube of Reporter Probes (NanoString Technologies);
- 10 or 20 µl of master mix were added to 12 empty PCR tubes;
- 46-100 ng of total RNA (maximum volume 5 µl) or 5-7 µl of lysate sample were added to each tube and if necessary DEPC H_2O was added to bring the volume of each reaction to 25 or 27.5 µl;
- 2.5 or 5 µl of Capture Probe (NanoString Technology) were added to each tube.

Hybridizations were performed in the termocycler TC-4000 (Techne) at 65° C for 12-30 hours. Prep Station and Digital analyzer were used according manufacturer's instructions. Prep Station was programmed in high sensitive mode and Digital Analyzer was set up at 600 fields of view (FOV, discrete units that indicates the number of readings for each lane).

To assess the efficiency of hybridization, code-sets contain probes used as positive and negative controls. Positive controls are probes designed against 6 ERCC transcripts sequences (External RNA Consortium) transcribed *in-vitro* and mixed in the Reporter CodeSet at a determined concentration during manufacturing. Negative controls are 8 probes that have not target transcripts.

Data were analysed using the software nSolverAnaysisSoftware 1.1 (NanoString Technologies). The software performs a quality control analysis that provides information about:

- The FOV counted by the Digital analyzer (if less than 75% of the FOV attempted are successfully imaged, data are discarded).
- The probe binding density to determine if data collection is compromised due to image saturation (binding density is set up between 0.05 and 2.25 as default).
- Linearity of the counts of the positive controls (if regression value is less than 0.9, data are discarded).
- Limit of detection of the positive controls (if the counts of 0.5fM positive control are less than the following value: 2 ·standard deviations of negative controls, data are discarded).

To eliminate variability unrelated to the sample, the software uses the positive controls to normalize data. For each sample the sum of counts and the mean of counts of positive controls are calculated and used to have a normalization factor (geometric mean/sum of counts). All the counts of a sample are multiplied by the normalization factor.

In Nanostring nCounter experiments performed in this study, following the positive normalization, all the counts were adjusted relative to the counts of ubiquitin, used as reference gene, to correct differences in sample input between assays. For experiments showed in chapter 4, this normalization was calculated using the software that calculates the geometric mean of the reference gene; whereas, for experiments showed in chapter 4, the mean of the counts of ubiquitin was calculated to have a normalization factor (mean of counts/counts of ubiquitin from a single time-point) and all the counts of a sample were multiplied by the normalization factor.

The negative controls were used to estimate the background of the experiment. For each sample, the average and standard deviations of all the negative control counts were calculated to have a threshold value as follow: average of negative control counts + 2· standard deviation of negative control counts.

2.4.4 *In-vivo* GFP image analysis and luciferase assay.

Embryos and larvae injected with GFP reporter constructs were analysed using a Carl Zeiss Axio Image 1 fluorescent microscope with AxioVision software. Images were processed using Adobe Photoshop CS5.1 software.

Bioluminescence assays were performed for larvae injected with luciferase constructs and uninjected larvae (negative control). Larvae were plated in 96-multiwell plates in number of 2, 5 or 10 per well. In all the experiments, each well contained 200µl FASW and 0.5 mM of luciferin (250 mM, Promega). In addition, in order to improve permeability of embryos to luciferin, 0.004% DMSO (100%, Sigma) was diluted in FASW. Luciferase assays were performed using a Packard TopCount NXT Microplate Scintillation & Luminescence Counter (kindly provided by Prof. David Whitmore at UCL) at the temperature of 15 or 18°C in constant dark conditions over 24, 48 or 72 hours. Each well was counted for emission of bioluminescence at intervals of 30 or 60 min. Data were imported into Microsoft Excel by using a macro software gently offered by Whitmore lab.

2.4.5 Whole Mount *in-situ* Hybridization (WMISH).

To detect the spatial expression pattern of specific genes, *in-situ* hybridization techniques were employed on whole fixed sea urchin embryos and larvae. In this paragraph reports procedures to synthesize an antisense RNA probe and protocols of *in-situ* hybridization.

Amplification of a DNA template for RNA probe synthesis.

The first step to synthesize an antisense RNA probe consists in amplify by PCR the desired DNA fragment, previously cloned, using primers that sit outside both RNA polymerase promoter sites, pSPORT Forward and pSPORT Reverse (Appendix A). Each PCR reaction was set up using the *Taq* Invitrogen DNA polymerase kit (Invitrogen) in a final volume of 50µl following the manufacturers instructions and using 1ng of DNA template. Amplification was carried out using the following cycle conditions: initial denaturation at 95 °C for 5 minutes, 30 amplification cycles as follows: denaturation at 95 °C for 30 seconds, annealing at 55°C for 30 seconds, elongation at 72°C for X minutes (depending by the length of the fragment) and a final elongation step of 72°C for 5 minutes. Electrophoretic gel analysis was performed to check the amplification of the PCR product and then the template was purified using NucleoSpin® Extract II kit (Macherey-Nagel) as described previously.

RNA probe synthesis for WMISH.

Probe templates were used to synthesize antisense RNA probes labeled with Dinitrophenol (DNP) or Digoxigenin (DIG) or Fluorescein (Fluo) Transcription reactions were carried out in a total volume of 20 µl using either SP6 RNA Polymerase (Roche) or T7 RNA Polymerase (Roche) depending on the orientation of the DNA fragment in the clone.

The synthesis of DNP labeled probes was carried out in a two-step process. First, a non-labeled probe (cold probed) was synthesized as follows: 1 µg of DNA template, 1mM NTP mix (2.5mM) (Promega), 1X transcription buffer (10X), 0.2 U of T7 or Sp6 RNA polymerase (2 Units/µl), 0.1 U of RNase Inhibitor (2 Unit/µl), nuclease-free H_2O up to 20 µl. All transcription reactions were incubated 2 hours at 37 °C. To stop the reaction and remove the template DNA, 1µl of DNAseI/RNase-free (1Unit/µl; Roche) was added to the reaction and incubated at 37 °C for 15 minutes. The reaction was cleaned from unincorporated nucleotides by precipitation using 10µl of 7.5 M LiCl (Ambion) at −20°C overnight. Afterwards samples were centrifuged for 10 min at maximum speed in a micro-centrifuge (Eppendorf, model 5424) and washed twice with 1ml 80% ethanol (the samples were centrifuged at maximum speed after each wash). Ethanol was removed from tubes as much as possible and pellets were air dried until all residual ethanol evaporated. Probes were dissolved in 30 µl of DEPC H_2O and their concentrations were determined using NanoDrop 2000c Spectrophotometer. Cold probes were stored at -80°C. The second step includes the DNP labeling reaction using the Label It DNP labeling Kit (Mirus Corporation). Reactions were carried out in a total volume of 50µl using the following reagents: 1 µg of “cold” RNA probe, 5 µl Mirus Labelling Buffer A (10X), 5 µl Label It DNP reagent and DEPC H_2O up to 50 µl. The reaction was incubated for 2 hours at 37°C. To remove any unincorporated DNP, the RNA probes were purified using twice a Mini Quick Spin RNA Column G50 Sephadex (Roche), following manufacturer’s instructions. Probes were diluted at the concentration of 50ng/µl and stored at -80°C.

DIG or Fluo labeled probes were synthesized as follows: 0,5 µg of template DNA, 2 µl DIG or Fluo RNA labeling mix (10x), 2 µl transcription buffer (10X), 1.6 µl of T7 or Sp6 RNA polymerase (2 Units/µl), 0.4 µl of RNase Inhibitor (1 Unit/µl), Nuclease-free H_2O up to 20 µl. The transcription reaction was incubated for 2-7 hours at 37°C. After incubation with 1µl of DNAse/RNAse free (1Unit/µl; Roche) for 15 minutes at 37°C, to precipitate the RNA probe, 30 µl of DEPC H_2O and 10 µl of 7.5 M LiCl were added to

the reaction and incubated at −20°C overnight. Washing and resuspension of the probe were performed as previously described. Probes were diluted to 50ng/µl and stored at -80 °C. Probe concentrations were determined using NanoDrop® 2000c Spectrophotometer, while successful synthesis and absence of degradation of RNA probes was confirmed by using gel electrophoresis.

Fixation of embryos and larvae for WMISH.

To fix for WMISH, sea urchin embryos and larvae were collected at the right developmental stage and left to settle down by addition of a few microliter of, respectively, fixative solution II (4% paraformaldehyde (Electron Microscopy Sciences), 32.5% FASW, 32.5 mM MOPS at pH 7, 162.5 mM NaCl) and fixative solution I (4% paraformaldehyde, 0.1 M MOPS pH 7, 0.5 M NaCl). Samples were washed in fixative solution three times and incubated overnight at 4°C. The following day, they were washed 5 times in MOPS buffer (0.1 M MOPS pH7, 0.5M NaCl, 0.1 % Tween-20 in DEPC-treated H_2O) and stored in 80 % ethanol at −20 °C indefinitely.

WMISH in sea urchin embryos and larvae.

Two WMISH protocols were used in this project: one adopted from Minokawa *et al.* (2004) was used to perform double fluorescent *in-situ*, the second adopted from Croce *et al.* (2010) for single enzymatic *in-situ.*

Double fluorescent *in-situ* hybridization*.*

Fixed embryos and larvae were rehydrated with gradual washes of ethanol (50% and 30%) and washed four times with 1ml MOPS buffer. After that, samples were, first, pre-hybridized in 500 µl of fresh hybridization buffer (70% formamide, 0.1M MOPS pH7, 0.5M NaCl, 0.1% Tween-20, 1mg/ml BSA) for 3 hours at 50°C and then hybridized for one week at 50°C in fresh hybridization buffer containing 0.1 ng/µl of two probes labelled with DIG, Fluo or DNP. After a week of hybridization, samples were washed five times with 1ml MOPS buffer at room temperature and then incubated in 500 µl of hybridization buffer or 3 hours at 50 °C to remove excess of probe. Samples were washed a further three times with 1ml MOPS buffer at room temperature and, first, incubated in 500 µl of Perkin Elmer Blocking reagent (0.5% PEBR in MOPS buffer) for 30 minutes at room temperature and then in an antibody solution (1:1000 dilution of anti-DIG or anti-Fluo POD Fab fragments (Roche) in 500 µl of Perkin Elmer Blocking reagent) over night at 4°C. The excess of antibody was removed by washing the

samples five times with 1ml MOPS buffer at room temperature. For probe detection, samples were washed with a diluent amplification solution (TBS containing 0.0015 % H_2O_2) and stained with fresh amplification diluent (PerkinElmer) containing 1:400 dilution of CY5 or CY3 (PerkinElmer) for 15min. Stains were developed in the dark, at room temperature and stopped by washing samples five times in MOPS buffer. To eliminate the horseradish peroxidase activity, samples were washed once in 1.5 ml of 1% H_2O_2 in MOPS and then washed five times with 1ml MOPS. Samples were then blocked and incubated overnight, using a second antibody (anti-DNP POD, antibody (Perkin Elmer)) as described above for the first antibody. After antibody incubation, samples were washed five times with 1 ml MOPS, and then washed with the amplification diluent for 15 minutes at room temperature. Samples were stained, as mentioned above, using CY3 or CY5 (PerkinElmer). Higher expressing genes or the DIG probes were used in combination with CY5, whereas lowest expressing genes or DNP probes with CY3. This combination was used to better discriminate CY5 signal that tends to have more background than CY3. Moreover, CY5 was used as first dye in order to be washed more times. Finally, samples were washed four times in MOPS buffer and stored at 4°C.

DAPI (4,6-diamidino-2-phenylindole) staining was performed to visualize the nuclei of cells upon imaging. 1µl of 200µg/ml DAPI (Sigma) was added to the 1 ml MOPS buffer containing samples.

Single enzymatic *in-situ* hybridization.

Fixed larvae and embryos were rehydrated with gradual washes of ethanol (50% and 30%) and washed five times in TBST (0.2M Tris pH 7.5, 0.15M NaCl, 0.1% Tween-20). Larvae were, first, transferred to 1:1 ratio of TBST:hybridization buffer (50%deionizedformamide,10%polyetheleneglycol (PEG; Sigma), 0.6 M NaCl, 0.02M Tris pH7.5, 0.5 mg/ml yeast tRNA, 1X Denhardts solution, 0.1%Tween-20, 5mM EDTA) and then pre-hybridised in 500 µl of fresh hybridization buffer for 1 hour at 60°C. Samples were then hybridized overnight at 60°C in hybridization buffer containing a labeled RNA probe at the concentration of 0.05 ng/µl. After hybridization, samples were washed in a 1:1 ratio of TBST:hybridization buffer at 60°C, then washed two times in TBST at 60°C. This was followed by two washes in 1X SSC at 60 °C and then a single wash in 0.1X SSC at 60 °C. Samples were, then, washed twice in TBST at room temperature, and probe detection started with incubation of samples for 30 minutes in blocking buffer (TBST, 5% sheep serum) at room temperature and with an antibody

solution (1:2000 dilution of Anti-Digoxigenin-AP, Fab fragments (Roche) or Anti Fluorescein-AP, Fab fragments (Roche) in blocking buffer) for 1 hour at room temperature. To remove excess of antibody, samples were washed four times with TBST buffer at room temperature and then washed twice with alkaline phosphatase buffer (0.1M Tris pH9.5, 50mM $MgCl_2$, 0.1M NaCl, 1mM Levamisole, 0.1% Tween-20) for 30 minutes at room temperature. Samples were stained in 500 µl of staining buffer (alkaline phosphatase Buffer, 10% dimethylformamide, 0.8 µl of NBT/BCIP stock solution (Roche)). Stains were developed for different amounts of time in the dark at room temperature or 4°C and monitored under the microscope. The staining reaction was stopped by washing three times in TBST buffer containing 0.05M EDTA and transferred initially to 25% glycerol and then 50% glycerol. Samples were stored at 4°C.

2.4.6 Differential Interference Contrast (DIC), epi-fluorescent and confocal microscopy.

Bright-field and DIC images were taken with a Zeiss Axio Imager M1 coupled to a Zeiss Axio Cam HRc using 20X or 40X magnification. For fluorescent stained embryos, each embryo was imaged multiple times using different channels (Cy3, Cy5 and DAPI) and DIC. For confocal microscopy, images were collected using an inverted Zeiss confocal laser scanning microscope LSM510 and a Leica SP8 available at UCL imaging facility. Optical sections were analysed using ImageJ software package (NIH).

2.4.7 Images processing, diagrams and graphs.

Adobe Photoshop CS5 was used for images processing and merges all pictures of the different fluorescent channels. Figures were made using Adobe Illustrator CS5 or Adobe Photoshop CS5; schematic representations were drawn using Adobe Illustrator CS5 or Microsoft Power Point 2008; graphs showing temporal expression data were made by using Microsoft Excel 2008.

2.4.8 Statistical analysis.

Statistical tools as ANOVA and cosinor method were performed on temporal expression data to statistically validate the presence of a 24hrs rhythmic oscillation. One-way ANOVA was used to assess if the variance measured between time points within a temporal series was significantly different from the variance of time points between independent experiments. If ANOVA test was significant, post hoc tests (Fisher's Least

Significant Difference, Tukey's Honestly Significant Difference and Scheffe's) were applied to the analysed data in order to estimate which time points were significantly different. One-way ANOVA and post hoc analysis were performed using the macro for Microsoft Excel QI Macro 2014 (http://www.qimacros.com/).

Cosinor analysis is based on linear least-squares regression analysis to define the best-fitting cosine curve out of time series data. The model uses a cosine function: $y = M + A \cos(\omega t + \Phi)$, where M is the mesor (the mean level of the adjusted curve), A is the amplitude (distance between the mesor and the maximum or minimum value of the adjusted curve), Φ is the acrophase (time of the maximum value of the adjusted curve), ω is a fixed frequency that in the case of circadian rhythmicity is 24h.

The method uses F statistic to imply absence of amplitude as null hypothesis and, thereby, absence of 24h rhythmicity. In order to analyse time series data with the cosinor method a script for MATLAB was downloaded from www.mathworks.co.uk/matlabcentral/fileexchange/20329-cosinor-analysis.

Cosinor method was applied for each single batch of temporal data, and the average values of amplitude, mesor and acrophase were compared using Student t test. All statistical tests were considered significant if p-value was lower than 0.05.

Chapter3

The circadian system in sea urchin: a genomic overview.

The first part of this study consisted of compiling a list of candidate genes to be analysed for their potential involvement in the circadian system of the sea urchin. The list can be divided into six categories according to the position (reported in brackets) that a gene may have in such system: canonical clock genes (core clock); genes encoding bHLH-PAS domains (core clock); cryptochromes and photolyases (core clock, input and output pathways); opsins (input pathway); neuropeptides and melatonin pathway (signaling molecules); and a set of genes expressed in the sea urchin larval apical organ, encoding transcription factors linked to neural and photoreceptor differentiation (clock-controlled genes; see paragraph 3.5 for references). For most of the genes, the genome survey was based on reciprocal BLAST methodology using as a query the corresponding *Drosophila* and/or mouse sequences (called reference database, see Materials and Methods for details). Furthermore putative protein domains have been identified in key canaonical clock proteins. Sea urchin genes encoding opsins, neuropeptides and transcription factors of the apical organ were previously described (detailed references in following paragraphs), however only a set of genes for each gene family was included in this project. The reasons for their inclusion, together with their descriptions, are reported in this chapter.

3.1 Identification of core clock genes and characterization of conserved protein domains.

3.1.1 Identification of canonical core clock genes.

In order to understand whether the sea urchin genome encodes for all the components of a canonical animal core clock, we created a reference database that including genes encoding transcription factors, co-regulators of transcription factors, kinases, ubiquitination proteins etc. shown to be involved in insect and vertebrate transcriptional/translational feedback loops responsible for circadian oscillation. Particularly, our analysis was focused on genes encoding transcription factors and co-regulators that are potential key elements necessary to understand how the regulatory network of clock genes is assembled in sea urchin. The genome survey identified one sea urchin sequence for each canonical clock gene, except for *period* (Table 3.1).

Table 3.1 List of sea urchin genes homologous to canonical clock genes. The table reports the blast result of canonical clock genes from insects and/or vertebrates, identified in the sea urchin genome version 3.1; the type of encoded protein, the accession number for the sea urchin; accession number for the transcriptome database and the best BLAST X against the NR database, hit when sea urchin clock genes are used as queries. If necessary, sea urchin circadian clock genes were renamed accordingly to scientific literature. BLAST X was performed in NCBI against the non-redundant protein database. Genes indicated by (*) are derived from the phylogenetic analysis performed in Rubin et al. (2006); Reitzel et al. (2013). This analysis was performed by the student Matthias Turner.

Clock genes	**Gene name in *Sp***	**Gene type**	**Gene Model(s)**	**Transcriptome**	**Best Blast X (E-value, common name)**
clock	*clock*	b-HLH-PAS	SPU_017407, SPU_017408	WHL22.335679	*Aplysia californica* ($2e^{100}$, sea hare) *
bmal	*bmal*	b-HLH-PAS	SPU_020284	WHL22.253511	*Cricetulus griseus* ($6e^{-177}$, hamster)*
timeless	*tim*	Arm/ HEAT	SPU_028411	WHL22.140308	*Ixodes scapularis* ($7e^{-27}$, deer tick)*
timeout	*timeout*	Armadillo repeats	SPU_006230, SPU_025518	WHL22.737890	*Pteropus alecto* (0.0, black fruit bat)*
rev-erb	*rev-erb*	Nuclear receptor	SPU_017492	WHL22.595563	*Aplysia californica* ($3e^{-68}$, sea hare)
rorα	*rorα*	Nuclear receptor	SPU_022678	WHL22.499606	*Heterocephalus glaber (4e-12, naked mole-rat)*
hlf,tef, dbp, pdp1	*hlf*	b-zip	SPU_004414	WHL22.306206	*Loxodonta Africana ($7e^{-57}$, African bush elephant)**
nfil3, vrille	*nfiL3*	b-zip	SPU_024307	WHL22.733532	*Xiphophorus maculatus ($7e^{-14}$, southern platy fish)**

Continue table 3.1

cwo	*hey*	b-HLH	SPU_009465	WHL22.578435	*Saccoglossus kowalevski (3e^{-100})*
btrcp	*slimb*	F-box; WD-repeats	SPU_026972, SPU_024120	WHL22.78830	*Saccoglossus kowalevskii (0.0)*
jetlag	*fbxl15*	F-box; LR repeats	SPU_020231	WHL22.314548	*Branchiostoma floridae (5e^{-59})*
cbp	*cbp*	Creb binding	SPU_019024	WHL22.581111	*Pelodiscus sinensis (0.0, softshell turtle)**
ck1d	*ck1d*	Kinase_CK1	SPU_001500	WHL22.557027	*Saccoglossus kowaleskii (0.0)*
shaggy	*gsk3b*	serine/ threonine kinase	SPU_009263, SPU_012832, SPU_027914	WHL22.70457	*Saccoglossus kowaleskii (0.0)*
period	-	PAS	-	-	-

The best blast hit of the sea urchin clock genes versus the non-redundant (NR) protein database identifies mostly deuterostome genes, as expected for a non-vertebrate deuterostome; while *sp_clock*, *sp_tim and sp_rev-erb* are more closely related to protostome genes. Sea urchin genome encodes a complete set of transcription factors necessary to drive rhythmic expression in a canonical animal clock: b-HLH transcription factors Sp_Bmal and Sp_Clock; the b-zip transcription factors Sp_Hlf and Sp_Nfil3; the orphan nuclear receptors Sp_Rorα and Sp_Rev-Erb. Interestingly, the sea urchin is the only deuterostome so far investigated that encodes for a homolog of *timeless* (or *tim*). *Tim* and *timeout* are two paralogous genes and it was suggested that they evolved from gene duplication at the base of bilaterians (Rubin et al., 2006; Reitzel et al., 2010). Both genes are present broadly in bilaterians, with *tim* independently lost in nematodes and chordates. *Timeout,* retained in chordates, is involved in the following different functions in *Drosophila* and mouse: maintenance of chromosome integrity, light entrainment of the circadian clock, embryonic development, and regulation of DNA replication (Gotter et al., 2000; Barnes et al. 2003; Benna et al., 2010).

On the other hand, no homolog of *period* (*per*)*,* encoding a PAS domain protein was found in the sea urchin genome. Similarly to cnidarians (Reitzel A.M. et al., 2010), the BLAST search for a homolog of *per* returned as best hit the gene encoding bHLH-PAS domains *arnt*. Genes of the class bHLH-PAS present in the sea urchin genome were

included in this study as genes that might substitute for the lack of *period* function (Table 3.2).

Table 3.2 bHLH-PAS domain genes in the sea urchin genome.

Gene name in Sp	**Gene type**	**Gene Model(s)**	**Transcriptome**	***Best Blast X (E-value, common name)***
arnt	b-HLH-PAS	SPU_000129	-	*Saccoglossus kowaleskii* (0.0)
sim	b-HLH-PAS	SPU_013962	WHL22.424996	*Saccoglossus kowaleskii* (0.0)
ahr	bHLH-PAS	SPU_013788	WHL22.676940	*Xenopous laevis* ($6e^{-116}$)
ncoa	b-HLH-PAS	SPU_021430	WHL22.507984	*Saccoglossus kowaleskii* ($6e^{-66}$)

The sea urchin was used in previous studies to determine the phylogenetic relationships of different clock genes in Metazoa because of its key phylogenetic position as a non-vertebrate deuterostome (Rubin et al., 2006; Reitzel et al., 2013). These studies confirmed the relationships of homology advanced by the BLAST survey (see table 3.1 for details).

3.1.2 Characterization of conserved protein domains and motifs.

Functional domains and motifs of Cycle/Bmal, Clock and Tim have been extensively studied in different organisms to characterize their role in transcriptional regulation, sub-cellular localization and interactions at protein level (Hirayama and Sassone-Corsi *et al.*, 2005, Vodovar et al., 2002). To conduct better evolutionary and comparative studies, putative domains, NLS (nuclear localization signal) and NES (nuclear export signal) motifs were analysed in Sp_Bmal, Sp_Clock and Sp_Tim using, respectively, the database software SMART and NLS/NES predictive software (Fig. 3.1; see Material and methods for details). In addition, potential functional domains, characterized experimentally in mouse and insects, were identified in corresponding sea urchin proteins by using sequence alignment software (see Material and methods for details).

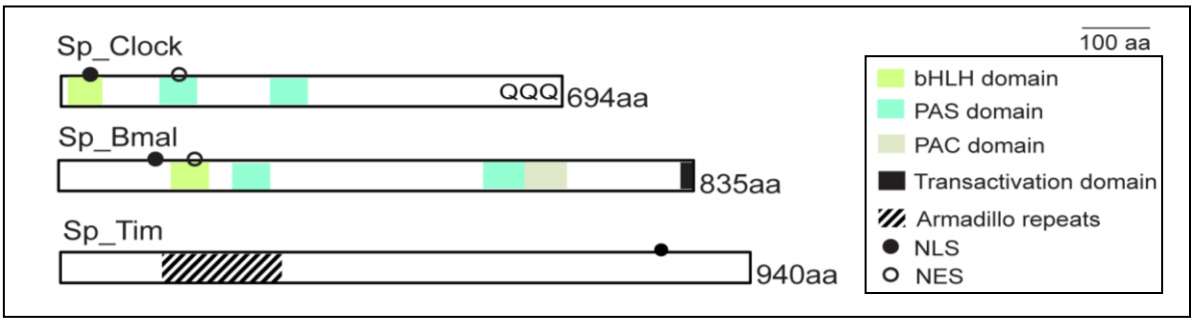

Fig. 3.1 Schematic representation of Sp_Clock, Sp_Bmal and Sp_Tim with identified protein domains and motifs. See legend for domain and motif identity and text for additional details. Position of domains and motifs are reported in Appendix D, table D1 and D2.

As expected Sp_Clock and Sp_Bmal contain b-HLH, PAS (Per Arnt Sim) and PAC domains, which are essential for them to work as heterodimeric transcription factors. Moreover, putative NLS and NES signals were identified at the N-terminal of both proteins as described also in insects and mammals (Chang et al., 2003; Hirayama and Sassoni-Corsi, 2005; Rubin et al., 2006). Both Sp_Clock and Sp_Bmal possess putative transactivation domains at the C-terminus. Sp_Clock is characterized by poly-glutamine stretches (polyQ) similarly to *Drosophila* Clock (Darlington et al., 1998; Allada et al., 1998).

Whereas the C-terminus of Sp_Bmal is conserved with that of mouse and the ant *A. pernyi* (see alignment in appendix D, fig. D1) where a transactivation domain with transcriptional activity was localised experimentally (Takahata et al., 2000; Chang et al. 2003). Based on these observations, Sp_Bmal and Sp_Clock are likely to have a similar function to orthologous proteins already described in other organisms.

The characterization of protein domains of Timeless has been well performed in the insects *Drosophila*, *Antheraea pernyi* and *Bombyx* (Vodovar et al., 2002; Saez and Young, 1996; Ousley et al., 1998; Chang et al., 2003; Iwai et al., 2003). Insect Timeless has two Armadillo (Arm)/HEAT regions, two PER interaction sites, an NLS and a C-terminal cytoplasmatic localization domain (CLD). Interestingly, Sp_Tim shows low sequence similarity when aligned with *Drosophila* Timeless (17.2% of identities, 31.5% of similarities and 39.2% of gaps, alignment in appendix D Fig.3) despite that phylogenetic analysis of the timeless/timeout family in Eumetazoa (Rubin et al., 2006) shows that *sp_tim* is an artholog of the insects timeless (Appendix D Fig.3). Sp_Tim is characterized by a single Armadillo (ARM/HEAT) region at the N-terminal and a putative

NLS at the C-terminal. Interestingly, a conserved CLD domain was not found and the regions corresponding to the Per-binding domains show low levels of conservation The first domain (position 546-608) is not conserved in Sp_Tim; the second domain (position 746-907) show low levels of identity (31 %). This may suggest the absence of Per interaction sites in Sp_Tim likely as example of mechanism of co-evolution along with the loss of a *period* gene.

3.2 The cryptochrome/photolyase family.

3.2.1 Identification of cryptochrome and photolyase genes.

The cryptochrome/photolyase gene family (CPF) was extensively studied in sea urchin for its potential role in photoreception and regulation of the core clock. The most relevant results obtained from this analysis were published in "The cryptochrome/photolyase family in aquatic organisms" (Oliveri et al., 2014), where CPF members from different marine and fresh water organisms (diatoms, sea urchin and annelid, teleost) were characterized to gain new insights into the evolutionary and functional relationships within the CPF family. The genome survey for the identification of CPF genes led to the identification of 5 distinct sequences located in different scaffolds and corresponding to predicted gene models (Table 3.3).

Table 3.3 CPF genes identified in *Strongylocentrotus purpuratus*. The table reports, from left to right: CPF genes in insects and vertebrates, identified putative homologous genes in sea urchin, the accession number for the sea urchin genome version 3.1, the accession number for the transcriptome database and the best BLAST X hit when sea urchin CPF genes are used as queries. BLAST X was performed in NCBI against the non-redundant protein database.

CPF genes	**Gene name in *Sp***	**Gene Model(s)**	**Transcriptome**	**Best Blast X (E-value, common name)**
vertebrate-like cry	*vcry*	SPU_007204	WHL22.732419	*Mustela putorius* (0.0, forest polecat)
drosophila-like cry	*dcry*	SPU_000282	WHL22.613873	*Capitella telata* (0.0, polichaete worm)
6-4 photolyase	*6-4 photolyase*	SPU_019722	WHL22.156161	*Xenopus laevis* (0.0)
cry-dash	*cry-dash*	SPU_009619 SPU_027694	WHL22.91720 WHL22.96269	*Xenopus laevis* (0.0)

Continue Table 3.3.

cpd photolyase	*cpd photolyase*	SPU_001597 SPU_024091 XM_003726260	WHL22.469818 WHL22.469821	*Crassostera gigas* (0.0, pacific oyster)

The 5 sea urchin genes belong to 5 different classes of animal CPF genes as described in the phylogenetic analysis reported in Oliveri et al., 2014 (Fig. 3.2). All the identified genes were renamed accordingly to the scientific literature: *sp_vcry, sp_dcry, sp_6-4 photolyase, sp_cryDASH, sp_CPD photolyase*. From the phylogenetic analysis and Blast result *sp_vcry, sp_6-4 photolyase* and *sp_cryDASH* are evolutionary close to the corresponding vertebrate CPF genes; while, s*p_dcry* and s*p_cpd photolyase* are more closely related to protostome genes. *Sp_vcry* and *sp_dcry* are both homologous, respectively, to a *vertebrate-like cry* (*vcry*) and a *drosopila-like cry* (*dcry*). So far the presence of an ortholog to *dcry* in deuterostomes was reported only in Echinoderms. This is confirmed by the identification of a *dcry* gene in brittle stars and the absence of orthologous in hemichordates (*Saccoglossus kovalevskii*), urochordates (*Ciona intestinalis*) and cephalochordates (*Branchiostoma floridae*) (Oliveri et al., 2014).

Figure 3.2 (Following page). Phylogenetic analysis of CPFs in Metazoans (Oliveri et al., 2014). The ML tree was generated on a final set of 76 sequences using Mega 5.2 (Tamura et al., 2011) with JTT model and gamma distribution. Topological and nodal support was estimated by 1000 bootstrap pseudoreplicates in ML and are indicated in percentage value only if higher than 60. For this analysis, CPF sequences from 13 aquatic animals were used including, sponges and corals (identified by diamond symbols) lophotrocozoan protostomes (identified by triangles) and deuterostomes (identified by circles). Sea urchin is indicated with a green circle.

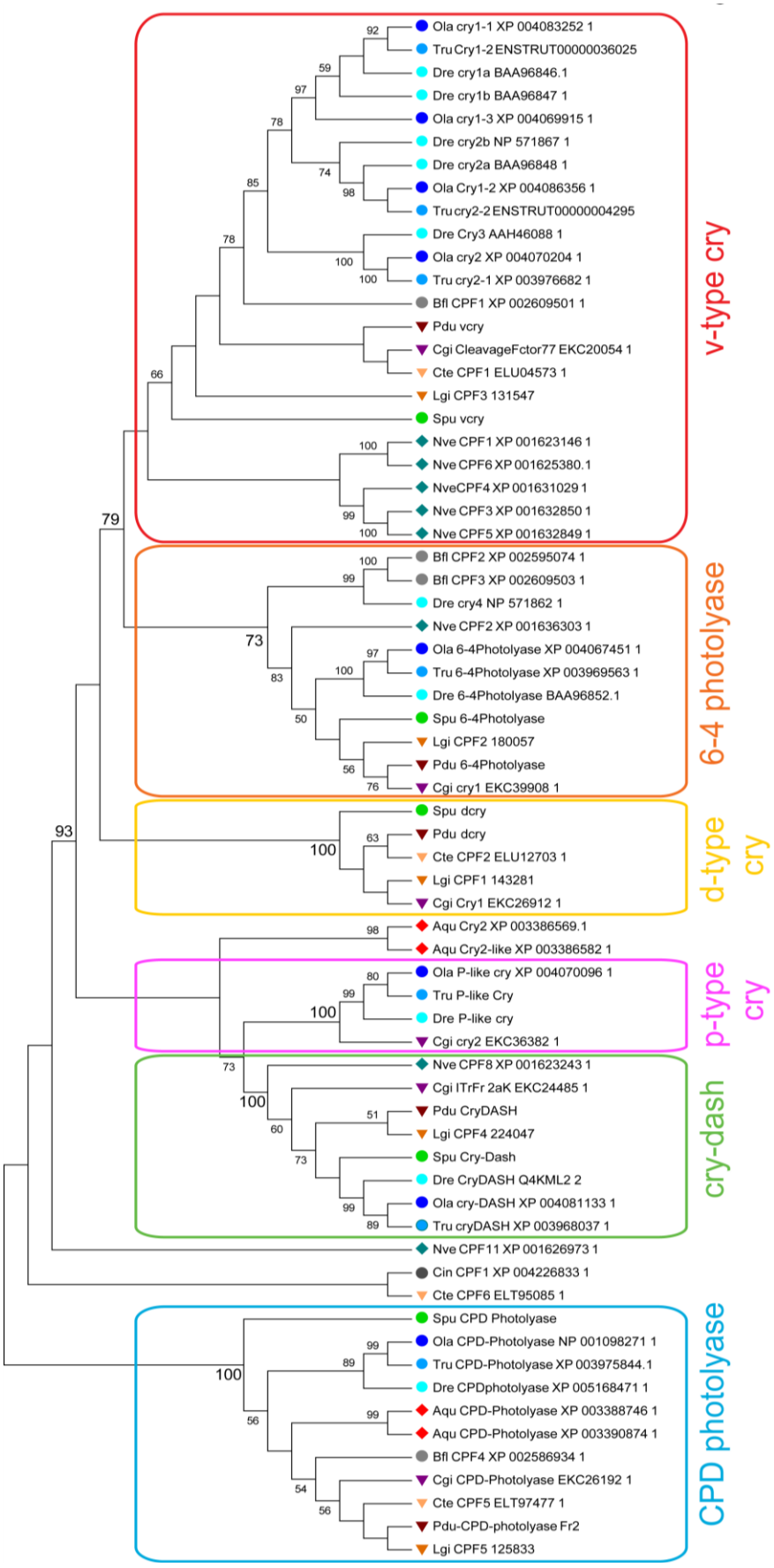
Ola cry1-1 XP 004083252 1
Tru Cry1-2 ENSTRUT00000036025
Dre cry1a BAA96846.1
Dre cry1b BAA96847 1
Ola cry1-3 XP 004069915 1
Dre cry2b NP 571867 1
Dre cry2a BAA96848 1
Ola Cry1-2 XP 004086356 1
Tru cry2-2 ENSTRUT00000004295
Dre Cry3 AAH46088 1
Ola cry2 XP 004070204 1
Tru cry2-1 XP 003976682 1
Bfl CPF1 XP 002609501 1
Pdu vcry
Cgi CleavageFctor77 EKC20054 1
Cte CPF1 ELU04573 1
Lgi CPF3 131547
Spu vcry
Nve CPF1 XP 001623146 1
Nve CPF6 XP 001625380.1
NveCPF4 XP 001631029 1
Nve CPF3 XP 001632850 1
Nve CPF5 XP 001632849 1
v-type cry
Bfl CPF2 XP 002595074 1
Bfl CPF3 XP 002609503 1
Dre cry4 NP 571862 1
Nve CPF2 XP 001636303 1
Ola 6-4Photolyase XP 004067451 1
Tru 6-4Photolyase XP 003969563 1
Dre 6-4Photolyase BAA96852.1
Spu 6-4Photolyase
Lgi CPF2 180057
Pdu 6-4Photolyase
Cgi cry1 EKC39908 1
6-4 photolyase
Spu dcry
Pdu dcry
Cte CPF2 ELU12703 1
Lgi CPF1 143281
Cgi Cry1 EKC26912 1
d-type cry
Aqu Cry2 XP 003386569.1
Aqu Cry2-like XP 003386582 1
Ola P-like cry XP 004070096 1
Tru P-like Cry
Dre P-like cry
Cgi cry2 EKC36382 1
p-type cry
Nve CPF8 XP 001623243 1
Cgi ITrFr 2aK EKC24485 1
Pdu CryDASH
Lgi CPF4 224047
Spu Cry-Dash
Dre CryDASH Q4KML2 2
Ola cry-DASH XP 004081133 1
Tru cryDASH XP 003968037 1
cry-dash
Nve CPF11 XP 001626973 1
Cin CPF1 XP 004226833 1
Cte CPF6 ELT95085 1
Spu CPD Photolyase
Ola CPD-Photolyase NP 001098271 1
Tru CPD-Photolyase XP 003975844.1
Dre CPDphotolyase XP 005168471 1
Aqu CPD-Photolyase XP 003388746 1
Aqu CPD-Photolyase XP 003390874 1
Bfl CPF4 XP 002586934 1
Cgi CPD-Photolyase EKC26192 1
Cte CPF5 ELT97477 1
Pdu-CPD-photolyase Fr2
Lgi CPF5 125833
CPD photolyase

To reveal important characteristics and to determine if the gene predictions were correct, the structure of the CPF genes were studied using gene models (GLEAN3 predictions), transcriptome data available in the SpBase (www.spbase.org/SpBase/) and NCBI (www.ncbi.nlm.nih.gov/), PCR, RACE and cDNA cloning. Correct gene annotation was available for *sp_vcry* and *sp_6-4 photolyase,* whereas other genes had to be manually annotated.

The gene prediction SPU_000282 and the corresponding transcript WHL22.613873 define *sp_dcry*, the models lack of the 3' end and, theoretically, encodes for a truncated protein. To have a complete *sp_dcry* sequence a 3' RACE was performed and the 3' of the transcript was extended to completeness including a 3'UTR of 1114 bp. *Sp_cpd_photolyase* is located in a part of the genome characterized by the presence of several small contings and gaps that are likely to be the cause of an incorrect gene model. A further BLAST analysis and conserved protein domain prediction allowed the manual assembling of *sp_cpd_photolyase* gene that encompasses the SPU_024091 and the SPU_001597 sequences, corresponding to the WHL22.469818 transcript, and the XM_003726260 sequence present in the NCBI database. Further extension of the gene at the 5' end was obtained using the transcript WHL22.469821, which partially overlaps with the XM_003726260 sequence and it is located in the same scaffold of the other SPU gene models of *sp_cpd_photolyase*. The final version of *sp_cpd_photolyase* gene was, then, manually annotated. *Sp_crydash* sequence was initially identified in the SPU_009619 gene model. From the transcriptome data three mRNA isoforms that differ in the length of 5' UTR were identified. However, the BLAST analysis revealed that the SPU_009619 gene model is lacking of the 3' end of the gene and encodes for an incomplete protein. To search in the genomic sequence if the rest of the protein was annotated in another scaffold, further BLASTP analysis was conducted using only the C-term of *Xenopus laevis crydash*; the missing sequence was indeed identified in the SPU_027694 gene model present in a different DNA scaffold. Interestingly, also in this case the relative RNA-seq transcript model (WHL22.96269) shows 4 different isoforms that differ in the 3' UTR length, furthermore an alignment of all the sequences (data not shown) shows the partial overlap of the two SPU gene models. The entire coding sequence, spanning both gene models, has been validated by PCR and a fragment of 1602 bp has been successfully amplified from a cDNA pool. The manual annotation of the sequences in the two scaffolds predicted a total of 14 exons, however the small

contigs and the presence of several repetitive sequences did not allow accomplishing a complete analysis of the gene structure.

3.2.2 Characterization of conserved protein domains.

Characterization of putative functional domains and motifs of the sea urchin CPF proteins was performed as described in paragraph 3.1.

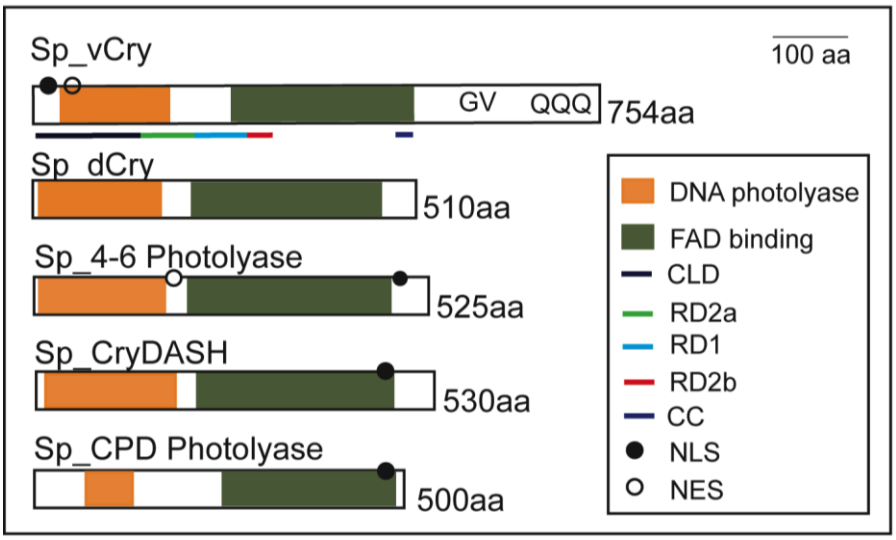

Fig. 3.3 Schematic representation of sea urchin CPF proteins with identified conserved domains and protein motifs. For each protein, FAD (Flavin Adenin Dinucleotide) binding domains and DNA photolyase domains are reported. For Sp_vCry other conserved domains similar to the mouse CRY1 protein were identified (see text for description). CLD, cytoplasmic localization domain; CC, coiled coil region; GV, region rich in GV (Glycine-Valine) repeats; QQQ, region rich in glutamine stretches; RD (see text for description). The exact position of domains and motifs are reported in Appendix D, table D1 and D2.

As expected, all sea urchin CPF proteins contain two conserved photoactive domains: a DNA photolyase domain at the N-terminal and a FAD (Flavin Adenin Dinucleotide) binding domain at the C-terminal end essential for them to work as light sensing proteins.

It is important to notice that clear NLS and NES motifs are both predicted in Sp_vCry and Sp_6-4 Photolyase suggesting a regulated trafficking between cytoplasm and nucleus. In the case of Sp_vCry, this is in agreement with the role that orthologs of this protein have in the circadian clocks of other animals. NLS and NES motifs are absent in Sp_dCry as expected for a protein belonging to the dCry class of CPF and with a potential light-sensing function.

Animal cryptochromes have been extensively studied in several organisms for their important role in the circadian clock (for review see Chaves et al., 2011). To better characterize the two sea urchin cryptochromes, further analyses were performed to identify regions that show similarity with Cry proteins of other organisms. In particular, Sp_dCry was compared to the *Drosophila* Cry and Sp_vCry to both the zebrafish Cry1 and the mammalian mCry1 and mCry2.

A recent structural study showed that the *Drosophila* Cry protein is characterized by recognizable domains (phosphate binding loop, protrusion domain and a C-terminal lid), auxiliary to the DNA photolyase and FAD binding domains (Levy C. et al., 2013; Czarna A. et al., 2013). The sequences corresponding to the phosphates motif and the C-terminal lid are partially conserved in Sp_dCry (43% and 50% of identities respectively, see Appendix D fig. D4). On the contrary low sequence similarities have been found for the sequence corresponding to the protrusion motif (0 % of identities, Appendix D fig. D4). In addition, the C-terminal of Sp_dCry has low sequence similarity with the C-terminal tail of *Drosophila* dCry (17% of identities, Appendix D fig. D4) that is involved in regulation of light response and interaction with TIM (Busza et al., 2004; Dissel et al., 2004; Hemsley et al., 2007). If Sp_dCry works as a circadian photoreceptor, these sequence differences may imply the presence of a different mechanism of light regulation and interaction with other clock proteins.

The other sea urchin cryptochrome, Sp_vCry, belongs to the v-type class or transcriptional regulator of CPF proteins. Three conserved functional regions along with the already described DNA photolyase and FAD binding domains characterize this class of CPF proteins. The three regions, called RD2a, RD1 and RD2b, were initially identified in the zebrafish Cry1 and have been shown to participate in protein-protein interaction. More specifically RD1, RD2b are responsible for the interaction with the Clock:Bmal protein dimer and RD1, RD2a for the regulation of nuclear localization (Hirayama et al., 2003). Sea urchin vCry shows clear conservation at least with the RD1 and RD2b domains (RD2a: 39% of identities, RD1: 68%, RD2b: 56%; Appendix D Figure D5), suggesting a potential interaction with Clock:Bmal dimer and involvement in circadian regulation.

In addition, the mammalian Crys differ in their repression activity (Khan et al., 2012) with mCry1 being a stronger repressor compared to mCry2. This difference in the repressive activity is caused by the presence of 6 critical amino acids in mCry1 identified in a photolyase homology region (PHR), which are not conserved in mCry2. Protein

alignment revealed that Sp_vCry conserves four of the six critical amino acids (Appendix D Fig. D5), indicating a potential repressive capability of Sp_vCry similar to mCry1. A CLD (cytoplasmic localization domain) at the N-terminal and a coiled coil region at the C-terminal were also identified in Sp_vCry (58% and 60% of identities respectively; Appendix D Fig. D5). All these structural similarities with vertebrate CRY proteins strongly suggest a similar function of the Sp_vCry protein as transcriptional repressor. Furthermore, the sea urchin vCry, contrastingly to vertebrate, is characterized by a long C-term tail (~ 200 aa) containing a polyQ domain (Fig. 3.2 and Appendix D Fig.D5), which may be involved in protein-protein interaction and transcriptional regulation.

3.3 The opsin gene family.

Sea urchin opsins, previously described in Raible et al., 2006; Delroisse et al., 2014, were investigated as potential photoreceptors that entrain the clock in sea urchin larvae. Opsins that are expressed during sea urchin larval stage were included in this project by combining quantitative expression data described in Raible et al., 2006 and data derived from sea urchin transcriptome (www.spbase.org:3838/quantdev/). These are *sp_opsin1* member of the ciliary opsin family, *sp_opsin 2,* an echinoderm-specific opsin (D'aniello et al., 2015), *sp_opsin 3.2*, member of the Go rhodopsin lineage and *sp_opsin4,* that groups in the rhabdomeric lineage.

3.4 Signaling molecules: neuropeptides and melatonin.

Signaling molecules, such as neuropeptides and melatonin, are responsible for the interconnection between clock neurons, the coordination of peripheral clocks and regulation of physiological and behavioral outputs (Granados-Fuentes and Herzog, 2013; Helfrich-Forster, 2005; Stehle et al., 2003; Tosches et al., 2014). For this reason, genes encoding neuropeptides were included in this project and the presence of the melatonin pathway was investigated in the sea urchin.

A genome survey for genes encoding neuropeptides was previously described in Rowe and Elphick 2012. The neuropeptide system of the nervous system of the free-living larva has been analysed in terms of spatial expression patterns (spatial expression patterns of *sp_trh* (thyrotropin-realising hormone), *sp_gkmide*, *sp_ppln2* (pedal peptide-like neuropeptide 2) and *sp_p-18* are described in Chapter 4). Based on this expression analysis, neuropeptides that are expressed at considerable level in sea urchin larvae

were included in this project (table 3.4). In addition, the gene *sp_secretogranin7B2L* (SPU_015798) was included in the list as putative clock controlled gene. *Sp_secretogranin7B2L* belongs to a class of genes encoding auxiliary proteins necessary for the secretion of neuropeptides.

Table 3.4 List of genes encoding neuropeptides used in this study.

Gene name in *Sp*	Neuropeptide family	Gene model (SPU/NCBI)	Reference
f-type salmfamide	SALMFamide (Echinodermata only)	SPU_015798	Elphick and Thorndyke 2005
ngfffamide	Neurophysin-containing neuropeptide	SPU_030074	Elphick and Rowe 2009
gnrh (Spnp2 SpGnRHP)	gonadotropin-releasing hormone (GnRH)-like neuropeptide	SPU_019680	Rowe and Elphick 2012
trh (Spnp3 SpTRHLP)	thyrotropin-releasing hormone	SPU_008352	Rowe and Elphick 2012
gkamide (Spnp5 SpANPP)	No sequence similarities with neuropeptides identified in other phyla.	SPU_018666	Rowe and Elphick 2012
ppln-2 (Spnp7)	pedal peptide-like neuropeptide precursor 2	SPU_024381	Rowe and Elphick 2012
p-18 (Spnp18)	No sequence similarities with neuropeptides identified in other phyla.	GI: 115839524	Rowe and Elphick 2012

The melatonin pathway appears to be conserved in all animals so far investigated (Hardeland and Poeggeler, 2003). We analysed the presence of endogenous melatonin in sea urchin by searching for homologous genes that encode key enzymes involved in this pathway, such as tryptophan hydroxylase (TPH*),* Hydroxyindole O-methyltransferase (HIOMT), and aralkylamine N-acetyltransferase (AANAT).

Surprisingly, the sea urchin genome encodes homologs for the TPH (*sp_5ht*; Spu_003725) an aromatic amino acid decarboxylase that produce serotonin, but not two downstream components necessary for melatonin synthesis, the enzymes HIOMT and AANAT, suggesting the absence of endogenous melatonin in sea urchin. This does not exclude the possibility that the sea urchin may use exogenous melatonin through its algal diet. Indeed, the genome survey led to the identification of potential melatonin receptors; however, their function was not investigated in this study.

Serotonin modulates the response of the circadian system to light in *Drosophila* and mouse (Yuan et al., 2006; Ciarleglio et al., 2011) and its production is under circadian regulation because of the rhythmic expression of *tph* (Florence et al., 1996; Green et al., 2004). Thus, we considered in the analysis the gene *sp_5ht* to monitor if serotonin production is rhythmic in sea urchin larvae.

3.5 Hypothetical output genes regulated by sea urchin circadian clock.

In sea urchin embryos and larvae, several transcription factors expressed only in serotonergic neurons of the apical organ are involved in neurogenesis and development of the nervous system (table 3.5 for references). We included in our analysis a set of such genes in order to assay them as potential clock-controlled genes and thus to investigate neurogenesis as a putative clock output.

Gene name in *Sp*	**Synonyms**	**Gene type**	**Gene model**	**Transcriptome**	**References**
atbf1	*znhx3*	TF-Znfn HD	SPU_017348	WHL22.369567	Yaguchi et al., 2013
ac-sc		TF	SPU_028148	WHL22.128311	Burke et al., 2006
brain 1/2/4		TF	SPU_016443	WHL22.40221	Yuh C.H. et al., 2005
collier	*ebf3*	TF	SPU_004702	WHL22.113329	Jackson et al., 2010

Continue table 3.5

ets1/2		TF	SPU_002874	WHL22.238821 WHL22.238821	Rizzo et al., 2006
fez	*z133*	ZNF	SPU_027491	WHL22.580602	Yaguchi et al., 2011
glass 2		TF	SPU_007599	WHL22.204563	Oliveri P.; unpublished
hbn		TF-homeobox	SPU_023177	WHL22.523959 WHL22.523959	Burke et al., 2006
lhx2	*lhx2_1 limc1*	TF_lim HD	SPU_021313 SPU_004021	WHL22.91758	Howard-Ashby et al., 2006
mox		TF-homeobox	SPU_025486	WHL22.737621	Pouska et al., 2007
neuroD	*neuroD1*	TF	SPU_024918	WHL22.694980	Burke et al., 2006
ngn		TF	SPU_007147	WHL22.677570	Burke et al., 2006
otp		TF	SPU_19290	WHL22.286934	Di Bernardo et al., 1995
pea		TF	SPU_014576	WHL22.166439	Rizzo et al., 2006
rx		TF-homeobox	SPU_014289	WHL22.523971	Burke et al., 2006
soxC		TF- HMG	SPU_002603	WHL22.622787	Howard-Ashby et al., 2006
z167	*glass*	ZNF	SPU_015362	WHL22.171389	Poustka et al., 2007
z60	*egr*	ZNF	SPU_015358	WHL22.280477	Materna S.C. et al., 2006
znhb	*z81, smadip*	TF	SPU_022242	WHL22.553144	Yaguchi et al., 2011

Table 3.5 List of genes encoding transcription factors expressed in serotonergic neurons of the apical organ in sea urchin embryos and larvae investigated as putative clock-controlled. The table reports, from left to right, gene names in *S. purpuratus*; synonyms, type of encoded transcription factor; the accession number for the sea urchin genome version 3.1, accession number for the transcriptome database and references where genes have been described. Modified from Avi Lerner thesis.

3.6 Summary.

The genome survey and the characterization of protein domains performed for canonical clock genes give an indication of the composition of the core clock in the sea urchin.

The set of transcription factors that drive rhythmic expression of clock genes is conserved in the sea urchin; particularly the sequences of Sp_Bmal and Sp_Clock show a high degree of conservation with their corresponding orthologs, suggesting that they may have a similar function in the core clock of the sea urchin.

Unlike in insects and vertebrates, there is no *period* gene in the sea urchin. The loss of a *period* gene implies that the negative part of the canonical feedback loop diverges from what is observed in other model organisms. The negative loop may be controlled by either Sp_vCry and/or Sp_Tim, or have a different composition with the involvement of a different PAS domain protein. For this reason sea urchin genes encoding PAS domains have been analysed in this study.

Sp_vCry shows structural similarities with vertebrate Cry proteins suggesting a similar role as transcriptional co-repressor. The long C-terminal, characterized by a polyQ domain, may indicate the acquisition of new functions in protein interactions and possibly in transcriptional regulation.

Interestingly, the sea urchin genome encodes homologs of *tim* and *dcry* suggesting the presence of a mechanism of circadian photoreception similar to that which has been observed in insects.

Sp_dCry has all structural characteristics of a light-sensing cryptochrome and might work as a circadian photoreceptor, though its C-terminal diverges from the *Drosophila* Cry where sites of regulation to light and interaction with dTim have been mapped. On the other side, the sequence differences observed between Sp_Tim and dTim may suggest functional divergence for Sp_Tim with respect to the insect ones.

The second part of this study consisted in understanding which genes, described in this chapter, are under circadian transcriptional control by analyzing their daily transcripts levels and assessing the presence of 24 hours rhythmicity.

Chapter 4

Rhythmic and spatial expression patterns of putative clock and clock-controlled genes.

Circadian rhythmicity has never been described in the sea urchin at any level of analysis from molecular to behavioural. An initial question to be addressed is: when does the circadian clock start to oscillate in the ontogeny of the sea urchin and which are the genes that drive such rhythmicity?

Any investigation of the development of circadian rhythmicity must take into account at least three aspects. The first is the establishment of an intrinsic rhythm driven by core clock genes. The second regards the formation of input pathways linked to the development of specialized cells, able to perceive information from the environment. The third is the maturation of output pathways that generate rhythmicity in physiological and behavioural processes.

Previous experiments carried out in the Oliveri's laboratory showed that many gene orthologues of core clock genes are maternally transcribed and expressed during embryonic development of the sea urchin, however, none of them exhibit clearly 24 hour rhythmic changes in mRNA levels in a light-dark cycle (data not shown). For this reason my work was focused on analyzing the presence of a circadian system in sea urchin larvae. The sea urchin larva is a free-living self-sustaining organism with a fully differentiated nervous system, and it is likely that it possess all the molecular and cellular components to exhibit circadian activity and, therefore, to interact actively with the marine environment. To this purpose, the following aspects were investigated:

- The gene expression at different times of day to investigate the presence of circadian rhythmicity at the molecular level and to identify genes involved hypothetically in the core clock, light input and output pathways (genes described in the previous chapter).
- The spatial expression patterns of putative core clock genes (*sp_bmal*, *sp_clock*, *sp_vcry*, *sp_tim*, *sp_hlf*), genes potentially involved in photoreception (*sp_dcry*, *sp_opsin3.2*) and genes encoding neuropeptides in embryos and larvae to analyse the cellular distribution of the circadian system.

4.1 Rhythmic expression of genes in sea urchin larvae.

In order to investigate the presence of circadian rhythmicity in sea urchin larva at mRNA level, profiles of expression of putative clock and clock-controlled genes (described in chapter 3) were measured at the larval stage 1 week post fertilization (wpf) using nCounter Nanostring technology (see Materials and Methods for details).

Embryos were entrained to LD cycles (12 hours light, 12 hours dark with zeitgeber time 0 (ZT0) at 7am and ZT12 at 7pm) for 6 days. The day before the sampling, cultures were split in two fractions: one exposed to the same LD cycles, the second moved to constant dark (DD, free running condition). Larvae were collected every four hours over 36 hours for the LD conditions or over 44 hours for the DD conditions and processed for RNA extraction (Fig. 4.1). Experiments were performed in two independent batches. The two cultures were obtained at the same time and treated in the same way, and levels of expression where quantified using Nanostring nCounter technology (see Methods, paragraph 2.4.3).

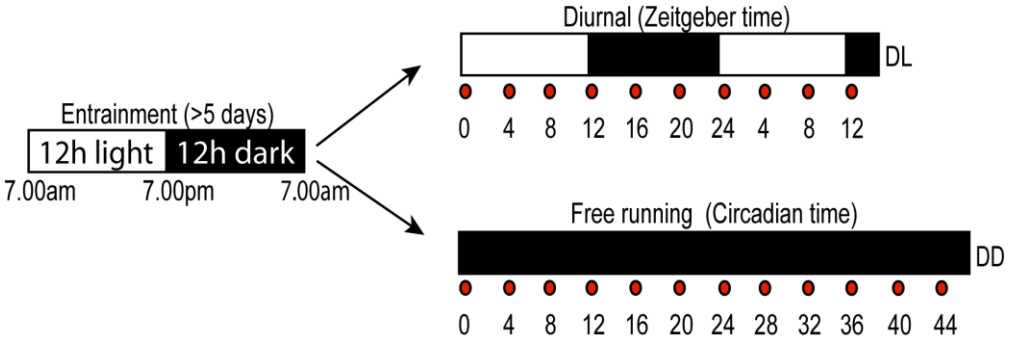

Fig. 4.1 Schematic representation that describes how the sampling of sea urchin larvae was organized. After at least 5 days of entrainment in 12h/12h light/dark cycles larvae from the same culture were split in two conditions, light/dark (LD or zeitgeber time) and free running (DD or circadian time), and collected every four hours (red dots indicate the time of sampling).

The results of this analysis are presented in Fig. 4.2 and 4.3 as numbers of normalised counts/100 ng of RNA measured at different ZT. For each gene, two main graphs illustrate the profiles of expression detected in the two independent batches (F1 and F2) exposed to LD (e.g. graph A for *sp_vcry*) and DD (e.g. graph B for *sp_vcry*) conditions. ANOVA and cosinor methods were used to evaluate statistical significance of the detected time series (see Methods). ANOVA analysis was performed to measure variance between maximum and minimum points of expression. Whereas, the cosinor

analysis was used to adjust a cosine curve to the measured 24h time series assuming that a rhythm is sinusoidal in shape. The results of cosinor analysis are reported for each independent batch (e.g. for *sp_vcry,* graphs AI-AII describe samples in LD; graph BI-BIV describe samples in DD) and a rhythm was considered significant if p-values< 0.05 were observed in the two batches, for at least the first 24h in DD. A significant fit is described with values of amplitude, mesor and acrophase (table 4.1, see Methods paragraph 2.4.8). From these results two genes, *sp_vcry* and *sp_tim,* show circadian expression, indicating the presence of circadian rhythmicity in sea urchin larvae (fig. 4.2 A, B, C, D). They are characterized by 24h oscillatory profiles both in LD and DD conditions. *Sp_hlf*, *sp_opsin3.2* and the other components of the CPF family, show an oscillatory cycle only in presence of light, whereas they are arrhythmic in free running conditions (fig. 4.2 E, F, G, H, J, I; fig. 4.4 A, B). On the contrary, all other analysed genes (appendix D, Fig. D6) did not show any oscillatory expression profile in either condition, suggesting their exclusion from the list of clock-controlled genes. This does not exclude the possibility that some of them such *sp_bmal* and *sp_clock* (discussed below) as well as genes involved in post-translational regulation of the core clock, as *sp_ck1d,* are involved in the circadian system of the sea urchin larva. For example, in other model organisms genes encoding kinases involved in the post-translational regulation of the circadian system are constitutively expressed.

Fig. 4.2 (Following page). Daily profiles of expression of *sp_vcry* (A, B), *sp_tim* (C, D), *sp_hlf* (E, F), *sp_dcry* (G, H), *sp_opsin3.2* (I, J) detected in LD and DD conditions by nCounter Nanostring. The profile of expression of the two indipendent batches are reported by the blue line (F1) and red line (F2). For *sp_tim* expression profiles of F1 and F2 were averaged and normalized (scale 0-1) with respect to the maximum level of its expression (green line). Grey boxes indicate the dark phase to which larvae were exposed. For the experiments performed in light/dark cycles, time points are reported as zeitgeber time (ZT) or, in constant dark as circadian time (CT). For sp_vcry and sp_tim ANOVA results are reported: p-value < 0.01 (**), p-value < 0.001 (***). To the right of the main graphs, the comparisons between the cosinor model (black line) and experimental time series (colour code as explained above) are reported with the corresponding p-values.

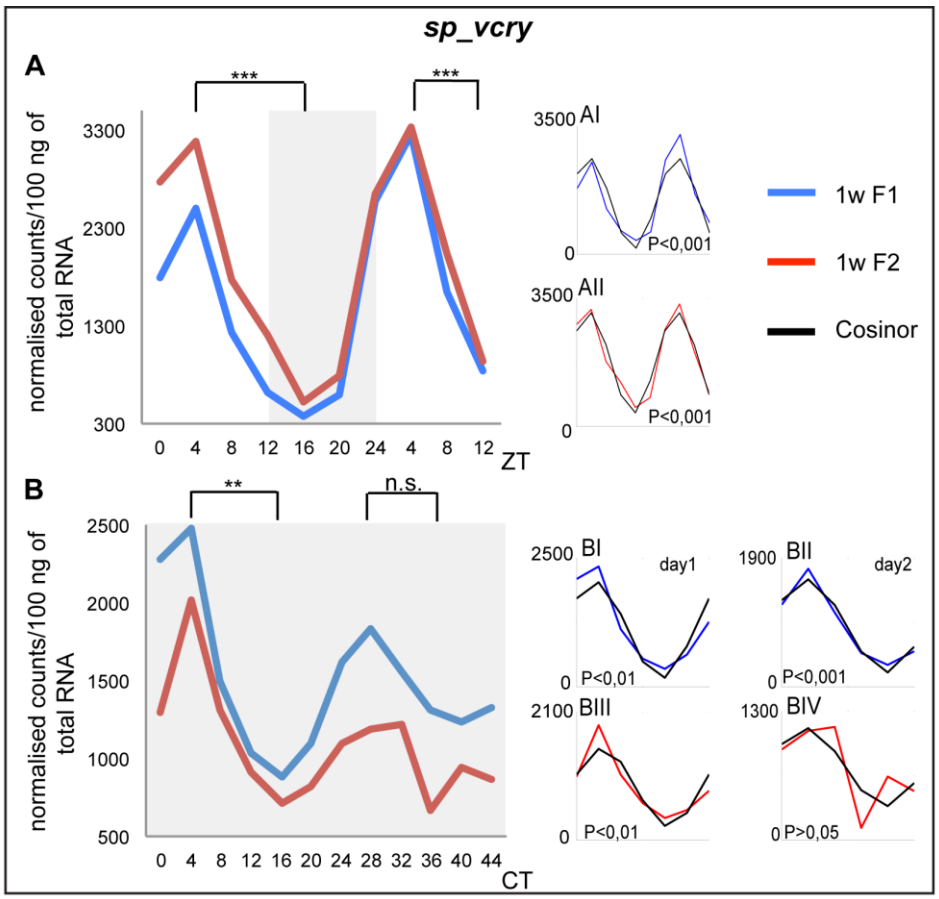
sp_vcry
A
normalised counts/100 ng of total RNA
***
***
3300
2300
1300
300
0 4 8 12 16 20 24 4 8 12
ZT
3500 AI
0
P<0,001
3500 AII
0
P<0,001
1w F1
1w F2
Cosinor
B
normalised counts/100 ng of total RNA
**
n.s.
2500
2000
1500
1000
500
0 4 8 12 16 20 24 28 32 36 40 44
CT
2500 BI
day1
0
P<0,01
1900 BII
day2
0
P<0,001
2100 BIII
0
P<0,01
1300 BIV
0
P>0,05

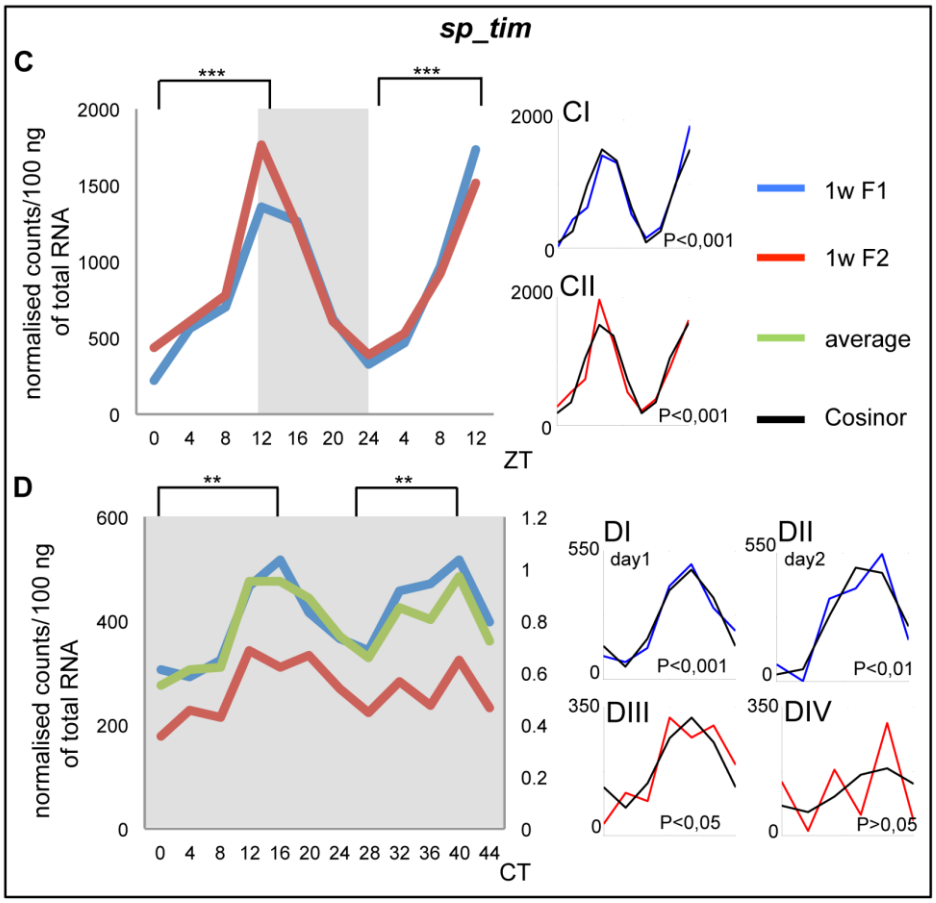
sp_tim
C
normalised counts/100 ng of total RNA
***
***
2000
1500
1000
500
0
0 4 8 12 16 20 24 4 8 12
ZT
2000 CI
0
P<0,001
2000 CII
0
P<0,001
1w F1
1w F2
average
Cosinor
D
normalised counts/100 ng of total RNA
**
**
600
400
200
0
1.2
1
0.8
0.6
0.4
0.2
0
0 4 8 12 16 20 24 28 32 36 40 44
CT
550 DI
day1
0
P<0,001
550 DII
day2
0
P<0,01
350 DIII
0
P<0,05
350 DIV
0
P>0,05

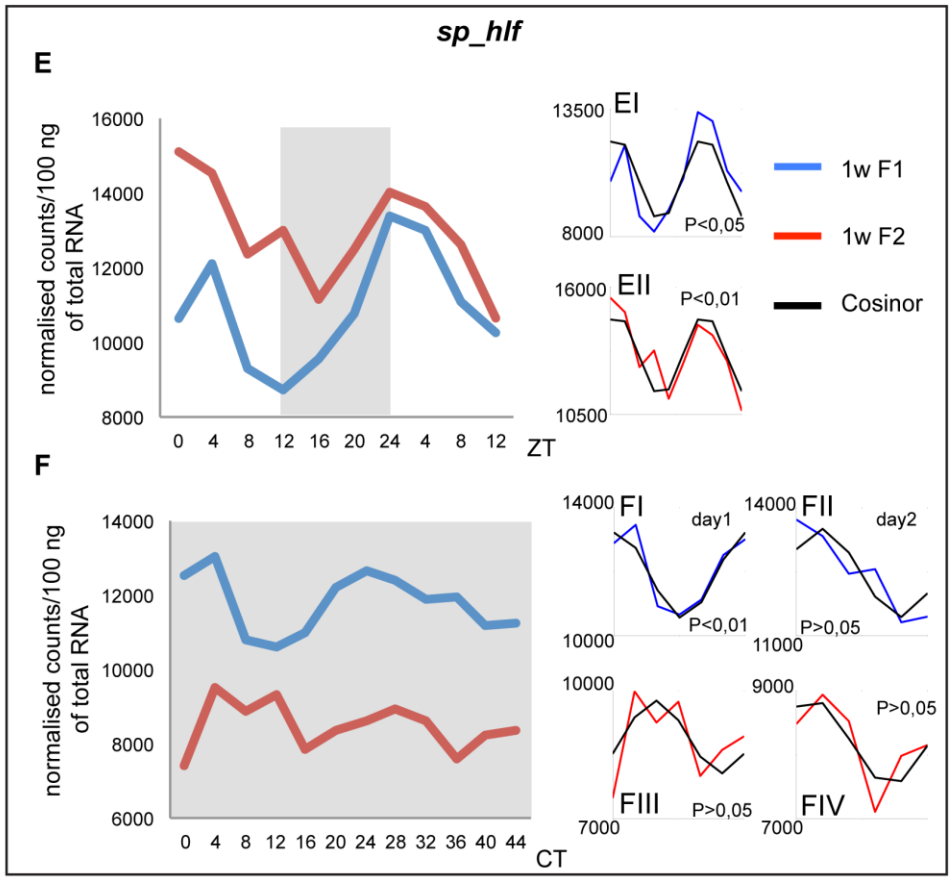
sp_hlf
E
normalised counts/100 ng of total RNA
16000
14000
12000
10000
8000
0 4 8 12 16 20 24 4 8 12
ZT
EI
13500
8000
P<0,05
EII
16000
10500
P<0,01
1w F1
1w F2
Cosinor
F
normalised counts/100 ng of total RNA
14000
12000
10000
8000
6000
0 4 8 12 16 20 24 28 32 36 40 44
CT
FI
day1
14000
10000
P<0,01
FII
day2
14000
11000
P>0,05
FIII
10000
7000
P>0,05
FIV
9000
7000
P>0,05

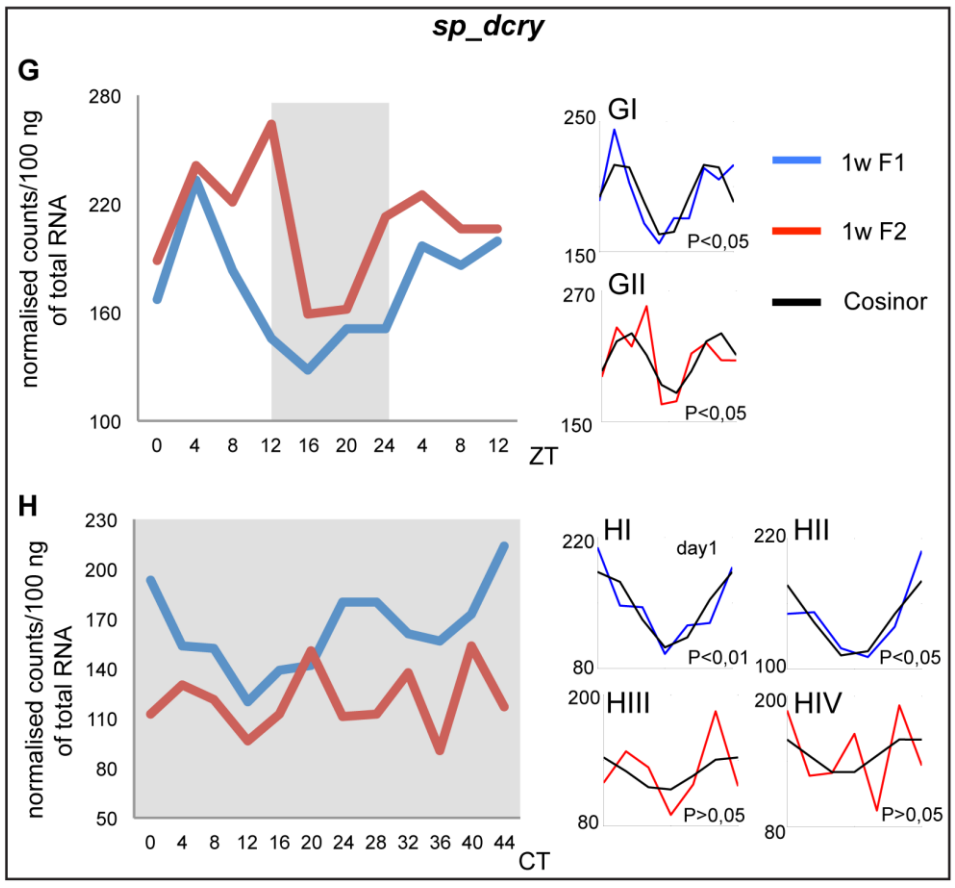
sp_dcry
G
normalised counts/100 ng of total RNA
280
220
160
100
0 4 8 12 16 20 24 4 8 12
ZT
GI
250
150
P<0,05
GII
270
150
P<0,05
1w F1
1w F2
Cosinor
H
normalised counts/100 ng of total RNA
230
200
170
140
110
80
50
0 4 8 12 16 20 24 28 32 36 40 44
CT
HI
day1
220
80
P<0,01
HII
220
100
P<0,05
HIII
200
80
P>0,05
HIV
200
80
P>0,05

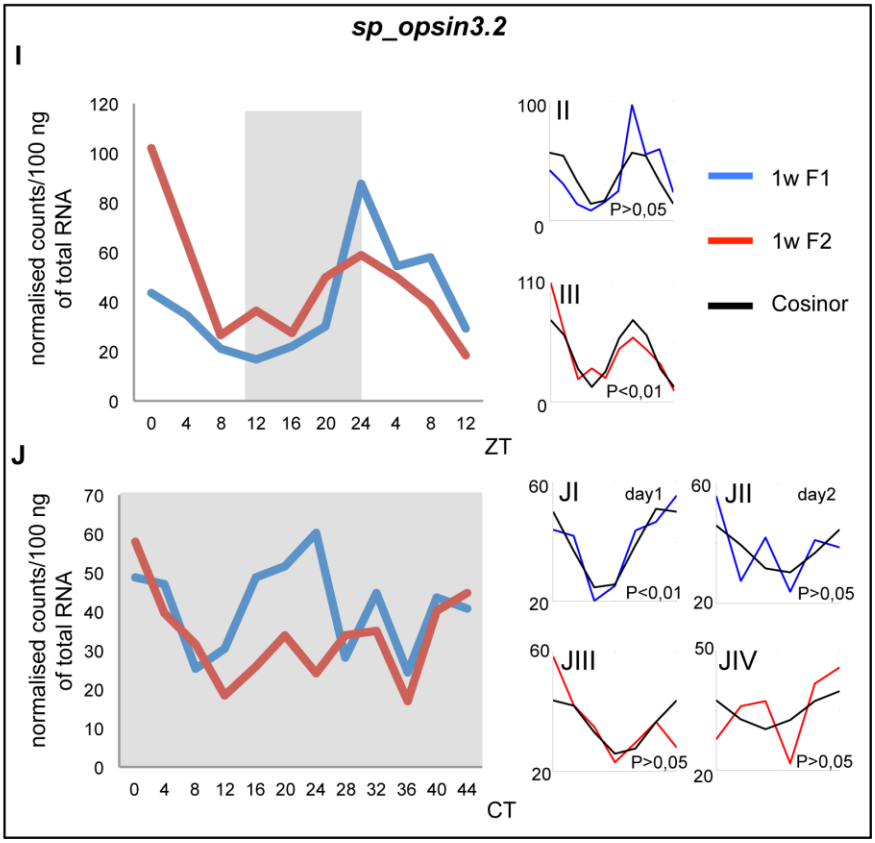

Table 4.1 Summary table indicating values of amplitude, mesor and acrophase detected for the genes described in this paragraph. These values were calculated using the cosinor analysis (see Materials and Methods for details) when the cosinor model was statistically significant (p-value < 0.05). Amplitude and mesor values are expressed in normalized counts of transcripts, acrophase values in degrees of circumference (°). For each value the standard deviation mean is reported (± value). When possible the values obtained from the two batches were averaged.

Gene name/light condition	Amplitude (counts of transcripts)	Mesor (counts of transcripts)	Acrophase (°)
sp_vcry DL	1311±70	1558±177	-0.87±0.01
sp_vcry DD day1	653.5±103	1311.5±171.5	-1.03±0.17
sp_vcry DD day2	290	1479	-0.98
sp_tim DL	591.5±13.5	879±26	-3.425±0.05
sp_tim DD day1	113	393	-4.1
sp_hlf DL	1601.5±20.5	11793±1027	-0.46±0.02
sp_dcry DL	43±8	185.5±17.5	-1.6±0.1
sp_opsin3.2 DL	25.75	203.5	-0.05
sp_crydash DL	500.5±11.5	543.85±64.15	-2.11
sp_6-4 photolyase DL	261.3±38.7	636.4±232.9	-1.65±0.02

In detail, *sp_vcry* mRNA levels reach a peak in the first hours of the subjective day (ZT4), thereafter they decrease with a trough at ZT16 and increase again in absence of light in both LD and DD conditions (Fig. 4.2 A, B). With respect to the former conditions, the amplitude of oscillation and mesor are reduced in free running (table 4.1) and, in particular, the oscillation is less robust during the second day (see values of amplitude, mesor (table 4.1) and cosinor analysis (Fig 4.2, BI-BIV)) with an increased variability between the two batches.

Differently from *sp_vcry*, the *sp_tim* mRNA profile (Fig. 4.2 C, D) exhibits minimum values at ZT0 in LD; its expression, then, increases during the light phase to reach its maximum at ZT12 (when light is off) and decreases during the subjective night. In DD the phase of oscillation is shifted by 4h (see cosinor model, Fig. 4.2 DI-DII) with a peak and a trough at ZT16 and ZT4, respectively. In these conditions ANOVA analysis was not significant, hence the profile of expression was reported as relative to the maximum value of transcripts to validate statistically the difference between peak and trough (green line, fig. 4.2 D). Similarly to the *sp_vcry* mRNA profile in DD, the amplitude and mesor of *sp_tim* are reduced in free-running conditions with respect to LD conditions. Again, in constant dark the oscillation during the second day is less robust (Fig., 4.2 DIII-DIV). Taken together, these results describe the presence of circadian rhythmicity in 1 week post fertilization (wpf) sea urchin larvae. LD cycles entrain the clocks of several larvae (1000 larvae/time-point were collected) to the same rhythm that is also maintained in free running conditions for at least the first 24 hours. After that the oscillation becomes less pronounced, with notable variability for *sp_vcry* and *sp_tim* in the two independent batches of larvae.

The genes that exhibit 24h rhythmicity in LD conditions, detected in this experiment, show very similar profiles of expression (Fig. 4.2 E, G, I; Fig. 4.3). Their mRNA levels increase during the first hours of the day, an exception being *sp_opsin3.2* which has a peak at ZT0 (Fig. 4.2 I), and then decreases, reaching a minimum in the night phase. *sp_hlf*, *sp_dcry* and *sp_opsin3.2* expression profiles all show a degree of variability between the two batches, making ANOVA analysis irrelevant (for this reason ANOVA results are not shown). For the first two genes, however, cosinor models confirm their rhythmic expression (Fig. 4.2 EI-II, GI-II). Whereas, variability observed for *sp_opsin3.2* is likely caused by technical limitations in reproducing consistent quantification when a gene is expressed at very low levels. Its rhythmic oscillation was confirmed in further experiments (see Appendix D, table D9). We concluded that the three genes do not

cycle in DD because any significant rhythmicity was observed at least 24 hours in both batches. However, we realized that batch F2 is prone to variability, thus, daily expression patterns of the genes described above were measured in at least a third independent batch using qPCR (see Appendix D, table D4). These experiments confirmed that: 1) *sp_vcry* and *sp_tim* oscillation dampens in the second day of free running conditions; 3) *sp_hlf* and *sp_dcry* oscillatory patterns are prone to variability in LD conditions not showing always consistent cosine curves (see also table D9 in Appendix) and do not oscillate at all in DD conditions.

Furthermore, the profiles of expression for *sp_crydash* and *6-4 photolyase* are typical of genes with 24h rhythmic expression in LD condition (Fig. 4.3). *sp_crydash* and *6-4 photolyase* mRNA levels increase rapidly after light is on (ZT4-8) then slowly decrease reaching a minimum at ZT24 and ZT16, respectively. Thereafter they increase rapidly again in presence of light. Conversely, in free running conditions, transcript levels are similar to the trough points detected in LD and can be considered constant during the entire 44 hours. The oscillatory expression profile of *sp_cpd photolyase* in LD conditions was detected by qPCR and reported in Appendix D, fig. D7.

Fig. 4.3 (Following page). Daily profiles of expression of *sp_crydash* (A) and *sp_6-4 photolyase* (B) detected in LD and DD conditions by nCounter Nanostring. Profiles of expression in the two indipendent batches are reported by the blue line (F1) and red line (F2) for LD samples; the green line (F1) and purple line (F2) for DD samples. On abscissa, time points are reported as zeitgeber time (ZT) and circadian time (CT) for LD and DD samples, respectively. For *sp_crydash,* ANOVA results are reported as: p-value < 0.001 (***). For *sp_6-4 photolyase* ANOVA (not shown) was calculated by using values normalized to the maximum level of its expression. In AI, AII, BI, BII, the comparisons between the cosinor model (black line) and experimental time series for LD samples (colour code as explained above) are reported with the corresponding p-values.

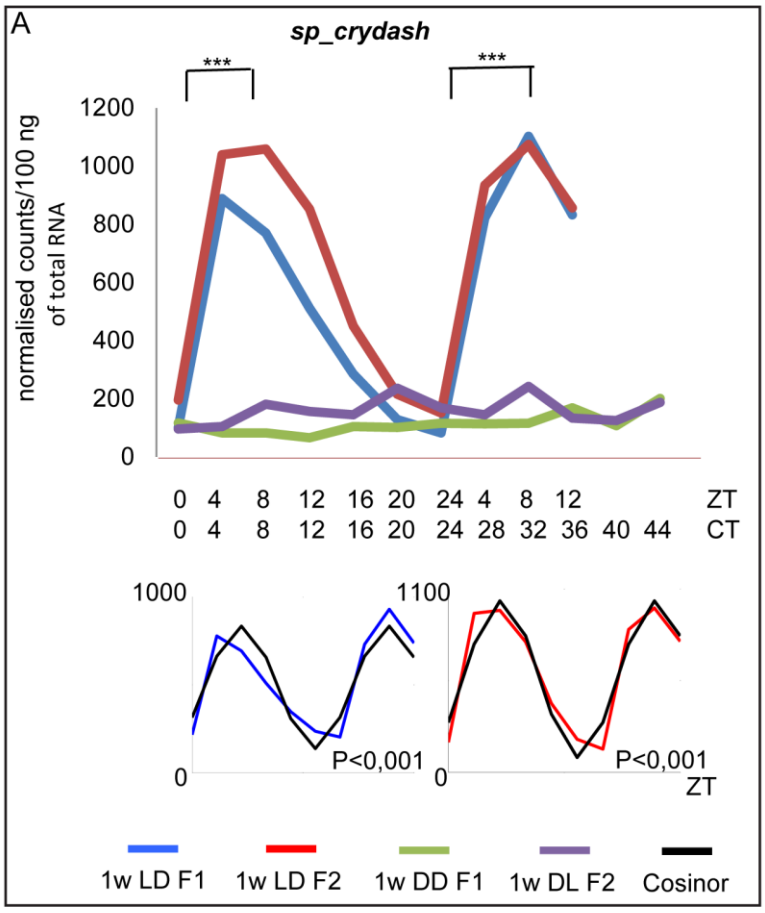
A
sp_crydash
***
***
normalised counts/100 ng of total RNA
1200
1000
800
600
400
200
0
0 4 8 12 16 20 24 4 8 12 ZT
0 4 8 12 16 20 24 28 32 36 40 44 CT
1000
0
P<0,001
1100
0
P<0,001
ZT
1w LD F1
1w LD F2
1w DD F1
1w DL F2
Cosinor

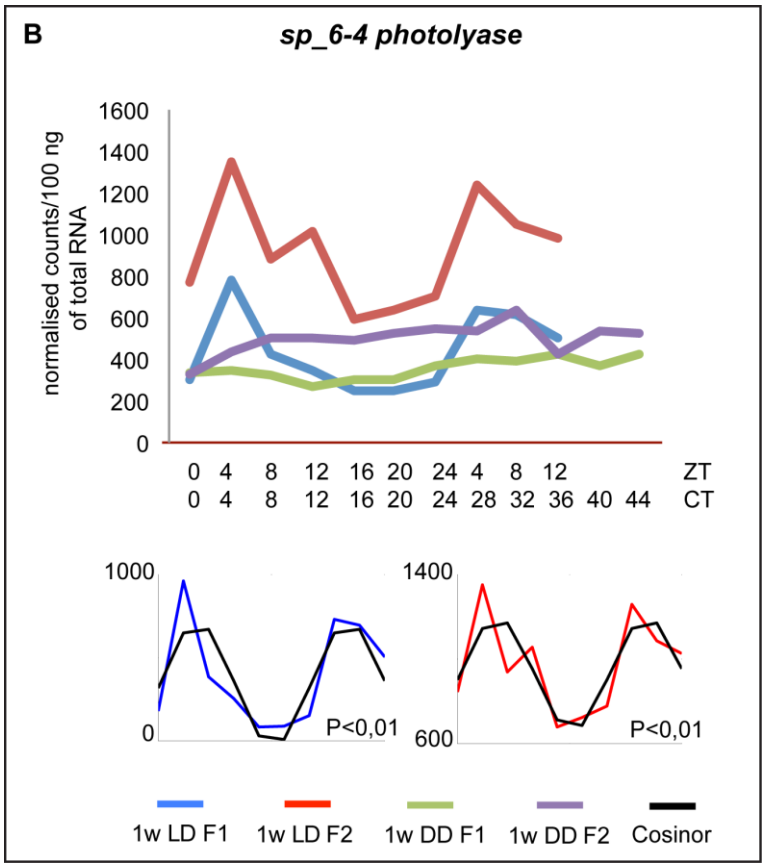
B
sp_6-4 photolyase
normalised counts/100 ng of total RNA
1600
1400
1200
1000
800
600
400
200
0
0 4 8 12 16 20 24 4 8 12 ZT
0 4 8 12 16 20 24 28 32 36 40 44 CT
1000
0
P<0,01
1400
600
P<0,01
1w LD F1
1w LD F2
1w DD F1
1w DD F2
Cosinor

Importantly, all the other genes do not show rhythmic changes in their mRNA levels (Appendix D, fig. D6), including *sp_bmal* and *sp_clock*. In other model organisms, at least one of the two orthologs show circadian expression being involved in the secondary loop, whereas, in sea urchin both are arrhythmic. Nevertheless, their function was hypothesized to be conserved in driving circadian rhythmicity, due to the high degree of protein sequence conservation between orthologs. All these observations could suggest: 1) the absence of their transcriptional regulation under circadian control; 2) that their expression may be rhythmic with asynchronous oscillatory patterns in different tissues, thus other techniques should be used to investigate them; 3) they might be regulated at post-transcriptional level in order to have circadian rhythmicity in protein activity and 4) that they do not have a role in the circadian system.

Fig. 4.4 shows the profiles of expression of *sp_bmal* and *sp_clock* detected by qPCR and nCounter Nanostring at different larval stages (5dpf, 1wpf, 2wpf) and different conditions (LD and DD). For each graph a correlation value was calculated indicating the similarity in the patterns of expression of the two genes and suggesting that their transcription could be under the same regulatory control. Moreover, they are arrhythmic even at an advanced larval stage (2 wpf) (Fig. 4.4 B) excluding the possibility that the architecture of the core clock undergoes to changes during post-embryonic development of this larval stage.

Fig. 4.4 (Following page). Daily profiles of expression of *sp_bmal* and *sp_clock* detected by qPCR (A, B) and nCounter Nanostring (C, D). The expression levels were measured from different larval stages and in LD and DD conditions: 5 dpf DL (A), 2 wpf DL (B), 1 wpf DL and DD (C, D). Correlation values between the two profiles of expression was calculated and reported for each condition. Colour codes are described in the figure.

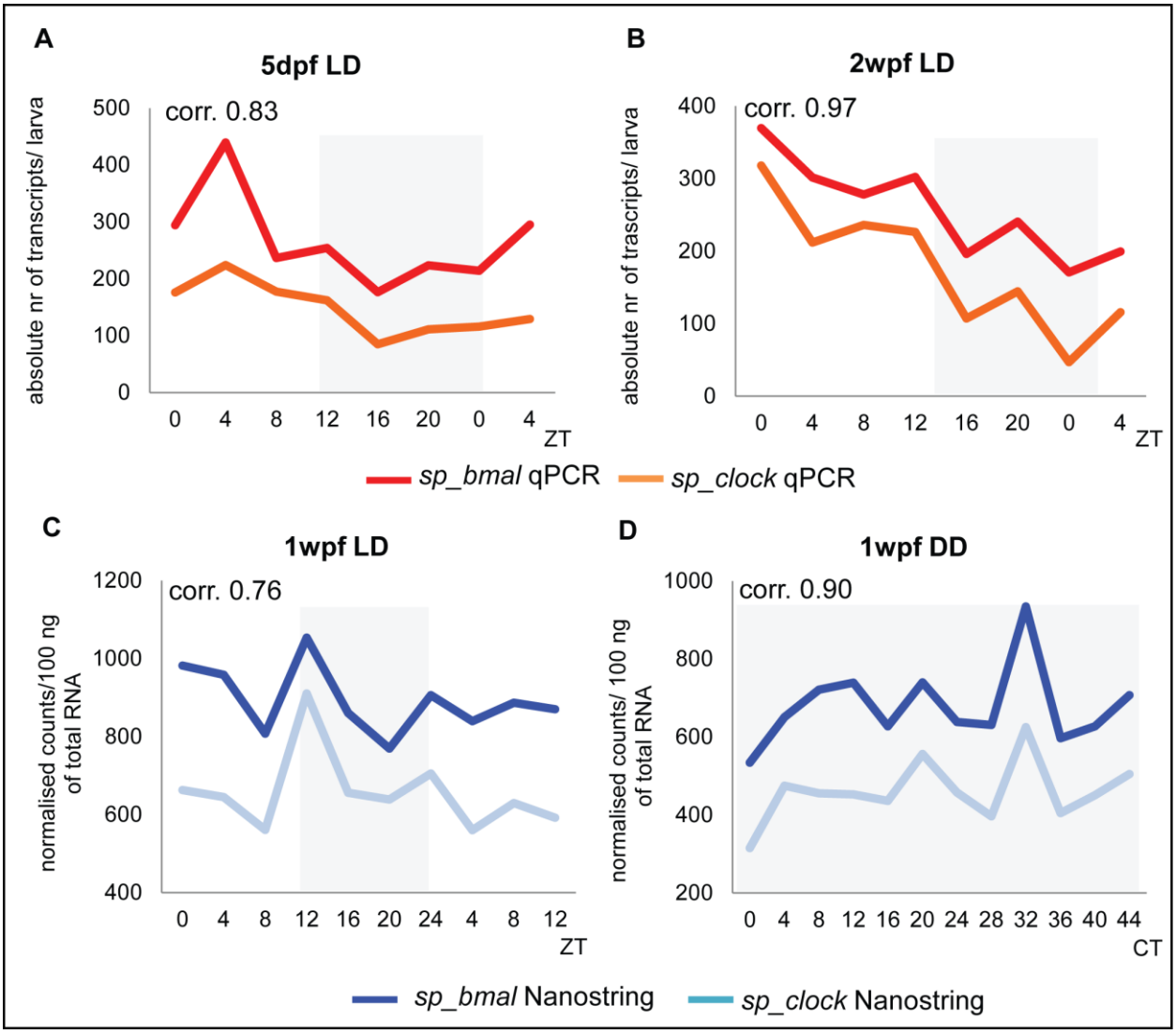

4.2 Spatial expression analysis of putative clock genes in embryos and larvae.

Spatial expression patterns of clock genes (*sp_vcry* and *sp_tim*) and other candidate genes, such as light responsive genes and neuropeptides, were analysed during embryonic development and in the larva to elucidate the cellular organization of the circadian system. Even if no rhythmicity was detected during embryonic development, this analysis was useful to investigate the dynamics of expression of these genes during embryogenesis and, eventually, follow the processes of specification and differentiation of specific cellular populations involved in the circadian system. Finally, analysis of their spatial expression in the larva could delineate the presence of clock, sensory and effector cells and their distribution in the organism.

4.2.1 Clock genes during embryogenesis.

Whole mount *in-situ* hybridization (WMISH) was performed on embryos and larvae cultured in chambers in absence of light (blastula (B), mesenchyme blastula (MB), gastrula (G) and pluteus stages (P)). Fig. 4.5 shows the patterns of expression of genes evaluated that are important to dissect the cellular organization of the clock. These are genes with circadian expression (*sp_vcry* and *sp_tim*), light responsive genes (*sp_hlf*, *sp_dcry*, *sp_opsin3.2*) and *sp_bmal* and *sp_clock*.

Fig.4.5 (Following page). Spatial expression patterns of clock genes during embryonic development. Spatial expression patterns were detected at the stages of early blastula (EB, 16 hpf) or blastula (B, 18 hpf), mesenchyme blastula (MB, 24 hpf), gastrula (G, 48hpf) and pluteus (P, 72hpf or 96hpf) for *sp_bmal*, *sp_clock*, *sp_vcry*, *sp_tim* and *sp_dcry.* Spatial expression patterns for *sp_hlf* were detected in the gastrula and pluteus (96 hpf) and *sp_opsin3.2* at 1wpf. Almost all the experiments were performed using single probe chromogenic *in-situ* technique; exceptions are *sp_tim* and *sp_dcry*, which have been detected with single fluorescent *in-situ* technique at gastrula and pluteus stages, respectively. For the expression of *sp_tim* at pluteus stage, the green arrow indicates the midgut, the red arrow the blastocoeliar cells, the yellow arrow the apical organ. For the expression of *sp_dcry,* the blue arrow indicates the three cells of the pluteus apical organ positive to this gene. Unless otherwise specified embryos and pluteus are presented in lateral view with the apical domain at the top. OV (oral view), AV (apical view), AbV (aboral view). *sp_bmal*, *sp_clock* and *sp_vcry in-situs* were performed by Edmondo Iovine; *sp_tim in-situ* was performed by Agnieszka Chomka, *sp_hlf* and *sp_opsin3.2 in-situs* were performed by Harriet Stephenson and Wendy Hart respectively.

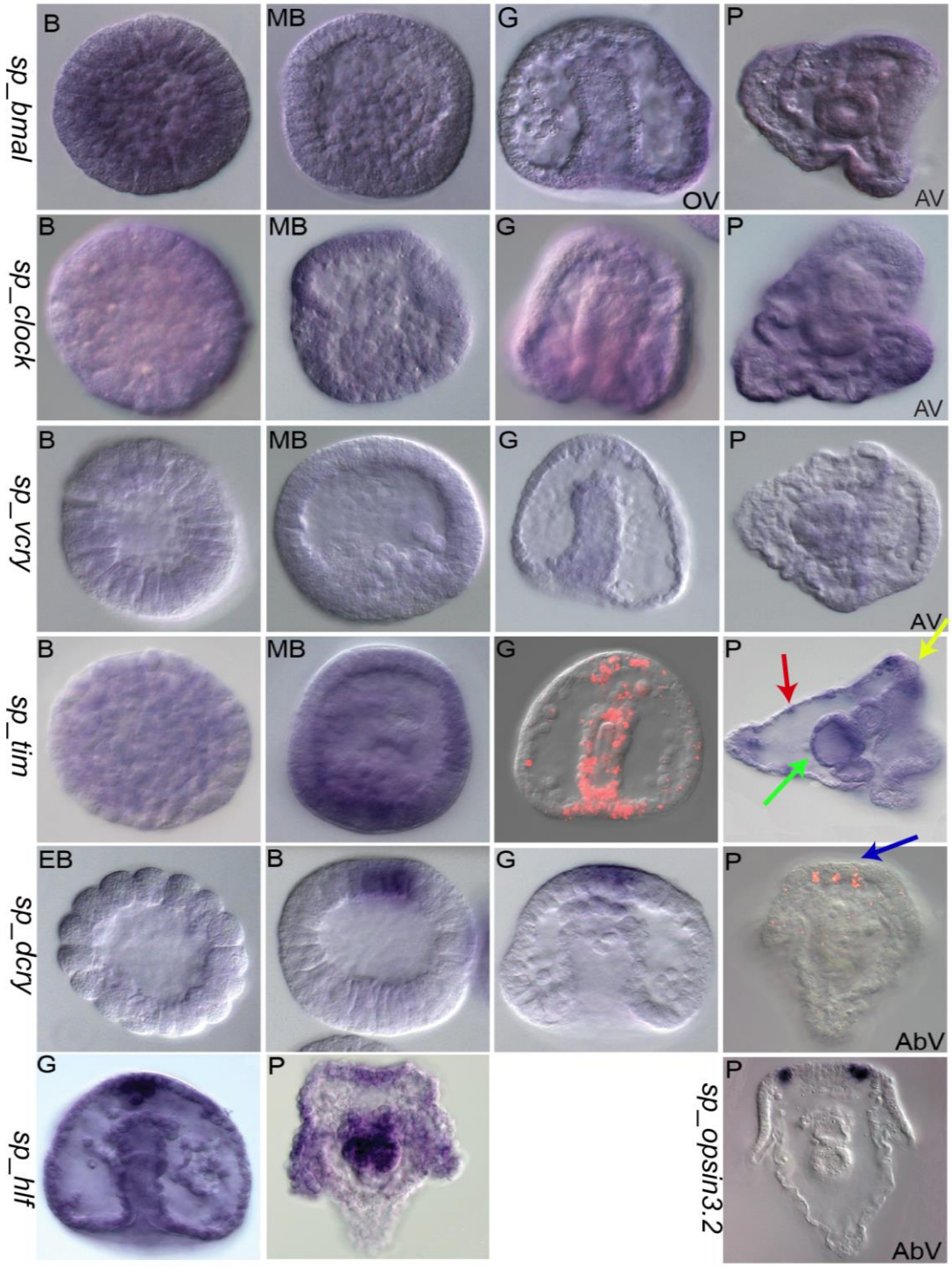

The analysis revealed that *sp_bmal*, *sp_clock*, *sp_vcry* are ubiquitously expressed in embryos and larvae suggesting the presence of clock pacemakers in all the cells of the organism. In contrast, *sp_tim*, *sp_dcry*, *sp_hlf* show pronounced or localized expression in specific cellular domains during embryogenesis suggesting the presence of molecular pathways for the circadian system already in the developing embryos. The exception is *sp_opsin3.2,* expression which was analysed only at the larval stage because of the

absence of expression early in development as reported by the sea urchin developmental transcriptome (http://www.spbase.org/SpBase/rnaseq/).

Notably, *sp_tim* is ubiquitously expressed in the early stages of development, then, from the gastrula stage, its expression is localized to the developing archenteron, the secondary mesenchyme cells (SMC), located at the tip of the archenteron and that will form the blastocoelar, and a subset of cells in the neurogenic apical domain. This pattern is maintained in the larva where *sp_tim* again shows expression in the midgut, blastocoeliar cells and apical organ cells.

Sp_hlf, whose expression in the early embryonic stages was described in Howard-Ashby et al., 2006, is ubiquitously expressed with enriched transcripts levels in the apical domain at gastrula stage. Later in development, its expression increases in both the gut and the ciliary band.

Sp_dcry is maternally expressed and ubiquitously distributed until early blastula stage, after which its expression becomes restricted to the apical domain. Still, its domain of expression reduces in the gastrula until it appears only in three cells of the larval apical organ.

Finally, *sp_opsin3.2* is expressed in two cells adjacent to the apical organ and at the base of the anterolateral arms of the pluteus larva (see below for details).

Taken together these data suggest the possible presence of specialized cells in the apical organ and gut that might have a role as clock and/or photoreceptor cells. However, this does not exclude the possibility that some of these genes may have roles independent of circadian regulation, especially during embryonic development where no rhythmicity was detected.

4.2.2 Cellular characterization of the larva's apical organ.

We focused our study in better understanding the cellular composition of the apical organ within the circadian system as a structure that potentially may contain clock neurons, input and output pathways.

The apical organ is a larval neurosensory structure, present in many marine organisms, that detects the external environment with one of its functions being to regulate swimming behaviour (Rentzsch et al., 2008). In sea urchin larvae, the apical organ has been well described regarding its neuronal composition (Burke et al., 2006) but information about the presence of molecules that response to the environment are lacking. In addition, to my knowledge there are few studies that have investigated its

function as sensory structure (Wada et. al., 1997; Yaguchi and Katow, 2003) and none of them describe any molecular mechanism that integrates environmental stimuli and translation into behavioural outputs. The analysis performed in the previous section led to the identification of cells of the apical organ expressing clock genes and potential photoreceptors. In order to characterize these cells further for their potential involvement as clock neurons or light responding cells, a series of the following double fluorescent *in-situs* were performed in the sea urchin larva:

- *sp_dcry*/*sp_z167* (Fig. 4.6) to characterize *sp_dcry*-positive cells as potential clock neurons. *Sp_z167* is a homolog of *Drosophila* glass gene that encodes a transcription factor required for the differentiation of photoreceptor cells (Poutka et al., 2007; Moses et al., 1989). In *Drosophila*, *glass* and *dcry* are co-expressed in a subset of clock neurons (Klarsfeld et al., 2004). To discriminate better between different cells, larvae were stained for serotonin using immunohistochemistry techniques. This experiment was performed by Dr. Avi Lerner.
- *sp_dcry*/*sp_tim* (Fig. 4.7) to verify the co-expression of the two genes which homologous interact at protein level in *Drosophila*.
- *sp_dcry*/*sp_ppln2*, *sp_p18*/*sp_5ht*, *sp_ppln2*/*sp_p18*, *sp_gkmide*/*sp_p18, sp_trh/sp_5ht* (Fig. 4.8, Fig. 4.9 A) to analyse the connection between the neuropeptide and neurotransmitter system of the apical organ and circadian system and to have a better understanding of the neuronal organization of the apical organ. Experiments were performed by Teresa Mattiello.
- *sp_trh/sp_opsin3.2* (Fig. 4.9 B) to define the two *sp_opsin3.2*-positive cells as potential photoreceptors cells, with molecular signatures different from *sp_dcry*-positive cells.

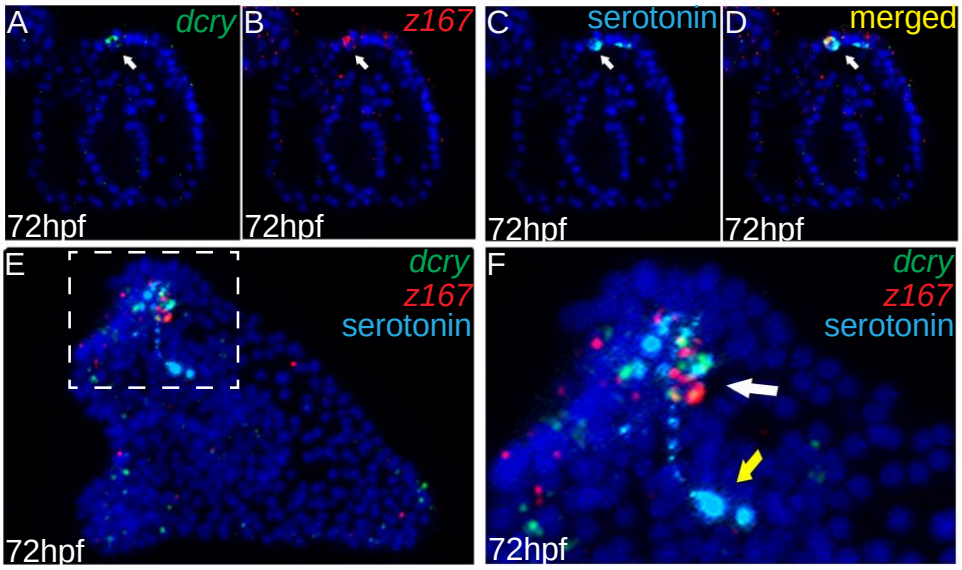

Fig.4.6 Double fluorescent *in-situ* to detect the expression of *sp_dcry* and *sp_z167*. Because the apical organ is characterized by a group of serotonergic cells, after *in-situ*, an antibody against serotonin was used to detect the type of neuronal cells expressing *dcry* and *z167*. In A, B, C and D larvae are viewed from an oral view, in E from a lateral view. In A, B and C are illustrated images of the same pluteus (oral view) with a different fluorescent channel; in D all the images have been merged to analyse the co-expression of *sp_z167* and *sp_dcry*. In E, a different larva is reported (lateral view) with merged different fluorescent channels to underline that *sp_dcry* and *sp_z-167* are co-expressed in a subset of serotonergic neurons. Details of the co-expression (dashed box in E) are reported in F; the white arrow indicates serotonergic cell expressing *sp_dcry* and *sp_z167,* the yellow arrow indicates other serotoninergic neurons. Nuclei were stained with DAPI (blue). In A, B, C and D images are projections of 4 confocal slices; in E and F images are full projections of confocal slices.

Fig. 4.6 shows *sp_dcry* co-expressed with *sp_z167* in a subset of serotonergic cells of the pluteus apical organ. Larvae labeled with the serotonin antibody show two clear and distinct types of serotonergic neurons in the sea urchin apical organ: serotoninergic cells expressing *sp_dcry* and *sp_z167* (Fig. 4.6 F, white arrow) and serotoninergic cells not expressing *sp_dcry* and *sp_z167* (Fig. 4.6 F, yellow arrow).

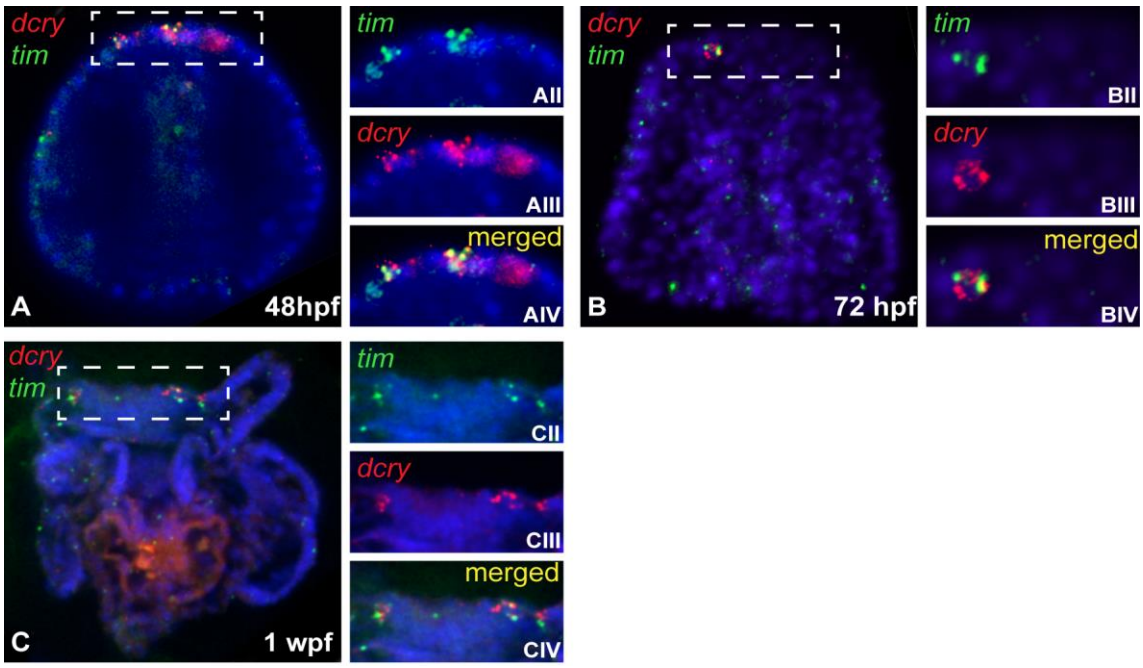

Fig.4.7 Double fluorescent *in-situ* to detect the co-expression of *sp_dcry* and *sp_tim* at 48hpf (A), 72hpf (B) and 1Wpf (C). In A and B, the embryo and the larva are viewed from an oral view; in C, the larva is viewed from an abanal view. Images of the region in the dashed boxes were enlarged to show in detail the expression of *sp_tim* (AII, BII, CII), *sp_dcry* (AIII, BIII, CIII) and co-expression in the merged picture (AIV, BIV, CIV).

sp_dcry and *sp_tim* genes show partial co-expression during embryonic development at the gastrula stage in two cells of the apical domain (fig. 4.7). Co-expression is complete at the larval stage where all 3 cells are positive for both genes. Interestingly, *sp_dcry* seems to turns on in the gut of fed larvae at 1 wpf suggesting the potential presence of a light input system in this tissue of the larva. This observation has been made several times (Appendix D, Figure D8): indeed, at 72 hpf, *sp_dcry* is expressed only in cells of the apical organ, while at 1 wpf its expression has been detected in the gut as well.

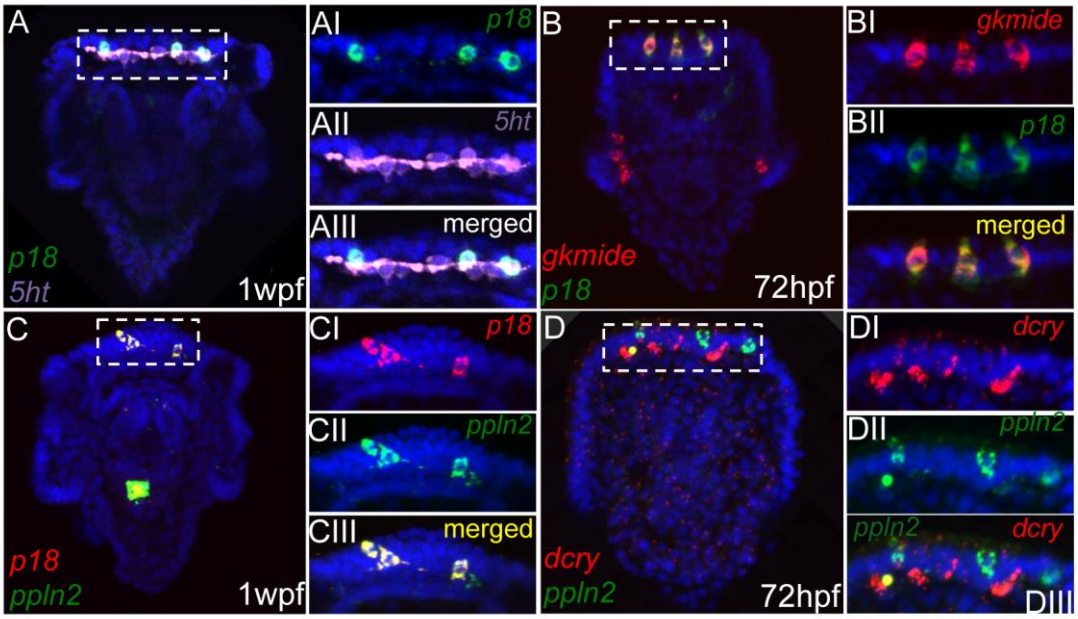

Fig.4.8 Double fluorescent *in-situ* *sp_p18/sp_5ht* (A), *sp_gkmide/sp_p18* (B), *sp_p18/sp_ppln2* (C), *sp_dcry/sp_ppln2* (D) performed in sea urchin larva. For the organization of the figure, see caption fig. 4.6 and 4.7. All larvae are viewed from an abanal view. The enlarged figures are confocal projections of 4 slices.

Fig.4.8 shows the patterns of co-expression of the neuropeptides *sp_gkmide*, *sp_p18* and *sp_ppln2* in 3 serotonergic cells of the apical organ. In these figures it is important to appreciate the expression pattern of *sp_5ht* that indicates the presence of an interconnected cluster of serotoninergic neurons constituting the anterior ganglion (Burke, 2014). However, the neuropeptides so far analysed are expressed in cellular types different from the *sp_dcry*-positive cells. Indeed, *sp_ppln2* was detected in adjacent cells to *sp_dcry*-positive cells (Fig. 4.8 D).

Interestingly, another neuropeptide gene, *sp_trh* is expressed outside the domain marked by *sp_5ht* in two adjacent cells that express also the *sp_opsin3.2* and it seems they send projections to the serotorinergic cells (Fig. 4.9, next page).

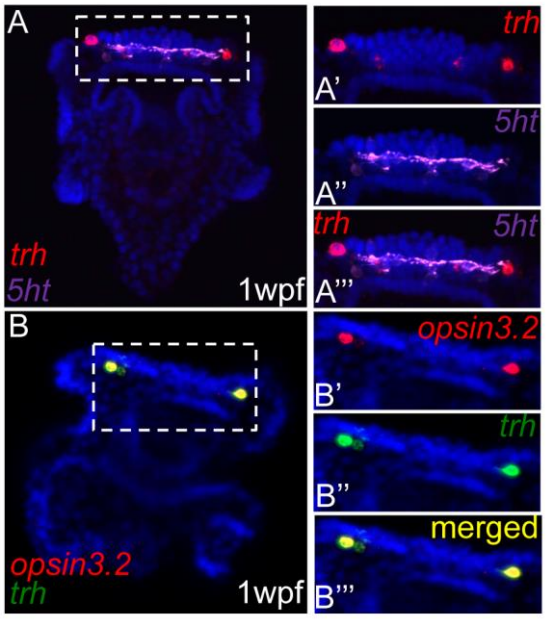

Fig.4.9 Double fluorescent *in-situ* *sp_trh/sp_5ht* and *sp_opsin3.2/sp_trh* performed in sea urchin larva. Organization of the figure is as described in Fig. 4.5 and 4.6. In A, the larva is viewed from an abanal view; in B, the larva is viewed from an oral-posterior view.

Results obtained from the WMISH experiments showing genes with localized expression have been summarized in the table 4.2.

Gene name in *Sp*	*tim*	*dcry*	*opsin3.2*	*ppln2*	*p18*	*gkmide*	*trh*	*z167*
tim		3 s + g						3 s
dcry	3 s + g							3 s
opsin 3.2							2 al. ar.	
ppln2					3 s	3 s		
p18				3 s		3 s		
gkmide				3 s	3 s			
trh			2 al. ar.					
z167	3 s	3 s						

Table 4.2 The table summarizes the spatial expression patterns of the genes with localized expression described in this chapter. Number of cells and domain of expression is indicated for each gene. The presence of co-expression is depicted by a colour code: red for serotorinergic neurons (s) *sp_dcry*$^{+}$ and/or gut (g), green for serotoninergic neurons *sp_dcry*$^{-}$, yellow for the two cells in the anterolateral arms (al. ar.); white for absence of co-expression. *sp_vcry*, *sp_hlf*, *sp_bmal* and *sp_clock* have not been inserted in the table because they are characterized by ubiquitous expression.

This analysis led to the characterization of different cell types within the apical organ of the larva. This neurosensory structure is characterized by: 1) three serotoninergic neurons that have the molecular signatures of clock neurons and light-sensing cells (*sp_dcry*, *sp_tim*, *sp_z167* are expressed in these cells with *sp_vcry*, *sp_hlf*, *sp_bmal* and *sp_clock* ; 2) three serotoninergic neurons that do not express *sp_dcry* and *sp_tim* but are characterized by the co-expression of three neuropeptides (*sp_ppln2*, *sp_p18*, *sp_gkmide*) *;* 3) two potential photoreceptor cells (*sp_opsin3.2* positive), adjacent to the domain marked by the serotoninergic neurons, with a potential neuro-signaling function (*sp_trh*).

4.3 Spatial expression patterns of *sp_vcry*, *sp_bmal*, *sp_clock* in larvae entrained to light/dark cycles.

The previous WMISH experiments were performed on embryos and larvae not synchronized to LD cycles. Importantly, the rhythmic expression detected for *sp_vcry*, *sp_tim*, *sp_hlf*, *sp_dcry*, *sp_opsin3.2* in LD conditions (paragraph 4.1) seems to pinpoint that all the processed larvae are synchronized to the same light/dark rhythm. This hypothesis was tested by performing WMISH on batches of larvae raised under 12h/12h light/dark cycles and collected at different ZT (ZT4, ZT10, ZT17). Experiments were performed by master student Harriet Stephenson. *Sp_vcry* was tested for this experiment because it shows the most robust rhythmic expression in LD and DD conditions. *sp_foxa,* not likely to be under circadian control was used as negative control (Fig. 4.10, next page).

Sp_vcry shows ubiquitous expression with a higher intensity at ZT4 that decreases at ZT10 and ZT17 in agreement with the trend of mRNA levels detected by nCounter Nanostring. Notably, changes in levels of expression are more pronounced in the gut and apical organ from ZT4 to ZT17. On the contrary, *sp_foxa* has levels of expression that do not change at the different time-points assuring the sensitivity of the technique in discriminating between visible changes in expression of a gene with rhythmic expression. This result confirms that mRNA levels of *sp_vcry* changes rhythmically in all cells of the sea urchin larvae indicating that all cells are synchronized to the same rhythm in LD conditions.

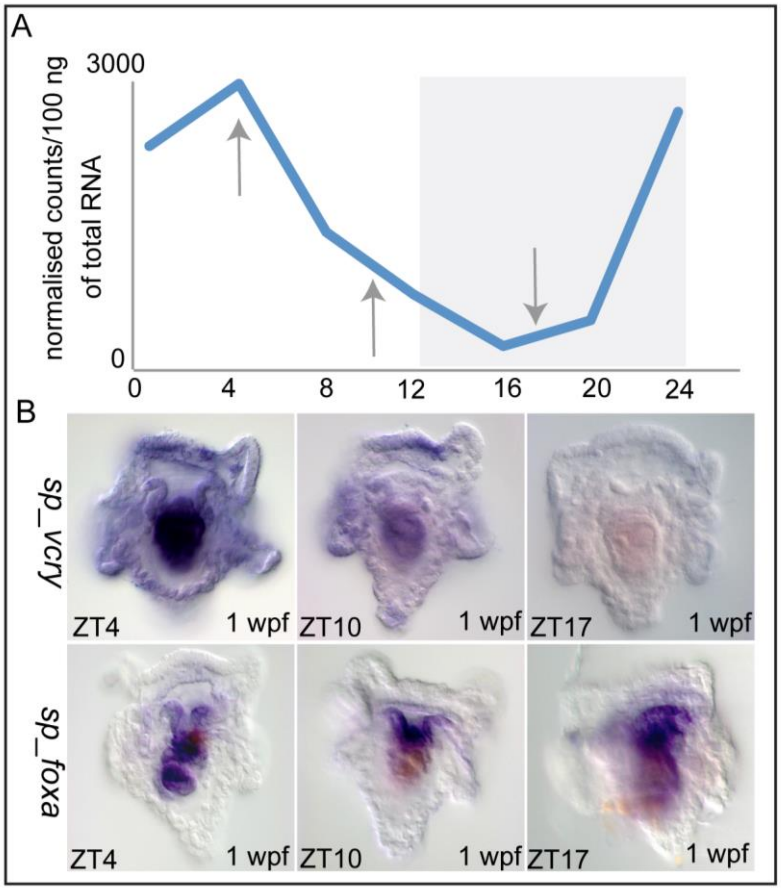

Fig.4.10 Spatial expression of *sp_vcry* detected in larvae (1wpf) collected at ZT4, ZT10 and ZT17. In A, the daily expression profile of *sp_vcry* measured by Nanostring nCounter is shown. The arrows indicate the levels of expression of *sp_vcry* at ZT4, ZT10 and ZT17. In B, spatial expression patterns of *sp_vcry* and *sp_foxa* are shown. All larvae are viewed from an abanal view.

Same experiment was performed for *sp_bmal* (fig. 4.11, next page) and *sp_clock* (fig. 4.12, page 114) to verify the absence of rhythmicity detected by the quantitative analysis (paragraph 4.1) or, conversely, the presence of rhythmicity either in specific cells of the larva or in all the cells with different phases. Both experiments show the presence of variability in the intensity of expression in the same batches of larvae rendering the analysis of daily changes in gene expression difficult. For *sp_bmal*, patterns of expression vary from ubiquitous with pronounced expression in the ciliary band to the absence of expression at ZT4 (Fig. 4.11 A, B); pronounced expression in the ciliary band with different intensity at ZT10 (Fig. 4.11 C, D); and ubiquitous expression to pronounced expression in the ciliary band at ZT17 (Fig. 4.11 E, F). A similar result occurred for *sp_clock* which is ubiquitously expressed with particular

enrichment of transcripts levels in the ciliary band (Fig 4.12). The variability in the intensity of expression for both genes may have been caused by technical problems (e.g. problems with tissue penetration of the antisense probes).

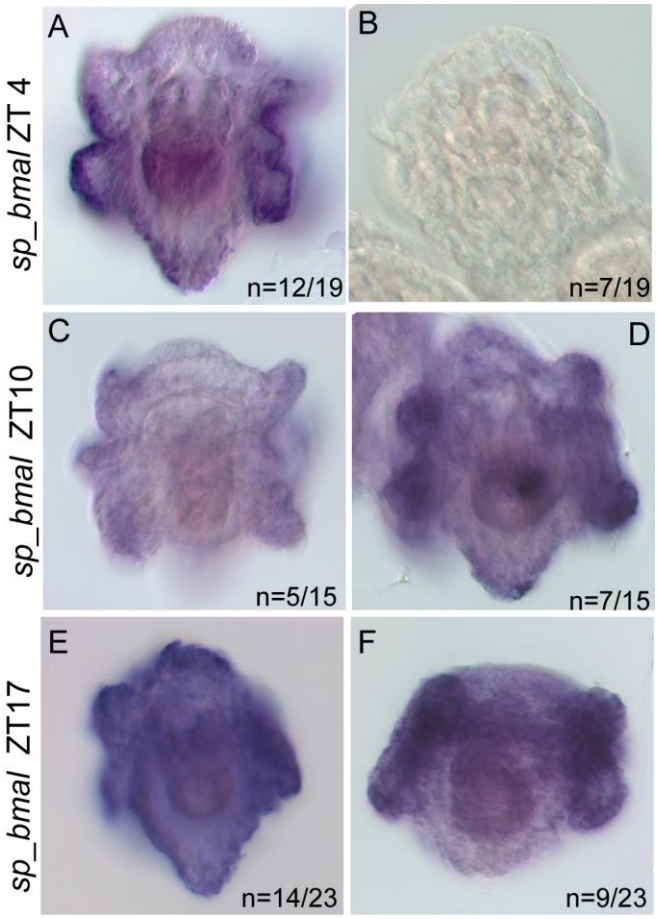

Fig.4.11 Spatial expression of *sp_bmal* was detected in 1wpf larvae collected at ZT4 (A, B), ZT10 (C, D), ZT17 (E, F). Variability in intensity of expression was detected at each time point, thus larvae were counted and grouped according the different pattern of expression. All larvae are viewed from an abanal view.

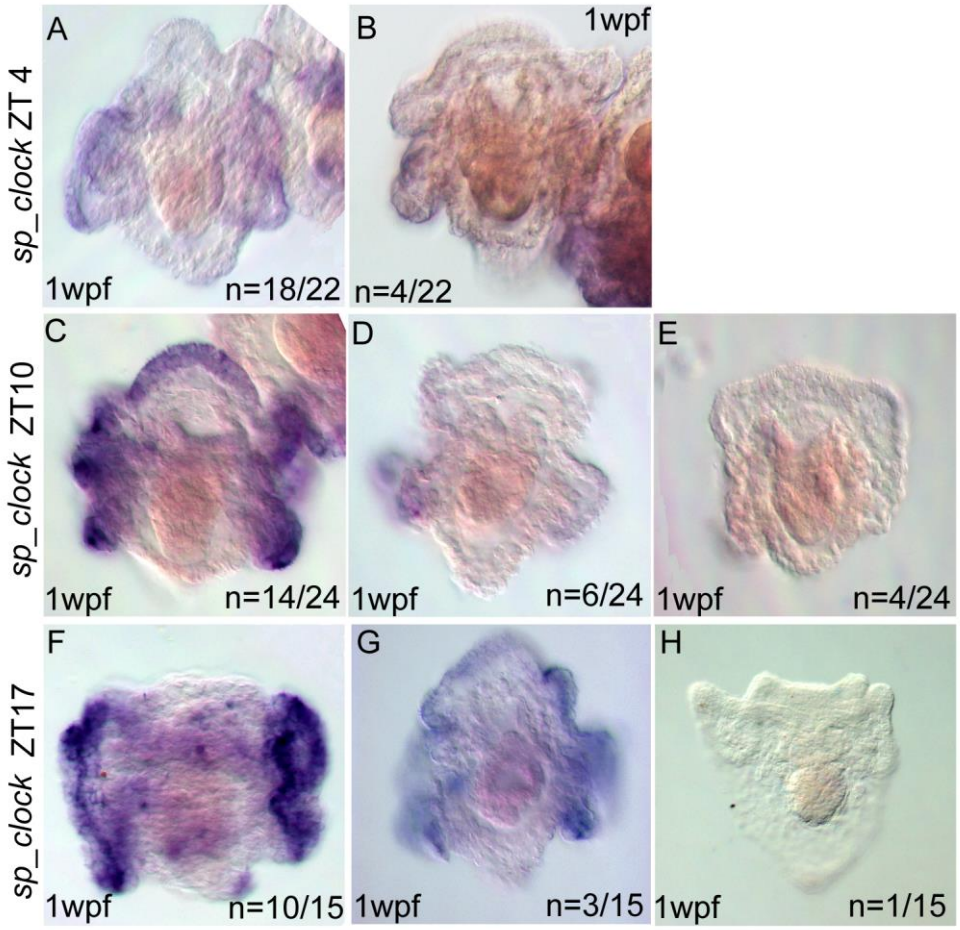

Fig.4.12 Spatial expression of *sp_clock* detected in larvae collected at ZT4 (A, B), ZT10 (C, D, E) and ZT17 (F, G, H). Variability in intensity of expression was detected in each time point, thus larvae were counted and grouped according the different intensity of expression. All larvae are viewed from an abanal view.

4.4 Summary.

For the first time, a circadian rhythm has been detected in the sea urchin larva. I have identified two genes with circadian expression (*sp_vcry* and *sp_tim*), several genes that oscillate in LD conditions (sp_hlf, sp_dcry, sp_opsin3.2, sp_crydash, *sp_6-4 photolyase*, *sp_cpd photolyase*), and genes (in particular *sp_bmal* and *sp_clock*) with absence of rhythmicity. The presence of only two genes with circadian expression suggest that the GRN that drives circadian rhythmicity in sea urchin larvae may have been rewired from that which has been reported in other organisms (discussion in chapter 6).

In addition, the WMISH analysis gives first insights into the cellular organization of the circadian system of the larva. Two tissues might have a primary role in such a system. Indeed, cells co-expressing *sp_vcry* and *sp_tim* have been localized in the apical organ and the gut. The apical organ has a complex neural organization characterized by at least two different types of serotoninergic neurons. One type possesses all the molecular signatures of clock neurons and/or photoreceptor cells (expression of *sp_dcry*, *sp_tim*, *sp_z167* and other candidate genes). The second type expresses a set of neuropeptides and other genes described in this chapter (except *sp_dcry* and *sp_tim*) and may have neuro-signaling functions. A third cellular type was identified adjacent to the apical organ where two cells possess all the characteristics for a photoreceptor function: *sp_opsin3.2* is a potential photoreceptor and the neuropeptide *sp_trh* might be involved in spreading the signal triggered by *sp_opsin3.2*.

Conversely, the gut of the sea urchin larva might be the tissue where clock cells are involved in the regulation of output pathways involved in the metabolism.

Finally, information obtained in this chapter together with the analysis of protein domains described in chapter 3, indicates the need to study the functional linkages between clock and light-dependent genes to truly discern the architecture of the core clock network and light input system in the sea urchin larva. In order to compile a provisional network model, functional experiments were carried out in which linkages between genes were analysed by perturbing the expression of *sp_vcry*, *sp_tim*, *sp_dcry* and *sp_opsin3.2* (described in the next chapter).

Chapter 5

Functional analysis provides a provisional model of the circadian system of sea urchin larva.

The sea urchin embryo has been used as powerful model system to dissect gene regulatory networks, which drive specification and differentiation processes during embryogenesis (Davidson et al 1995; Oliveri and Davidson, 2004). Such studies are facilitated by the availability of the genome and transcriptome sequences (Sodergren et al., 2006; Tu et al., 2012); the ease in obtaining millions of gametes in the laboratory; the rapid and synchronous development of transparent embryos and larvae making them ideal for microscopy. Embryos are robust to experiments of manipulation, such as microinjection, and allow for easy gene transfer and reporter gene expression. All this facilitates studies involved in analysing and perturbing gene expression and function. A consolidate strategy used to assess functional linkages between regulatory genes in sea urchin is based on generating knockdown of a specific gene through microinjection of specific MOs into fertilized eggs. At a desired developmental stage, spatio-temporal expression patterns of candidate network genes are monitored in perturbed samples and compared with unperturbed ones to assess if the knockdown affects their mRNA levels (Materna and Oliveri, 2008). In addition, another strategy widely used in different model organisms for the study of the circadian clock is the *in-vivo* luciferase assay. This technique uses a luciferase encoding cassette fused to regulatory regions of specific clock genes as real-time reporter gene. Thus, it allows to precisely monitor daily rhythms in gene expression in individual organisms and cultured tissues and cells. This avoids issues related to the use of homogenised samples of several animals and the application of time-consuming experiments such as samplings and RNA extractions (Yu and Hardin, 2007).

We applied two strategies to gain provisional insights into the architecture of the circadian system in the sea urchin larva. The first approach (paragraph 5.1) consisted of constructing a luciferase reporter gene that provided a reliable representation of the endogenous clock of *S. purpuratus* larvae. Such a reporter would have been used in knockdown studies of various candidate clock genes to monitor if the endogenous clock was affected in such conditions. Whereas the second strategy (paragraph 5.2) was

based on perturbation of gene function by MO injections and analysis of daily expression profiles of candidate genes by qPCR and Nanostring technology.

5.1 *In-vivo* luciferase assay in sea urchin.

The *in-vivo* luciferase assay is a powerful technique because luciferase has a fast turn-over and catalyses a reaction in presence of luciferin that emits light. Thus it is suitable to study temporal changes in transcription for several days with light automatically measured by a luminescence counter. In this way molecular rhythms are detected as daily changes of bioluminescence emission in single injected or transgenic organisms. In this paragraph the experimental strategy used to perform for the first time this technique in sea urchin is described. Experiments shown in this paragraph were performed by master student Louise Cleal except microinjections that were performed by Dr Paola Oliveri or the undersigned.

5.1.1 Generation of *sp_vcry* luciferase and GFP reporter genes.

In order to monitor the sea urchin circadian clock *in-vivo*, reporter constructs were generated with the luciferase cassette under the control of the regulatory regions of *sp_vcry*, the gene that shows the most robust rhythmic expression in LD and DD conditions. The intergenic region upstream *sp_vcry* locus (~ 37 kb) was analysed for the presence of potential regulatory elements that may drive its rhythmic expression using the software ConSite, a transcription factor binding site search tool (http://asp.ii.uib.no:8090/cgi-bin/CONSITE/consite/). The analysis has been focused on the search of E-box elements (CATGTG) bound by b-HLH transcription factors and D-box elements (TTATGTAA) bound by b-zip transcription factors. This led to the identification of three canonical and 4 non-canonical E-box elements within 1 kb from the start codon (for details see figure 5.1 A and Appendix D table D4 for sequences), and 2 D-box elements in positions -9280 bp and -11275 bp (Figure 5.1 A).

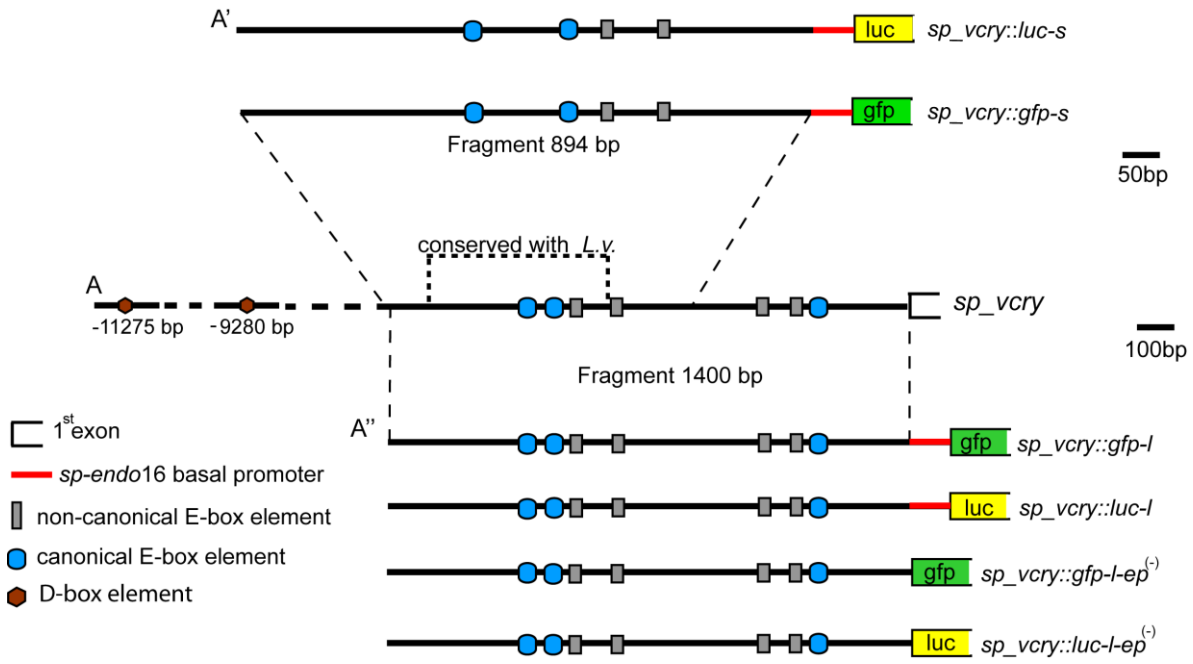

Fig.5.1 Schematic representation of the intergenic region of *sp_vcry* (A) *and* reporter genes used in this project (A'-A''). In A, in the rectangle the 564 bp region conserved with *Lytechinus variegatus* is indicated. Two different fragments have been cloned to generate reporter constructs: GFP and luciferase cassettes are under the transcriptional control of an 894bp fragment (A') and a 1400 bp fragment (A''). See figure key for details.

In addition, a BLASTn alignment search between this region with the genomic sequence of *Lytechinus variegatus* (another species of sea urchin for which a partial genome sequence exists) revealed a 564bp conserved sequence between the two sea urchin species (fig. 5.1 A for details). The conserved region includes two canonical E-boxes and one non-canonical E-box reinforcing the possibility that it might contain regulatory elements to drive rhythmic expression of *sp_vcry*.

Two DNA fragments were amplified and cloned to generate reporter constructs: a shorter fragment of 894bp (named "s" (short)), containing the conserved region with *L. variegatus*; and a longer fragment of 1400bp (named "l" (long)), which additionally encompassed other non-canonical E-boxes, the promoter region and the 5' UTR of *sp_vcry*. These fragments were used to generate GFP (used as positive control; *sp_vcry::gfp-s, sp_vcry::gfp-l, sp_vcry::gfp-l-ep$^{(-)}$*) and luciferase reporter constructs (*sp_vcry::luc-s, sp_vcry::luc-l, sp_vcry::luc-l-ep$^{(-)}$;* schematic representation is reported in Fig.5 A' – A"; for detailed maps see Appendix B). Furthermore, because of the

presence of the *sp_vcry* basal promoter in the 1400bp fragment and the presence of *sp_endo16* basal promoter in the reporter vectors, the latter promoter was removed to generate luciferase and GFP constructs only under the *sp_vcry* promoter (Fig. 5.1 A").

5.1.2 Pilot experiments based on microinjection of GFP reporter vectors.

First we assessed the functionality of the microinjection experiments for injections of exogenous DNA molecules in sea urchin embryos and verified that the cloned regulatory regions of *sp_vcry* drive expression of reporter genes. Injected DNA molecules form concatemers in the egg cytoplasm (McMahon et al., 1985; Livant et al., 1991) and are stably incorporated in a single nucleus at 2nd, 3rd or 4th cleavage causing a mosaic pattern of expression of the reporter gene (Flytzanis et al., 1985; McMahon et al., 1985; Hough-Evans et al., 1988; Franks et al., 1990; Livant et al., 1991). Thus, for each experiment, injected embryos and larvae were observed for their normal morphology and expression of GFP in expected cellular domains. Additionally, they were counted to estimate the average number of embryos that incorporate a specific reporter construct. To control for batch differences and other potential problems of the microinjection experiments the constructs *sp_he::gfp and sm50::gfp* were used as positive control. The first is a construct in which the GFP is under the control of the hatching enzyme regulatory region and is expressed in all domains of the embryo except skeletogenic mesenchyme cells. A previous study showed that GFP expression driven by *sp_he* regulatory regions is detectable on average in 95% of the injected embryos (Cameron et al., 2004). In our case, GFP signal from the *sp_he::gfp* was scored on average in 84% of injected embryos (Appendix D, table D5 and fig. 5.2 A) confirming the functionality of the microinjection experiments.

Sm50::gfp is specifically expressed only in skeletogenic cells (Cameron et al., 2004). Indeed *sp-sm50* encodes a spicule matrix protein that is expressed exclusively in the skeletogenic mesenchyme cells (Benson et al., 1987; Killian and Wilt, 1989; Sucov et al., 1988; Katoh-Fukui et al., 1992). Although the expression of *smp::gfp* was clonal, from the onset of gastrula stage, all the 32 skeletogenic mesenchyme cells express GFP (high number for a clonal expression). In fact, these cells establish filipodial contacts with one another and fuse at the onset of gastrulation, and thus GFP diffuses into all of them. In average, *smp::gfp* is detectable in 50.8% of injected embryos (Arnone et al., 1997). In the present work *smp::gfp* showed expression in an average of

53 % of injected embryos consistent with the published data (Appendix D table D5 and Figure 5.2 C).

In order to assess that the cloned *sp_vcry* regulatory regions were capable to drive the expression of the reporter gene, the GFP reporter constructs *sp_vcry::gfp-s*, *sp_vcry::gfp-l*, *sp_vcry::gfp-l-ep*$^{(-)}$ were also monitored for their GFP expression in injected embryos. A summary of the results of the different injections of *sp_vcry::gfp-s*, *sp_vcry::gfp-l*, *sp_vcry::gfp-l-ep*$^{(-)}$ is reported in table D5. *Sp_vcry* is expressed ubiquitously during embryonic development and larval stages, thus if the constructs faithfully reproduce the expression of the endogenous gene, they should drive the expression of the GFP in a mosaic way, but in all cells (Figure 5.2 B) of the larva.

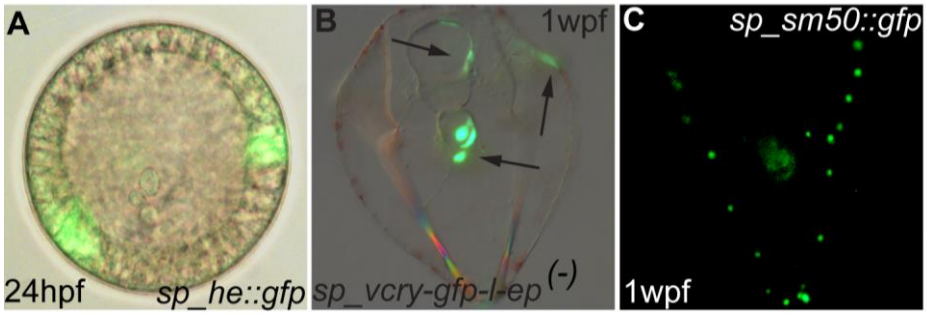

Fig.5.2 Sea urchin embryo injected with *sp_he*::gfp (A) and larvae (B, C) injected with, *sp-vcry*::*gfp-l-ep*$^{(-)}$ *and smp::gfp ,* respectively. In A and B bright-field and fluorescent-field images were superimposed to show expression of *sp_he::gfp* in 2 patches of a mesenchyme blastula (A); and expression of *sp_vcry*::*gfp-l-ep*$^{(-)}$ in cells of the gut and ectoderm of the larva (black arrows). In C, GFP signal was detected in the skeletogenic cells of a larva injected with *sp_sm50::gfp*.

GFP expression was detected for all the constructs, however, *sp_vcry::gfp-s* injection mostly caused aberrant development with an average of 29% of embryos expressing GFP and *sp_vcry::gfp-l* produced a GFP signal not strong enough to permit a significant evaluation of it and it was scored in average only in 19% of the embryos (Appendix D table D5). Additionally, GFP signal from *sp_vcry::gfp-l-ep*$^{(-)}$ was scored in an average of 58% of embryos and larvae. These results taken together suggest that the cloned 1400 bp regulatory region of *sp_vcry* is capable of driving the expression of the GFP in a manner comparable to the endogenous *vcry* gene and that the corresponding luciferase reporter *sp-vcry::luc-l-ep*$^{(-)}$ may be the most efficient construct to use in the luciferase assay.

5.1.3 *In-vivo* luciferase assay.

An *in-vivo* luciferase assay has never been performed in sea urchins, and so in order to troubleshoot this technique, the construct *smp::luc* (luciferase cassette under the control of *sp_sm50* regulatory region) was generated and used as a positive control for its potential in driving high levels of expression of a reporter gene. In order to test if the luciferase system works in sea urchin embryos and larvae, two independent pilot luciferase assays were run using embryos (fig. 5.3 A) and larvae (fig 5.3 B) injected with *smp::luc* not entrained to light/dark cycles. The assay was performed using Packard TopCount NXT Microplate Scintillation & Luminescence Counter (Whitmore laboratory, UCL) in constant dark conditions because the machine was not equipped with a system to induce light/dark cycles. The luciferase assay was performed in embryos for 48 hours (24hpf-72hpf) in batch1, and during larval stage for 24h (72hpf-96hpf) in batch2. As it was unknown how strong the signal would have been from a single embryo or larva, we plated in different wells different numbers of embryos or lavae, from 1 to 10, in duplicates. Fig. 5.3 shows a graph in which light emitted by the reaction catalysed by luciferase was measured as counts/second every hour in each well. The highest counts were measured from wells containing 10 individuals, although appreciable levels of luminescence was detected even in wells containing 2 or 5 individuals. These experiments proved that an *in-vivo* luciferase assay can be applied to study the expression of luciferase driven by regulatory regions in sea urchin embryos and larvae. Thus, we performed this technique using embryos and larvae injected with the three luciferase reporter constructs generated in this project and described above. Results for *sp_vcry::luc-s* and *sp_vcry::luc-l* are summarized in table D6, appendix D. In both experimental replicas, the construct *sp_vcry::luc-s* shows values of luminescence close to the background level identified by the uninjected embryos and larvae, whereas *sp_vcry::luc-l* shows high variability within the same batch of larvae and with respect of a second independent one.

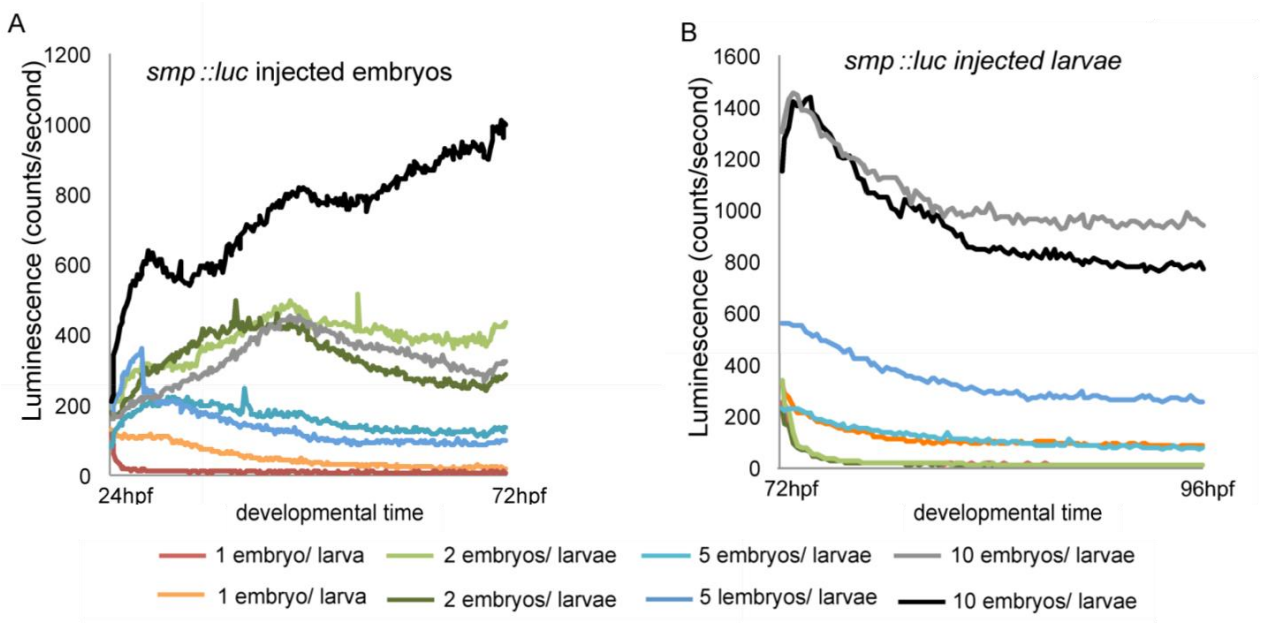

Fig. 5.3 Luminescence signal detected in embryos (A) and larvae (B) injected with *smp::luc.* Injected embryos/larvae were plated, from 1 to 10 individuals, in duplicates in different wells (see figure key for details). The different coloured lines indicate the luminescence signal counted from wells containing different nr. of embryos (graph A) and larvae (graphB). Same colour code has been used for graph A (embryo) and B (larvae).

Results of luciferase assays for larvae injected with *sp_vcry_luc-ep*$^{(-)}$ are described in fig. 5.4 (next page). Injected embryos were raised until the larval stage (at least up to 72 hours after fertilization) in light/dark conditions (12h/12h L/D), whereas the assays were run in constant dark for 46h or 70h. In both experiments, *sp_vcry::luc-I-ep*$^{(-)}$ emitted luminescence signals (Figure 5.4 A, B) characterized by an initial peak and decrease of signal with values above the background level (uninjected larvae, Appendix D, table D7 for details).

This suggests that the regulatory regions of the 1400bp fragment were sufficient to drive the expression of luciferase. However, no 24 hour rhythmic oscillation of the signal was recorded for any of the experiments. Different hypothesis may explain the absence of rhythmic oscillation in luminescence signal. First, absence of rhythmicity may not have been observed because luciferase assays were run in constant dark, thus to exclude the possibility that this condition may have affected the putative rhythmic expression of *sp_vcry::luc-I-ep*$^{(-)}$, in future, luciferase assays will be performed in a Packard TopCount NXT Microplate Scintillation & Luminescence Counter equipped with a light system for

the light/dark cycles. Second, the cloned regulatory regions may be sufficient to drive expression of the reporter gene, but might not contain the regulatory elements that convey rhythmic expression. For this reason BACs, containing the whole genomic locus of *sp_vcry* and its upstream region, will be used in the future to build a new luciferase construct.

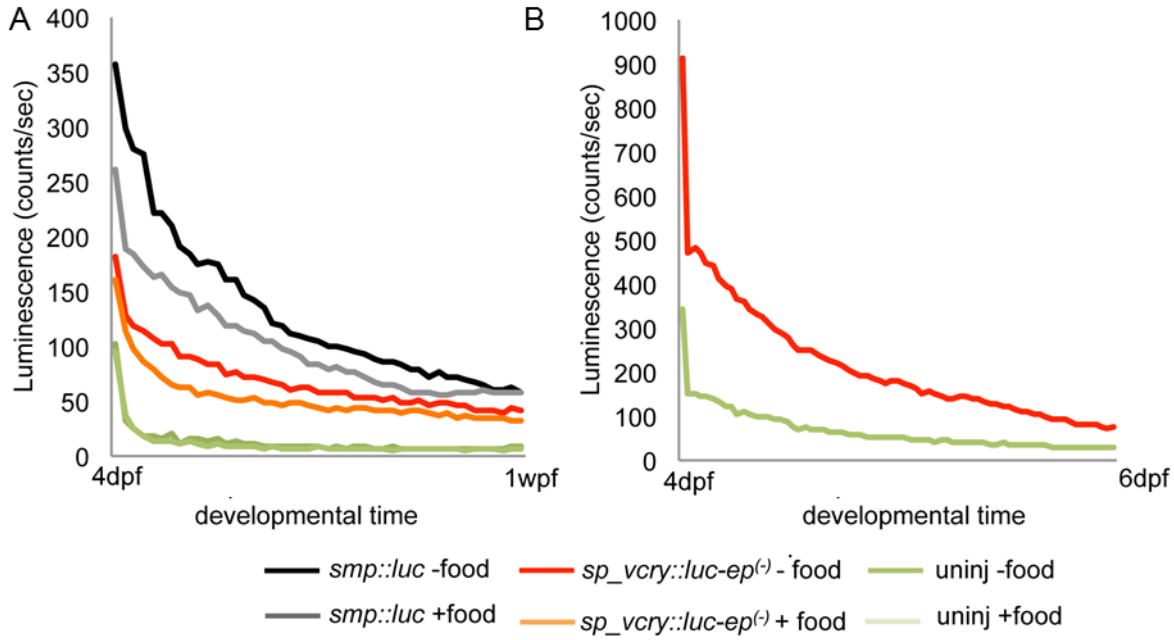

Fig.5.4 Luminescence signal detected in larvae injected with *sp_vcry::luc-I-ep*$^{(-)}$ in two independent experiments. In experiment 1 (A), 5 larvae were plated in triplicate for each condition. In addition, in order to troubleshoot the assay, absence/presence of algae (+/- food) was tested. Uninjected larvae were used as a negative control, *smp::luc* injected larvae as positive control. In B, experiment 2 was performed by plating, in triplicate, 10 larvae/well. Only unfed uninjected and unfed *sp_vcry::luc-I-ep*$^{(-)}$ larvae were used in this experiment. Because luciferase signal for each triplicates were similar, results are shown as average count/sec.

Future troubleshooting of the assay is important because this may be a very useful technique in order to study in detail the mechanism of circadian clock in the sea urchin larva. Nevertheless, in order to perform functional analysis we decided to apply a second experimental approach consisting of the knockdown of key clock genes and assessing perturbation in expression of clock candidate genes by analysing their mRNA levels.

5.2 Perturbation analysis of *sp_vcry*, *sp_tim*, *sp_dcry* and *sp_opsin3.2*.

In order to perform functional analysis we generated the knockdown of *sp_vcry* and *sp_tim,* genes characterized by circadian expression and likely components of the core clock, and the knockdown of *sp_dcry* and *sp_opsin3.2* encoding potential circadian photoreceptors and characterized by light-dependent expression.

Consequently, entrained uninjected and injected larvae were processed to analyse daily expression profiles of genes described in chapter 3 using nCounter Nanostring technology. Finally, in order to assess what roles *sp_vcry*, *sp_tim*, *sp_dcry* and *sp_opsin3.2* have within the circadian system, daily expression profiles in both conditions were compared for the presence/absence of rhythmicity, changes in amplitude of oscillation and/or levels of expression. Microinjections described in these paragraphs were performed by Dr. Paola Oliveri.

5.2.1 Set up of the sampling experiment.

First, we established a new system of entrainment and sampling to avoid overnight sampling. Embryos were entrained under light/dark conditions in two tents with inverted light/dark cycles (Materials and methods, paragraph 2.3.3 for details). A tent (tent 1) was characterized by a 12:12 light/dark cycle (ZT0 at 7 am, ZT12 at 7 pm) and the other (tent 2) characterized by an inverted cycle 12:12 dark/light (ZT0 at 7 pm (light on), ZT12 at 7am (light off)). Based on the property of entrainment of the circadian clock, larvae were collected in the presence of light at ZT0, ZT6 and ZT12 in tent1, and in the absence of light at ZT18 and ZT24 in tent2 (see figure 5.5 for details). Larvae were processed for quantitative analysis as described in Materials and methods paragraph 2.3.3.

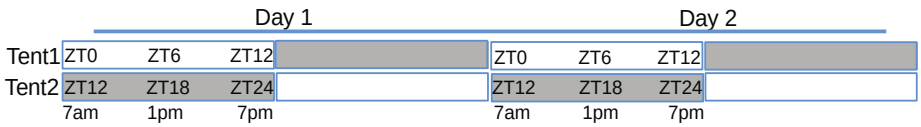

Fig.5.5 Schematic representation of the sampling of microinjected larvae using the two lightproof tents with inverted light cycles. White boxes represent time frames when light was on, dark boxes when light was off. ZT are reported within the boxes, time of sampling is reported underneath the boxes.

In order to ensure if this system of sampling did not generate high variability in gene expression between samples collected in the two tents, a pilot experiment was performed. This involved collecting 1 wpf larvae over two days as described in figure 5.5 with similar ZT between the tents: ZT12 in tent 1 and tent 2; ZT24 in day 1 and ZT0 in day2. Daily expression profiles of *sp_vcry* and *sp_tim* (fig. 5.6) were measured by qPCR.

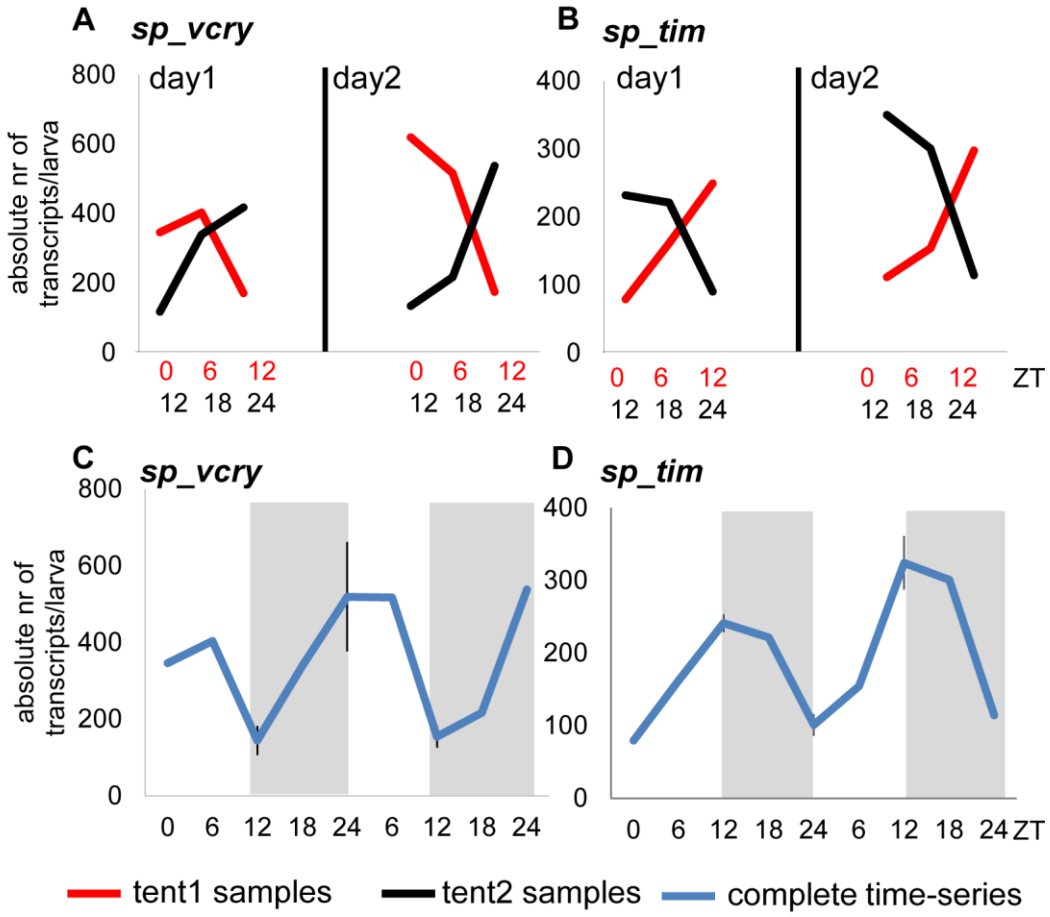

Fig.5.6 Quantitative expression analysis of *sp_vcry* and *sp_tim* from larvae collected in tents characterized by inverted light/dark cycles. In A and B, expression patterns measured from larvae collected in tent 1 (red line) and tent2 (black line) were overlapped to show the inverted profiles of expression typical of clock genes when entrained to inverted light/dark cycles. In C and D, the same expression profiles detected in tent1 and tent2 are described as a continuous representation of subjective day and night. Expression values measured in common ZT were averaged and standard deviations were calculated (bars).

In A and B quantitative data (absolute nr of transcripts/larva) are reported with the time-series of tent 1 (red line) compared with the time series of tent 2 (black line). As

expected the profiles of expression measured in the two tents are inverted: maximum level of expression is at ZT0 or 6 and minimum at ZT12 for *sp_vcry*, while maximum level is at ZT12 and minimum at ZT0 for *sp_tim*. In C and D the transcripts levels measured in tent 1 and tent 2 have been joint to show the typical 24h expression profiles of the two genes (as described in chapter4) and observe the acceptable standard deviation measured between the common time-points (fig. 5.6 C, D). From this control experiment we concluded that this system can be used to investigate daily expression profiles of clock and light-responsive genes.

5.2.2 Microinjection of morpholino antisense oligonucleotides (MO) in sea urchin fertilized eggs.

In order to generate knockdown of *sp_vcry*, *sp_tim*, *sp_dcry* and *sp_opsin3.2,* MOs specific for each gene were injected into fertilized sea urchin eggs. They were designed to act as a translation blocker, using sequences (Appendix A, table A5) from the sea urchin transcriptome database while their uniqueness was assessed by executing BLASTn against the sea urchin genome. In addition to the specific MOs, a control MO with random sequence (Appendix A, table A5) and non-specific targeting, was injected as a control to assess that the morphology of the larvae was not affected by general toxicity of morpholino oligonucleotides. Considering the embryonic expression of *sp_vcry*, *sp_tim* and *sp_dcry* and, consequently, their potential involvement in developmental processes, MOs were initially injected at different concentrations (50 μM to 300 μM) to identify the optimal conditions of knock-down, which correspond to the highest possible dose that do not interfere with normal development of the larvae. In this way the perturbation analysis was only focused on the effects of knockdown in the larva's circadian system.

Microinjection of *sp_dcry*MO and *sp_opsinmo*3.2MO at 300 and 250 μM respectively did not affect embryogenesis (Fig. 5.7 C, D, Appendix D table D8); whereas microinjections of *sp_tim*MO and *sp_vcry*MO at the same concentrations caused interference with development suggesting a general toxicity of these morpholino oligonucleotides (Appendix D, table D8). Embryos injected with *sp_tim*MO at 300 μM do not form a normal gut and have a round shape with a shortened skeleton. Injections of *sp_vcry*MO at 300 μM also generated perturbed larvae with a shortened skeleton (Fig. 5.7 E, G).

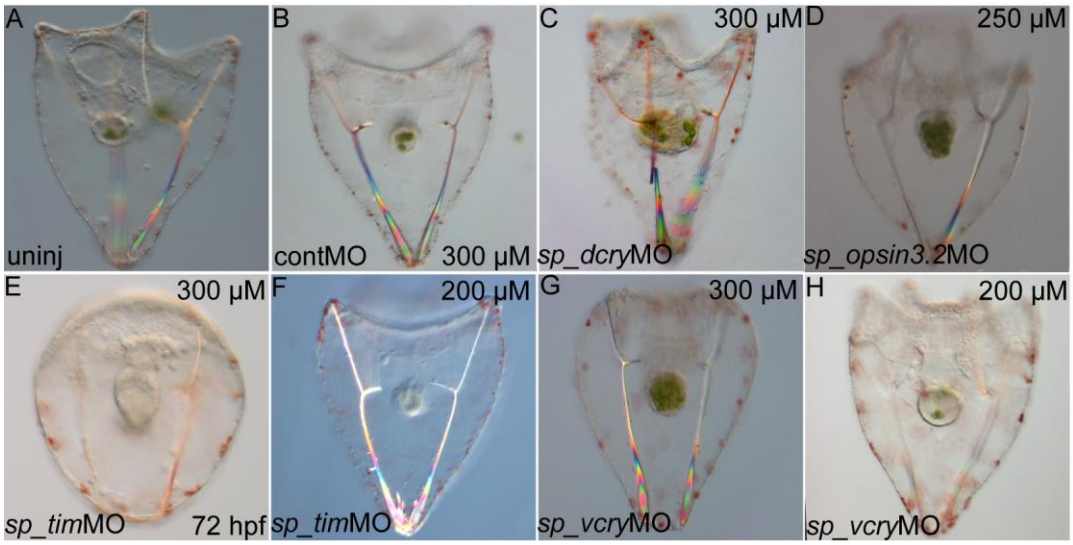

Fig.5.7 Morphological analysis of larvae injected with different MOs. Larvae were pictured alive. All larvae are at the stage of 1 wpf, except for the one injected with *sp_opsin3.2MO* (5 dpf, D) and the ones injected with *sp_tim*MO 300 µM (E).

For *sp_tim*MO a concentration of 200 µM was found optimal to allow normal development (Fig 5.7 F, Appendix D, table D7); instead, for *sp_vcry* the same concentration was found to be batch dependent (Fig. 5.7 H, Appendix D, table D8). In fact, injections of *sp_vcry*MO at 200 µM in more than one experiment (2/4) generated perturbed larvae with a shortened skeleton in comparison to the controlMO. In the present study, *sp_vcry* knockdown was obtained in two independent batches injected with different concentrations of MO (200 µM and 150 µM). To conclude, in single microinjection experiments, embryos were injected with *sp_dcry*MO at 300 µM, *sp_opsin3.2* at 300 and 250 µM, *sp_tim*MO at 200 µM and *sp_vcry* at 200 and 150 µM; they were cultured as described above and collected to be processed for quantitative analysis at the larval stage of 1 wpf.

5.2.3 Daily expression profiles of candidate genes of the circadian system in knock down conditions.

Functional analysis was performed in at least two independent batches of larvae cultured as described in paragraph 5.2.1. In the first batch injected and uninjected larvae were sampled for two consecutive days, while in the second batch larvae were sampled for 24 hours. Quantitative analysis of the genes listed in chapter3 was

performed using nCounter Nanostring technology, using lysate samples directly in the hybridization reaction. The exception to this is *sp_dcry* knock down, where microinjections were performed in 4 independent batches of embryos and quantitative analysis was performed with both qPCR (2 batches) and nCounter Nanostring technology (2 batches). Statistical significance of rhythmicity, values of amplitude, mesor and acrophase were measured using cosinor analysis. For genes with rhythmic expression, perturbation of gene expression was assessed by comparing presence/absence of rhythmicity and, changes in amplitude, mesor or acrophase between uninjected or contMO with knockdown conditions. For all other genes, perturbation effects were assessed by comparing levels of expression in the two conditions. Due to changes in the protocol required to set up hybridization reactions for nCounter Nanostring experiments (the use of lysated sample instead of extracted total RNA and the dilution of reagents such as capture and reporter probes), expression profiles for *sp_dcry* were detected below the background level for almost all the experiments (see Appendix D, table D9). Thus Nanostring data derived from *sp_dcry* quantification were not informative. In this paragraph, only genes whose expression was consistently affected by the different knockdown experiments are described. In appendix D, table D10 summarizes results obtained from cosinor analysis for *sp_vcry*, *sp_tim*, *sp_dcry*, *sp_hlf*, *sp_opsin3.2* and *sp_crydash* in all the experiments. Quantitative expression data for non-rhythmic genes (Appendix D, fig. D6) that do not show any perturbation are not reported and, as example of this category, profiles of expression of *sp_f-salmfamide* are described in Appendix D fig. D9.

Fig. 5.8 shows that daily expression profiles of *sp_dcry*, *sp_tim* and *sp_vcry* are perturbed in larvae injected with *sp_dcry*MO with respect to contMO conditions (Fig 5.8).

Fig. 5.8 (Following page). Daily expression profiles detected in larvae injected with contMO and *sp_dcry*MO by qPCR. Experiments were performed in two independent batches. In batch 1, contMO larvae were collected over 24 hours and *sp_dcry*MO larvae over 36 hours, whereas in batch 2 samples were collected for 48 hours.

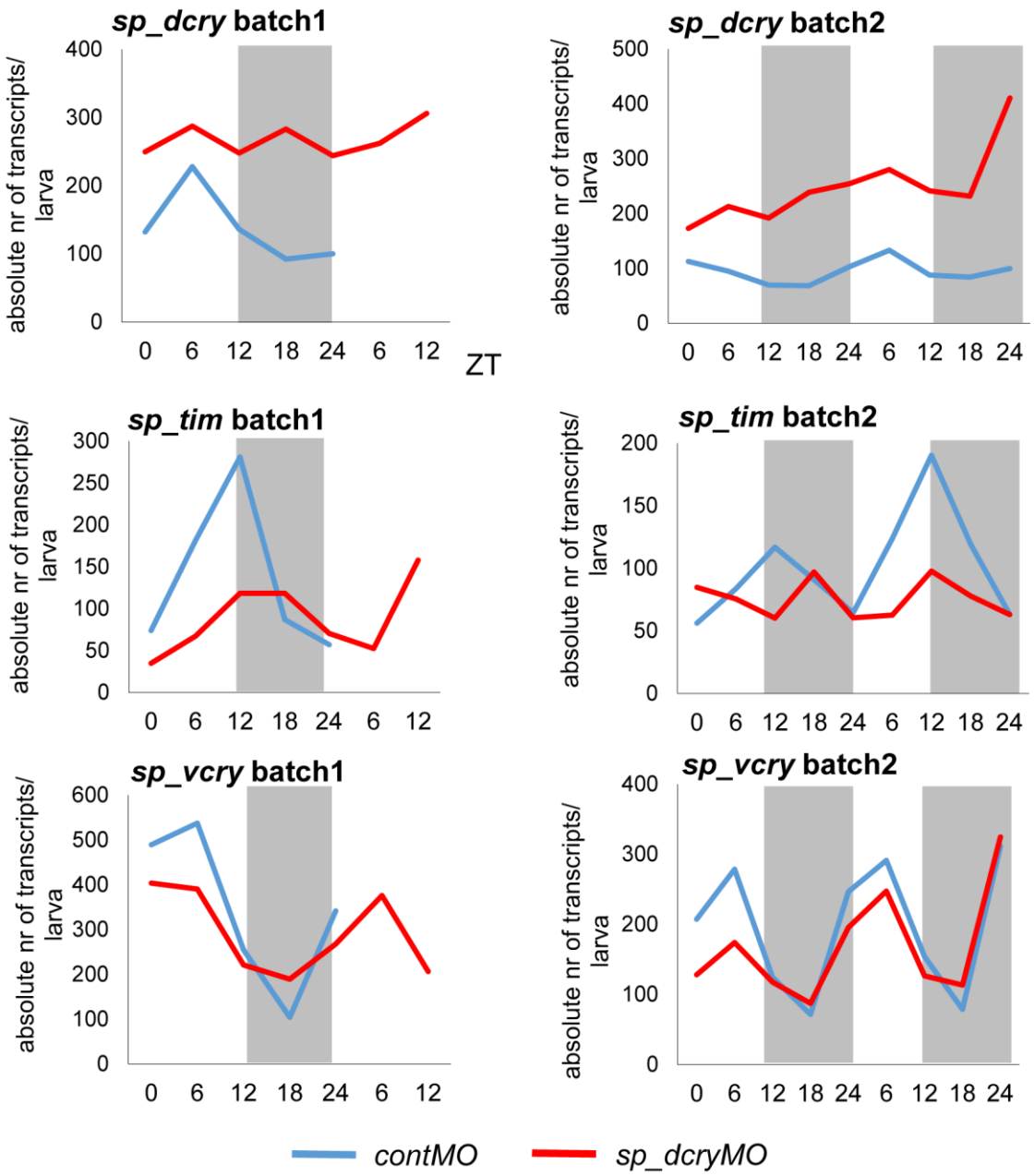

The expression profile of *sp_dcry* is characterized by absence of rhythmicity (Appendix D, table D9) and by increased levels of expression. *Sp_tim*, on the other side, shows reduced values of amplitude and mesor with its profile of expression that remains significantly rhythmic (except in batch 2, first day of sampling, for details see Appendix D, table D10). Similarly, *sp_vcry* shows decreased values of amplitude (Appendix D, table D10). In the first batch its pattern of expression remains rhythmic, whereas in the second batch is arrhythmic (even though visual inspection confirms 24h oscillatory expression both in contMO and *sp_dcry*MO samples). Rhythmicity and reduction of

amplitude of *sp_vcry* mRNA were even detected in a third independent batch where uninjected larvae were compared to injected ones and quantitative analysis was performed by nCounter Nanostring (appendix D, table D10). Taken together these results suggest that *sp_dcry* influences the light dependent expression of itself and has indirect inputs on the expression of *sp_tim* and *sp_vcry.*

The knock down of *sp_opsin3.2* results in the downregulation of the expression of *sp_hlf* mRNA (fig. 5.9). Reduction in the levels of expression is observable in both batches, although there is a degree of variability in the data. In batch one, *sp_hlf* is characterized by arrhythmicity in perturbed conditions (see Appendix D, table D9 for details); whereas arrhythmicity was detected for both conditions in batch2. These observations might suggest that *sp_opsin3.2,* a G0 opsin type, has a positive input on the light dependent rhythmic expression of *sp_hlf* and the lack of an effective downregulation may be explained by the restricted expression of *sp_opsin3.2* in only two cells of the larva compared to the ubiquitous expression of *sp_hlf*.

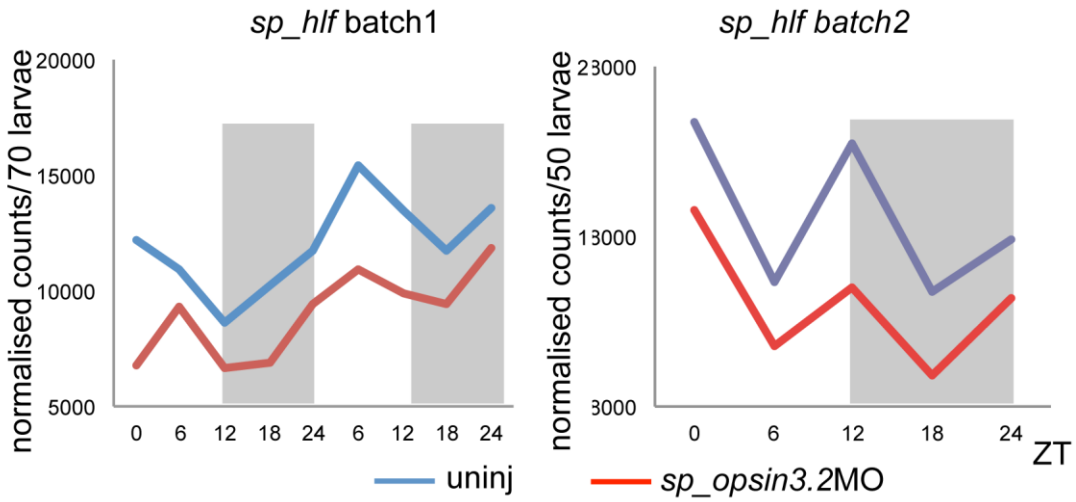

Fig. 5.9 Daily expression profiles detected in larvae injected with *sp_opsin*MO. In batch 1 nCounter Nanostring was performed using a lysate sample equivalent to 70 larvae, in batch2 with 50 larvae.

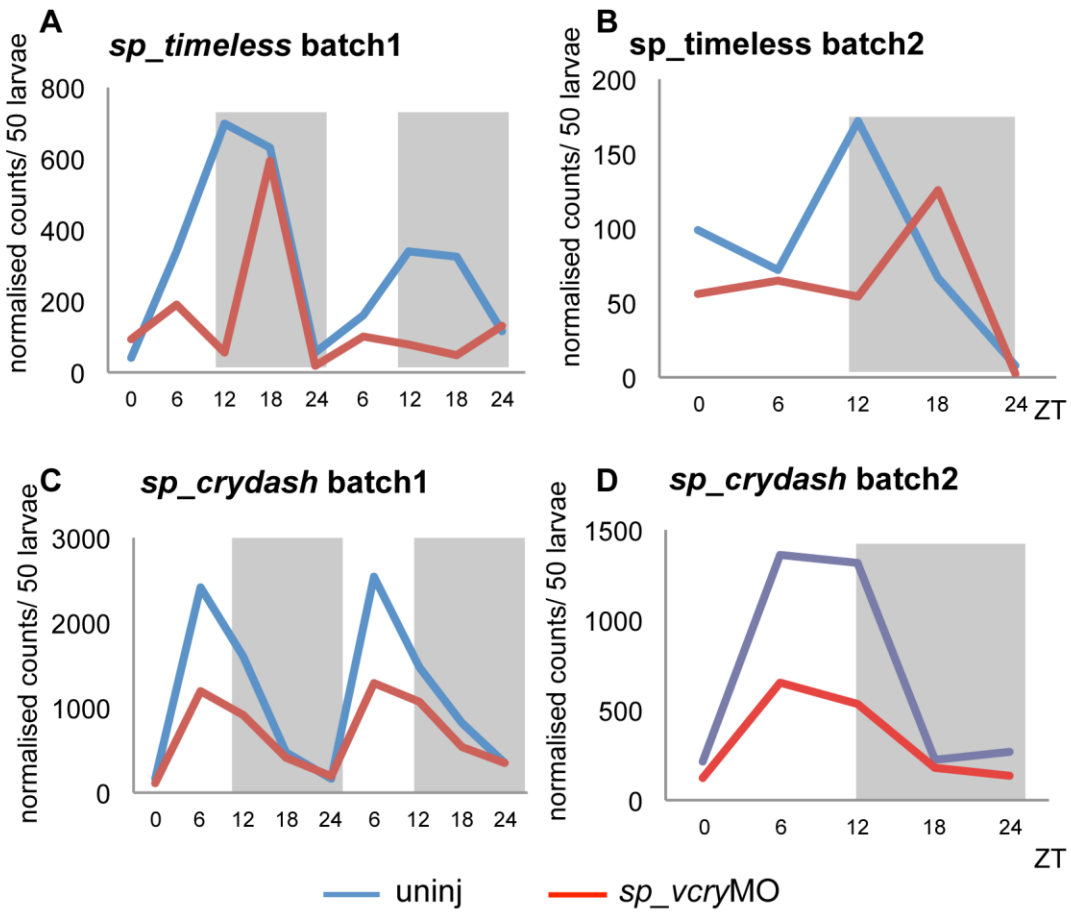

Fig. 5.10 Daily expression profiles detected in larvae injected with *sp_vcry*MO. In A and B, expression profiles of *sp_tim* detected by nCounter Nanostring and qPCR respectively (qPCR experiment performed by Wendy Hart). In C and D, expression profiles of *sp_crydash*.

Knockdown of *sp_vcry* induces arrhythmicity in *sp_tim:* in batch one the loss of rhythmicity is statistically significant (Fig. 5.10 A); in batch two (Fig. 5.10 B) a similar pattern of expression was detected even though it was not possible to detect significant rhythmicity by cosinor analysis. Interestingly, *sp_tim* mRNA expression seems to have a shift of 6 hours in knockdown conditions with a maximum peak of expression at ZT 12 in uninjected samples and ZT 18 in *sp_vcry*MO samples. This might suggest also a phase delay of *sp_tim* mRNA expression in the knockdown of *sp_vcry*.

The other gene affected in *sp_vcry*MO larvae is *sp_crydash* that, in both batches, shows a significant reduction in amplitude (3 fold of difference) and mesor (2 fold of difference) (Fig. 5.11). These results suggest that *sp_vcry* might work as a core clock

gene and influences the expression of both the clock gene *sp_tim* and the light-dependent gene *sp_crydash*.

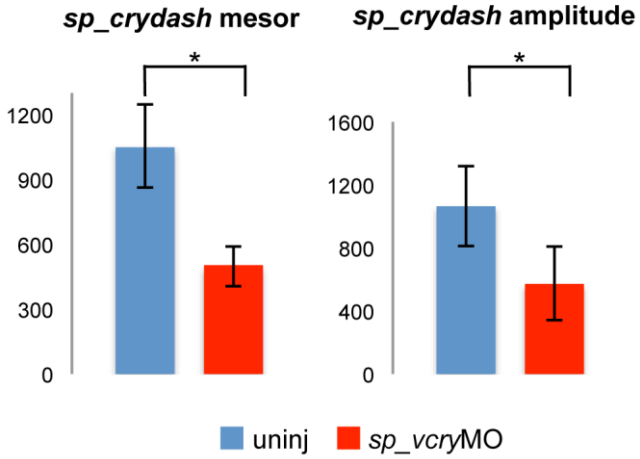

Fig. 5.11 A comparison of amplitude and mesor values of *sp_crydash* detected in *sp_vcry*MO and uninjected larvae. Bars indicate standard deviation. Statistical significance was measured by Student t-test, * indicates a p-value < 0.05.

Interestingly in *sp_timMO* knockdown, no consistent effect was detected in the expression patterns of the key genes (see Appendix D, table D9). The only affected gene is *sp_ngn,* whose expression was found perturbed in *sp_dcryMO* and *sp_opsin3.2*MO larvae as well but not in sp_vcryMO larvae (fig 5.12, next page). In *sp_dcry*MO, *sp_opsin3.2*MO, *sp_tim*MO, levels of expression of *sp_ngn* are consistently down regulated implying a positive input of the respective genes (*sp_dcry*, *sp_opsin3.2* and *sp_tim*) on its expression. *Sp_ngn* encodes a b-hlh transcription factor and has been linked to neurogenesis in sea urchins (Burke et al., 2006; Burke at al., 2014) suggesting that these genes might be involved in the regulation of this process.

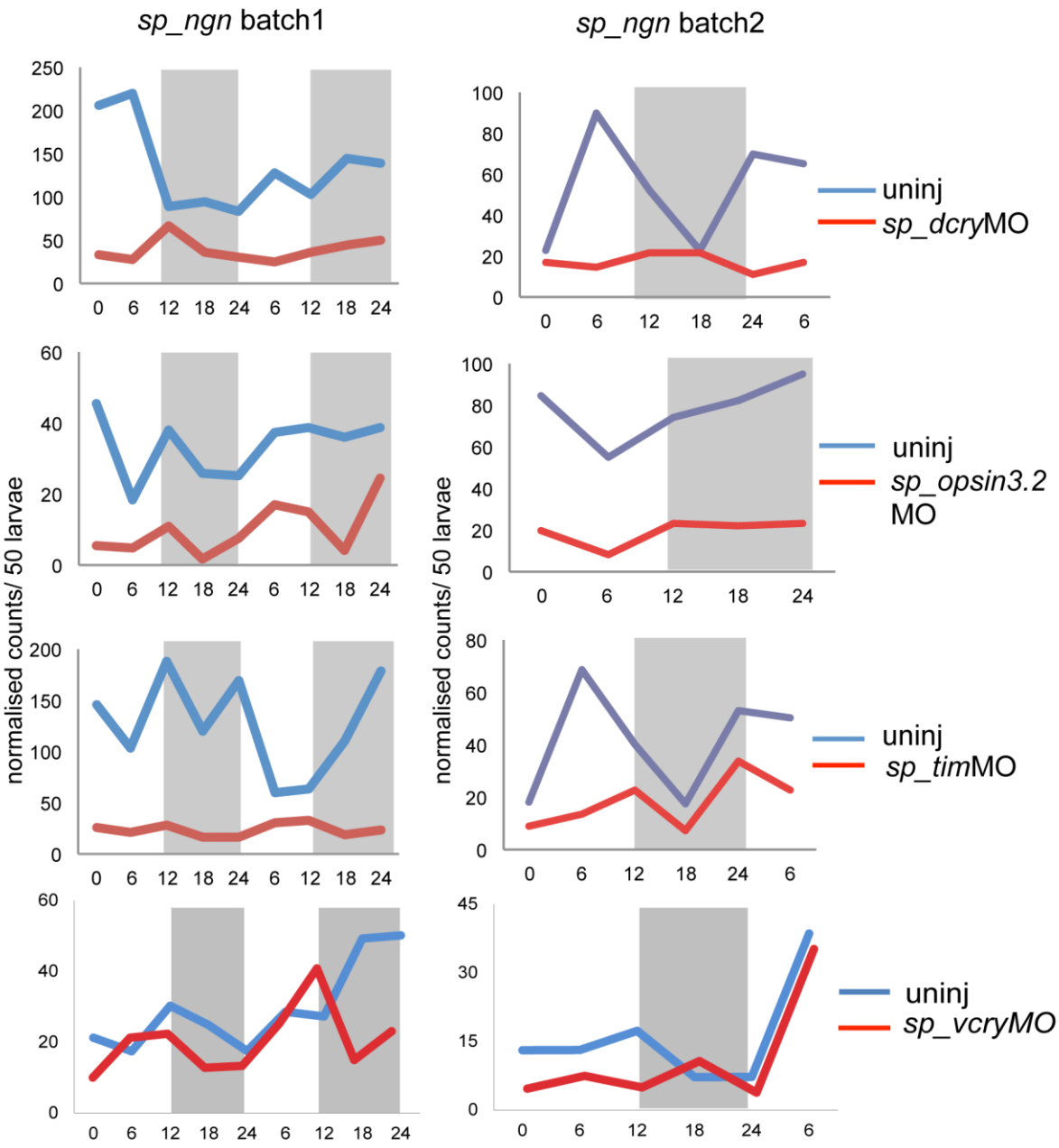

Fig.5.12 Daily expression profiles of *sp_ngn* detected in larvae injected with *sp_dcry*MO, *sp_opsin3.2*MO, *sp_tim*MO and *sp_vcry*MO. In the knockdown of *sp_opsin3.2,* batch 2, nCounter Nanostring was performed using lysate sample equivalent to 70 larvae.

Finally fig. 5.13 describes daily expression profiles of *sp_vcry* detected in *sp_opsin3.2*MO, *sp_vcry*MO and *sp_tim*MO experiments as a control of a gene with 24h oscillatory expression that is not affected in the different knock down conditions. Values of amplitude and mesor of *sp_vcry* mRNA have not been significantly affected in

*sp_opsin3.2*MO, *sp_vcry*MO and *sp_tim*MO (the ratio between uninjected/knockdown values are less than two fold of difference; see Appendix D, table D9 for details) suggesting that the results obtained for the other genes described in this paragraph are not biased.

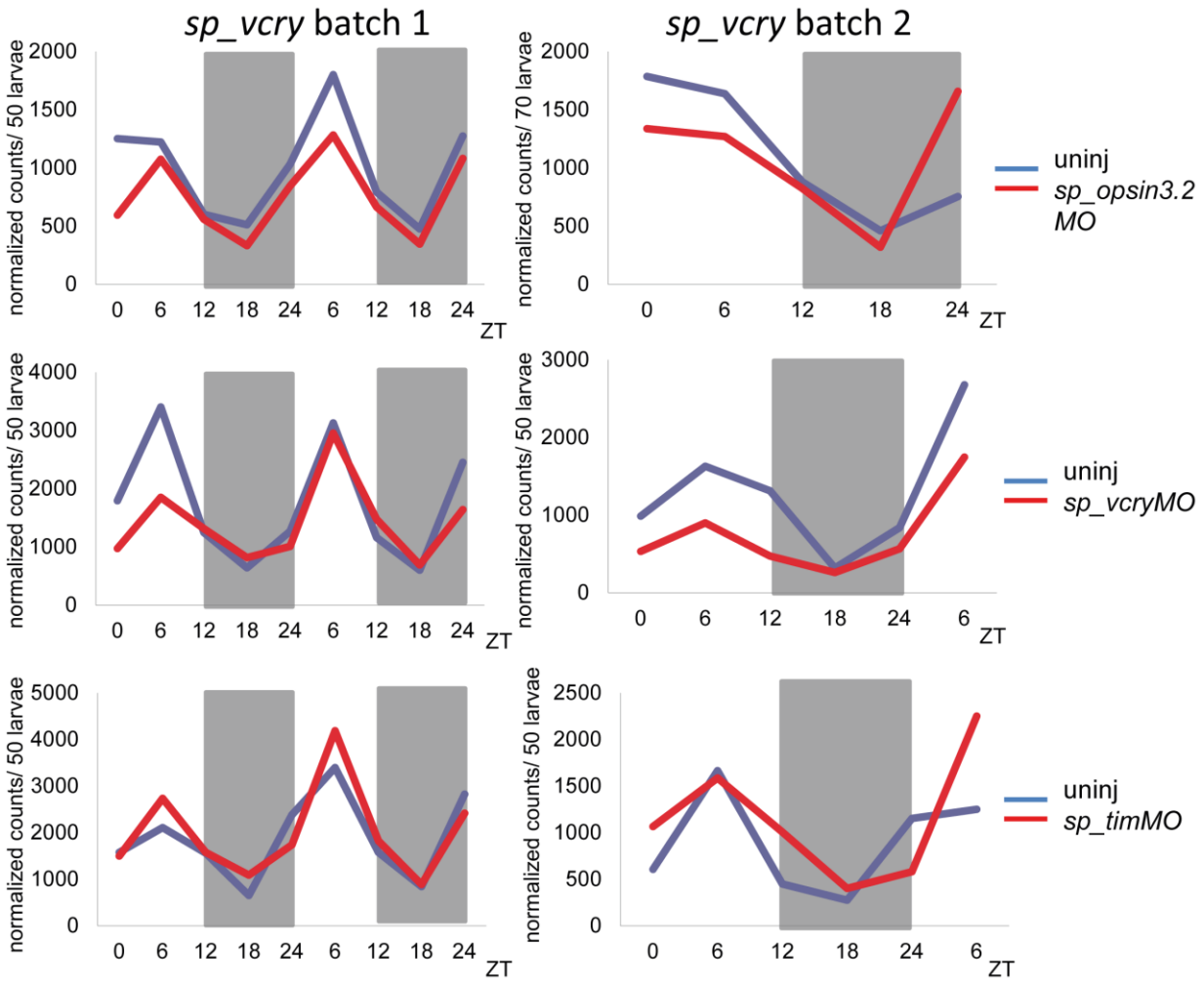

Fig.5.13 Daily expression profiles of *sp_vcry* detected in larvae injected with *sp_opsin3.2*MO, *sp_vcry*MO and *sp_tim*MO. In the knockdown of *sp_opsin3.2,* batch 2, nCounter Nanostring was performed using lysate sample equivalent to 70 larvae.

5.3 Summary.

In this chapter I have described results obtained using two different experimental strategies to perform functional experiments and have provisional insights in the architecture of the circadian system of the sea urchin larva.

For the first time an *in-vivo* luciferase assay was applied using a real-time reporter gene in sea urchin. Regulatory regions of *sp_vcry*, characterized by the presence of b-zip elements, have been used as molecular marker to monitor the molecular clock in the sea urchin larva. The 1400 bp regulatory region of *sp_vcry* cloned in the construct *sp_vcry::gfp-l-ep*$^{(-)}$ were capable of driving the expression of GFP (the GFP signal from was scored in 58% of embryos and larvae) and was used in the reporter construct *sp-vcry::luc-l-ep*$^{(-)}$ to perform the *in-vivo* luciferase assay.

The results obtained by using *smp::luc* (luciferase cassette under the control of *sp_sm50* regulatory region) proved that *in-vivo* luciferase assay can be applied to study the expression of luciferase driven by regulatory regions in sea urchin embryos and larvae. However, despite that *sp_vcry::luc-l-ep*$^{(-)}$ was sufficient to drive the expression of luciferase in injected embryos and larvae, we could not observe any oscillatory rhythmic pattern of the luciferase signal. The second strategy was based on knock down of the clock genes *sp_vcry*, *sp_tim*, and light dependent genes *sp_dcry* and *sp_opsin3.2* and analysis of daily expression profiles of candidate genes. These experiments allowed the identification of functional linkages between some of the clock and light-dependent genes: the influence of *sp_dcry* on the expression of itself and *sp_vcry* and *sp_tim*; the input of *sp_vcry* on *sp_tim* and *sp_crydash*; and the input of *sp_opsin3.2* on *sp_hlf*.

These results together with the ones described in the previous chapters are discussed in chapter 6 to delineate a provisional model of circadian clock in the sea urchin larva.

Chapter 6
Discussion

6.1. The sea urchin genome encodes components typical for both protostome and deuterostome circadian clocks.

Studies carried out in several animals, from sponges to mammals, suggest that the animal circadian clock dates back at least to the common ancestor of the extant Eumetazoa (Reitzel, 2013). Based on this observation and to reveal new details in the evolution of the animal circadian clock, we have examined the presence of the canonical set of core clock genes in sea urchin using a reciprocal BLAST strategy. Sea urchin genes homologous to canonical core clock genes were already identified in other studies carried out to elucidate phylogenetic relationships of clock genes in cnidarians and insects (see table 3.1). Nevertheless, in order to have a better annotation of the sea urchin gene models, we investigated *de-novo* the presence of these genes using the version 3.1 of the sea urchin genome (http://www.echinobase.org/Echinobase/; Cameron et al., 2009), which integrates sequencing data of transcriptomes derived from different embryonic stages, larvae and adult tissues. In addition we extended the query list by including not only the canonical transcription factors, corepressors and cryptochromes but also canonical genes involved in post-translational regulation of the TTFL and genes encoding photolyases. This resulted in a much broader overview of the hypothetical composition of the sea urchin circadian clock.

In case gene predictions were revealed as incorrect (e.g. s*p_dcry*, *sp_cpd_photolyase* and *sp_crydash*) genes were manually annotated (paragraph 3.2). In this way we had well annotated sequences to use for analysis of protein domains, to reveal important characteristics of proteins, to design primers for cloning and qPCR experiments, and as probes for the nCounter Nanostring technology and the design of morpholino oligonucleotides.

The finding that sea urchin genome contains sequences corresponding to both protostome and deuterostome canonical clock components (Table 3.1 and 3.2) suggests that the last common ancestor of all bilaterians might have a more complex clock toolkit than what seen in the so far analysed species.

Firstly, the sea urchin genome encodes the canonical set of genes encoding transcription factors that drive rhythmic expression (*sp_bmal*, *sp_clock*, *sp_hlf*, *sp_nfil3*,

sp_ror, *sp_rev-erb*), and secondly, the sea urchin genome encodes also homologs of *timeless* and *drosophila*-like *cry*, so far identified only in protostomes; thirdly, the sea urchin genome lacks a homolog to the *period* gene.

We identified one clear homolog to *bmal* and *clock* that encode for b-HLH transcription factors as suggested by the protein domain analysis (Fig. 3.1). The presence of *bmal*/*cycle* and *clock* homologs is widespread in Eumetazoa, reinforcing the idea that these b-HLH transcription factors may be factors in driving rhythmic expression in the animal core clock. Apart from the well-documented role described in insects and vertebrates, their function in the circadian clock has recently been described in *Platynereis* (Zantke et al., 2013) and in the crustacean *Eurydice pulchra* (Zhang et al., 2013). In cnidarians, in absence of functional studies, their conserved function has been hypothesized based on the findings that at least one of them has rhythmic expression (*clock*) and that the proteins undergo to heterodimerization *in-vitro* (Reitzel et al., 2010). Despite the lack of rhythmic expression of these two genes in sea urchin larva (Figure 4.4) and based on the widely conserved function in animal circadian clock, it is plausible that the two b-HLH transcription factors might still be involved in driving rhythmic expression of other clock genes. However, functional experiments are needed to elucidate their real function.

PAR-b-ZIPs transcription factors and orphan nuclear receptor factors involved in the secondary loop of circadian clocks and in the regulation of circadian outputs have been well-described in insects and vertebrates (see introduction for details). On the contrary there has been very little research directed towards their functional characterization in other animals. In the cnidarians *N. vectensis* and *A. digitifera* (Shinzato et al. 2011) three genes that match to bilaterian PAR-bZIPs have been identified with two of them being rhythmically expressed (Reitzel et al., 2013). Moreover cnidarian genomes do not contain members of the nuclear receptor 1 (NR1) family, including the homologs of *rev-erb* and *ror*. Similarly, in *Platynereis* only the homologs to b-ZIP transcription factors have been investigated showing that both have rhythmic expression (Zhang et al., 2013). In the present study, the reciprocal BLAST showed that the sea urchin b-ZIP transcription factors *sp_hlf* and *sp_nfil3* and nuclear receptor factors *sp_rev-erb* and *sp_rorα* are more closely related to the vertebrate ones, consistent with the phylogenetic position of the sea urchin as non-vertebrate deuterostome (table 3.1). However our results related to the lack of rhythmic oscillation of *sp_bmal* and *sp_clock* in addition to the finding that only *sp_hlf* is characterized by rhythmic expression in light

dependent conditions (Fig. 4.2) might suggest the absence of a secondary feed-back loop in the sea urchin circadian clock. In fact, this is the first time that it has been suggested that a secondary loop is lacking in a metazoan clock. Further investigation on the role of these genes in sea urchin and other organisms such as cnidarians are needed to comment on their evolutionary context.

So far *sp_dcry* and *sp_tim* were found only in protostome genomes, thus their presence in sea urchin has revealed new details about the evolution of circadian clock components and suggested that the sea urchin clock shares some common aspects with the protostomes clock mechanisms and divergences with the vertebrates ones. Our analysis, published in Oliveri et al. (2014) and in agreement also with previous analyses (Levy et al., 2007; Shoguchi et al., 2013) reports that the dCry photoreceptor class is present only in bilaterians. In particular the phylogenetic analysis carried out using aquatic animals, diatoms and plants revealed important findings about the evolution of the CRY/6–4 Photolyase superclass (Oliveri et al., 2014). The last common eukaryotic ancestor of these organisms might have possessed a precursor gene with double function of light sensing and DNA repair activity. Lately duplication and functional diversification events might have given rise to the 6–4 Photolyase, vCry and dCry classes at least in the common ancestor of bilaterians. This implies also the possibility that some animal cryptochromes and photolyases might have retained a double function and for this reason we have analysed all genes belonging to the CPF family for their possible involvement in the sea urchin circadian clock.

Regarding the evolutionary history of *tim*, the presence of both *tim* and *timeout* in sea urchin reveals that the duplication event that originated *timeless* as a duplication of *timeout* must have occurred at the base of bilaterians. In particular, the *tim* gene seems to be under strong evolutionary selection as suggested by its loss in nematodes, chordates and also within some insects (Rubin et al., 2006; Reitzel et al., 2010; Gu et al., 2014). This might suggest the reason for the low sequence similarities observed between Sp_tim and Drosophila Tim (Fig. 3.1; Appendix D Fig. D2).Finally our analysis allowed to have a further understanding of the evolution of the animal circadian clock consisting in sequence conservation of positive elements of the circadian TTFL as *bmal*/*cycle* and *clock* and sequence divergence of negative components as *tim*, *per* and *cryptochromes*. This is also suggested by the analysis of protein domains as shown in chapter 3: while Sp_Bmal and Sp_Clock retain conserved domains typical of b-HLH transcription factors (Fig. 3.1) that drive rhythmic expression, other proteins show

important sequence dissimilarities with their relatives (*sp_tim*) or acquisition of additional domains as for example *sp_vcry,* characterized by a unique poly-Q at the C-terminus (Fig. 3.3).

Another interesting finding that derives from the genome survey analysis is the lack of a pathway that produces melatonin in the sea urchin. Melatonin has been identified broadly throughout the tree of life, in animals, plants, and fungi, supporting a deep evolutionary origin for this signalling molecule (Hardeland and Poeggeler, 2003). Melatonin production is under circadian control in the majority of examined organisms suggesting its involvement in the circadian clock. Its function has been well documented in vertebrates as modulator of sleep (Dollins et al., 1994), while its role outside vertebrates is poorly understood. A recent study shows that melatonin regulates circadian swimming behaviour in the larva of *Platinereis* suggesting an ancient role in regulating locomotion in invertebrates (Tosches et al., 2014). Rhythmic melatonin production also occurs in *Nematostella* suggesting that a link with circadian clock is conserved also in cnidarians (Peres et al., 2014). Interestingly, the sea urchin genome encodes genes that might belong to the class of the melatonin receptors (not shown in this study). Although the function of these genes need to be investigated, the observation of their retention in the sea urchin genome, in absence of endogenous synthesis of melatonin, has driven us to propose the hypothesis of their possible involvement in binding exogenous melatonin which might be derived from the diet of the sea urchin larva. Indeed the alga *Dununiella sp,* used in our experiments, may encode the pathway that produce melatonin (Hardeland, 2015) as also identified in the metabolites pathway database MetaCyc (Caspi et al., 2014).

6.2. Molecular evidence for a circadian clock and light input pathways in the sea urchin larva.

6.2.1 *Sp_vcry* and *sp_tim* are components of the circadian clock.

So far the circadian clock has never been extensively investigated in echinoderms, only few studies report light driven processes, as phototaxis, in larvae and adults (Sharp and Gray, 1962; Emlet; 1986; Ullrich-Lüter et al., 2010). The oscillatory expression of *sp_vcry* and *sp_tim* in light/dark and free-running conditions (Fig. 4.2 A, B, C, D and Fig. 6.1) establishes for the first time that the sea urchin larva possesses a circadian clock entrained by light. Rhythmic expression of these two clock genes has been detected from the larval stage of 5 days post fertilization (Table D3) indicating that a molecular

clock starts to oscillate at completion of embryonic development. At this stage the larvae feed on phytoplankton and need to interact actively with the environment to allow optimal growing and a successful metamorphosis.

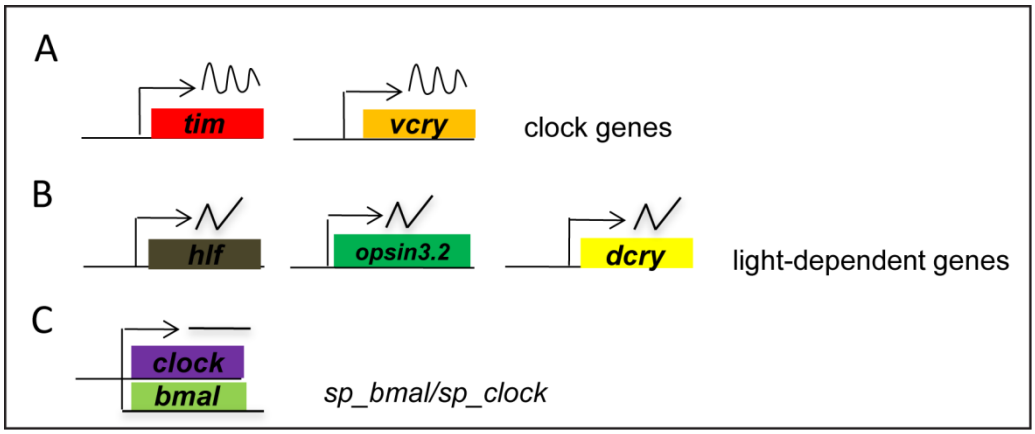

Fig. 6.1 Schematic resume of clock and light dependent genes identified in the sea urchin larva. Only genes that have been analysed more in details in this study are reported in the figure. In A, the two clock genes, *sp_vcry* and *sp_tim;* in B, the light-dependent genes *sp_hlf*, *sp_opsin3.2*, *sp_dcry*; in C, *sp_bmal* and *sp_clock*, that may be under the same regulatory control, and, although characterized by absence of rhythmic expression, have been proposed as components of the sea urchin circadian clock.

Interestingly, none of the canonical clock genes encoding transcription factors shows oscillatory circadian expression in the sea urchin larva (Fig. 4.2 F for *sp_hlf,* Fig. 4.4 for *sp_bmal* and *sp_clock*, Fig.D6 for *sp_nfil3*, *sp_rev-erb and sp_rorα*). This might highlight significant differences in the structure of the circadian TTFL in the sea urchin larva with respect to what has been observed in other organisms so far investigated. In particular these differences might be related to the absence of a secondary loop in the core clock of the sea urchin larva that regulates rhythmic expression of *sp_bmal* and *sp_clock.* If cis-regulatory modules for the binding of b-zip transcription factors or nuclear orphan receptors are conserved in *sp_bmal* or *sp_clock,* the absence of circadian expression of the typical components of the secondary loop (*sp_hlf, sp_nfil3*, *sp_rev-erb* and *sp_rorα*) may explain the arrhythmic expression of the two genes encoding b-HLH transcription factors. In addition, the light dependent oscillatory expression of *sp_hlf* might be regulated by a light input pathway potentially triggered by Sp_Opsin3.2 (Fig. 5.9) suggesting that *sp_hlf* might encode for a transcription factor

involved only in light responsive processes. This would also be in agreement with the absence of inputs of *sp_hlf* in driving expression of *sp_clock* and *sp_bmal.*

sp_vcry and *sp_tim* are characterized by dampened oscillations in free running conditions. This might be linked to an issue of desynchronization of free-running periods between the different larvae seen that the experiments of quantitative analysis shown in chapter 4 have been performed by extracting RNA from 100 whole larvae. In addition, it is not to exclude that molecular oscillators might undergo desynchronization in different tissues within a single larva when in free running.

This aspect has been well documented in *Drosophila*: molecular rhythms were characterized by dampened oscillations within 2-4 days of free-running when measured by extracting RNA from 30-50 individuals, in contrast behavioural rhythms were able to maintain rhythmicity for at least five weeks (Veleri et al., 2003). To overcome this contradiction, molecular oscillations were measured in single flies by using a *per-luciferase* construct that generated a fusion protein in only a subset of the clock neurons (Veleri et al., 2003). These experiments showed the heterogeneity of molecular oscillators in the different neurons of a single fly. Indeed the lateral neurons s-LNv, LNd and the dorsal neurons DN2 and DN3 are characterized by self-sustained molecular oscillations in free-running conditions with DN2 that oscillates in anti-phase with respect to the others. In contrast, the neurons l-LNv and DN1 contain a dampened oscillator. Heterogeneity of molecular oscillators is a characteristic also of the mouse circadian clock where studies on SCN slices and dispersed SCN cells revealed that SCN cells have a broad distribution of periods and amplitudes (Welsh et al., 1995; Westermark et al., 2009).

It has been evident that in order to have a clear understanding of the molecular features of the sea urchin circadian clock other experimental procedures had to be used in addition to the qPCR and nCounter Nanostring. For this reason WMISH has been tested as a qualitative tool to discern rhythmic expression of clock genes among individuals and to not miss the cycling of clock genes in specific tissues. *Sp_vcry* WMISH (Fig. 4.10) performed on larvae entrained to light/dark cycles has confirmed the result observed in the whole animal qPCR analysis (Fig. 4.2 A). Indeed, in light/dark conditions, larvae are synchronized to the same rhythm and within one larva mRNA levels of *sp_vcry* change rhythmically with the same trend in all cells. Therefore WMISH could be used in future experiments as qualitative tool to better characterize patterns of

circadian rhythmicity of *sp_tim, sp_vcry* and other candidate genes in larvae collected over 48 hours in free-running conditions.

We applied for the first time an *in-vivo* luciferase assay in sea urchin larvae to precisely monitor daily rhythms in gene expression in single larvae and to avoid issues related to the use of homogenised samples of several larvae. However the lack of a 24h rhythmic pattern of the luciferase signal using the *sp_vcry::luc-I-ep*$^{(-)}$construct indicates that the experiment needs to be optimized and repeated by performing it in light/dark conditions.

The study of a circadian behavioural output is a strategy that may be used to clarify features of the sea urchin circadian clock at the systemic level. In well-established model systems as *Drosophila*, zebrafish and mouse the study of circadian rhythmicity at the molecular level has been always coupled with the control of a behavioural output such as locomotor activity, facilitating the study of different aspects of a circadian clock (Rosato, 2007). For example the measuring of locomotor activity rhythms in *Drosophila* has been used in large-scale to screen for novel clock mutants (e.g. Konopka and Benzer 1971; Dubruille *et al.* 2009) and is continually used to dissect and understand clock function *in vivo*. The sea urchin larva may exhibit circadian rhythmicity in processes as swimming activity and may undergo diel vertical migration for the necessity of avoiding the harmful effects of light or for feeding necessities. There are some examples of marine larvae in which swimming activity has been proposed to be linked to the circadian clock or presence/absence of light. *Platinereis* larvae (Tosches et al., 2014) are characterized by rhythmic production of melatonin that regulates swimming behaviour, whereas the swimming activity of sea urchin sand dollar larvae have been shown to respond to UV light (Pennington and Emlet, 1986).

In this project, some attempts have been performed in establishing an experimental system to monitor swimming activity in sea urchin larvae entrained to light/dark cycles (data not shown). One attempt consisted of using the device that monitors locomotor activity in *Drosophila.* Based on the assumption that sea urchin larvae may be characterized by diel vertical migration, larvae entrained to light/dark cycles should swim up and down in the column of water with a 24 hours rhythm both in light/dark and free running conditions. In order to prove this hypothesis, sea urchin larvae were placed in tiny glass tubes (filled with sea water) crossed by an infra-red light beam hitting photovoltaic cells. An electronic signal would have been emitted by the photovoltaic cells, each time a larva had crossed the beam (the hypothesis was once every 24h).

However, the infrared system was unable to detect the passage of sea urchin larvae probably because larvae are too small or transparent.

A second attempt consisted of filming swimming activity of larvae placed in a small chamber and recording their distribution in the column of water at different time points. This system has been troubleshooted in order to optimize the application of a transparent chamber where to place the larvae and the use of a camera to record their swimming activity, the number of larvae to insert in the chamber, the tracking of the larvae in dark conditions. However some of these aspects need still to be resolved to optimize the system and allow the study of the swimming activity in the sea urchin larva.

6.2.2 Genes with light-dependent oscillatory expression.

Light-dependent signalling is a feature common in most of the living forms from cyanobacteria to plants, fungi, and animals to trigger mechanisms that are related to the presence/absence of light such as photosynthesis, growing, repair of UV-induced DNA damage, entrainment of the circadian clock and vision. Most of genes involved in these mechanisms show light dependent mRNA regulation (e.g. Wijnen et al., 2006) likely as adaptive strategy to optimize the molecular response during exposure to sunlight. Moreover it is more and more evident that components of the circadian clock are also subject to a light-dependent expression in addition to a circadian one. Examples are given by the light-response expression of *mper1* in mice (Albrecht et al., 1997) and *zfper2* and *zfcry1a* in zebrafish (Vallone et al., 2004; Mracek et al. 2012). In particular the mechanism how light induces the expression of clock and light-dependent genes has been studied in zebrafish where D-box elements bound by b-zip transcription factors have been characterized as critical light-responsive regulatory modules (Vatine et al., 2009; Laura et al., 2012).

In this project, apart from the two clock genes *sp_vcry* and *sp_tim*, several genes show oscillatory expression in light/dark but not in constant dark conditions (Fig. 4.2 E, F, G, H, J for *sp_dcry*, *sp_hlf*, *sp_opsin3.2*; Fig. 4.3 for *sp_crydash* and *sp_6-4 photolyase*; Fig. D7 for *sp_cpd photolyase*) giving the possibility to analyse the presence of light input pathways and their possible role in the entrainment of the circadian clock of the sea urchin larva.

Sp_dcry and *sp_opsin3.2* might encode for photoreceptors and their light dependent pattern of expression indicates that they are not under circadian control. *Sp_hlf* is characterized by light-dependent oscillatory expression and likely it might be involved in

light input pathways similar to what has been described in zebrafish (Vatine, 2011). Light signalling pathways might regulate the expression of *sp_hlf* and, in turn, regulate the expression of clock genes and/or other classes of genes including those involved in the repair of UV-damaged DNA. We identified also genes of the photolyase-cryptochrome class linked to mechanisms of DNA repair (*sp_6-4 photolyase*, *sp_cpd photolyase*, *sp_crydash*) although their role in this activity was not analysed in this study, their diurnal oscillation in mRNA levels suggests the presence of light-sensing pathways that may trigger the activation of their expression.

6.2.3 The hypothetical output genes.

Regarding molecular outputs, none of the 29 genes, described as hypothetical output genes in Chapter 3, show circadian expression. This might be explained by different hypotheses: 1) some genes might not be involved in circadian output mechanisms; 2) others might be not under circadian transcription or control but regulated rhythmically at other levels of regulation. This might be the case of neuropeptides given that in mouse and fruit fly there are examples of neuropeptides which mRNA levels are not under circadian regulation but the peptide undergoes into a cellular rhythmic release (GRP and AVP in mouse (Francl et al., 2010) and PDF in *Drosophila* (Park et al., 2000)); 3) the whole larva approach or desyncronization issues might have made impossible the detection of output genes.

6.3. Cellular organization of the circadian system in the sea urchin larva.

Studies performed in *Drosophila*, zebrafish and mouse have revealed so far two different typologies of circadian system within an organism: 1) hierarchical in mouse with a master clock in the suprachiasmatic nuclei (SCN) that communicate timing information to most cells of the body via a range of direct and indirect cues; 2) cell autonomous organization with light that can directly entrain the rhythms of most of the cells in fruit fly and zebrafish (see introduction for details).

The WMISH experiments showed in chapter 4 give first insights into the cellular organization of the clock and light input system of the sea urchin larva although this experiments were not sufficient to reveal the type of circadian organization (hierarchical or cell-autonomous, Fig. 6.2). The co-expression of *sp_vcry* (Fig. 4.5, 4.10) and *sp_tim* (Fig. 4.5) in the apical organ and gut suggests a primary role for these organs in the circadian system of the larva. This hypothesis is also reinforced by the observation of

the expression of *sp_dcry* (Fig. 4.5, 4.7, 4.8; Fig. D8) in these two structures of the larva (Fig. 6.2).

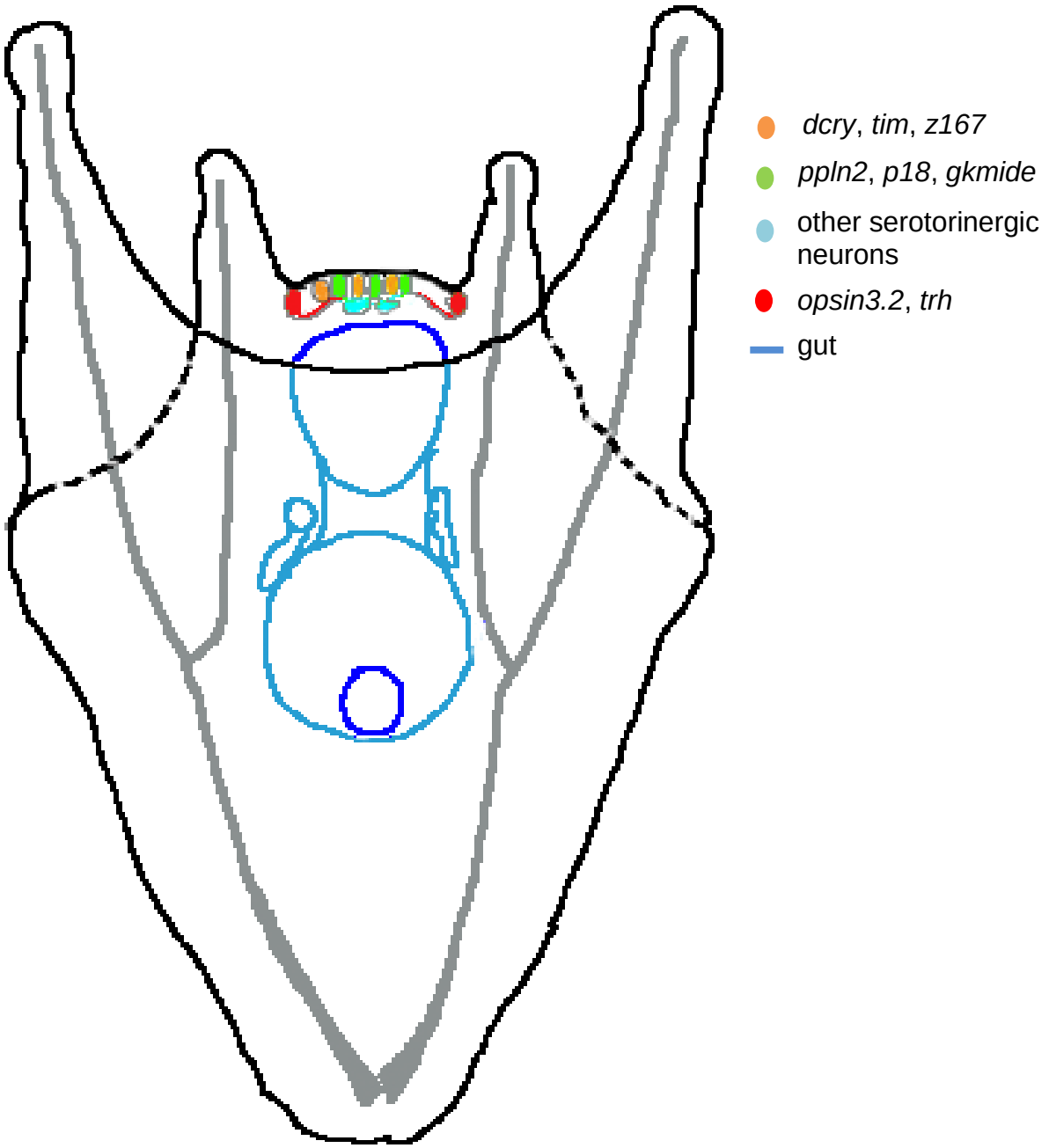

Fig.6.2 Cellular organization of the circadian clock in the sea urchin larva. Drawing of a four arms pluteus (1 week old sea urchin larva viewed from an abanal view) with apical organ (different coloured cells) and gut (blue) in highlights. All cells of the larva express *sp_vcry*, *sp_hlf*, *sp_clock* and *sp_bmal*. The apical organ is organized in at least two different types of serotoninergic neurons: three serotorinergic neurons are characterized by the expression of *sp_dcry*, *sp_tim* and *sp_z167* (orange); other three serotorinergic neurons express the neuropeptides *sp_ppln2*, *sp_gkmide* and *sp_p18* (green). Two cells (red), localized in the antolateral arms, express *sp_opsin3.2* and *sp_trh* and send projections to the serotorinergic neurons. The gut is characterized by the localized expression of *sp_tim* and *sp_dcry*. The drawing of the larva has been made by Dr. Paola Oliveri.

6.3.1 Clock neurons and light sensing cells in the apical organ of the sea urchin larva.

At the larval stage the apical organ is a complex neurogenic structure and might be contain cells organized in a network of clock neurons with *sp_dcry* expressing cells that might integrate light input stimuli. Similarly to mouse and *Drosophila* where SCN (Yan, 2009) and clock neurons (Veleri and Wulbeck, 2004) are organized in diverse subpopulation of cells that have different functions within the circadian system, the sea urchin larva apical organ might possess different cell types involved in different circadian functions. The cell heterogeneity of the apical organ has been already observed in Avi Lerner's PhD thesis (Development of the sea urchin apical organ: cellular mapping of gene expression and FGF signalling, 2013) where at least two different types of serotoninergic neurons were identified (Fig. 4.6, 4.7). One type of serotorinergic neurons (three cells) is characterized by the co-expression of *sp_dcry*, *sp_tim* and *sp_z167* (Fig. 4.6) describing these cells as possible light-sensing and/or clock neurons likely involved in the entrainment of the circadian clock of the sea urchin larva. This hypothesis is supported by the similarities of expression patterns found with *Drosophila* clock neurons DN1. *Sp_z167* is homolog to *Drosophila glass*, encoding a zinc finger transcription factor necessary for the development of photoreceptor cells in *Drosophila* (Moses et al., 1989). Glass is not only expressed in the visual system of *Drosophila* but is also co-expressed with *dcry* in the subset of DN1 clock neurons (Klarsfeld et al., 2004). The double mutant glass^{60j}cry^{b}, which lacks all known photoreceptors, loses the ability to entrain the circadian clock to light (Helfrich-Forster et al., 2001) indicating that *Drosophila* utilizes at least three photoreceptors systems for entrainment: DN1 neurons, the compound eyes, and the H-B eyelet. Therefore an interesting experiment that might delineate the role for the *z167-dcry* neurons as circadian photoreceptor cells will consist in analysing the knock down of *sp_z167* in the sea urchin larva.

The second type of serotoninergic neurons (three cells) express a set of neuropeptides (*sp_gkmide*, *sp_ppln2*, *sp_18*, Fig. 4.8) and other genes (*sp_vcry*, *sp_hlf*, *sp_bmal* and *sp_clock* (Fig. 4.5)) except *sp_dcry* and *sp_tim* suggesting that these cells might have neuro-secreting functions. In general, genes encoding neuropeptides have been found to have no circadian expression in other organisms but their protein products carry out their signalling action through cellular release with circadian rhythmicity (Francl et al., 2010; Helfrich-Forster et al. 2000). In the future, it will be possible to analyse the

involvement of sea urchin neuropeptides in the signalling of circadian information for the synchronization or regulation of physiological/behavioural outputs.

A new cellular type has been identified adjacent to the apical organ at the base of the anterolateral arms where two non-serotoninergic cells express *sp_opsin3.2* and *sp_trh* (Fig. 4.9) possess all the characteristics to have light sensing and neuro-signalling functions. Indeed *sp_opsin3.2* groups in the subfamily of the Go opsins and it is associated to ciliary photoreceptor cells in other metazoans (Kojima et al., 1997). This suggests that a potential photoreceptor and neuropeptide might be involved in a light input pathway with the signal triggered by Sp_Opsin3.2 that might extend to the adjacent apical organ and/or other cells of the larva through the action of Sp_Trh.

These findings fall also in the context to better discern the functions of the apical organ in different marine larvae and whether this structure shares a common evolutionary origin within metazoans (Nielsen, 2005a; Raff, 2008; Sly et al., 2003). Apical organs play a role in the detection of settlement cues for the induction of metamorphosis (Conzelmann et al., 2013; Hadfield et al., 2000; Rentzsch et al., 2008) and regulation of the activity of ciliary bands and musculature (Croll and Dickinson, 2004; Goldberg et al., 1994; Satterlie and Cameron, 1985). Here I suggest that the sea urchin apical organ may also have role in the circadian system at least as light sensing organ. The relationship between the apical organ and the circadian clock has also been described in the larva of *Platinereis* (Tosches et al., 2014) where expression patterns of clock genes and ciliary opsin have been shown in the apical organ. In contrast to bilaterians, in the *Nematostella vectensis* larva, distinct nerve cells have not been identified within the apical organ (Chia and Koss, 1979; Nakanishi et al., 2012) and clock genes are expressed only in endodermal territories (Peres et al., 2014).

6.3.2 Possible roles of the gut within the circadian system of the sea urchin larva.

The pronounced or localized expression of *sp_vcry* and *sp_tim* (Fig. 4.5, Fig. 4.10, and Fig.6.2) in the gut might suggest different roles for this organ in the circadian system of the sea urchin larva.

In mouse, it is becoming more and more evident that food acts as input for the cyclicng of clock genes in metabolic organs without affecting the central clock in the SCN suggesting the presence of two self-sufficient clocks: the SCN entrained by light and the metabolic clock entrained by food. Both coordinate each other to provide effective energy homeostasis (Stephan et al., 1979; Damiola et al., 2000; Hara et al., 2001;

Stokkan et al., 2001). Nevertheless, molecular mechanisms driving the food-entrainable clock are not yet known.

In addition metabolism is under circadian control in all well studied model systems: genes encoding enzymes involved in glucose, fatty acid and cholesterol metabolism exhibit circadian expression (Sahar et al., 2012; Eckel-Mahan et al. 2013).

Feeding activity is very important in the sea urchin larva to guarantee optimal growing and success in metamorphosis, thus it should not be surprising if the gut might contain a self-sustained clock or display metabolic activitities circadian-dependent.

The molecule that might trigger food entrainment might be the exogenous melatonin absorbed from the algal diet as hypothesized in paragraph 6.1. Moreover, the expression of *sp_dcry* in the gut needs to be further investigated. There are some evidences that this gene is also expressed in this organ from 1 week post fertilization (Fig. D8) suggesting that these cells might be able to perceive light information.

Therefore, future research lines could be directed in analysing: 1) food as zeitgeber that entrain the circadian system of the sea urchin larva; 2) gut as location of an independent cellular clock; 3) metabolism under circadian regulation.

6.4 Provisional functional linkages in the regulatory network of sea urchin clock genes.

The functional analysis described in Chapter 5 allowed the identification of functional linkages between some of the genes described in this study: the influence of *sp_dcry* on the expression of itself and *sp_vcry* and *sp_tim* (Fig. 5.8), the input of *sp_opsin3.2* on *sp_hlf* (Fig 5.9) and the input of *sp_vcry* on *sp_tim* and *sp_crydash* (Fig. 5.10).

In order to discuss the results of the functional analysis some considerations need to be made. First, in this study injected and uninjected larvae were collected only in light/dark conditions to analyse the possible effects of the different knockdowns on genes with light dependent expression. However the circadian clock is an endogenous mechanism and, to really discern the function of the clock genes *sp_vcry* and *sp_tim*, functional analysis need to be performed on uninjected and injected larvae exposed to constant conditions.

Second, based on the localized expression of *sp_dcry* and *sp_opsin3.2*, our quantitative analysis performed on the use of whole larvae (paragraph 5.2) cannot completely distinguish the effects of their knock down on the expression of *sp_vcry*, *sp_hlf* and *sp_tim*. These genes are characterized by broader spatial expression patterns. Thus, in

order to understand if Sp_dCry and Sp_Opsin3.2 act only in their domain of expression or trigger signalling pathways that expand in the whole larva, quantitative analysis need to be supported by WMISH experiments. This will allow analysing spatial expression patterns of putative affected genes in MO-injected larvae collected at different time-points.

Third, the functionality of morpholino oligonucleotides used in this project need to be tested with the use of antibodies in order to confirm the downregulation of the protein of interest in MO-injected larvae. In particular the efficiency of their knockdown after 1 week from the microinjection needs to be tested. Nevertheless, we based our analysis on the observation that morpholino oligonucleotides injected in fertilized eggs were shown to be still functional in 1wpf sea urchin larvae in a previous study (Oliveri et al., 2008). Finally, the functional analysis performed in this study is incomplete for the lack of information about the expression of *sp_dcry* in the different knockdown experiments. This because of technical problems related to the quantification of *sp_dcry* probe in nCounter Nanonstring experiments (paragraph 5.2, Table D9 for details).

Further experiments will be performed in future to resolve all these considerations.

From the results obtained in this study, provisional functional linkages can be described in the cells of the apical organ and the gut where *sp_vcry*, *sp_tim* and *sp_dcry* are co-expressed (Fig. 6.3 A) and in the two cells at the base of the anterolateral arms of the sea urchin larva expressing *sp_opsin3.2* and *sp_trh* (Fig. 6.2 B).

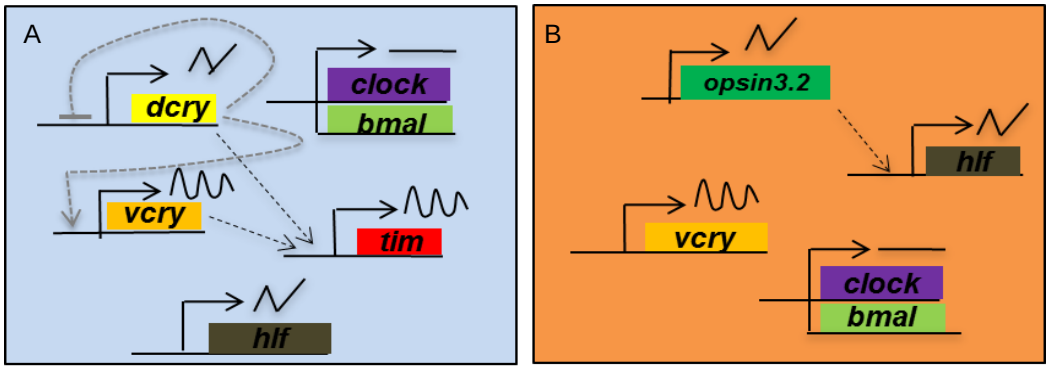

Fig.6.3 Provisional networks of the genes described in this study. In A, the functional linkages between genes expressed in the three serotoninergic neurons *sp_dcry*$^{+}$ and gut^{+} in B the linkages described in the two cells of the anterolateral arms adjacent the apical organ. Dashed arrowed lines indicate possible indirect linkages.

Results obtained from *sp_dcry*MO and *sp_opsin3.2*MO suggest that sea urchin larva might possess at least two light input pathways. *Sp_dcry* might encode a light sensing protein regulating *sp_vcry* and *sp_tim* expression in the apical organ serotoninergic neurons and likely in the gut. In *sp_dcry*MO both genes seem to maintain their rhythmic expression with reduction of levels of amplitude for *sp_vcry* and amplitude and mesor for *sp_tim* (Fig. 5.8).

The function of Sp_dCry as light sensing protein is also supported by the protein domain analysis that individuates all typical features of a light-sensing cryptochrome (Fig. 3.2). Interestingly its C-terminal diverges from that of *Drosophila* Cry (Appendix D, Fig. D4) involved in regulation to light and interaction with dTim (Busza et al., 2004; Dissel et al., 2004; Hemsley et al., 2007). This suggests that Sp_dCry may respond to light or interact with proteins in a different way with respect to *Drosophila* Cry. *Drosophila* Cry, after the removal of 20 C-terminal residues, can still entrain the clock under low levels of light (Busza et al., 2004; Dissel et al., 2004). This observation, for example, suggests that Sp_dCry might activate itself in presence of low levels of light.

Interesting research avenues that might help in elucidating mechanisms of regulation to light and protein interactions of Sp_dCry involve the analysis of protein interactions in heterologous systems *in-vitro*, the heterologous expression of *sp_dcry* in *Drosophila* cry^{b} and thus the behavioural analysis of the mutant fruit flies to different light conditions.

In addition *sp_dcry* has a negative indirect input on itself (Fig. 5.8) suggesting that the pathway triggered by *sp_dcry* may be involved in regulating its own light-dependent expression likely in a feedback mechanism to control rhythmic levels of the protein Sp_dCry as expected for a light-dependent mechanism. Interestingly, this result finds similarities with what have been described in *Drosophila* where the *Drosophila cry* participates directly or indirectly in its own transcriptional regulation (Stanewsky et al., 1998).

The second light input pathway involves *sp_opsin3.2* and *sp_hlf* in the two cells located at the base of the two anterolateral arms. These cells, as discussed before, might have characteristics of photoreceptor cells. Our result does not elucidate if *sp_opsin3.2*MO induce arrythmicity in *sp_hlf* expression most likely because of issues of variability related to this gene (Fig. 4.2, Table D3 and Table D9). Furthermore it would be interesting to analyse, by using WMISH, if the effect of *sp_opsin3.2*MO on *sp_hlf* expression is localized in the two *sp_opsin3.2*$^{+}$ cells or extended to the whole larva,

given the ubiquitous expression of *sp_hlf*. This experiment may elucidate if the light input pathway triggered by Sp_Opsin3.2 has a global action in the whole larva. Without excluding the possibility of masking effects because of the presence of other photoreceptors, the *sp_opsin3.2*MO does not affect the rhythmic expression of *sp_vcry* and *sp_tim* suggesting that *sp_opsin3.2* might not have a role in the clock of the sea urchin larva.

The effect of *sp_vcry*MO on the expression of the clock gene *sp_tim* (Fig. 5.10) suggests that *sp_vcry* might be a core clock gene. Interestingly its knockdown does not induce arrhytmicity on itself (Fig 5.13 and Table D9) as we would have expected in the knock down of a core clock gene involved in a transcriptional-translational feedback loop. This result might be explained by the presence of light input pathways that are involved in driving rhythmic expression of *sp_vcry* independently by the core clock, given that experiments have been performed on larvae collected in light/dark conditions. If this is the case, functional analysis performed on *sp_vcry*MO-injected larvae kept in free running conditions might verify this hypothesis.

The protein domain analysis for Sp_vCry identifies typical domains for the hypothetical interaction with Bmal and Clock as a canonical vertebrate-like Cry. In addition the poly-Q at the C-terminal of Sp_vCry might have conferred novel functions with respect to corresponding orthologs analysed so far in insects and vertebrates (Fig. 3.2). Poly-Qs have been shown to be involved in protein–protein interactions and transcriptional regulation (Mitchell and Tjian, 1989; Schaefer et al., 2012). Sp_vCry with its 24 hours rhythmic activity might bind Sp_Bmal and Sp_Clock on the regulatory regions of clock genes and repress their transcriptional activity. In this way the interaction between Sp_vCry and Sp_Bmal/Clock might confer 24h rhythmicity at the two transcription factors in driving transcription of clock genes. Moreover *sp_vcry*MO has a consistent effect on the expression of *sp_crydash*, characterized by oscillatory expression only in LD conditions (Fig. 5.10) reducing significantly its amplitude of oscillation and values of expression (mesor, Fig. 5.11). This result suggests the influence of the sea urchin circadian clock on *sp_crydash*, characterized by only light-dependent oscillatory expression. It will be interesting to analyse its function in the sea urchin larva in future experiments.

Sp_tim does not have any effect on the expression of *sp_vcry* and itself in LD conditions, as normally would be from a typical core clock gene (Table D9). The only gene that was affected in *sp_tim*MO is *sp_neurogenin*, which was also downregulated

in *sp_dcry*MO and *sp_opsin3.2*MO but not in *sp_vcry*MO (Fig. 5.12). This suggests that *sp_tim*MO may have worked and induced the knockdown of *sp_tim* in the injected larvae. If this is the case, the absence of effects on *sp_vcry* expression and itself expression in LD condition might be explained by the presence of other inputs that induce rhythmic expression of the two clock genes in LD conditions. In order to better elucidate the effects of the knockdown of *sp_tim,* functional analysis will be performed on *sp_tim*MO-injected larvae kept in free running conditions.

The downregulation of *sp_neurogenin* in *sp_tim*MO, *sp_dcry*MO and *sp_opsin3.2*MO suggests that the three genes are involved in regulating *sp_neurogenin* expression. Neurogenin encodes a b-HLH transcription factor likely involved in neurogenesis processes (Burke et al., 2006; Burke at al., 2014).

Based on the data described in this study I have suggested a provisional model of the core clock in the sea urchin larva (Fig. 6.4, next page). The core clock might be composed of *sp_vcry* and *sp_tim* that are regulated in a circadian manner at mRNA level; *sp_bmal* and *sp_clock* that might exhibit circadian activity only at protein level. Sp_Clock and Sp_Bmal might form a heterodimer and drive the circadian expression of *sp_vcry* and *sp_tim*. Differences in phase of oscillation of these two genes might be caused by the presence of mechanisms of post-transcriptional regulation. Sp_vCry and Sp_Tim might be the components of the negative feedback loop. Sp_vCry might be involved in the interaction with Clock/Bmal and inhibition of their transcriptional activity on the regulatory regions of the clock and clock controlled genes. This interaction might confer 24h rhythmicity to the activity of the two transcription factors. However, it is not to exclude the presence of post-translational mechanisms (e.g. phosphorylation), not been taken in consideration in this study, that might confer 24h rhythmicity to the activity of the proteins. Sp_dCry might function as light sensing protein involved in a mechanism of entrainment that regulates the light-dependent expression of *sp_vcry*, *sp_tim* and itself.

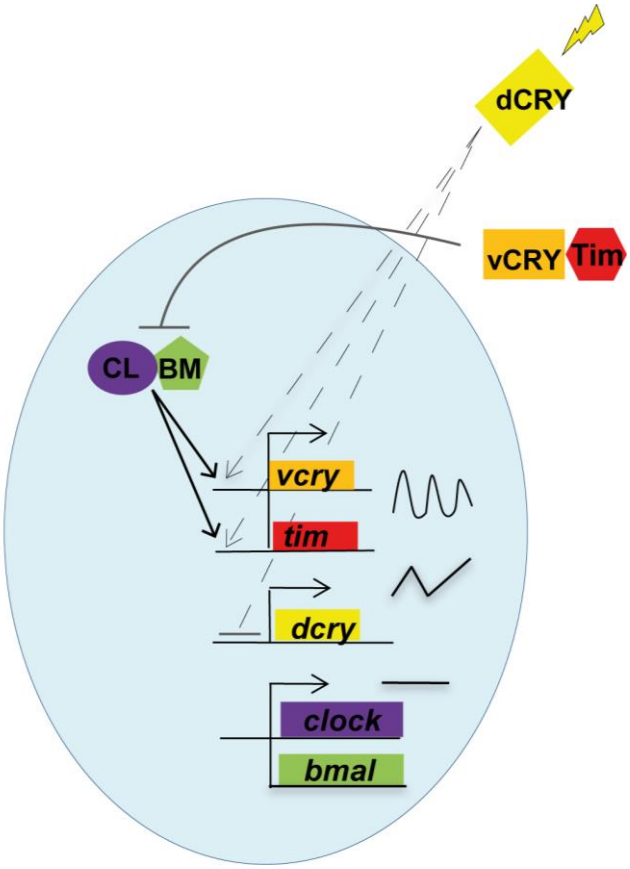

Fig. 6.4 Provisional model of the circadian TTFL in the sea urchin larva. Although the results obtained in this study are preliminary I have suggested a provisional model of the circadian TTFL in cells where co-expression of *sp_vcry*, *sp_tim* and *sp_dcry* has been identified (three serotoninergic neurons of the apical organ and gut). Hypothetical direct linkages have been depicted with continue lines, hypothetical indirect linkages with dotted lines. Sp_Clock (CL), Sp_Bmal (BM). See text for details.

Despite the functional analysis obtaining consistent results for *sp_vcry*MO knockdowns, we also realized that it is prone to variability likely caused by the experimental procedures and/or genetic variability. As discussed in paragraph 6.2 if food is an important zeitgeber its use during circadian experiments needs to be revaluated. Another issue may be related to the exposition of larvae cultured in tent 2 to different and prolonged times at red dim light during procedures of washing and feeding. Larvae may sense dim red light when exposed for a long time and thus gene expression might be sensible to this exposition.

Moreover, variability detected in the different experiments might be linked to genetic variability. Indeed, apart from *sp_vcry*, *sp_tim*, *sp_crydash*, *sp_6-4 photolyases* that have showed consistent expression patterns in different experiments (Fig 4.2, Fig. 4.3, Table D3, Table D9) other genes are more variable in gene expression. This is the case

of *sp_hlf* and *sp_dcry* that have been found variable by quantitative analysis (Fig 4.2, Fig. 4.3, Table D3 and Table D9).

6.5 Conclusion and future directions.

For the first time the mechanism of circadian clock has been analysed in the sea urchin larva. Genome survey identified almost all canonical clock genes known in protostomes and deuterostomes, with exception of *period*, indicating that the last common ancestor of all bilaterians already had a complex clock toolkit. The circadian clock starts to oscillate consistently in the free-living larva as shown by the rhythmic expression of *sp_vcry* and *sp_tim* in both light/dark and free running conditions. Interestingly, our analysis allowed the identification of only two rhythmically-expressed clock genes suggesting that the circadian clock might be organized in a simple feed-back loop in the sea urchin larva. On the other hand, several genes are characterized by light dependent rhythmic expression (*sp_dcry*, *sp_opsin3.2*, *sp_hlf*, *sp_crydash*, *sp_6-4 photolyase, sp_cpd photolyase*) and might be involved in light-dependent pathways. Furthermore, the spatial expression analysis ascribes to apical organ and gut a primary role in the circadian system of the sea urchin larva. The apical region of the larva, that might also be location of clock neurons, is characterized by the presence of at least two types of light perceiving cells: serotoninergic cells expressing *sp_dcry* and non-serotoninergic cells expressing *sp_opsin3.2*. The functional analysis based on MO approach, although has yielded variable results, has given also first insights in the functional linkages between the genes analysed in this project. *Sp_dcry* might be involved in a light sensing pathway that might regulate the expression of *sp_vcry*, *sp_tim* and itself expression. On the contrary, *sp_opsin3.2* and *sp_hlf* might be involved in a second light input pathway not related to the circadian clock. Finally, *sp_vcry* knockdown induces arrythmicity in the clock gene *sp_tim* indicating that *sp_vcry* might be a core clock gene.

Importantly, our study highlights differences in the architecture and gene regulation of the sea urchin larval circadian clock compared to other metazoan clocks. This might have occurred through changes in cis-regulatory regions (which might explain the absence of rhythmic expression in *sp_bmal* and *sp_clock*), loss of genes (a homolog to *period* is absent in sea urchin), functional diversification with acquisition or loss of protein domains (see the polyQ in Sp_vCry, the C-terminal of Sp_dCry and the probable lack of Per binding sites in Sp_Tim).

On the other hand, this study does not provide information about the roles of transcription factors in the circadian clock of the sea urchin larva: functional analysis of *sp_bmal*, *sp_clock* and *sp_hlf, sp_rev-erb, sp_rorα, sp_nfil3* is fundamental to discern a circadian network and it will be analysed in future experiments implementing information and critical points obtained in this study.

Being the first time that the circadian clock has been analysed in the sea urchin larva, it has been important to define some critical points regarding the experimental approach that has been used in this study. The whole larva approach and the use of several larvae to determine molecular oscillations may have been factors that have prevented the study of circadian clock in details. In order to overcome possible issues of desynchronization between the different larvae, future analysis will implement other experiments based more on a single larva approach. WMISH and immunohistochemistry will be used as qualitative tool to discriminate rhythmic expression patterns of genes and proteins in single larvae. In particular WMISH will be performed on larvae collected in free running conditions to better understand the cellular organization of the circadian clock.

A reliable behavioural output of the sea urchin circadian clock, useful as standard readout of the clock function, has not been found in this study. Next experiments will be directed in improving the monitoring of the swimming activity of the larva in LD and DD conditions. The filming of the swimming activity of the larvae will be troubleshooted in order to record their distribution in the column of water at different time points.

The luciferase assay using *sp_vcry* regulatory regions as molecular marker of the sea urchin circadian clock show some promising preliminary data of expression of luciferase but did not allow for measuring rhythmic gene expression yet. The assay will be troubleshooted and used to discern the involvement of candidate genes within the circadian clock of the sea urchin larva.

In addition, the functional analysis described in this thesis needs to be supported by other experiments. To really discern the functional linkages of the clock genes *sp_vcry* and *sp_tim*, functional analysis will be performed in uninjected and injected larvae exposed to free-running conditions and, additionally, WMISH experiments will be performed in MO-injected larvae collected at different time-points.

Furthermore, morpholino oligonucleotides might dilute and be less efficient as development go forward from a single cell to the 1500-2000 cells of a larva. Thus, the

functionality of morpholino oligonucleotides used in this project will be tested by using antibodies against the protein of interest in MO-injected larvae.

The functional analysis could be improved by adopting other techniques. The CRISPR system (clustered regularly interspaced short palindromic repeat), consisting in editing a genome at a precise position to generate loss-of-function mutations, is a methodology successfully applied to sea urchin embryos (Che-Yi and Yi-Hsien, 2016). This technique could be used to overcome possible issues related to the variations in morpholino efficiency after 1 week from micro-injection.

The functional analysis should also be supported by a complete bioinformatic analysis for the identification of putative regulatory sequences of genes such as *sp_tim*, *sp_bmal*, *sp_clock*, *sp_hlf*, *sp_dcry*. Regulatory regions have been analysed for *sp_vcry* that is characterized by E-box elements suggesting that the circadian expression of this gene might be driven by Sp_Bmal and Sp_Clock. This analysis may facilitate the understanding of the functional linkages between genes analysed in this study.

The experimental strategy described in this thesis, based on the analysis of mRNA expression of canonical clock genes, has allowed the identification of two clock genes and the description of a provisional model of the core clock of the sea urchin larva. Nevertheless, a different experimental approach, based on the analysis of the activity of the proteins, needs to be used in order to have a more clear understanding of the role of the candidate genes in the core clock of the sea urchin larva. For example, *Drosophila*-like Crys from fruit fly and butterfly undergo a light-dependent reduction in protein levels in S2 cells because of proteasome-mediated degradation (Lin et al., 2001; Zhu et al., 2005). If *sp_dcry* functioned as light-sensing protein, a reduction in its protein levels might be observed after that *sp_dcry*-transfected S2 cells have received a light-pulse treatment. *sp_vcry and sp_tim* activity could be assessed in S2 cells as well by co-transfecting them with *sp_bmal*, sp_*clock* and a E-box-containing luciferase construct. *sp_bmal* and *sp_clock* might induce activation of luciferase activity while the presence of *sp_vcry* or *sp_tim*, if they worked as negative repressor, might mediate a reduction of luciferase expression.

Additionally, the experimental design used in this project has been focused on a candidate gene approach based on the observation that the main components of the circadian clock are well conserved in bilaterians. However, it is not to exclude the hypothesis that different genes, not necessarily related to those identified in other organisms, might be involved in the circadian clock of the sea urchin. Thus, future

experiments will be focused also in using higher throughput technologies such as RNA seq for screening other genes characterized by circadian expression. New candidate genes will be then analysed for their role in the circadian system by functional analysis.

Finally, this study is a first attempt to characterize the circadian clock in the sea urchin larva. *Sp_vcry* and *sp_tim* have been identified as clock genes, other genes such as *sp_dcry*, *sp_hlf*, *sp_opsin3.2*, *sp_6-4 photolyase*, *sp_cydash* and *sp_cpd photolyase* are characterized by oscillatory light dependent expression. The spatial expression patterns described in this study have provided first insights into the cellular organization of the circadian system of the larva. The preliminary set of knockdown experiments have aimed at establishing a provisional model of the core clock of the sea urchin larva.

.

Appendix A

The present appendix contains a list of primers sequences used for qPCR, cloning and sequencing; a list of clones, with their details; a list of probe sequences used for the Nanostring nCounter experiments; and a list of MO sequences used for knockdown experiments.

Table A1 List of primer sequences used for qPCR reactions.

Gene name in Sp	**Forward primer**	**Reverse primer**
bmal	CAAGCAACCAGCAGATCGTA	TGGCTACTGCAACCAGACAG
clock	GGACGTTAGAACCGGACAAA	ACTAAGCTGCGTGGAGAGGA
tim	CATGCCATCCAACAGTTCAC	TCTCGCAGGAAGGACAAAGT
vcry	CTGCAGATGTGCTTCCAAGA	CCTCCTGCGCTAAGGTACTG
dcry	GGGTGTGCGTTATCTGACCT	CTCAATGCACTCGACCTTCA
arnt	GCTTCTGCCATCTGAGGAAC	GATGGTGGCCAGTTCTTGAT
sim	TGCAACAGCTTGTGAGGTTC	GGTAGCCTGCTGCGTAACTC
hlf	TGAAGGAGCGTCTCCTGTTT	CTCATTGGTGGTGGAGGACT
ahr	ACATTCGATGATGCCCTCTC	CACTGCAAGCGTGTCAAGAT
ncoa	CACACCACCATTCAGGTCAG	GCGTTGCAGGGTTGTTATTT
rev-erb	ATGAAGACGGAGCAGCTCAT	CGCCGTTATTGTTGTTGTTG
rorα	CCACACCATCACAACCATGT	AAGACTTTGGCACGGCTTTA
nfil3	AACTACGCGCAACGTTTCTA	GTGCGGAACCTCATCATCTT
6-4 photolyase	TCCACCAGATGGAGGAGAAC	CAGCCTTCGGTCCTTAGTTG
crydash	TGACCTTCGATACCGTGACA	GAGGAACTTGAGGCGATGAG
cpd photolyase	CGCATGTACTGGGCTAAGAA	TCGTGGATGCCACAAATAGA
ubiquitin	CACAGGCAAGACCATCACAC	GAGAGAGTGCGACCATCCTC
18S	CAGGGTTCGATTCCGTAGAG	CCTCCAGTGGATCCTCGTTA

Table A2 List of primer sequences used for cloning and sequencing.

Gene name/Use	Forward	Reverse
sp_dcry/3' RACE	GAGAAGCTCAAGGCATGGAC (inner)	TGCCTGATCCTATCCTCACC (outer)
sp_dcry/directional cloning	CCGGAATTCATGCCTGGCGGTGCCT	TCCGCTCGAGATTAAGAAAAAGGAACAAAC
sp_crydash/directional cloning	TACGCTCGAGTCACTTCTGGCTAGGATTAG	TACGCTCGAGTCACTTCTGGCTAGGATTAG
sp_vcry/ amplification regulatory region (894bp)	TGGTATACTGGTTTTCATGAATGG	GCCGGATCGGTAAATTTTGT
sp_vcry/ amplification regulatory region (1646bp)	TGGTATACTGGTTTTCATGAATGG	GCTACAAGATCCTGCGAACC
sp_vcry/ directional cloning (913bp)	GATGAGCTCTGGTATACTGGTTTTCATGAATGG	GGTCACGCGTGCCGGATCGGTAAATTTTGT
sp_vcry/ directional cloning (1664bp)	GATGAGCTCTGGTATACTGGTTTTCATGAATGG	GACACGCGTGCTACAAGATCCTGCGAACC
sp_opsin 3.2/ cloning	CCACTCATTTCGTGCGGATT	CTCTAGTGATGACGGGCGAT
sp-nfil3/cloning	CCGATTCGGATACCAAAGAA	CGGATTCTGAGGGAATTCAA
pSPORT/ Probe template	GTGCTGCAAGGCGATTAA	TGTGGAATTGTGAGCGGATA
GFP-20/ sequencing	CTAGCAAAATAGGCTGTC	
GFP-REV/ sequencing		TGGTTTGTCCAAACTCATCAA
Luciferase-R/ sequencing		CTCGAAGTACTCGGCGTAGG
Sp6/sequencing	TATTTAGGTGACACTATAG	
T7/sequencing	TAATACGACTCACTATAGGG	
pGEX6p1/ sequencing	GGGCTGGCAAGCCACGTTTGGTG	CGGGAGCTGCATGTGTCAGAGG

Table A3 List of clones used in this work. Their use is reported in the info column; in case of probe for WMISH, type of RNA polymerase is reported in brackets.

Clone name	Gene name in *Sp*	Vector	Clone size	Info
sp_dcry 3'	*dcry*	pGEMT-easy	1672 bp	3' end of *dcry* cloned by RACE
sp_dcry full length 21	*dcry*	pGEX6p1	1553 bp	Complete cds of *dcry*
sp_opsin 3.2	*opsin 3.2*	pGEMT-easy	1175 bp	Probe synthesis (SP6 RNA pol)
sp_crydash cds	*crydash*	pGEX6p1	1641 bp	Complete cds of *crydash*
sp-vcry-1.6reg	*vcry*	pGEMT-easy	1646 bp	Vcry regulatory regions (+183 to -1463)
sp-vcry-894reg	*vcry*	pGEMT-easy	894 bp	Vcry regulatory regions (-569 to -1463)
sp_bmalB	*bmal*	pSPORT1	1867 bp	Probe synthesis (SP6 RNA pol)
sp_clock	*clock*	pGEMT-easy	1206 bp	Probe synthesis (T7 RNA pol)
sp_tim	*tim*	pGEMT-easy	1717 bp	Probe synthesis (T7 RNA pol)
sp_dcry	*dcry*	pGEMT-easy	1288	Probe synthesis (SP6 RNA pol)
sp_vcry	*vcry*	pGEMT-easy	1887 bp	Probe synthesis (SP6 RNA pol)
sp_hlf	*hlf*	pSPORT1	1700 bp	Probe synthesis (SP6 RNA pol)
sp_tph	*5ht*	pGEMT-easy	1062 bp	Probe synthesis (T7 RNA pol)
RNSP-9L6	*p18*			Rowe and Elphick 2012
RNSP-5B10	*ppln2*			Rowe and Elphick 2012
RNSP-5K1	*gkmide*			Rowe and Elphick 2012
RNSP-9P21	*trh*			Rowe and Elphick 2012
	foxa			Tu et al., 2006

Table A4 List of probe sequences used for Nanostring nCounter experiments. Name of the target genes, corresponding accession number and target sequences used to design the probes are listed in the present table.

Gene name	Accession number	Target sequence
p18	EC439524	TATCCGTTAGAGACGAGAAGACAAACAATAAATAACCA ATAAAGTAAAGGCAGTAAAGCTCGTGCATTCGGTCCGA AATTACAAAAGAGGAACGCAGAAA
ets1/2	Materna el al., 2010	GCTCATCGCCACACGTACAGAAGCCGAGTAATTCCTG GTCGACGATTCGAGTTCGACCTCCAACAAGAGCCGCG CTGAGCATCAATCATGGCGTCTATGC
foxA	Materna el al., 2010	CACGCGCATACACATCAGTGGAGGCTGACACTATATAC TTTAGCAGATATATACAAACATACACTCAGCTCACGATC GAGAGAGAGAGAGGAACACAACG
arnt	GLEAN3_00129	CAAGCCAAAAGTCGAGACTGGGTGTGGCTTCGAACCA GCTGCTTCAGCTTTCAGAATCCTTACACCGATGAAGTG GAGTACATCGTCTGCACCAATACAG
collier	GLEAN3_04702	GGCCGGAGAGCGAGAAGACTTGACCCATCTGAAGGAG CTACGCCGTGCATCAAGGCAATCAGCCCTAGCGAAGG ATGGACAACAGGGGGCGCCACTGTCA
sim_1	GLEAN3_13962	CAGTTACTTAAAGATGCGTGCCCTATTCCCTGAAGCAT CGCCAGGTAATGGAGCGGTAAACCGGAGCACCGATCT TATTTGCAATTTTCGCTCCGATTGC
rx	GLEAN3_14289	GCACGCAGCAGCGGTCGCTGTCGCTGCAGCCGCCAG CCAAACAGCTATGTTTCCTTTGCTCAGCCCGACTCATC TCACATCGCCTCCTGGCCGCCCTGGG
z60	GLEAN3_15358	AGTTTGATCAACGAAGCGGTATCGGCTCAGCCTATCGT ATCCTGCGAGACGGCTTGTTTCACACCTAGCTGCACCT CAAGCTTTCAGATCGCCAGCACTC
rev-erb	GLEAN3_17492	TCAGATGAAGACGGAGCAGCTCATACTAAGCATCCATG AAGCACAGAAGAAGACCTTATGGGATTGGGGCATCCT GCAATGCAGGAGTTATAACCTTCTA
fez	GLEAN3_19089	TCACCCAAACTCGCATTTTCAATTGATAGCATCTTAGGA ATCAAGAAGATGAAGAAATCTAAACTTGAGCCATCGGT GAACGAGGATGCATTCCATAAAG
ubq	GLEAN3_21496	TTGTCAAGACCCTCACCGGCAAGACCATCACACTCGAG GTCGAGCCAAGTGACTCCATCGAGAACGTAAAGGCCA AGATCCAGGACAAAGAAGGCATCCC
acsc	GLEAN3_28148	GTCGCACGCCGTAACGAACGGGAGCGAAACCGCGTCA AACTCGTCAACCATGGATTCGCCAATTTACGCCAGCAG CTCCCTAACGGCGCCAATAATAAGA
lhx2	Materna el al., 2010	CACTACGAAACCCTCTTCGTTCCGTCCTCCGATCAGAG CACCTATCACCATCTCCACCACGCCTCGCCTCCTCCTC CGCAACCAACCCTCCATAATCTCT
hbn	LOC575572	AGGCGCAGCAGCGGCTCACGACGGCGCCAAGCTCTC CCATTCCCTTCCAATCTCCATCCCGAAACTCTACATGTC GCCTGCCGAGAAAGGAAGGAGAATG
brain 1/2/4	LOC577601	GGGTGTTCTGGGACCAGGTGGTGGTCAGTTACCTAGT CATAATGGTTCCGAAACGGTGATCGAAGACGATGCACC GTCATCGGATGATCTCGAGCAGTTT
otp	LOC579386	CCACCGTACTCGATTCACACCGGCCCAACTGAACGAA CTGGAGAGAAACTTTGCCAAGACACACTATCCTGATAT CTTCATGCGGGAGGAGATTGCGATG

Continue Table A4

pea	LOC580556	TGGAATGCGGCAGGGCGTTCTATGATGATGCAAGCGTACCGGAAAAGGCTCAAGAACAACACAATGAGCCGAGGCATGAGGTGGTGCGAGAAGGGCCTCT
ngn	LOC580598	CTGACGAAGATTGAAACCCTTCGCTTCGCCCACAACTACATCTGGGCCCTGTCTCAGATGCTCAACATGGTGGACAGCAGCGAAAATGGTTGCCCAGGAA
hlf	LOC593063	GTGCACCTTTACCGCGGAGGAGCTCAAGCCGCAGCCTATGATCAAGAAGTCACGAAAGATCTACGTGCCCGATGAGCAGAAGGACGACAAGTACTGGGAG
soxc	LOC593520	GCTGCTAAGACCACCAGCAGCAAACCAAAAGCCAACAAGCCCAAGTCATCATCGAAATTGACGAAGATGAATGGCATCGTGATCGACCAGATGCACCCGC
atbf1	LOC593587	GAGGAGAGGAGATTTGATGAAAGAAATGAAGTGAAGAGTTGGGAGGAGCGAAATGAGAGAGAGATGCAGTCACGGATATCTAGCCATAAAGGTAGTGAGA
opsin1	SPU_005569	GCCTGGTCGTCCCTGTATCAAGAACAACGTATAACTACCTAACAGTCTATACAGGATTTCTGACCATCTTCGGTATACTCAACAACGGTATCGTGATGAT
opsin4	SPU_022851	GTCACGACAGCCCTTCCGCATGGCTTGAATAAACCTACGATTGAAGCTCGCTGGACCAAGTCTCTGAGGACACCACCTAACATGTTGATTGTGAATCTTG
bmalb	WHL22.117376.1	TGGTCTTAATACAAGAGGTCTGTGCGTGGACTTAAAGTTTACGGTCCAGGTCTTAATCTTGGTCCATCTTCCTCAGAGCCTTGGTCTACTCAGGGTAAGA
tim	WHL22.140308.0	TTCAACATTAATGACATGGGAAGCATACGTCCAGGCGAGCAATCAAAGGAACAACGATAGCAAATCAAACTCGGACTTCAAAATCTTGAACATGCAGGCC
6-4 photolyase	WHL22.156161.0	TCACCTCCATGCTCAAGAAGAAATAGACTACAGGCTTGTTATAGTAGGAAGGAAAGATCTTGGCAATAGCATTCCGAAATGGTAACTTGAACCCACTTTG
gkmide	WHL22.164432.1	AGGGTGTGTTGTAGTTTGTACGAGCCGATCGATCCGGCCTATTCCTCAGACCACAAATTACAATCGAAAGTCTGGGATCAAAGGACCAATGGCCGACTTG
z167	WHL22.171389.2	TCTTCGTCGCTCTGTTGACATGGGATTGCCCGGGTCTGATCTAAGCATGTATGGTAGTAGGGATGGATTCAGCAACTTTCTAAACATCTCCTCGGAGTCT
grL1	WHL22.18108.0	TGAGCCCACAAATCGTAAGCTGCGAGAGAGCATCCATCATTTCTGCAACGTTCCTTCAGACATAACACTGACTCGTAACCTTCAACTACTCAGCCGCTCC
glass 2	WHL22.204563.0	TTCAGCTGGCGTTCGTCCGCTACTGTCTTGTAGAGGATGTTTACCTGTCAAGCTATTCTGTACTCAGAGTCGCCTCTATACGATCTATGTGTTCACCCGA
ngfffamide	WHL22.20926.0	AAACAACAGTGGAGAATAGGCACGAGCTATACGTGGAGAAAAGGTTTTCGTTAGATTTAGGTGCCTCGAGAAAAGATCGCAGGTCGATTGGTTTAAGGGA
opsin2	WHL22.272775.0	TCAGAGCAGTGTTAACGCGGACAGTGGTGTTTTTGAAACGAGCCCAAATTGCAACACGGCAAAGAAATCACAAATTAGCGTGCAAAGGCAAATAGAAAAT
trh	WHL22.3018.0	GGCTACTTTACTTTGCTAAAGCGTCGTCACTGTCTGCGGCAATAAAAAAGCCAGCTTGAAATCGGTGGAACGATTTATCACACGCAGTCAGTCCTTAGTG
fbxl15	WHL22.314548.0	AGCATCGCCAATGTCCTTGTCTTTTGGTACGGTATCCAGGTTAACTAGGGGCAAGTCATGCCCTTCTGAATACGGATGAGGTGAGTATGTAGTGTTGTCC

Continue Table A4

clock	WHL22.335679.0	TACTTATACAGGAGCTATGCTCAATGGTTTCGACCAAGACGAGAAAGCTGGACAAGTCCGCAGTCCTCAGAGCCACCATACACTTCTTAAAGGCTCATAA
opsin3.2	WHL22.338995.0	CTGAATAAAAGATTGCAAGAACTTGGAAAGGCGGGGAAGCATATTCGAGAGGATAAGCGAGACCACTCATTTCGTGCGGATTCGACCACAATGAATTCTT
secretogranin	WHL22.347132.0	ATGTGGTACGTGATTCTAAGCATGTTGCTCCTCGGAGCATTGGCAAGCAGCGAGTACTCAGGGATGTCTCTGAGGGATCGAATCGCCTTGAGGAATCTTC
ror-alpha	WHL22.499606.0	ATGACCAAGGAAGAGATCTTAACACGATTATCAGTCCTATTAGGCAGTCAGTACGAACGCATCGTCCAGTTCGCAGAGTCCATACCAGGCTTTGGAGAAT
znHb	WHL22.553144.0	TGATATTTGGGACTGTGGGATTCTGCCTTCTTCTGCCGACTGGCTTGTGTTTTGGAACATACCTACGTATGGGAGCTACTATGGCAGATTCCGCTATAAT
ck1d	WHL22.557027.0	CGATGAGAAGCCTGACTACTCCTTTCTCAGACAGTTGTTCCGCAATCTCTTCCACCGATTAGGCTACACATACGACTATGTCTTTGACTGGAACATGCTC
hey	WHL22.578435.1	AAGCGGACCACACGCTTACTTGACACTTCAAGAAAACTTGATCAAAACCTTCCACTCTTCAAAAACACAGAGACAGTCAGCGAGCCCAATTCTTTTCTCA
dcry	WHL22.613873.1	TTGATTTTGCATCTATACACACAAGATCCAAACGTCGACAGTGACGGTACTCGGAGCAGTCGACAGGAGAGCTAAAACAGATTAAGTAAGCCATCATTTC
5ht	WHL22.635790.0	CTCAGATCCAAGCAAGACGCTCACGTTAACAAGCGATACAAAACGTCTCTCCAGAACGCCCTTCATTTTGTCGTCTTTGAGGGCAATAAGGCATGAACCA
ppl2	WHL22.656375.0	ATGAGAAGCGGATTCTTTAAGAGATTCGGATCCGGTAGCTTGGAGCCAATGTCGAGCGGATTTTACAAGAAAAACTTCGGCGGCTCGCTCGATGCGATGC
ahr	WHL22.676940.0	AAATTGTGGATTTCGAAGGAACGTTACATTTAGCTCAGCCGCGACATGGATTCCATAGGATCTAAACTTTATGCTGGCAAAAGGCGTCGTCGTCCTGCCA
neuroD	WHL22.694980.1	TCGAGACTCTACGCCTCGCAAAGAATTACATCCATGCTCTAGCTGACATTCTCAGGACAGGTGTCGTTCCCGACAACATCTCATTCGCGCAGACATTATC
vcry	WHL22.732419.0	TTCTAGACCCTTGGTTCGCAGGATCTTGTAGCAAAGGAGTCAACAGATGGAGGTTTCTATTAGAATGTTTGGAGGACCTAGACTCCAGTCTGAGGAAGCT
nfil3	WHL22.733532.0	CTCAGCCAAGGCCTCTGAAAGAACTCGTCCTTTGGTCGAATCTCCCATCGCGGAGTCTAAGCCAGTATCAGCTATTGAAGATGTCTGTAAACCAGTATCG
mox	WHL22.737621.0	CATAGTGTCGAACCACAGTACGGATAGCGCGTGCGGTTTGGACAACGGTTCAGACGCGAGTAATTACGGCGGTTCGGATAATGGGGATCCAAATAGTCCG
timeout	WHL22.737890.1	AATCCACTCATGTATGCTGTCAAGGACCATATTCTTCACCGTCGTGCTCAGGAGAATGATGAGTCCTACTACTTCTGGGCAATGCAATTCTTCATGCAGT
f-salmfamide	WHL22.752571.0	GAGGTCTGATGCCGAGTTTTGCGTTCGGTAAGAGGCCACATGGCGGTTCAGCATTCGTATTTGGACGTCGAGATTGGGCGCCGAGGGAACAGGACTTTGC
crydash	WHL22.91720.0	ACCGTGACAATGAGGTTCTCTTTTGGGCACACAAGAATGCAACCAATGTGATTCCTCTCTACTGCTTTGATCCTCGTCACTATAAGGGCACGCATCAGTT

TableA5 List of MASO sequences used for the knock down experiments. Name of genes and corresponding sequences against which MASOs were designed and types of action executed are listed in the present table.

Gene name in *Sp*	**Sequence 5'- 3'**	**Type of MASO**
vcry	CTATGCTTTCGCTTCGGCATTTTGC	Translation blocker
dcry	ATGCAGGCACCGCCAGGCATCTTGA	Translation blocker
tim	ATTTAAGCCACCTCCCATAATAAGC	Translation blocker
opsin3.2	ATGTGGTCGAATCCGCACGAAATGA	Translation blocker
controlMO	TTTTTTTTTT	control

Appendix B

The present appendix contains maps of reporter vectors used in this study. For each map, enzymatic restriction sites, sites of primers annealing and cloned regions are reported. The Endo16 cassette marks the basal promoter (from -117 to +20) and the SV40 A+ cassette marks the polyadenilation sequence from Simian Virus. All the vectors are ampicillin resistant.

Fig.B1 Ep::GFPII vector (A) (Cameron et al., 2004) was used to generate a luciferase vector (Ep::Luc, in B) by replacing the GFP cassette with a luciferase cassette.

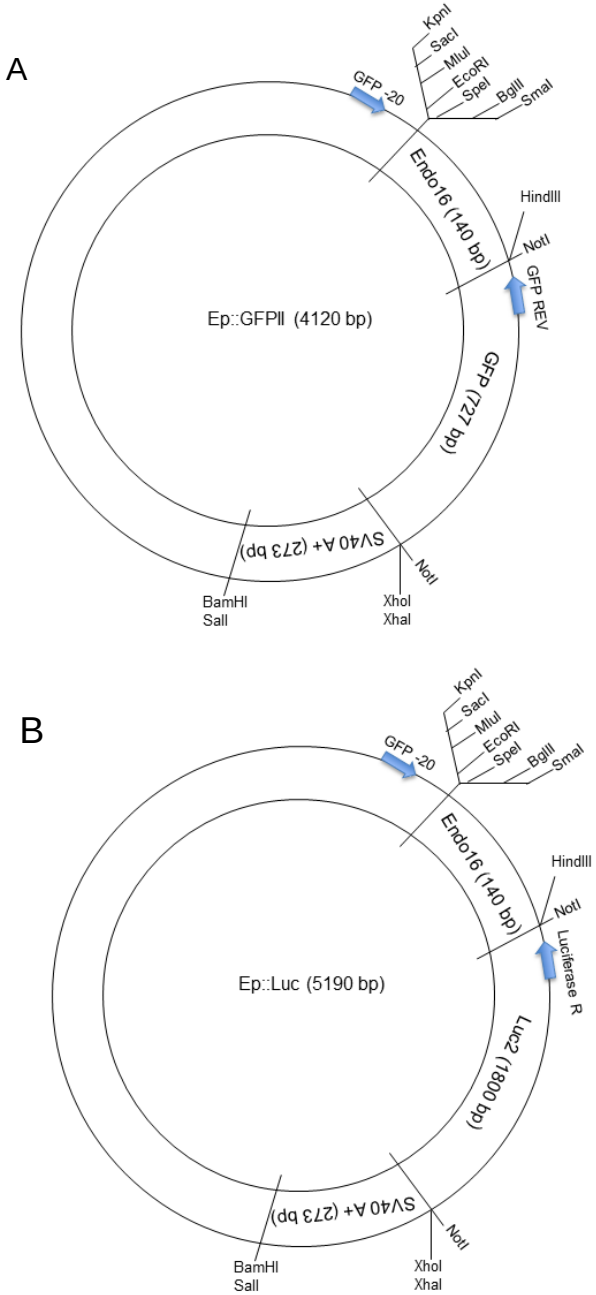

Fig.B2 Restriction maps of the SMp-GFP vector (A) containing the *sp_sm50* regulatory regions from -432 to +109 was used to generate the SMp-Luc vector (B) by swapping the GFP cassette with the Luc cassette.

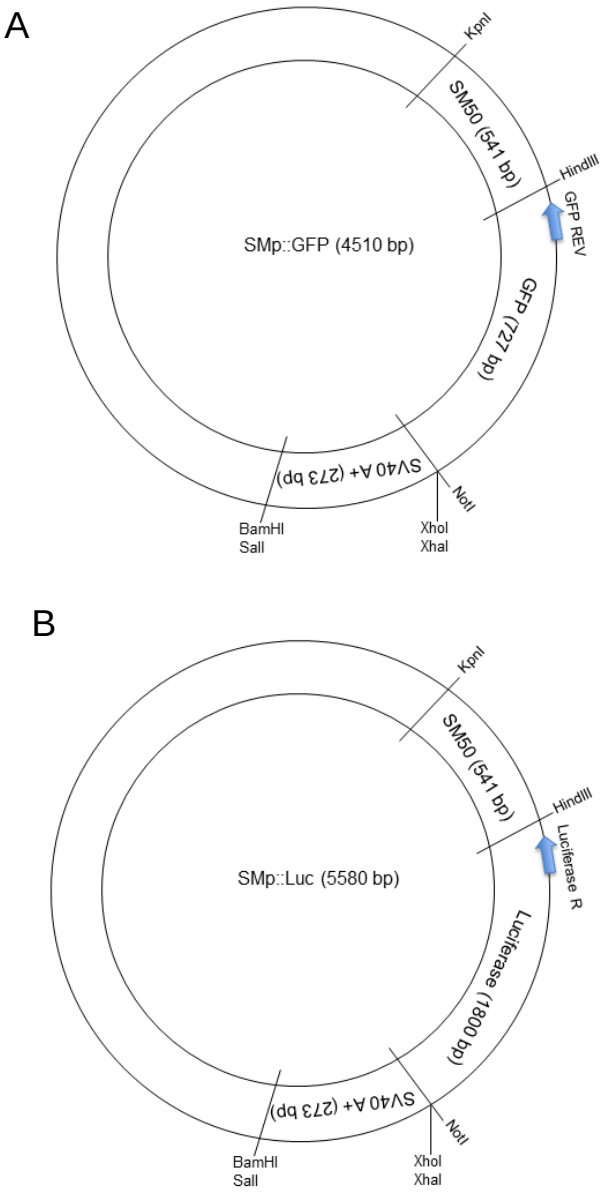

Fig.B3 Restriction maps of the *sp_vcry*::GFP-l (A), *sp_vcry*::GFP-s (B), *sp_vcry*::Luc-l (C) and *sp_vcry*::Luc-s (D) vectors containing the *sp_vcry* regulatory regions:, L form, from -1463 to -51 bp; S form, from -569 to -1463 bp.

A

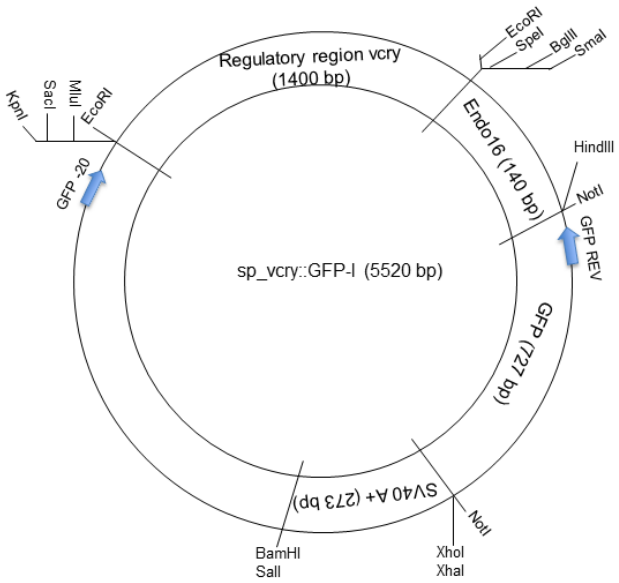

B

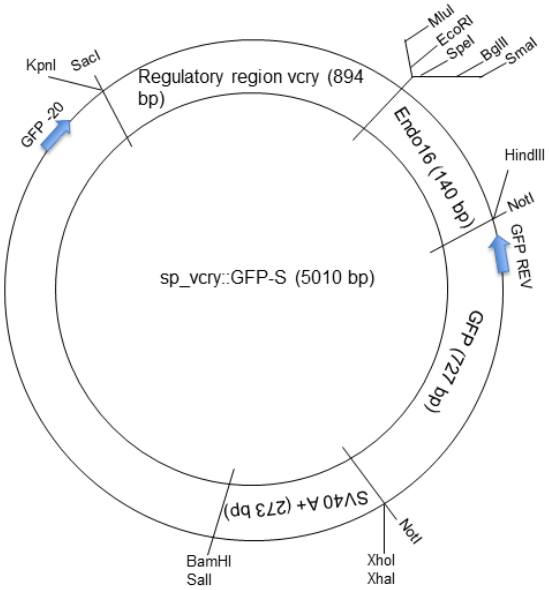

C

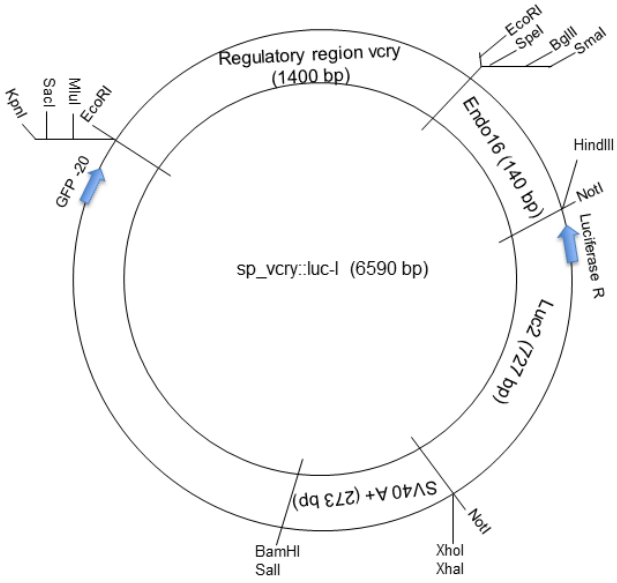
Regulatory region vcry
(1400 bp)
EcoRI
SpeI
BglII
SmaI
KpnI
SacI
MluI
EcoRI
Endo16 (140 bp)
HindIII
NotI
Luciferase R
GFP -20
sp_vcry::luc-l (6590 bp)
Luc2 (727 bp)
SV40 A+ (273 bp)
NotI
BamHI
SalI
XhoI
XhaI

D

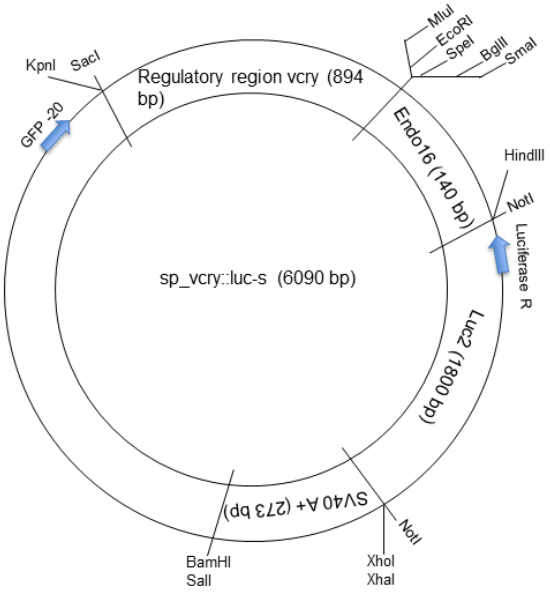
MluI
EcoRI
SpeI
BglII
SmaI
KpnI
SacI
Regulatory region vcry (894
bp)
GFP -20
Endo16 (140 bp)
HindIII
NotI
Luciferase R
sp_vcry::luc-s (6090 bp)
Luc2 (1800 bp)
SV40 A+ (273 bp)
NotI
BamHI
SalI
XhoI
XhaI

Fig.B4 Restriction maps of the *sp_vcry*::GFP-I-ep$^{(-)}$ (A) and *sp_vcry*::Luc-I-Ep$^{(-)}$ (B), vectors where the ENDO16 basal promoter was removed.

A

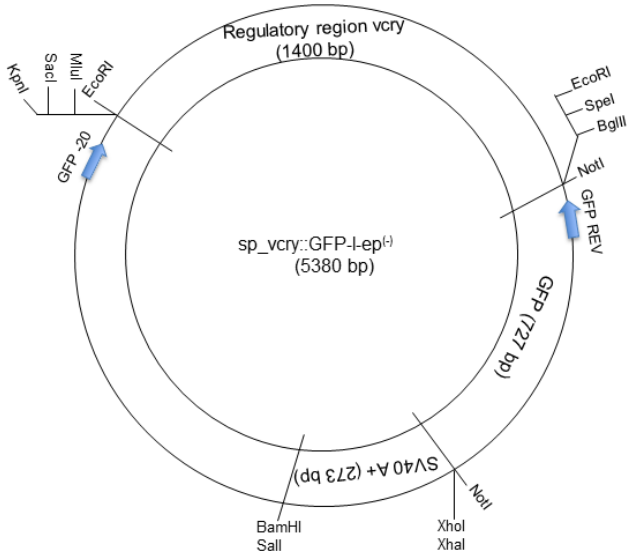

B

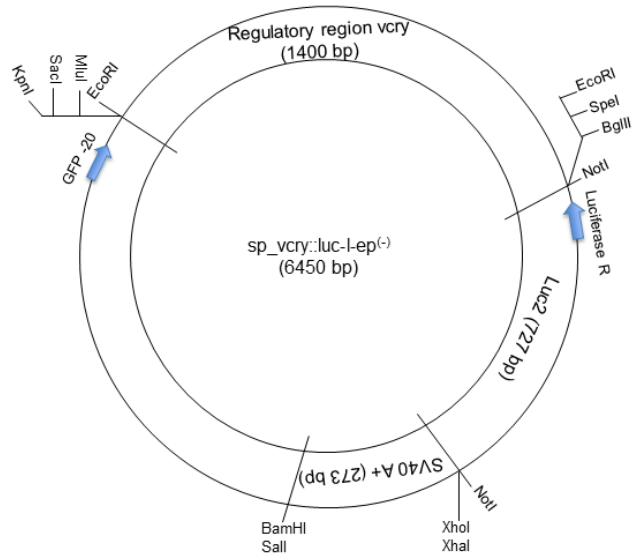

Appendix C

Appendix C contains the recipes to prepare artificial sea water (ASW) and PABA sea water.

Table C1 ASW formula for 1 litre. Salinity and pH were adjusted to 36 ppt and pH 8.2**.**

Reagent	**Amount (g)**
NaCl	28.32
KCl	0.77
$MgCl_2.6H_2O$	5.41
$MgSO_4.7H_2O$	7.13
$CaCl_2$	1.18
$NaHCO_3$	0.20

Table C2 PABA Sea Water formula

Reagent	**Amount**
Para-aminobenzoc acid sodium salt (SIGMA)	150mg
Filtered ASW	500ml

Appendix D

Appendix D includes supplementary tables and results commented in chapter 3, 4 and 5.

Table D1 Sea urchin proteins analysed for the presence of conserved domains using Smart software or Phyre2 in the case of Sp_Tim. For each protein, name of domains, their aminoacidic position and respective E-value is reported. This information allowed the elaboration of figure 3.1 and 3.2.

Protein name in Sp	**Domain 1 (aa position; E-value)**	**Domain 2 (aa position; E-value)**	**Domain 3 (aa position; E-value)**	**Domain 4 (aa position; E-value)**
Clock	b-HLH (36-86; 3.18 e^{-43})	PAS (105-169; 5.04 e^{-7})	PAS (256-308; $2.9*10^{-4}$)	
Bmal	b-HLH (133-186; 5.9 e^{-17})	PAS (105-169; 2.9 e^{-9})	PAS (499-565; 9.5 e^{-8})	PAC (575-615; $2.6*10^{-2}$)
Tim	Arm/HEAT (105-264)			
vCry	DNA photolyase (20-184;1.4 e^{-43})	FAD binding (227-503; 1.1 e^{-99})		
dCry	DNA photolyase (6-172;3.1 e^{-40})	FAD binding (212-491; 5.9 e^{-88})		
6-4 Photolyase	DNA photolyase (6-171;7.9 e^{-42})	FAD binding (213-489; 7.7 e^{-99})		
Cry-DASH	DNA photolyase (8-185; 3 e^{-39})	FAD binding (219-486; 2.6 e^{-73})		
Cpd photolyase	DNA photolyase (79-141; 4 e^{-9})	FAD binding (265-495; 7.6 e^{-32})		

Table D2 Identification of putative NLS and NES motifs in sea urchin clock proteins, cryptochromes and photolyases. The software NLS mapper, Nucpred and NLStradamus (see Materials and Methods for details) were used to predict the position of putative NLS motifs; NetNES software was used to predict the position of NES motifs. These information are schematized in Figure 3.1 and 3.2.

	NLS mapper	Nucpred	NLStradamus	NetNES
Clock (aa position)	35-66	29-44	31-43	111-119
Bmal (aa position)	92-103	94-97	-	169-172
Tim (aa position)	653-664	658-660	-	-
vCry (aa position)	3-31	3-11	3-11	76-90
dCry (aa position)	-	-	-	-
6-4 photolyase (aa position)	495-519	-	493-524	196-203
Cpd photolyase (aa position)	479-489	489-488	-	-
CryDASH (aa position)	482-512	-	488-511	-

Fig. D1 Multi-alignment between the C-terminal of Sp_Bmal, ApBmal (AAR14937.1) and mBmal1b (BAA81898.1) where a transactivation domain was localized. Alignment was performed using Clustal Omega (see Material and Methods for details) using the full length sequences of the proteins and below the last 40 aa , corresponding to the transactivation domain of apBmal and mBmalb1, are reported. Ap is *Antheraea pernyi*; m is mouse. The asterix (*) indicates identities, the colon (:) indicates high similarity, the dot indicates low similarity.

```
SpBmal       EAAMAFIMSLLEADAGLGGSVDFNDLPWPL-  835
apBmal       EAAMAVIMSLLEADAGLGGQVNFSGLPWPLP  589
mBmal1b      EAAMAVIMSLLEADAGLGGPVDFSDLPWPL-  625
             *****.************* *:*. *****
```

Fig.D2 Alignment between the full length of Drosophila Tim (P49021.3) and Sp_Tim. The alignment was performed using EMBOSS Needle, pairwise sequence alignment with default setting. The alignment gives 17.2% of identities, 31.5% of similarities and 39.2% of gaps. The Armadillo (Arm)/HEAT region of Sp_Tim (highlighted in black) was identified with the software Phyre2 (see Methods); Per binding sites of dTim are highlighted in yellow; the CLD of dTim is highlighted in green. The line (I) indicates identities, the colon (:) indicates high similarity, the dot indicates low similarity.

```
dTim               1 ----------------------------MSRVRQLHNHIWNNQNFDKVKS     22
                                                 :....|       :..:.::|.
SpTim              1 MEEREQFGEDGVDAGAGQVIAYQRELTELPAAAQ-------SDTYKRLKL     43

dTim              23 VMDWLLATPQLYSAFSSLGCLEGDTYVVNPNALAILEEINYKLTYEDQTL     72
                     .|.||:....|.:..::||..|..:||:......:|:.:...:..|.:..
SpTim             44 RMQWLIMGGGLNATATNLGYHEETSYVITEECKDVLDVMVNNILQESKVK     93

dTim              73 RTFRRAIGFGQNVRSDLIPLL-ENAKDDAVLESVIRILVNLTVPVECLFS    121
                     ...||.:...:.::.||||:| .:.:|..|.:::::|:|::|::|:|.:..
SpTim             94 CQARRNVANSRLIQMDLIPILCHSTEDPEVFDAIVRLLMHLSMPLEVVMP    143

dTim             122 V-DVMYRTDVGRHTIFELNKLLYTSKEAFTEARSTKSVVEYMKHILE--S    168
                     : ..:.:.|..:..  ||.|:|.|.|:.||::.....:|..|..|:|  .
SpTim            144 ILKKLTKEDYEKRD--ELQKMLATIKKEFTQSTVISCLVGQMALIIEEAG    191

dTim             169 DPKLSPHKCDQINNCLLLLRNILHIPETHAHCVMPMMQSMPHGISMQNTI    218
                     ...:.....|.::|||.|:||:|::          ..:....|....:||
SpTim            192 SYAIDQTNADTLSNCLTLIRNVLYV----------NYERYKVGSLKNDTI    231

dTim             219 LWNLFIQSIDKLLLYLMTCPQRAFWGVTMVQLIALIYKDQHVSTLQKLLS    268
                     :..||......:|..:...|:.:.|..:::|::.|:|||.....:...|:
SpTim            232 IGKLFKADFQDVLKEMCRRPEGSKWLSSLLQVLHLMYKDTSSLKMMSYLN    281

dTim             269 LWFEASLSESSEDNESNTSPPKQGSGDSSPMLTSDPTSDSSDNGSNGRGM    318
                     ...|..|.|:....:..|:
SpTim            282 RKHEQKLREAEGAKDEQTT------------------------------    300

dTim             319 GGGMREGTAATLQEVSRKGQEYQNAMARVPADKPDGSEEASDMTGNDSEQ    368
                                                   .||...:|  |:|.
SpTim            301 -------------------------------------KEETKVVT--DAEG    312

dTim             369 PGSPEQSQPAGESMDDGDYEDQRHRQLNEHGEEDEDEDEVEEEEYLQLGP    418
                     |.||..|..:.|::
SpTim            313 PASPSLSTHSLETI-------------------------------------    326

dTim             419 ASEPLNLTQQPADKVNNTTNPTSSAPQGCLGNEPFKPPPPLPVRASTSAH    468
                                                .||..|.|....|.::|..
SpTim            327 -------------------------------QEPLSPGPSCKPRDTSSCE    345

dTim             469 AQMQKFNESSYASHVSAVKLGQKSPHAGQLQLTKGKCCPQKRECPSSQSE    518
                     ..:      |.:|.::....|..:...|.                ||||.
SpTim            346 RTL------SCSSTLTIDSSGDSTVQEGD---------------SSQSS    373

dTim             519 LSDCGYGTQVENQESISTSSNDDDGPQGKPQHQKPPCNTKPRNKPRTIMS    568
                     .|           |.|:.|:|||..:
SpTim            374 CS----------SSSSMSSDDDSEK----------------------    388
```

```
dTim            569 PMDKKELRRKKLVKRSKSSLINMKGLVQHTPTDDDISNLLKEFTVDFLLK    618
                     :....|:||           |||.|.|              |.:|::
SpTim           389 -VGNNYLKRK-----------NMKKLAQ--------------FGLDYI--    410

dTim            619 GYSYLVEELHMQLLSNAKVPIDTSHFFWLVTYFLKFAAQLELDMEHIDTI    668
                      .|.::.:.:|...:.|..:...:|.|.:.:|:.||...::....|...
SpTim           411 --KYGMDNILIQCKEDLKNMVTNHYFLWQMNFFIPFATHPDVSYTDIKLT    458

dTim            669 LTYDVLSYL------TYEGVSLCEQLELNARQEGSDLKPYLRRMHLVVTA    712
                    |:..|.|.|      |:|.........|..:..||.|    .:::..:.
SpTim           459 LSAPVFSQLLSSTLMTWEAYVQASNQRNNDSKSNSDFK----ILNMQAST    504

dTim            713 IREFLQAIDTYNKVTHLNEDDKAHLRQLQLQISEMSDLRCLFVLLLRRFN    762
                    :|:.|.||..:  .|:....|..|::.:...|:....:|..:.||:|:|.
SpTim           505 MRQMLHAIQQF--TTNPQNTDIIHMKTILATIALTDAVRNFYYLLIRKFQ    552

dTim            763 PSIHSKQYLQDLVVTNHILLLILDSSAKLGGCQ--TIRLSEHITQFATLE    810
                    |:.|:..:|::|:|.|.::|.|:|....:...|  .:.:::||.:|||..
SpTim           553 PNQHTLSFLRELIVGNDLVLRIIDQVQHIHRPQWGKLDMTKHIGKFATRP    602

dTim            811 VMHYYGILLEDFNNNGEFVNDCIFTMMHHIGGDLGQIGVLFQPIILKTYS    860
                    :|..|..:|..|:.|....|:.:.|||||:..|:.:..||:|..||.:::
SpTim           603 IMRVYNYMLSKFSLNTLEENEVVMTMMHHVVVDIAKPEVLYQIPILSSFA    652

dTim            861 RIWEADYELCDDWS-DLIEYVIHKF--MNTPPKSPLTIPTTSLTEMTKEH    907
                    .:|||........| :||:|:||:|  :.:..|.. .:.|.::.:..:..
SpTim           653 SLWEAGSGYVTKQSHELIDYIIHEFCVLGSANKEK-CLETVTMPDRVRPA    701

dTim            908 NQEHTVCSWSQEEMDTLYWYYVQSKKNNDIVGKIVKLFSNNGNKLKTRIS    957
                    .::|.                     .|::.|         ||:...:|
SpTim           702 KRKHV----------------------TDVISK---------NKMMKMLS    720

dTim            958 IIQQLLQQDIITLLEYDDLMKFEDAEYQRTLLTTPTSATTESGIEIKECA   1007
                    ..:.|             .:..::::.:...|.| :||:::|
SpTim           721 TAKGL-------------YVPRDESDVEEEELET-SSASSKS--------    748

dTim            1008 YGKPSDDVQI---LLDLIIKENKAQHLLWLQRILIECCFVKLTLRSGLKV   1054
                     .||..|:.:   |..|.:| ...:.:..||.:|:|.|:.||...   ||
SpTim           749 -AKPIQDLSVEECLAALRLK-GFGEEICELQNVLLEICYFKLNCP---KV    793

dTim            1055 PEGDHIMEPVAYHCICKQKSIPVVQWNNEQSTTMLYQPFVLLLHKLGIQL   1104
                        |:.||..:||:...||:|::.:............|..|||:||:..
SpTim           794 ----HVGEPHIWHCVSDGKSVPIIPFTESSENAHADTHFKALLHRLGLHT    839

dTim            1105 PADAGSIFARIPDYWTPETMYGLAKKLGPLDKLNLKFDASELEDATASSP   1154
                     ..|...::..:|.:|..:..|..|..||.:.:.||||:..::|.......
SpTim           840 AQDTCRLYPSVPAFWPSDMCYKTASMLGDILEGNLKFELDQIEKVPVECE    889

dTim            1155 SRYHHTGPRNSLSSVSSLDVDLGDTEELALIPEVDAAVEKAHAMASTPSP   1204
                     .:   :|.......|:..|:|||           ..|:||       |:.
SpTim           890 EK---SGMTQEGVMVNLEDLDLG-----------KEAMEK-------PTV    918

dTim            1205 SE-IFAVPKTKHCNSIIRYTPDPTPPVPNWLQLVMRSKCNHRTGPSGDPS   1253
                     :. .|.||....||.|.|...
SpTim           919 NRPYFQVPLQMWCNVIKRANK----------------------------    939
```

```
dTim          1254 DCVGSSSTTVDDEGFGKSISAATSQAASTSMSTVNPTTTLSLNMLNTFMG  1303

SpTim          940 --------------------------------------------------   939

dTim          1304 SHNENSSSSGCGGTVSSLSMVALMSTGAAGGGGNTSGLEMDVDASMKSSF  1353

SpTim          940 --------------------------------------------------   939

dTim          1354 ERLEVNGSHFSRANNLDQEYSAMVASVYEKEKELNSDNVSLASDLTRMYV  1403

SpTim          940 --------------------------------------------------   939

dTim          1404 SDEDDRLERTEIRVPHYH   1421

SpTim          940 ------------------    939
```

Fig. D3 Phylogenetic relationships of the Timeless and Timeout proteins from Rubin et al. (2006). The plant TIMELESS protein was used as an outgroup to root the tree. Support levels are shown only for the main protein lineages, which are separated slightly vertically for visual clarity (percentage of trees showing a branch in distance and parsimony bootstrapping, followed by percentage of maximum likelihood quartet puzzling steps). Distinct font styles are used to highlight major taxonomic lineages. Bold for insects, italics for vertebrates, underline for the sea urchin, and plain for all the others. The honey bee *Apis mellifera* is highlighted with an asterisk.

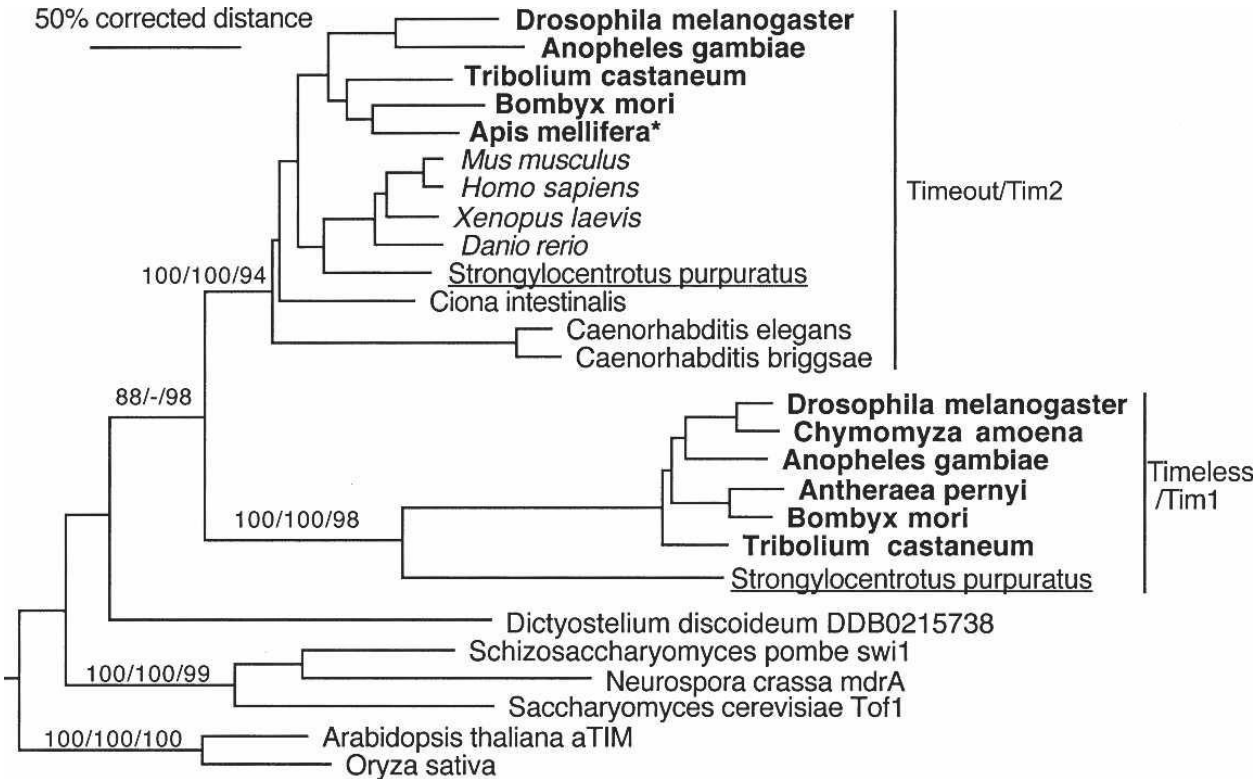

Fig. D4 Alignment of the full-length of Sp_dCry and *Drosophila* Cry (O77059.1). The alignment was performed using EMBOSS Needle, pairwise sequence alignment with default setting. The alignment gives 45.2% of identities, 61.5% of similarities and 9.8% of gaps. The sequence corresponding to the phosphates motif is highlighted in green, the sequence of the C-terminal lid in red and the one of the protrusion motif in blue, ΔΔdCry region, involved in the interaction with dTim, is highlighted in grey; ΔdCry region, involved in light regulation, is highlighted in yellow (Busza E. et al., 2004; Dissel S., 2004; Hemsley M.J., 2007).

```
dCry              1 MATRGANVIWFRHGLRLHDNPALLAALADKDQGIALIPVFIFDGESAGTK     50
                    ...||.:.|||||||||||||||..:.   .|....||||||.|.||||
SpdCry            1 -MPGGACIHWFRHGLRLHDNPALLEGMT---LGKEFYPVFIFDNEVAGTK     46

dCry             51 NVGYNRMRFLLDSLQDIDDQLQAATDGRGRLLVFEGEPAYIFRRLHEQVR    100
                    ..||||.|||.|.|.|:|:||:||   .|||.||.|:|..||:.:..:..
SpdCry           47 TSGYNRWRFLHDCLVDLDEQLKAA---GGRLFVFHGDPCLIFKEMFLEWG     93

dCry            101 LHRICIEQDCEPIWNERDESIRSLCRELNIDFVEKVSHTLWDPQLVIETN    150
                    :..:..|.|.||||.|||..:::||:|:.:::.:|:||||||:|.::||.|
SpdCry           94 VRYLTFESDPEPIWTERDRRVKALCKEMKVECIERVSHTLWNPDIIIEKN    143

dCry            151 GGIPPLTYQMFLHTVQIIGLPPRPTADARLEDATFVELDPEFCRSLKL--    198
                    ||.||:||.||:..|..||.||||..|..|...           ::|:
SpdCry          144 GGTPPITYSMFMECVTEIGHPPRPMPDPILTKV-----------NMKIPS    182

dCry            199 -FEQ---LPTPEHFNVYGDNMGFL--AKINWRGGETQALLLLDERLKVEQ    242
                     ||:   ||:.|   |.|.||...  .|..|:||||:||.|...|:..|:
SpdCry          183 DFEERCALPSLE---VMGVNMECTEQEKKVWKGGETRALELFRVRILHEE    229

dCry            243 HAFERGFYLPNQALPNIHDSPKSMSAHLRFGCLSVRRFYWSVHDLFKNVQ    292
                    .||:.|:.||||.:|::..:|||:||:|||||||||||||.:||.:..::
SpdCry          230 EAFKGGYCLPNQYMPDLLGTPKSLSAYLRFGCLSVRRFYWKIHDTYSELK    279

dCry            293 LRACVRGVQMTGGAHITGQLIWREYFYTMSVNNPNYDRMEGNDICLSIPW    342
                            :....:|:|.|:||||||||||.|.::::|:.|.|||:|.|
SpdCry          280 --------KEVSPSHLTAQVIWREYFYTMSVGNIHFNKMKENPICLNIEW    321

dCry            343 AKPNENLLQSWRLGQTGFPLIDGAMRQLLAEGWLHHTLRNTVATFLTRGG    392
                     |.::..|::|..|:||:|.||..|:||..|||:|...|:..|.|||||.
SpdCry          322 -KEDDEKLKAWTDGRTGYPWIDACMKQLKYEGWIHQVGRHATACFLTRGD    370

dCry            393 LWQSWEHGLQHFLKYLLDADWSVCAGNWMWVSSSAFERLLDSSLVTCPVA    442
                    ||.|||.|||.|.|||||||||:|||||||:||||||:.|......|||.
SpdCry          371 LWISWEDGLQVFDKYLLDADWSICAGNWMWISSSAFEKFLQCPNCFCPVR    420

dCry            443 LAKRLDPDGTYIKQYVPELMNVPKEFVHEPWRMSAEQQEQYECLIGVHYP    492
                    ..:|:||.|.|:::|:|.|.::|..::.|||:.....||:.:|::|..||
SpdCry          421 YGRRMDPTGEYVRRYLPVLKDMPIRYLFEPWKAPRAVQERAKCIVGKDYP    470

dCry            493 ERIIDLSMAVKRNMLAMKSLRNSLITPPPHCRPSNEEE---VRQFFWLAD    539
                    ..:::...|...|...|:.:.|.|       |.:.|:.   .|:..|
SpdCry          471 MPVVEHKSASAANHEQMEKVVNKL-------RDTGEKNGKVERRCTW---    510

dCry            540 VVV    542

SpdCry          511 ---    510
```

Fig.D5 Multiallignment between the full length of Sp_vCry, mCry1 (NP_031797) and mCry2 (NP_034093.1). The colour code follow the schematic representation reported in fig. 3.2. In addition the 6 amminoacids critical for the activity of mCry1 are highlighted in black; while the atypical polyQ of SpvCry is highlighted in yellow. The alignment was performed using CLUSTALOmega with default setting. Identity (*); high similarities (:); low similarities (.).

```
SpvCry      MPKR---KHRSSRRDREEKPGCLVHWFRKGLRLHDNPALKEGLKSASGFRCIYILDPWFA
mCry2       MAAAAVVAATVPAQSMGADGASSVHWFRKGLRLHDNPALLAAVRGARCVRCVYILDPWFA
mCry1       ------------------MGVNAVHWFRKGLRLHDNPALKECIQGADTIRCVYILDPWFA
                               ****************   ::.*  .**:********

SpvCry      GSCSKGVNRWRFLLECLEDLDSSLRKLNSRLFLIRGQPADVLPRLFKEWKVTQLSFEEDS
mCry2       ASSSVGINRWRFLLQSLEDLDTSLRKLNSRLFVVRGQPADVFPRLFKEWGVTRLTFEYDS
mCry1       GSSNVGINRWRFLLQCLEDLDANLRKLNSRLFVIRGQPADVFPRLFKEWNITKLSIEYDS
            .*.. *:*******:.*****:.*********::*******:******* :*:*::* **

SpvCry      EPFGRTRDKAISTLAQEAGVKVISKVSHTLYDPQEILALNNNEPPLTYKRFQDIISLMGI
mCry2       EPFGKERDAAIMKMAKEAGVEVVTENSHTLYDLDRIIELNGQKPPLTYKRFQALISRMEL
mCry1       EPFGKERDAAIKKLATEAGVEVIVRISHTLYDLDKIIELNGGQPPLTYKRFQTLVSKMEP
            ****: ** ** .:* ****:*: . ****** :.*: **  :********* ::* *

SpvCry      PIYPAEALEAEDVEGLDTFIDPNHEDKYGIPTLEELGFDPEDVPPPMWIGGETEAKQRLD
mCry2       PKKPAVAVSSQQMESCRAEIQENHDDTYGVPSLEELGFPTEGLGPAVWQGGETEALARLD
mCry1       LEMPADTITSDVIGKCMTPLSDDHDEKYGVPSLEELGFDTDGLSSAVWPGGETEALTRLE
               ** :: :: :    : :. :*::.**:*:******  : :   :* ******  **:

SpvCry      RHLERKAWVANFERPRMSPASLMASPAGLSPYLRFGCLSPRTFYWKLTELYQKVRKTTNT
mCry2       KHLERKAWVANYERPRMNANSLLASPTGLSPYLRFGCLSCRLFYYRLWDLYKKVKRNSTP
mCry1       RHLERKAWVANFERPRMNANSLLASPTGLSPYLRFGCLSCRLFYFKLTDLYKKVKKNSSP
            :**********:*****.  **:***:************ * **::* :**:**::.:.

SpvCry      PLSLHGQLLWREFFFTVACNNRQFDHMVDNPICIQIPWDKNTALLNKWANGETGYPWIDA
mCry2       PLSLFGQLLWREFFYTAATNNPRFDRMEGNPICIQIPWDRNPEALAKWAEGKTGFPWIDA
mCry1       PLSLYGQLLWREFFYTAATNNPRFDKMEGNPICVQIPWDKNPEALAKWAEGRTGFPWIDA
            ****.*********:*.* ** :**:*  ****:*****:*   * ***:*.**:*****

SpvCry      IMTQLRLEGWIHPLARHAVACFLTRGDLWISWEEGMKVFDEYLLDADWSVNAGNWIWLSC
mCry2       IMTQLRQEGWIHHLARHAVACFLTRGDLWVSWESGVRVFDELLLDADFSVNAGSWMWLSC
mCry1       IMTQLRQEGWIHHLARHAVACFLTRGDLWISWEEGMKVFEELLLDADWSINAGSWMWLSC
            ****** ***** ****************:***.*::**:* *****:*:***.*:****

SpvCry      SSFYQQFFHCYCPVKFGRRTDPNCDYVRKYLPFLKNFPSKYIFEPWTAPIEVQEKAKCII
mCry2       SAFFQQFFHCYCPVGFGRRTDPSCDYIRRYLPKLKGFPSRYIYEPWNAPESVQKAAKCII
mCry1       SSFFQQFFHCYCPVGFGRRTDPNCDYIRRYLPVLRGFPAKYIYDPWNAPEGIQKVAKCLI
            *:*:********** *******.***:*:*** *: **::**::**.**  :*: ***:*

SpvCry      GKDYPLPIVDHAEASHRNIERMRKVYNNLSRRGGPGILGSVPSSQAASAPPQLGKFNMSS
mCry2       GVDYPRPIVNHAETSRLNIERMKQIYQQLSRYRGLCLLASVPSCVEDLSHPV--------
mCry1       GVNYPKPMVNHAEASRLNIERMKQIYQQLSRYRGLGLLASVPSNSNGNGGLM--------
            * :** *:*:***:*: *****:::*::***  *  :*.****     .

SpvCry      KLMMTKQQHQQQTQETPMAPPAGNDSDLMPRPAKMRFMGTGMSHMQMLLGGNTSTGIGGT
mCry2       ------------------AEPGSSQAGSISN--------T---GPRALSSGPASP-----
mCry1       ------------------GYAPGENVPSCSS--------SGNGGLMGYAPGENVPSCSGG
                             .   ..:             :         *

SpvCry      GVVVGPGVSGVGAGVGVGGVSLGAGVSGIGPGVGVGPGVSGIGAGVSGIVSVGVPCVRGV
mCry2       ------------------KRKLEAAEEPPGEELTKRARV----------------------
mCry1       NCSQGSGILHYAHGDSQQTHSLKQGRSSAGTGLSSGK-----------------------
                               .*  . .  *  :
```

```
SpvCry      EVSGINVTDVTSHLPGSSGTNVLSYQPSLDMQQQHQRQQQQQQHQQQHQQQQQQLSQQIM
mCry2       -------TEMPTQEPASKD-----S-----------------------------------
mCry1       ---------RPSQEEDAQS-----VGPKV------QRQSSN--------------------
                        ::   :.

SpvCry      PVDMATLSQMDVPGTSGSLLKELEGTNWQTHWQFTNQ
mCry2       -------------------------------------
mCry1       -------------------------------------
```

Table D3 Summary table indicating values of amplitude, mesor and acrophase detected for genes which expression profiles where quantified by qPCR in larvae (5 dpf, 1 wpf, 2 wpf) entrained to DL cycles or in constant dark DD. These values were calculated using cosinor analysis. Amplitude and mesor values are expressed in normalized counts of transcripts, acrophase values in degrees of circumference (°). Values were considered statistically significant when p-value < 0.05.

Gene name/light condition	Larval stage	Amplitude (counts of transcripts)	Mesor (counts of transcripts)	Acrophase (°)	p-value
sp_vcry DL	5 dpf	283	257	-0.89	0.0012
sp_vcry DL	1wpf	271	282	-0.19	0.00026
sp_vcry DL	2 wpf	249	240	-1.11	0.016
sp_vcry DD day1	5 dpf	160	360	-0.84	0.00043
sp_vcry DD day2	5 dpf	92	364	-1.28	0.087
sp_vcry DD day1	1 wpf	193	335	-0.67	0.038
sp_vcry DD day2	1 wpf	85	302	-0.15	0.055
sp_tim DL	5 dpf	142	315	-3.53	0.015
sp_tim DL	1wpf	32	66	-3.18	0.004
sp_tim DD day1	5 dpf	61	201	-3.63	0.00076
sp_tim DD day2	5 dpf	53	242	-3.52	0.66
sp_tim DD day1	1 wpf	50	114	-3.37	0.0021
sp_tim DD day2	1 wpf	7	91	-5.6	0.86
sp_hlf DL	5 dpf	1258	6545	-5.9	0.1
sp_hlf DD day*1*	5 dpf	425	7582	-5.67	0.53
sp_hlf DD day2	5 dpf	1405	7428	-0.97	0.18
sp_dcry DL	5 dpf	31	103	-0.95	0.0029
sp_dcry DD	5 dpf	58	157	-5.15	0.47
sp_dcry DD	1 wpf	46	172	-0.32	0.49
sp_cpd photolyase DL	1 wpf	41	73	-1.81	0.014
sp_cpd photolyase DL	5 dpf	66	137	-1.72	0.0033

Fig.D6 (Following page) Daily expression profiles of genes not described in chapter4. Expression profiles detected in DL conditions are reported in a heatmap to show the arrhythmic mRNA profiles of the other genes potentially involved in sea urchin circadian system. *sp_vcry* mRNA profile is shown in the first row as example of rhythmic oscillation. For each gene, numbers of transcripts measured in the two batches were averaged and normalized to the maximum value of its expression (scale 0-1). Heatmap was built using Microsoft Excel, conditional formatting function, assigning to the low value (0) the yellow colour and to the maximum value (1) the red colour (colour code is reported at the bottom of the heat map). On the left, names of genes are reported, each square represents the level of expression measured at a specific ZT. ZT are reported on top of the figure; ZT of the dark phase are indicated in black squares.

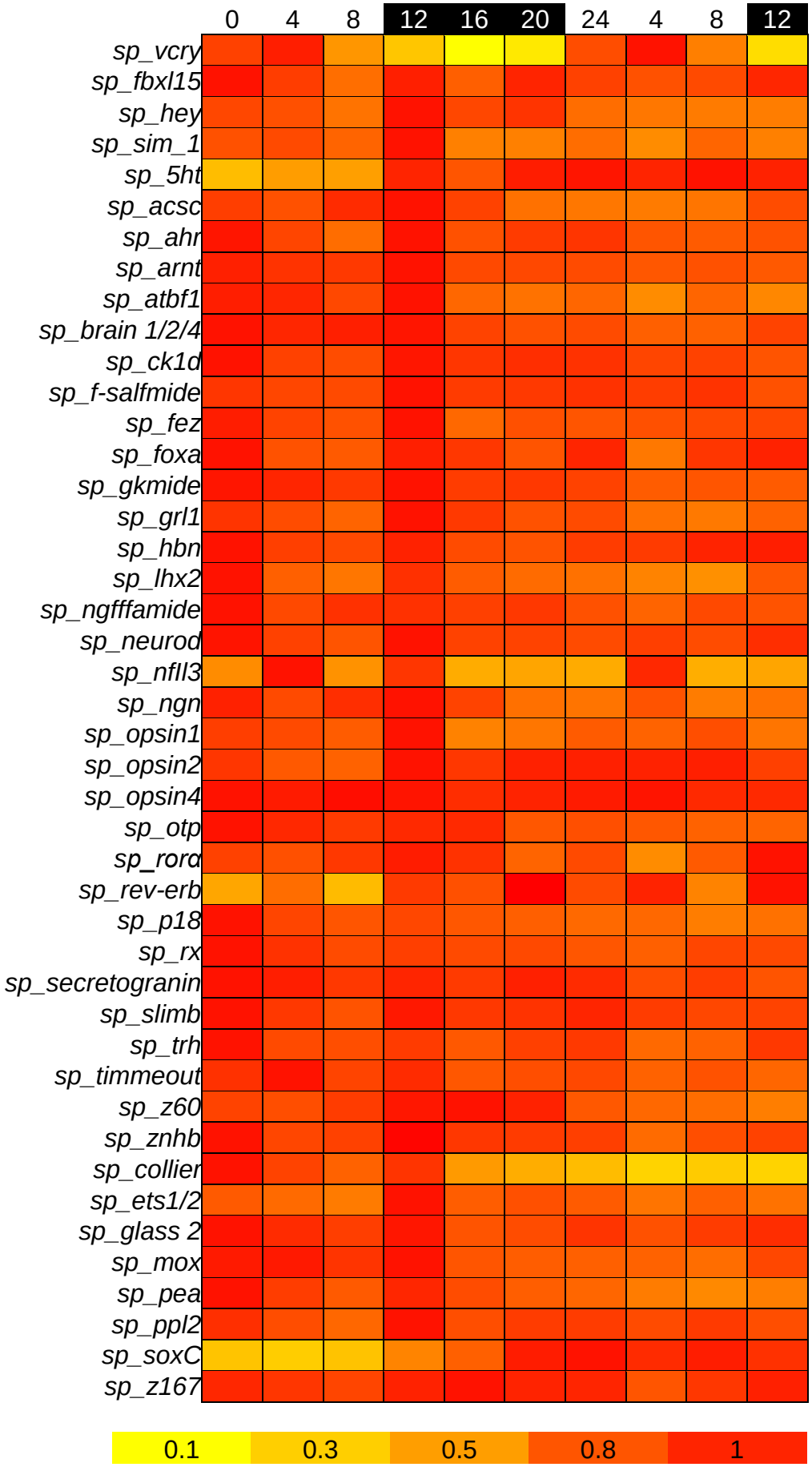
0
4
8
12
16
20
24
4
8
12
sp_vcry
sp_fbxl15
sp_hey
sp_sim_1
sp_5ht
sp_acsc
sp_ahr
sp_arnt
sp_atbf1
sp_brain 1/2/4
sp_ck1d
sp_f-salfmide
sp_fez
sp_foxa
sp_gkmide
sp_grl1
sp_hbn
sp_lhx2
sp_ngfffamide
sp_neurod
sp_nfil3
sp_ngn
sp_opsin1
sp_opsin2
sp_opsin4
sp_otp
sp_rora
sp_rev-erb
sp_p18
sp_rx
sp_secretogranin
sp_slimb
sp_trh
sp_timmeout
sp_z60
sp_znhb
sp_collier
sp_ets1/2
sp_glass 2
sp_mox
sp_pea
sp_ppl2
sp_soxC
sp_z167
0.1
0.3
0.5
0.8
1

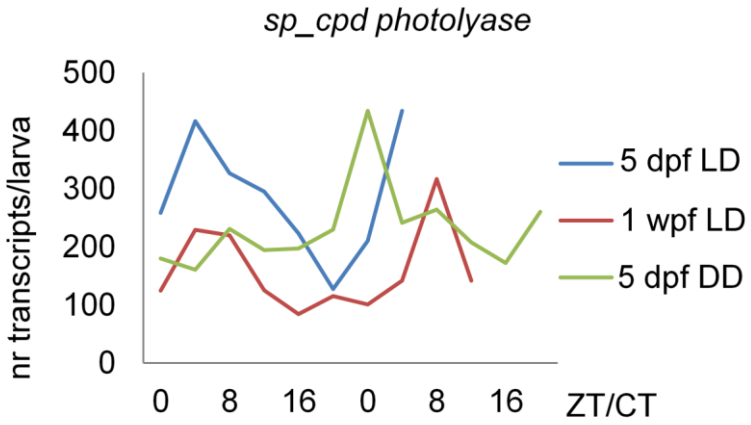

Fig. D7 Expression profiles of *sp_cpd photolyase* detected in 5dpf (blue and grey line) and 1wpf larvae (red line) exposed to LD cycles (blue and red line) and free running conditions (grey line). The gene shows 24h rhythmic oscillation in LD conditions and arrhythmic expression in free running conditions. The profiles of expression were measured by qPCR and are reported as number of transcripts/ larva. Results of cosinor analysis for LD samples are reported in table D3.

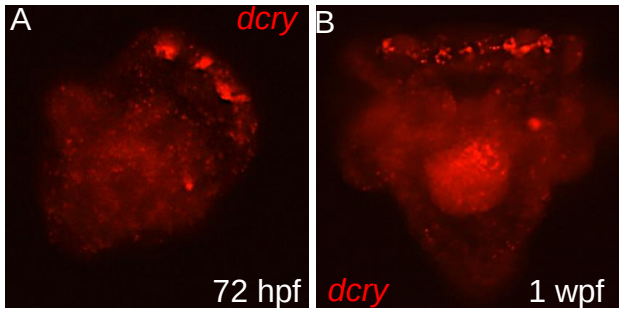

Fig.D8 Spatial expression pattern of *sp_dcry* at 72 hpf (A) and 1wpf (B) detected with single fluorescent *in-situ.* At 72 hpf, sea urchin larvae exhibit expression of *sp_dcry* in the apical organ, while, later in larval development, this gene turns on also in the gut. Experiment performed by Teresa Mattiello.

Table D4 Sequences of canonical and non-canonical E-box elements found in the 37 kb of intergenic region upstream sp_vcry locus. For each sequence, distance from *sp_cry* ATG is reported.

Ebox sequence	Distance from ATG (bp)
CATGTG	-249
AACGTG	-344
GACGTG	-478
CACGTT	-765
AACGTG	-824
CATGTG	-918
CATGTG	-1021

Table D5 Scoring for GFP signal in injected embryos in the different microinjection sessions. The percentage values are average of the different microinjection experiments.

Construct name	Number of indipendent microinjections	Total number of injected embryos	Average of embryos (%) expressing GFP
sp_he::gfp	3	86	84
smp::gfp	6	180	53
sp_vcry::gfp-s	3	69	29
sp_vcry::gfp-l	2	60	19
sp_vcry::gfp-l-ep$^{(-)}$	3	90	58

Table D6 Values of averaged luminescence detected in *sp_vcry::luc-s* and *sp_vcry::luc-l* injected larvae in two independent experiments. Luciferase assays were performed plating 10 larvae/well in duplicate for experiment 1 and triplicate for experiment 2. For each condition and replicate, luminescence counts detected during time were averaged. Again the obtained values were averaged between the replicates and standard deviation was calculated (in brackets). Uninjected larvae were plated to measure the background level of luminescence signal; smp::luc injected larvae were used as positive control. Values are expressed in counts of luminescence/second.

	Averaged luminescence (standard deviation) in exp1 (72hpf-96hpf)	Averaged luminescence (standard deviation) in exp2 (96 hpf- 144 hpf)
Uninjected	26 (±6)	17 (±2)
smp::luc	1000 (± 77)	812 (±336)
sp_vcry::luc-s	35.8 (± 3)	-
sp_vcry::luc-l	227 (± 176)	39 (±11)

Table D7 Values of averaged luminescence detected in *sp_vcry::luc-l-ep*$^{(-)}$ injected larvae in two independent experiments. Uninjected larvae were plated to measure the background level of luminescence signal; smp::luc injected larvae were used as positive control. Calculations made as explained in table D6. Values are expressed in counts of luminescence/second.

	Averaged luminescence (standard deviation) in exp1 (4dpf-1wpf)	Averaged luminescence (standard deviation) in exp2 (4 dpf- 6 dpf)
Uninjected (+food)	10 (±1)	
Uninjected (-food)	12 (±1)	66 (±29)
smp::luc (+food)	132 (±32)	
smp::luc (-food)	100 (±40)	
sp_vcry::luc-l-ep$^{(-)}$ (+food)	82 (±49)	
sp_vcry::luc-l-ep$^{(-)}$ (-food)	52 (±12)	215 (±31)

Table D8 Injected larvae were observed for normal development and counted (e.g. 2 larvae out of 15 showed normal development in *sp_tim*MO 300 µM batch1). For each microinjection experiment, morphological comparison was made between larvae injected with contMO (e.g. 7/16 in batch1 *sp_tim*MO 300 µM experiment) and the specific MO.

	***sp_tim*MO (300 µM) - contMO (300 µM)**	***sp_vcry*MO (300 µM) - contMO (300 µM)**	***sp_vcry*MO (200 µM) - contMO (200 µM)**
Batch1	2/15-7/16	0/11-10/10	13/13-8/8
Batch2			13/42-10/10
Batch3			10/10-10/10
Batch4			22/41-10/10

Continue Table D8

	***sp_dcry*MO (300 µM) - contMO (300 µM)**	***sp_opsin3.2* MO(300-250 µM) - contMO (300-250 µM)**	***sp_vcryMO* (150 µM) - contMO (150 µM)**	***sp_tim*MO (200 µM) - contMO (200 µM)**
Batch1	34/37-29/36	10/10-10/10	10/10-10/10	10/10-10/10
Batch2	8/8-10/10	10/10-10/10		9/10-10/12
Batch3	10/10-10/10			
Batch4				

Table D9 Comparison between background levels and *sp_dcry* mRNA levels detected in different microinjection experiments show that data derived from quantification of *sp_dcry* were not informative. Likely probes for the identification of this gene did not work properly because of changes in setting up the reaction of hybridization for nCounter Nanostring experiments. Background levels and *sp_dcry* mRNA levels were calculated for each time-point as described in Materials and Methods (paragraph 2.4.3). Then values were averaged and standard deviation (s.d.) was calculated.

	Background levels Normalized counts (s.d.)	***sp_dcry* mRNA levels Normalized counts (s.d.)**
*Sp_dcry*MO batch 1	8 (±2)	7 (±9)
*Sp_dcry*MO batch 2	6 (±2)	13 (±15)
*Sp_opsin3.2*MO batch 1	14 (±4)	3 (±2)
*Sp_opsin3.2*MO batch 2	8 (±3)	3 (±2)
*Sp_vcry*MO batch 1	12 (±3)	5 (±3)
*Sp_vcry*MO batch 2	25 (±9)	3 (±5)
*Sp_tim*MO batch 1	11 (±3)	35 (±24)
*Sp_tim*MO batch 2	22 (±6)	15 (±16)

Table D10 Summary table indicating values of amplitude, mesor and acrophase detected for genes which expression profiles where quantified in uninjected, conMO and knockdown conditions (chapter 5, paragraph 5.2). Amplitude and mesor values are expressed in normalized counts of transcripts, acrophase values in degrees of circumference (°). This values were calculating using the cosinor analysis (see methods) For each gene, condition of perturbation, day of sampling (day1 or day2), nr of independent experiments (batch1 or batch2) and comments about the effect of the knockdown are reported. Colours (grey and green) distinguish between different knockdown experiments. All statistical tests were considered significant if p-value was lower than 0.05.

Gene name	Condition	Amplitude	Mesor	Acrophase	p-value	Effect of knockdown
sp_dcry	ContMO day1 batch1	70	141	-1.79	0.025	Arrhythmicity/ increased levels of expression
	*sp_dcry*MO day1 batch1 qPCR	15	269	-3.18	0.39	
	ContMO day1 batch2 qPCR	21	88	-0.68	0.023	Arrhythmicity/ increased levels of expression
	ContMO day2 batch2 qPCR	25	100	-1.39	0.027	
	*sp_dcry*MO day1 batch2 qPCR	14	213	-5.24	0.81	
	*sp_dcry*MO day2 batch2 qPCR	44	282	-0.57	0.56	
sp_tim	ContMO day1 batch1	113	157	-2.71	0.0027	Rhythmicity with decreased levels of amplitude and mesor
	*sp_dcry*MO day1 batch1 qPCR	53	93	-3.76	0.0025	
	ContMO day1 batch2	38	95	-3.2	0.003	First day: rhythmicity with decreased level of amplitude. Second day: arrhythmicity
	ContMO day2 batch2	58	122	-3.1	0.0000 00003	
	*sp_dcry*MO day1 batch2 qPCR	12	80	-5.01	0.3	
	*sp_dcry*MO day2 batch2 qPCR	24	80	-3.47	0.03	

sp_tim	Uninj day1 batch1 nanostring	1	12.8	-5.28	0.8	No consistent
	Uninj Day2 batch1 nanostring	5	16	-3.1	0.00013	
	*sp_dcry*MO day1 batch1 nanostring	3	14	-3.8	0.2	
	*sp_dcry*MO day2 batch1 nanostirng	7	19	-4	0.9	
	Uninj Day1 batch2 nanostring	92	130	-1.7	0.7	No consistent
	*sp_dcry*MO day1 batch2	276	237	-3.1	0.06	
	Uninj day1 batch1 nanostring	172	228	-4.04	0.0031	Arrhythmicity
	Uninj Day2 batch1nanostring	258	304	-3.5	0.0048	
	sp_opsin3.2 MO day1 batch1 nanostring	198	235	-2.92	0.05	
	sp_opsin3.2 MO day2 batch1 nanostirng	54	101	-3.1	0.32	
	Uninj Day1 batch2 nanostring	3	8	-5.5	0.082	No consistent
	sp_opsin3.2 MO day1 batch2 nanostring	2	10	-0.43	0.72	
	Uninj day1 batch1 nanostring	439	464	-3.5	0.07	No effect
	Uninj Day2 batch1 nanostring	471	670	-2.83	0.0010	
	*sp_tim*MO day1 batch1 nanostring	725	975	-3.98	0.045	
	*sp_tim*MO day2 batch1 nanostirng	350	722	-2.92	$2.6\ e^{-5}$	

sp_tim	Uninj Day1 batch2 nanostring	71	100	-1.71	0.66	Not consistent, no effect
	*sp_tim*MO day1 batch2 nanostring	558	622	-2.94	0.0046	
	Uninj day1 batch1 nanostring	379	428	-3.5	0.0014	Arrhythmicity
	Uninj Day2 batch1 nanostring	158	229	-3.7	0.0021	
	*sp_vcry*MO day1 batch1 nanostring	203	194	-4.5	0.3	
	*sp_vcry*MO day2 batch1 nanostirng	24	73	-1.59	0.71	
	Uninj Day1 batch2 nanostring	135	177	-2.56	0.23	Not consistent. Decreased values of expression in sp_vcryMO
	*sp_vcry*MO day1 batch2 nanostirng	15	69	-4.24	0.85	
	Uninj day1 batch 1 qPCR	55	82	-3.6	0.27	Not consistent
	*sp_vcry*MO day1 batch 1 qPCR	42	62	-4.2	0.19	
sp_vcry	ContMO day1 batch1 qPCR	232	329	-1.2	0.008	Rhythmicity with decreased value of amplitude
	*sp_dcry*MO day1 batch1 qPCR	117	279	-1.019	0.006	
	ContMO day1 batch2 qPCR	114	178	-1.13	0.00075	arrhythmicity with decreased values of amplitude
	ContMO day2 batch2 qPCR	129	328	-0.96	0.0048	
	*sp_dcry*MO day1 batch2 qPCR	50	135	-1.05	0.089	
	*sp_dcry*MO day2 batch2 qPCR	89	194	-0.8	0.1	

sp_vcry	Uninj day1 batch1 nanostring	1140	1295	-1.23	0.0024	First day: rhythmicity with reduction of amplitude. Second day: not consistent.
	Uninj Day2 batch1 nanostring	683	1347	-6.18	0.42	
	*sp_dcry*MO day1 batch1 nanostring	589	964	-0.92	0.0093	
	*sp_dcry*MO day2 batch1 nanostirng	748	1645	-0.6	0.35	
	Uninj Day1 batch2 nanostring	845	993	-1.29	0.018	Rhythmicity with decreased value of amplitude.
	*sp_dcry*MO day1 batch2 nanostirng	396	751	-1.68	0.012	
	Uninj day1 batch1 nanostring	448	869	-0.9	0.0025	No effect
	Uninj Day2 batch1 nanostring	681	1044	-1.3	0.0036	
	sp_opsin3.2 MO day1 batch1 nanostring	378	667	-1.38	0.012	
	sp_opsin3.2 MO day2 batch1 nanostirng	493	814	-1.27	0.0027	
	Uninj Day1 batch2 nanostring	504	862	-1.24	0.16	Not consistent, No effect
	sp_opsin3.2 MO day1 batch2 nanostring	498	813	-0.89	0.036	

sp_vcry	Uninj day1 batch1 nanostring	776	1602	-1.22	0.08	No effect
	Uninj Day2 batch1 nanostring	1358	2103	-1.19	0.0006	
	*sp_tim*MO day1 batch1 nanostring	825	1731	-1.6	0.0089	
	*sp_tim*MO day2 batch1 nanostirng	1650	2201	-1.54	0.01	
	Uninj Day1 batch2 nanostring	651	765	-1.28	0.02	No effect
	*sp_tim*MO day1 batch2 nanostring	810	1038	-1.74	0.014	
	Uninj day1 batch1 nanostring	1406	1689	-1.5	0.018	No effect
	Uninj Day2 batch1 nanostring	1322	1691	-1.3	0.038	
	*sp_vcry*MO day1 batch1 nanostring	541	1211	-1.92	0.0032	
	*sp_vcry*MO day2 batch1 nanostirng	1122	1555	-1.7	0.018	
	Uninj Day1 batch2 nanostring	634	954	-1.65	0.0027	No effect
	*sp_vcry*MO day1 batch 2 nanostring	539	685	-1.67	0.010	
sp_hlf	Uninj day1 batch1 nanostring	10950	23276	-1.56	0.017	Not consistent
	Uninj Day2 batch1nanostring	2139	20140	-1.35	0.3	
	*sp_dcry*MO day1 batch1 nanostring	2490	26169	-1.2	0.2	
	*sp_dcry*MO day2 batch1 nanostirng	5578	31040	-1.2	0.077	
	Uninj Day1 batch2 nanostring	1516	15285	-1.7	0.86	Not consistent
	*sp_dcry*MO day1 batch2 nanostring	6757	13772	-5.5	0.17	

sp_hlf	Uninj day1 batch1 nanostring	1700	10404	-0.2	0.0007	Arrhythmicity with decrease value of mesor
	Uninj Day2 batch1 nanostring	1907	13285	-1.8	0.047	
	*sp_opsin3.2*MO day1 batch1 nanostring	1368	7670	-1.09	0.26	
	*sp_opsin3.2*MO day2 batch1 nanostirng	819	10235	-1.1	0.45	
	Uninj Day1 batch2 nanostring	6606	26360	-1.72	0.49	Not consistent but levels of expression decreased in knockdown
	*sp_opsin3.2*MO day1 batch2 nanostring	5747	18818	-1.3	0.40	
	Uninj day1 batch1 nanostring	2145	16881	-1.41	0.3	Not consistent, no effect
	Uninj Day2 batch1 nanostring	2139	20140	-1.35	0.3	
	*sp_tim*MO day1 batch1 nanostring	3618	12718	-1.45	0.33	
	*sp_tim*MO day2 batch1 nanostirng	2670	12966	-2.19	0.019	
	Uninj Day1 batch2 nanostring	3618	12718	-1.45	0.33	Not consistent, shift of 6 hours
	*sp_tim*MO day1 batch2 nanostring	2670	12966	-2.19	0.019	
	Uninj day1 batch1 nanostring	5310	18058	-1.86	0.11	Not consistent, decrease values of amplitude and mesor.
	Uninj Day2 batch1 nanostring	3644	21410	-2.24	0.41	
	*sp_vcry*MO day1 batch1 nanostring	2613	13030	-2.5	0.083	
	*sp_vcry*MO day2 batch1 nanostirng	2321	16046	-2.3	0.31	
	Uninj Day1 batch2 nanostring	4791	10818	-1.99	0.0077	Arrhythmicity
	*sp_vcry*MO day1 batch 2 nanostring	3897	8401	-1.6	0.16	

sp_opsin3.2	Uninj day1 batch1 nanostring	37	22	-0.1	0.018	arrhythmicity
	Uninj Day2 batch1 nanostring	17	49	-5.8	0.0085	
	*sp_dcry*MO day1 batch1 nanostring	5	40	-0.4	0.11	
	*sp_dcry*MO day2 batch1 nanostirng	22	57	-5.3	0.17	
	Uninj Day1 batch2 nanostring	16	46	-0.1	0.38	Not consistent
	*sp_dcry*MO day1 batch2	7	36	-5.83	0.26	
	Uninj day1 batch1 nanostring	13	20	-0.14	0.044	Consistent only first day with shift of 6 hours
	Uninj Day2 batch1 nanostring	8	29	-6.12	0.2	
	*sp_opsin3.2*MO day1 batch1 nanostring	13	21	-1.68	0.033	
	*sp_opsin3.2*MO day2 batch1 nanostirng	9	23	-1	0.075	
	Uninj Day1 batch2 nanostring	2	30.4	-4.4	0.97	Not consistent
	*sp_opsin3.2*MO day1 batch2 nanostring	9	22	-1	0.075	
	Uninj day1 batch1 nanostring	26	37	-6.04	0.022	No effect
	Uninj Day2 batch1 nanostring	26	52	-6.25	0.17	
	*sp_tim*MO day1 batch1 nanostring	22	55	-6	0.005	
	*sp_tim*MO day2 batch1 nanostirng	26	66	-6.01	0.002	

sp_opsin3.2	Uninj Day1 batch2 nanostring	12	35	-0.1	0.38	Not consistent, no effect
	*sp_tim*MO day1 batch2 nanostring	26	37	-6	0.02	
	Uninj day1 batch1 nanostring	17	56	-0.43	0.08	No effect
	Uninj Day2 batch1 nanostring	2.4	65	-5.8	0.8	
	*sp_vcry*MO day1 batch1 nanostring	12	34	-5.4	0.015	
	*sp_vcry*MO day2 batch1 nanostirng	12	43	-0.46	0.35	
	Uninj Day1 batch2 nanostring	6	48	-1.76	0.76	Not consistent, no effect
	*sp_vcry*MO day1 batch 2 nanostring	15	30	-0.29	0.00017	
sp_crydash	Uninj day1 batch1 nanostring	684	711	-2.2	0.008	No effect
	Uninj Day2 batch1 nanostring	494	697	-2.9	1.5 e^{-05}	
	*sp_dcry*MO day1 batch1 nanostring	309	525	-2.6	0.013	
	*sp_dcry*MO day2 batch1 nanostirng	716	925	-3	0.03	
	Uninj Day1 batch2 nanostring	732	615	-1.9	0.049	Rhythmicity with decreased values of amplitude
	*sp_dcry*MO day1 batch2 nanostirng	377	567	-2.6	0.0077	
	Uninj day1 batch1 nanostring	392	612	-2.7	0.011	No effect
	Uninj Day2 batch1 nanostring	557	729	-2.4	0.007	
	sp_opsin3.2 MO day1 batch1 nanostring	385	513	-2.4	0.007	
	sp_opsin3.2 MO day2 batch1 nanostirng	366	588	-2.6	1.9 e^{-5}	

sp_crydash	Uninj Day1 batch2 nanostring	233	405	-0.8	0.5	Not consistent, no effect
	sp_opsin3.2 MO day1 batch2 nanostring	401	502	-2.5	0.001	
	Uninj day1 batch1 nanostring	696	849	-2.66	0.00075	No effect
	Uninj Day2 batch1 nanostring	1137	1152	-2.26	0.0037	
	*sp_tim*MO day1 batch1 nanostring	624	1024	-2.3	0.064	
	*sp_tim*MO day2 batch1 nanostirng	942	1248	-3.7	0.041	
	Uninj Day1 batch2 nanostring	564	474	-1.96	0.049	No effect
	*sp_tim*MO day1 batch2 nanostring	694	636	-2.2	0.0026	
	Uninj day1 batch1 nanostring	1276	1145	-2.3	0.0076	Rhythmicity with decreased values of amplitude and mesor
	Uninj Day2 batch1 nanostring	1148	1236	-2.3	0.04	
	*sp_vcry*MO day1 batch1 nanostring	564	636	-2.4	0.01	
	Sp_vcryMO day2 batch1 nanostirng	571	766	-2.4	0.0067	
	Uninj Day1 batch2 nanostring	782	785	-2.3	$7.8\ e^{-7}$	Rhythmicity with decreased values of amplitude and mesor
	*sp_vcry*MO day1 batch 2 nanostring	317	367	-2.3	0.0011	

sp_6-4 photolyase	Uninj day1 batch1 nanostring	86	301	-2.3	0.065	First day: not consistent, second day: arrhythmicity
	Uninj Day2 batch1 nanostring	124	407	-3.5	$6.8\ e^{-6}$	
	*sp_dcry*MO day1 batch1 nanostring	8	134	-5.37	0.98	
	*sp_dcry*MO day2 batch1 nanostirng	401	638	-1.06	0.33	
	Uninj Day1 batch2 nanostring	473	574	-2.06	0.0002	No effect
	*sp_dcry*MO day1 batch2 nanostirng	317	767	-2.5	0.01	
	Uninj day1 batch1 nanostring	116	351	-2.27	0.0013	No effect
	Uninj Day2 batch1 nanostring	359	537	-2.39	$1.59\ e^{-6}$	
	sp_opsin3.2 MO day1 batch1 nanostring	202	403	-1.9	0.002	
	sp_opsin3.2 MO day2 batch1 nanostirng	348	545	-2.36	0.00089	
	Uninj Day1 batch2 nanostring	181	221	-1.16	0.24	Not consistent , no effect
	sp_opsin3.2 MO day1 batch2 nanostring	139	307	-1.99	0.014	
	Uninj day1 batch1 nanostring	439	764	-2.36	0.00095	No effect
	Uninj Day2 batch1 nanostring	691	1028	-2.19	0.00049	
	*sp_tim*MO day1 batch1 nanostring	320	821	-2.26	0.088	
	*sp_tim*MO day2 batch1 nanostirng	633	1021	-3.7	0.019	
	Uninj Day1 batch2 nanostring	364	442	-2.05	0.00022	No effect
	*sp_tim*MO day1 batch2 nanostring	450	667	-2.45	0.028	

sp_6-4 photolyase	Uninj day1 batch1 nanostring	267	551	-2.11	0.067	Arhythmicity with increased values of expression
	Uninj Day2 batch1 nanostring	260	568	-2.09	0.04	
	*sp_vcry*MO day1 batch1 nanostring	107	935	-2.9	0.39	
	*sp_vcry*MO day2 batch1 nanostirng	270	1066	-1.85	0.23	
	Uninj Day1 batch2 nanostring	965	1173	-1.8	0.013	Arhythmicity with decreased values of amplitude and mesor
	*sp_vcry*MO day1 batch 2 nanostring	577	651	-1.58	0.06	

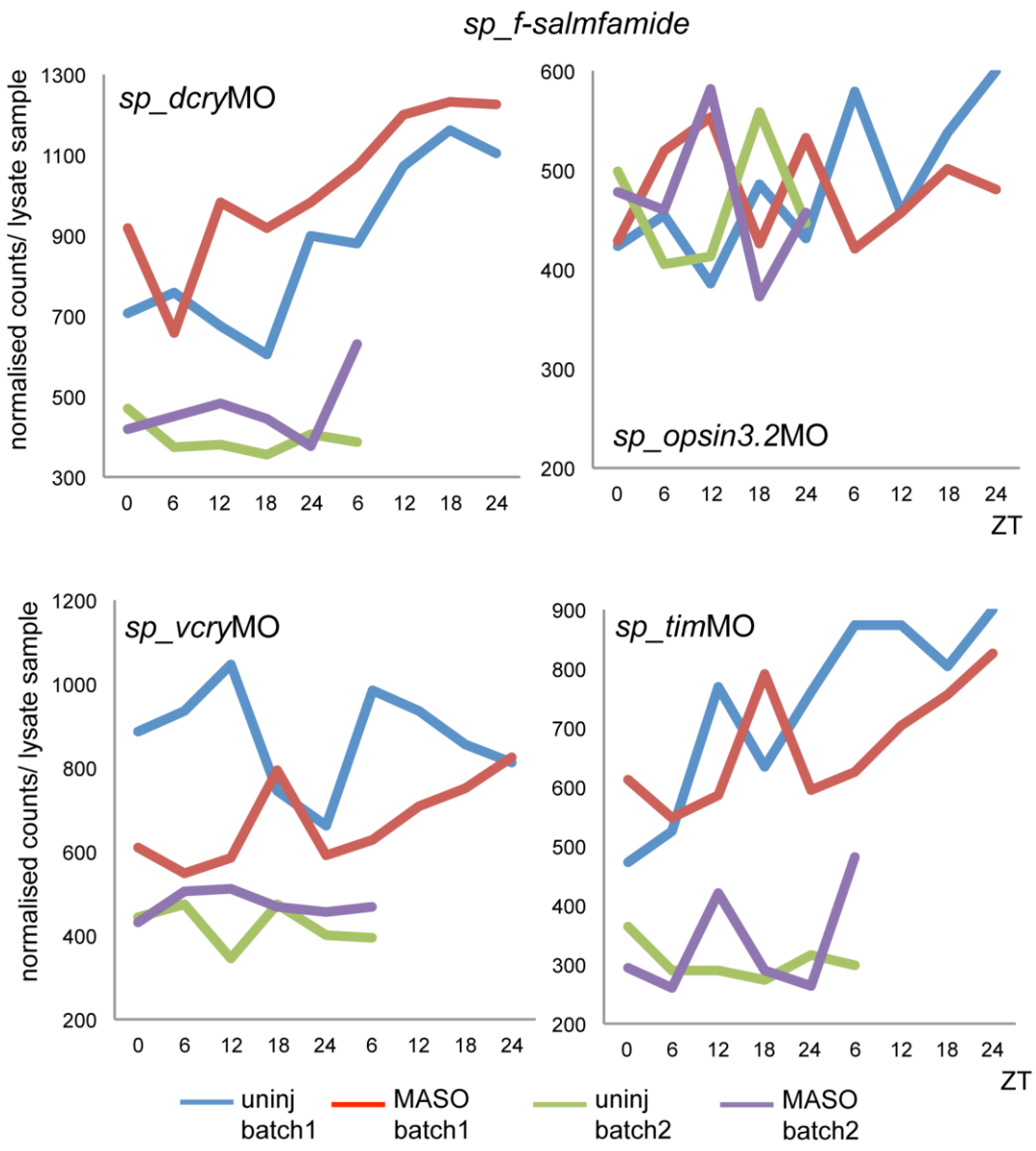

Fig.D9 Daily expression profiles of *sp_f-salmfamide* detected in uninjected and larvae injected with *sp_dcry*MO, *sp_opsin3.2*MO, *sp_vcry*MO, *sp_tim*MO. For details see the legend.

List of references

Abrahamson, E. E. and R. Y. Moore (2001). "Suprachiasmatic nucleus in the mouse: retinal innervation, intrinsic organization and efferent projections." Brain Res 916(1-2): 172-191.

Abruzzi, K. C., J. Rodriguez, J. S. Menet, J. Desrochers, A. Zadina, W. Luo, S. Tkachev and M. Rosbash (2011). "Drosophila CLOCK target gene characterization: implications for circadian tissue-specific gene expression." Genes Dev 25(22): 2374-2386.

Agca, C., M. C. Elhajj, W. H. Klein and J. M. Venuti (2011). "Neurosensory and neuromuscular organization in tube feet of the sea urchin Strongylocentrotus purpuratus." J Comp Neurol 519(17): 3566-3579.

Akten, B., Jauch, E., Genova, G.K., Kim, E.Y., Edery, I., Raabe, T. and Jackson, F.R. (2003) A role for CK2 in the Drosophila circadian oscillator. Nat. Neurosci. 6, 251–257.

Albrecht, U., Z. S. Sun, G. Eichele and C. C. Lee (1997). "A differential response of two putative mammalian circadian regulators, mper1 and mper2, to light." Cell 91(7): 1055-1064.

Allada, R., N. E. White, W. V. So, J. C. Hall and M. Rosbash (1998). "A mutant Drosophila homolog of mammalian Clock disrupts circadian rhythms and transcription of period and timeless." Cell 93(5): 791-804.

Amoutzias, G. D., A. S. Veron, J. Weiner, 3rd, M. Robinson-Rechavi, E. Bornberg-Bauer, S. G. Oliver and D. L. Robertson (2007). "One billion years of bZIP transcription factor evolution: conservation and change in dimerization and DNA-binding site specificity." Mol Biol Evol 24(3): 827-835.

Arendt, D. (2003). "Evolution of eyes and photoreceptor cell types." Int J Dev Biol 47(7-8): 563-571.

Arendt, D., H. Hausen and G. Purschke (2009). "The 'division of labour' model of eye evolution." Philos Trans R Soc Lond B Biol Sci 364(1531): 2809-2817.

Arendt, D., K. Tessmar-Raible, H. Snyman, A. W. Dorresteijn and J. Wittbrodt (2004). "Ciliary photoreceptors with a vertebrate-type opsin in an invertebrate brain." Science 306(5697): 869-871.

Arnone, M. I., L. D. Bogarad, A. Collazo, C. V. Kirchhamer, R. A. Cameron, J. P. Rast, A. Gregorians and E. H. Davidson (1997). "Green Fluorescent Protein in the sea urchin: new experimental approaches to transcriptional regulatory analysis in embryos and larvae." Development 124(22): 4649-4659.

Arshavsky, V. Y., T. D. Lamb and E. N. Pugh, Jr. (2002). "G proteins and phototransduction." Annu Rev Physiol 64: 153-187.

Bae, K., X. Jin, E. S. Maywood, M. H. Hastings, S. M. Reppert and D. R. Weaver (2001). "Differential functions of mPer1, mPer2, and mPer3 in the SCN circadian clock." Neuron 30(2): 525-536.

Barnes, J. W., S. A. Tischkau, J. A. Barnes, J. W. Mitchell, P. W. Burgoon, J. R. Hickok and M. U. Gillette (2003). "Requirement of mammalian Timeless for circadian rhythmicity." Science 302(5644): 439-442.

Bayo, P., E. Ochola, C. Oleo and A. D. Mwaka (2014). "High prevalence of hepatitis B virus infection among pregnant women attending antenatal care: a cross-sectional study in two hospitals in northern Uganda." BMJ Open 4(11): e005889.

Beer, A. J., C. Moss and M. Thorndyke (2001). "Development of serotonin-like and SALMFamide-like immunoreactivity in the nervous system of the sea urchin Psammechinus miliaris." Biol Bull 200(3): 268-280.

Bell-Pedersen, D., V. M. Cassone, D. J. Earnest, S. S. Golden, P. E. Hardin, T. L. Thomas and M. J. Zoran (2005). "Circadian rhythms from multiple oscillators: lessons from diverse organisms." Nat Rev Genet 6(7): 544-556.

Belvin, M. P., H. Zhou and J. C. Yin (1999). "The Drosophila dCREB2 gene affects the circadian clock." Neuron 22(4): 777-787.

Benna, C., S. Bonaccorsi, C. Wulbeck, C. Helfrich-Forster, M. Gatti, C. P. Kyriacou, R. Costa and F. Sandrelli (2010). "Drosophila timeless2 is required for chromosome stability and circadian photoreception." Curr Biol 20(4): 346-352.

Ben-Shlomo, R. and C. P. Kyriacou (2002). "Circadian rhythm entrainment in flies and mammals." Cell Biochem Biophys 37(2): 141-156.

Benson, S., H. Sucov, L. Stephens, E. Davidson and F. Wilt (1987). "A lineage-specific gene encoding a major matrix protein of the sea urchin embryo spicule. I. Authentication of the cloned gene and its developmental expression." Dev Biol 120(2): 499-506.

Berson, D. M., F. A. Dunn and M. Takao (2002). "Phototransduction by retinal ganglion cells that set the circadian clock." Science 295(5557): 1070-1073.

Bishop, R. P., B. K. Sohanpal, S. P. Morzaria, T. T. Dolan, F. N. Mwakima and A. S. Young (1994). "Discrimination between Theileria parva and T. taurotragi in the salivary glands of Rhipicephalus appendiculatus ticks using oligonucleotides homologous to ribosomal RNA sequences." Parasitol Res 80(3): 259-261.

Bisgrove, B. W., and R. D. Burke. 1986. Development of serotonergic neurons in embryos of the sea urchin, Sfrongylocentrotus purpuratus. Dev. Growth Differ. 28: 569-574.

Blanton, E., S. Ombeki, G. O. Oluoch, A. Mwaki, K. Wannemuehler and R. Quick (2010). "Evaluation of the role of school children in the promotion of point-of-use water treatment and handwashing in schools and households--Nyanza Province, Western Kenya, 2007." Am J Trop Med Hyg 82(4): 664-671.

Bollinger, T. and U. Schibler (2014). "Circadian rhythms - from genes to physiology and disease." Swiss Med Wkly 144: w13984.

Bousema, T., W. Roeffen, H. Meijerink, H. Mwerinde, S. Mwakalinga, G. J. van Gemert, M. van de Vegte-Bolmer, F. Mosha, G. Targett, E. M. Riley, R. Sauerwein and C. Drakeley (2010). "The dynamics of naturally acquired immune responses to Plasmodium falciparum sexual stage antigens Pfs230 & Pfs48/45 in a low endemic area in Tanzania." PLoS One 5(11): e14114.

Brady, A. K., K. A. Snyder and P. D. Vize (2011). "Circadian cycles of gene expression in the coral, Acropora millepora." PLoS One 6(9): e25072.

Brameier, M., A. Krings and R. M. MacCallum (2007). "NucPred - Predicting nuclear localization of proteins." Bioinformatics 23(9): 1159-1160.

Bisgrove, B. W. & Burke, R. D. 1987. Development of the nervous system of the pluteus larva of Strongylocentrotus drobachiensis. Cell Tissue Res. 248, 335–343

Brameier M., Krings A., MacCallum R.M., NucPred, predicting nuclear localization of proteins Vol. 23 no. 9 2007, 1159–1160 bioinformatics applications note.

Brown, S. A., E. Kowalska and R. Dallmann (2012). "(Re)inventing the circadian feedback loop." Dev Cell 22(3): 477-487.

Buhr, E. D. and J. S. Takahashi (2013). "Molecular components of the Mammalian circadian clock." Handb Exp Pharmacol(217): 3-27.

Buijs, R., R. Salgado, E. Sabath and C. Escobar (2013). "Peripheral circadian oscillators: time and food." Prog Mol Biol Transl Sci 119: 83-103.

Bulimo, W. D., R. A. Achilla, J. Majanja, S. Mukunzi, M. Wadegu, F. Osunna, J. Mwangi, J. Njiri, J. Wangui, J. Nyambura, B. Obura, K. Mitei, D. Omariba, S. Segecha, M. Nderitu, A. Odindo, C. Adega, J. Kiponda, R. Mupa, F. Munyazi, G. Kissinger, M. Mwakuzimu, D. Kamola, E. Muhidin, D. Kamau, S. Kairithia, M. Koech, A. Sang, L. Onge'ta and D. C. Schnabel (2012). "Molecular characterization and phylogenetic analysis of the hemagglutinin 1 protein of human influenza A virus subtype H1N1 circulating in Kenya during 2007-2008." J Infect Dis 206 Suppl 1: S46-52.

Burke, R. D., L. M. Angerer, M. R. Elphick, G. W. Humphrey, S. Yaguchi, T. Kiyama, S. Liang, X. Mu, C. Agca, W. H. Klein, B. P. Brandhorst, M. Rowe, K. Wilson, A. M. Churcher, J. S. Taylor, N. Chen, G. Murray, D. Wang, D. Mellott, R. Olinski, F. Hallbook and M. C. Thorndyke (2006). "A genomic view of the sea urchin nervous system." Dev Biol 300(1): 434-460.

Burke, R. D., D. J. Moller, O. A. Krupke and V. J. Taylor (2014). "Sea urchin neural development and the metazoan paradigm of neurogenesis." Genesis 52(3): 208-221.

Burke, R. D., L. Osborne, D. Wang, N. Murabe, S. Yaguchi and Y. Nakajima (2006). "Neuron-specific expression of a synaptotagmin gene in the sea urchin Strongylocentrotus purpuratus." J Comp Neurol 496(2): 244-251.

Busza, A., M. Emery-Le, M. Rosbash and P. Emery (2004). "Roles of the two Drosophila CRYPTOCHROME structural domains in circadian photoreception." Science 304(5676): 1503-1506.

Byrne, M., Y. Nakajima, F. C. Chee and R. D. Burke (2007). "Apical organs in echinoderm larvae: insights into larval evolution in the Ambulacraria." Evol Dev 9(5): 432-445.

Caspi R, Altman T, Billington R, Dreher K, Foerster H, Fulcher CA, Holland TA, Keseler IM, Kothari A, Kubo A, Krummenacker M, Latendresse M, Mueller LA, Ong Q, Paley S, Subhraveti P, Weaver DS, Weerasinghe D, Zhang P, Karp PD. (2014) **“**The MetaCyc database of metabolic pathways and enzymes and the BioCyc collection of Pathway/Genome Databases”. Nucleic Acids Res.;42:D459-71.

Cameron, R. A., P. Oliveri, J. Wyllie and E. H. Davidson (2004). "cis-Regulatory activity of randomly chosen genomic fragments from the sea urchin." Gene Expr Patterns 4(2): 205-213.

Cameron, R. A., M. Samanta, A. Yuan, D. He and E. Davidson (2009). "SpBase: the sea urchin genome database and web site." Nucleic Acids Res 37(Database issue): D750-754.

Cameron, R. A., M. Samanta, A. Yuan, D. He and E. Davidson (2009). "SpBase: the sea urchin genome database and web site." Nucleic Acids Res 37(Database issue): D750-754.

Cashmore, A. R. (2003). "Cryptochromes: enabling plants and animals to determine circadian time." Cell 114(5): 537-543.

Cavallari, N., E. Frigato, D. Vallone, N. Frohlich, J. F. Lopez-Olmeda, A. Foa, R. Berti, F. J. Sanchez-Vazquez, C. Bertolucci and N. S. Foulkes (2011). "A blind circadian clock in cavefish reveals that opsins mediate peripheral clock photoreception." PLoS Biol 9(9): e1001142.

Cermakian, N. and P. Sassone-Corsi (2000). "Multilevel regulation of the circadian clock." Nat Rev Mol Cell Biol 1(1): 59-67.

Chang, D. C., H. G. McWatters, J. A. Williams, A. L. Gotter, J. D. Levine and S. M. Reppert (2003). "Constructing a feedback loop with circadian clock molecules from the silkmoth, Antheraea pernyi." J Biol Chem 278(40): 38149-38158.

Chaves, I., R. Pokorny, M. Byrdin, N. Hoang, T. Ritz, K. Brettel, L. O. Essen, G. T. van der Horst, A. Batschauer and M. Ahmad (2011). "The cryptochromes: blue light photoreceptors in plants and animals." Annu Rev Plant Biol 62: 335-364.

Che-Yi Lin, Yi-Hsien Su (2016). “Genome editing in sea urchin embryos by using a CRISPR/Cas9 system.” Developmental Biology 409, 15, 420–428.

Chen, G. and A. J. Courey (2000). "Groucho/TLE family proteins and transcriptional repression." Gene 249(1-2): 1-16.

Chen, K. F., N. Peschel, R. Zavodska, H. Sehadova and R. Stanewsky (2011). "QUASIMODO, a Novel GPI-anchored zona pellucida protein involved in light input to the Drosophila circadian clock." Curr Biol 21(9): 719-729.

Chia F.S., Koss R. Fine structural studies of the nervous system and the apical organ in the planula larva of the sea anemone Anthopleura elegantissima. J. Morphol, 160 (1979), pp. 275–298

Ciarleglio, C. M., H. E. Resuehr and D. G. McMahon (2011). "Interactions of the serotonin and circadian systems: nature and nurture in rhythms and blues." Neuroscience 197: 8-16.

Coesel, S., M. Mangogna, T. Ishikawa, M. Heijde, A. Rogato, G. Finazzi, T. Todo, C. Bowler and A. Falciatore (2009). "Diatom PtCPF1 is a new cryptochrome/photolyase family member with DNA repair and transcription regulation activity." EMBO Rep 10(6): 655-661.

Collins, B., E. O. Mazzoni, R. Stanewsky and J. Blau (2006). "Drosophila CRYPTOCHROME is a circadian transcriptional repressor." Curr Biol 16(5): 441-449.

Conzelmann M., Williams E.A., Tunaru S., Randel N., Shahidi R., Asadulina A., Berger J., Offermanns S., Jekely G. Conserved MIP receptor-ligand pair regulates Platynereis larval settlement. Proc. Natl. Acad. Sci. U.S.A. 2013;110:8224–8229.

Croll R.P., Dickinson A.J.G. Form and function of the larval nervous system in molluscs. Invertebr. Reprod. Dev. 2004;46:173–187.

Crump, J. A., H. O. Ramadhani, A. B. Morrissey, W. Saganda, M. S. Mwako, L. Y. Yang, S. C. Chow, S. C. Morpeth, H. Reyburn, B. N. Njau, A. V. Shaw, H. C. Diefenthal,

J. F. Shao, J. A. Bartlett and V. P. Maro (2011). "Invasive bacterial and fungal infections among hospitalized HIV-infected and HIV-uninfected adults and adolescents in northern Tanzania." Clin Infect Dis 52(3): 341-348.

Crump, J. A., H. O. Ramadhani, A. B. Morrissey, W. Saganda, M. S. Mwako, L. Y. Yang, S. C. Chow, B. N. Njau, G. S. Mushi, V. P. Maro, L. B. Reller and J. A. Bartlett (2012). "Bacteremic disseminated tuberculosis in sub-saharan Africa: a prospective cohort study." Clin Infect Dis 55(2): 242-250.

Czarna, A., A. Berndt, H. R. Singh, A. Grudziecki, A. G. Ladurner, G. Timinszky, A. Kramer and E. Wolf (2013). "Structures of Drosophila cryptochrome and mouse cryptochrome1 provide insight into circadian function." Cell 153(6): 1394-1405.

Damiola, F., N. Le Minh, N. Preitner, B. Kornmann, F. Fleury-Olela and U. Schibler (2000). "Restricted feeding uncouples circadian oscillators in peripheral tissues from the central pacemaker in the suprachiasmatic nucleus." Genes Dev 14(23): 2950-2961.

D'Aniello, S., J. Delroisse, A. Valero-Gracia, E. K. Lowe, M. Byrne, J. T. Cannon, K. M. Halanych, M. R. Elphick, J. Mallefet, S. Kaul-Strehlow, C. J. Lowe, P. Flammang, E. Ullrich-Luter, A. Wanninger and M. I. Arnone (2015). "Opsin evolution in the Ambulacraria." Mar Genomics.

Darlington, T. K., K. Wager-Smith, M. F. Ceriani, D. Staknis, N. Gekakis, T. D. Steeves, C. J. Weitz, J. S. Takahashi and S. A. Kay (1998). "Closing the circadian loop: CLOCK-induced transcription of its own inhibitors per and tim." Science 280(5369): 1599-1603.

Davidson, E. H., R. A. Cameron and A. Ransick (1998). "Specification of cell fate in the sea urchin embryo: summary and some proposed mechanisms." Development 125(17): 3269-3290.

Davidson, E. H., K. J. Peterson and R. A. Cameron (1995). "Origin of bilaterian body plans: evolution of developmental regulatory mechanisms." Science 270(5240): 1319-1325.

DeBruyne, J. P., D. R. Weaver and S. M. Reppert (2007). "CLOCK and NPAS2 have overlapping roles in the suprachiasmatic circadian clock." Nat Neurosci 10(5): 543-545.

DeBruyne, J. P., D. R. Weaver and S. M. Reppert (2007). "Peripheral circadian oscillators require CLOCK." Curr Biol 17(14): R538-539.

Delroisse, J., E. Ullrich-Luter, O. Ortega-Martinez, S. Dupont, M. I. Arnone, J. Mallefet and P. Flammang (2014). "High opsin diversity in a non-visual infaunal brittle star." BMC Genomics 15: 1035.

Delsuc, F., H. Brinkmann, D. Chourrout and H. Philippe (2006). "Tunicates and not cephalochordates are the closest living relatives of vertebrates." Nature 439(7079): 965-968.

Dissel, S., V. Codd, R. Fedic, K. J. Garner, R. Costa, C. P. Kyriacou and E. Rosato (2004). "A constitutively active cryptochrome in Drosophila melanogaster." Nat Neurosci 7(8): 834-840.

Dollins, A.B., Zhdanova, I.V., Wurtman, R.J., Lynch, H.J., and Deng, M.H. (1994). Effect of inducing nocturnal serum melatonin concentrations in daytime on sleep, mood, body temperature, and performance. Proc. Natl. Acad. Sci. USA 91, 1824–1828.

Ebling, F. J. (1996). "The role of glutamate in the photic regulation of the suprachiasmatic nucleus." Prog Neurobiol 50(2-3): 109-132.

Eckel-Mahan, K. and P. Sassone-Corsi (2013). "Metabolism and the circadian clock converge." Physiol Rev 93(1): 107-135.

Elphick Maurice R., Thorndyke Michael C. (2005). “Molecular characterisation of SALMFamide neuropeptides in sea urchins.” Journal of Experimental Biology 208: 4273-4282.

Elphick M.R., Rowe M.L., (2009). “NGFFFamide and echinotocin: structurally unrelated myoactive neuropeptides derived from neurophysin-containing precursors in sea urchins.” J. Exp. Biol. 212 1067–1077.

Emery, I. F., J. M. Noveral, C. F. Jamison and K. K. Siwicki (1997). "Rhythms of Drosophila period gene expression in culture." Proc Natl Acad Sci U S A 94(8): 4092-4096.

Emery, P., W. V. So, M. Kaneko, J. C. Hall and M. Rosbash (1998). "CRY, a Drosophila clock and light-regulated cryptochrome, is a major contributor to circadian rhythm resetting and photosensitivity." Cell 95(5): 669-679.

Emery, P., R. Stanewsky, J. C. Hall and M. Rosbash (2000). "A unique circadian-rhythm photoreceptor." Nature 404(6777): 456-457.

Ernst, S. G. (2011). "Offerings from an urchin." Dev Biol 358(2): 285-294.

Ettensohn, C. A., G. M. Wessel and G. A. Wray (2004). "The invertebrate deuterostomes: an introduction to their phylogeny, reproduction, development, and genomics." Methods Cell Biol 74: 1-13.

Falcon, J., H. Migaud, J. A. Munoz-Cueto and M. Carrillo (2010). "Current knowledge on the melatonin system in teleost fish." Gen Comp Endocrinol 165(3): 469-482.

Fernald R.D. (2006). “Casting a genetic light on the evolution of eyes.” Science 313:1914-1918.

Flytzanis, C. N., A. P. McMahon, B. R. Hough-Evans, K. S. Katula, R. J. Britten and E. H. Davidson (1985). "Persistence and integration of cloned DNA in postembryonic sea urchins." Dev Biol 108(2): 431-442.

Foster, R. G., I. Provencio, D. Hudson, S. Fiske, W. De Grip and M. Menaker (1991). "Circadian photoreception in the retinally degenerate mouse (rd/rd)." J Comp Physiol A 169(1): 39-50.

Francl, J. M., G. Kaur and J. D. Glass (2010). "Regulation of vasoactive intestinal polypeptide release in the suprachiasmatic nucleus circadian clock." Neuroreport 21(16): 1055-1059.

Franks, R. R., R. Anderson, J. G. Moore, B. R. Hough-Evans, R. J. Britten and E. H. Davidson (1990). "Competitive titration in living sea urchin embryos of regulatory factors required for expression of the CyIIIa actin gene." Development 110(1): 31-40.

Gallego, M. and D. M. Virshup (2007). "Post-translational modifications regulate the ticking of the circadian clock." Nat Rev Mol Cell Biol 8(2): 139-148.

Gehring, W. and M. Rosbash (2003). "The coevolution of blue-light photoreception and circadian rhythms." J Mol Evol 57 Suppl 1: S286-289.

Gekakis, N., D. Staknis, H. B. Nguyen, F. C. Davis, L. D. Wilsbacher, D. P. King, J. S. Takahashi and C. J. Weitz (1998). "Role of the CLOCK protein in the mammalian circadian mechanism." Science 280(5369): 1564-1569.

Gerlach, D., M. Wolf, T. Dandekar, T. Muller, A. Pokorny and S. Rahmann (2007). "Deep metazoan phylogeny." In Silico Biol 7(2): 151-154.

Giebultowicz, J. M. and D. M. Hege (1997). "Circadian clock in Malpighian tubules." Nature 386(6626): 664.

Gilbert S.F. Development Biology (2010). Palgrave Macmillan; 9th edition

Glossop, N. R. and P. E. Hardin (2002). "Central and peripheral circadian oscillator mechanisms in flies and mammals." J Cell Sci 115(Pt 17): 3369-3377.

Goldberg J.I., Koehncke N.K., Christopher K.J., Neumann C., Diefenbach T.J. Pharmacological characterization of a serotonin receptor involved in an early embryonic behavior of Helisoma trivolvis. J. Neurobiol. 1994;25:1545–1557.

Gooley, J. J., J. Lu, T. C. Chou, T. E. Scammell and C. B. Saper (2001). "Melanopsin in cells of origin of the retinohypothalamic tract." Nat Neurosci 4(12): 1165.

Gotter, A. L., T. Manganaro, D. R. Weaver, L. F. Kolakowski, Jr., B. Possidente, S. Sriram, D. T. MacLaughlin and S. M. Reppert (2000). "A time-less function for mouse timeless." Nat Neurosci 3(8): 755-756.

Goujon M, McWilliam H, Li W, Valentin F, Squizzato S, Paern J, Lopez R. A new bioinformatics analysis tools framework at EMBL-EBI (2010) Nucleic acids research 2010 Jul, 38 Suppl: W695-9 doi:10.1093/nar/gkq313

Granados-Fuentes, D. and E. D. Herzog (2013). "The clock shop: coupled circadian oscillators." Exp Neurol 243: 21-27.

Green C.B. and Besharse J.C. Tryptophan hydroxylase expression is regulated by a circadian clock in X*enopus laevis* retina. (1994). Journal of Neurochemistry. 62, issue 6, 2420:2428.

Grima, B., Lamouroux, A., Chelot, E., Papin, C., Limbourg-Bouchon, B. and Rouyer, F. (2002) The F-box protein slimb controls the levels of clock proteins period and timeless. Nature 420, 178–182.

Hadfield M.G., Meleshkevitch E.A., Boudko D.Y. The apical sensory organ of a gastropod veliger is a receptor for settlement cues. Biol. Bull. 2000;198:67–76.

Hai-Feng Gu, Jin-Hua Xiao, Li-Ming Niu, Bo Wang, Guang-Chang Ma, Derek W. Dunn, Da-Wei Huang (2014) Adaptive evolution of the circadian gene *timeout* in insects *Scientific Reports* 4, Article number: 4212

Hanai, S., Y. Hamasaka and N. Ishida (2008). "Circadian entrainment to red light in Drosophila: requirement of Rhodopsin 1 and Rhodopsin 6." Neuroreport 19(14): 1441-1444.

Hanai, S. and N. Ishida (2009). "Entrainment of Drosophila circadian clock to green and yellow light by Rh1, Rh5, Rh6 and CRY." Neuroreport 20(8): 755-758.

Hannibal, J., J. M. Ding, D. Chen, J. Fahrenkrug, P. J. Larsen, M. U. Gillette and J. D. Mikkelsen (1997). "Pituitary adenylate cyclase-activating peptide (PACAP) in the retinohypothalamic tract: a potential daytime regulator of the biological clock." J Neurosci 17(7): 2637-2644.

Hara, R., K. Wan, H. Wakamatsu, R. Aida, T. Moriya, M. Akiyama and S. Shibata (2001). "Restricted feeding entrains liver clock without participation of the suprachiasmatic nucleus." Genes Cells 6(3): 269-278.

Hardeland, R. and B. Poeggeler (2003). "Non-vertebrate melatonin." J Pineal Res 34(4): 233-241.

Hardeland, R. (2015). Melatonin in plants and other phototrophs: advances and gaps concerning the diversity of functions. *Journal of Experimental Botany*, *66*(3), 627–646.

Hardin, P. E. (2005). "The circadian timekeeping system of Drosophila." Curr Biol 15(17): R714-722.

Hardin, P. E. (2011). "Molecular genetic analysis of circadian timekeeping in Drosophila." Adv Genet 74: 141-173.

Harmer, S. L. (2009). "The circadian system in higher plants." Annu Rev Plant Biol 60: 357-377.

Helfrich-Forster, C. (2000). "Differential control of morning and evening components in the activity rhythm of Drosophila melanogaster--sex-specific differences suggest a different quality of activity." J Biol Rhythms 15(2): 135-154.

Helfrich-Forster, C. (2003). "The neuroarchitecture of the circadian clock in the brain of Drosophila melanogaster." Microsc Res Tech 62(2): 94-102.

Helfrich-Forster, C. (2005). "Neurobiology of the fruit fly's circadian clock." Genes Brain Behav 4(2): 65-76.

Helfrich-Forster, C., C. Winter, A. Hofbauer, J. C. Hall and R. Stanewsky (2001). "The circadian clock of fruit flies is blind after elimination of all known photoreceptors." Neuron 30(1): 249-261.

Hemsley, M. J., G. M. Mazzotta, M. Mason, S. Dissel, S. Toppo, M. A. Pagano, F. Sandrelli, F. Meggio, E. Rosato, R. Costa and S. C. Tosatto (2007). "Linear motifs in the C-terminus of D. melanogaster cryptochrome." Biochem Biophys Res Commun 355(2): 531-537.

Herring, P. J. The spectral characteristics of luminous marine organisms (1983). Proc. R. Soc. Lond. B 220, 183-217.

Hirano, A., K. Yumimoto, R. Tsunematsu, M. Matsumoto, M. Oyama, H. Kozuka-Hata, T. Nakagawa, D. Lanjakornsiripan, K. I. Nakayama and Y. Fukada (2013). "FBXL21 regulates oscillation of the circadian clock through ubiquitination and stabilization of cryptochromes." Cell 152(5): 1106-1118.

Hirayama, J., S. Cho and P. Sassone-Corsi (2007). "Circadian control by the reduction/oxidation pathway: catalase represses light-dependent clock gene expression in the zebrafish." Proc Natl Acad Sci U S A 104(40): 15747-15752.

Hirayama, J., H. Nakamura, T. Ishikawa, Y. Kobayashi and T. Todo (2003). "Functional and structural analyses of cryptochrome. Vertebrate CRY regions responsible for interaction with the CLOCK:BMAL1 heterodimer and its nuclear localization." J Biol Chem 278(37): 35620-35628.

Hirayama, J. and P. Sassone-Corsi (2005). "Structural and functional features of transcription factors controlling the circadian clock." Curr Opin Genet Dev 15(5): 548-556.

Hoadley, K. D., A. M. Szmant and S. J. Pyott (2011). "Circadian clock gene expression in the coral Favia fragum over diel and lunar reproductive cycles." PLoS One 6(5): e19755.

Howard-Ashby M, Materna SC, Brown CT, Tu Q, Oliveri P, Cameron RA, Davidson EH. High regulatory gene use in sea urchin embryogenesis: Implications for bilaterian development and evolution. Dev Biol. 2006 Dec 1;300(1):27-34.

Hough-Evans, B. R., R. J. Britten and E. H. Davidson (1988). "Mosaic incorporation and regulated expression of an exogenous gene in the sea urchin embryo." Dev Biol 129(1): 198-208.

Howard-Ashby, M., S. C. Materna, C. T. Brown, L. Chen, R. A. Cameron and E. H. Davidson (2006). "Gene families encoding transcription factors expressed in early development of Strongylocentrotus purpuratus." Dev Biol 300(1): 90-107.

Huang, Z. J., Edery, I., and Rosbash, M. (1993), “PAS is a dimerization domain common to Drosophila period and several transcription factors.” *Nature* 364, 259–262.

Hut, R. A. and D. G. Beersma (2011). "Evolution of time-keeping mechanisms: early emergence and adaptation to photoperiod." Philos Trans R Soc Lond B Biol Sci 366(1574): 2141-2154.

Jackson DJ, Meyer NP, Seaver E, Pang K, McDougall C, Moy VN, Gordon K, Degnan BM, Martindale MQ, Burke RD, Peterson KJ. Developmental expression of COE across the Metazoa supports a conserved role in neuronal cell-type specification and mesodermal development. Dev Genes Evol. 2010 Dec;220(7-8):221-34.

Jin, X., L. P. Shearman, D. R. Weaver, M. J. Zylka, G. J. de Vries and S. M. Reppert (1999). "A molecular mechanism regulating rhythmic output from the suprachiasmatic circadian clock." Cell 96(1): 57-68.

Jin Y, Yaguchi S, Shiba K, Yamada L, Yaguchi J, Shibata D, Sawada H, Inaba K. Glutathione transferase theta in apical ciliary tuft regulates mechanical reception and swimming behavior of Sea Urchin Embryos. Cytoskeleton (Hoboken). 2013 Aug;70(8):453-70.

Kaneko, M. and J. C. Hall (2000). "Neuroanatomy of cells expressing clock genes in Drosophila: transgenic manipulation of the period and timeless genes to mark the perikarya of circadian pacemaker neurons and their projections." J Comp Neurol 422(1): 66-94.

Kaneko, M., T. Hiroshige, J. Shinsako and M. F. Dallman (1980). "Diurnal changes in amplification of hormone rhythms in the adrenocortical system." Am J Physiol 239(3): R309-316.

Kaneko, M., K. Kaneko, J. Shinsako and M. F. Dallman (1981). "Adrenal sensitivity to adrenocorticotropin varies diurnally." Endocrinology 109(1): 70-75.

Katoh-Fukui, Y., T. Noce, T. Ueda, Y. Fujiwara, N. Hashimoto, S. Tanaka and T. Higashinakagawa (1992). "Isolation and characterization of cDNA encoding a spicule matrix protein in Hemicentrotus pulcherrimus micromeres." Int J Dev Biol 36(3): 353-361.

Kelley, L. A. and M. J. Sternberg (2009). "Protein structure prediction on the Web: a case study using the Phyre server." Nat Protoc 4(3): 363-371.

Kennedy, B., and J. S. Pearse. 1975. Lunar synchronization of the monthly reproductive rhythm in the sea urchin Centrostephanus coronatus Verrill. J. Exp. Mar. Biol. Ecol. 17:323–331.

Khan, S. K., H. Xu, M. Ukai-Tadenuma, B. Burton, Y. Wang, H. R. Ueda and A. C. Liu (2012). "Identification of a novel cryptochrome differentiating domain required for feedback repression in circadian clock function." J Biol Chem 287(31): 25917-25926.

Killian, C. E. and F. H. Wilt (1989). "The accumulation and translation of a spicule matrix protein mRNA during sea urchin embryo development." Dev Biol 133(1): 148-156.

Kimiwada, T., M. Sakurai, H. Ohashi, S. Aoki, T. Tominaga and K. Wada (2009). "Clock genes regulate neurogenic transcription factors, including NeuroD1, and the neuronal differentiation of adult neural stem/progenitor cells." Neurochem Int 54(5-6): 277-285.

Kiyohara, Y. B., S. Tagao, F. Tamanini, A. Morita, Y. Sugisawa, M. Yasuda, I. Yamanaka, H. R. Ueda, G. T. van der Horst, T. Kondo and K. Yagita (2006). "The BMAL1 C terminus regulates the circadian transcription feedback loop." Proc Natl Acad Sci U S A 103(26): 10074-10079.

Klarsfeld, A., S. Malpel, C. Michard-Vanhee, M. Picot, E. Chelot and F. Rouyer (2004). "Novel features of cryptochrome-mediated photoreception in the brain circadian clock of Drosophila." J Neurosci 24(6): 1468-1477.

Kobayashi, S., A. Meir, Y. Kokubo, K. Uchida, K. Takeno, T. Miyazaki, T. Yayama, M. Kubota, E. Nomura, E. Mwaka and H. Baba (2009). "Ultrastructural analysis on lumbar disc herniation using surgical specimens: role of neovascularization and macrophages in hernias." Spine (Phila Pa 1976) 34(7): 655-662.

Kobayashi, Y., T. Ishikawa, J. Hirayama, H. Daiyasu, S. Kanai, H. Toh, I. Fukuda, T. Tsujimura, N. Terada, Y. Kamei, S. Yuba, S. Iwai and T. Todo (2000). "Molecular analysis of zebrafish photolyase/cryptochrome family: two types of cryptochromes present in zebrafish." Genes Cells 5(9): 725-738.

Kojima D., Terakita A., Ishikawa T., Tsukahara Y., Maeda A., Shichida Y. 1997A novel Go-mediated phototransduction cascade in scallop visual cells. J. Biol. Chem. 272, 22 979–22 982

Korf, H. W., C. Schomerus and J. H. Stehle (1998). "The pineal organ, its hormone melatonin, and the photoneuroendocrine system." Adv Anat Embryol Cell Biol 146: 1-100.

Kosugi, S., M. Hasebe, M. Tomita and H. Yanagawa (2009). "Systematic identification of cell cycle-dependent yeast nucleocytoplasmic shuttling proteins by prediction of composite motifs (vol 106, pg 10171, 2009)." Proceedings of the National Academy of Sciences of the United States of America 106(31): 13142-13142.

Koyanagi, M. and A. Terakita (2008). "Gq-coupled rhodopsin subfamily composed of invertebrate visual pigment and melanopsin." Photochem Photobiol 84(4): 1024-1030.

Kramer, A., F. C. Yang, S. Kraves and C. J. Weitz (2005). "A screen for secreted factors of the suprachiasmatic nucleus." Methods Enzymol 393: 645-663.

Kramer, A., F. C. Yang, P. Snodgrass, X. Li, T. E. Scammell, F. C. Davis and C. J. Weitz (2001). "Regulation of daily locomotor activity and sleep by hypothalamic EGF receptor signaling." Science 294(5551): 2511-2515.

Krishnan, B., J. D. Levine, M. K. Lynch, H. B. Dowse, P. Funes, J. C. Hall, P. E. Hardin and S. E. Dryer (2001). "A new role for cryptochrome in a Drosophila circadian oscillator." Nature 411(6835): 313-317.

Kroeze, W. K., D. J. Sheffler and B. L. Roth (2003). "G-protein-coupled receptors at a glance." J Cell Sci 116(Pt 24): 4867-4869.

Kroidl, I., P. Clowes, J. Mwakyelu, L. Maboko, A. Kiangi, A. Rachow, K. Reither, J. Jung, A. Nsojo, E. Saathoff and M. Hoelscher (2014). "Reasons for false-positive lipoarabinomannan ELISA results in a Tanzanian population." Scand J Infect Dis 46(2): 144-148.

Kumar, M. B., P. Ramadoss, R. K. Reen, J. P. Vanden Heuvel and G. H. Perdew (2001). "The Q-rich subdomain of the human Ah receptor transactivation domain is required for dioxin-mediated transcriptional activity." J Biol Chem 276(45): 42302-42310.

la Cour, T., L. Kiemer, A. Molgaard, R. Gupta, K. Skriver and S. Brunak (2004). "Analysis and prediction of leucine-rich nuclear export signals." Protein Eng Des Sel 17(6): 527-536.

Laranjeiro, R. and D. Whitmore (2014). "Transcription factors involved in retinogenesis are co-opted by the circadian clock following photoreceptor differentiation." Development 141(13): 2644-2656.

Laura, R., D. Magnoli, R. Zichichi, M. C. Guerrera, F. De Carlos, A. A. Suarez, F. Abbate, E. Ciriaco, J. A. Vega and A. Germana (2012). "The photoreceptive cells of the pineal gland in adult zebrafish (Danio rerio)." Microsc Res Tech 75(3): 359-366.

Lear, B. C., C. E. Merrill, J. M. Lin, A. Schroeder, L. Zhang and R. Allada (2005). "A G protein-coupled receptor, groom-of-PDF, is required for PDF neuron action in circadian behavior." Neuron 48(2): 221-227.

Lesser, M. P., K. L. Carleton, S. A. Bottger, T. M. Barry and C. W. Walker (2011). "Sea urchin tube feet are photosensory organs that express a rhabdomeric-like opsin and PAX6." Proc Biol Sci 278(1723): 3371-3379.

Letunic, I., T. Doerks and P. Bork (2012). "SMART 7: recent updates to the protein domain annotation resource." Nucleic Acids Research 40(D1): D302-D305.

Levy, O., L. Appelbaum, W. Leggat, Y. Gothlif, D. C. Hayward, D. J. Miller and O. Hoegh-Guldberg (2007). "Light-responsive cryptochromes from a simple multicellular animal, the coral Acropora millepora." Science 318(5849): 467-470.

Li, Y., G. Li, H. Wang, J. Du and J. Yan (2013). "Analysis of a gene regulatory cascade mediating circadian rhythm in zebrafish." PLoS Comput Biol 9(2): e1002940.

Lin F.J., Song W., Meyer-Bernstein E., Naidoo N., Sehgal A. (2001). “Photic signaling by cryptochrome in the *Drosophila* circadian system.” Mol. Cell. Biol.;21:7287–7294.

Liu, H., B. Liu, C. Zhao, M. Pepper and C. Lin (2011). "The action mechanisms of plant cryptochromes." Trends Plant Sci 16(12): 684-691.

Livant, D. L., B. R. Hough-Evans, J. G. Moore, R. J. Britten and E. H. Davidson (1991). "Differential stability of expression of similarly specified endogenous and exogenous genes in the sea urchin embryo." Development 113(2): 385-398.

Lowrey, P. L. and J. S. Takahashi (2011). "Genetics of circadian rhythms in Mammalian model organisms." Adv Genet 74: 175-230.

Lucas, R. J., G. S. Lall, A. E. Allen and T. M. Brown (2012). "How rod, cone, and melanopsin photoreceptors come together to enlighten the mammalian circadian clock." Prog Brain Res 199: 1-18.

Martin H. S., Wanker E. E., Andrade-Navarro M. A. Evolution and function of CAG/polyglutamine repeats in protein–protein interaction networks Nucl. Acids Res. (2012) 40 (10):4273-4287.

Manyando, C., E. M. Njunju, D. Mwakazanga, G. Chongwe, R. Mkandawire, D. Champo, M. Mulenga, M. De Crop, Y. Claeys, R. M. Ravinetto, C. van Overmeir, U. D. Alessandro and J. P. Van Geertruyden (2014). "Safety of daily co-trimoxazole in pregnancy in an area of changing malaria epidemiology: a phase 3b randomized controlled clinical trial." PLoS One 9(5): e96017.

Materna SC, Howard-Ashby M, Gray RF, Davidson EH. The C2H2 zinc finger genes of *Strongylocentrotus purpuratus* and their expression in embryonic development. Dev Biol. 2006 Dec 1;300(1):108-20.

Materna, S. C., J. Nam and E. H. Davidson (2010). "High accuracy, high-resolution prevalence measurement for the majority of locally expressed regulatory genes in early sea urchin development." Gene Expr Patterns 10(4-5): 177-184.

Materna, S. C. and P. Oliveri (2008). "A protocol for unraveling gene regulatory networks." Nat Protoc 3(12): 1876-1887.

Matsumoto, A., M. Ukai-Tadenuma, R. G. Yamada, J. Houl, K. D. Uno, T. Kasukawa, B. Dauwalder, T. Q. Itoh, K. Takahashi, R. Ueda, P. E. Hardin, T. Tanimura and H. R. Ueda (2007). "A functional genomics strategy reveals clockwork orange as a transcriptional regulator in the Drosophila circadian clock." Genes Dev 21(13): 1687-1700.

McMahon, A. P., C. N. Flytzanis, B. R. Hough-Evans, K. S. Katula, R. J. Britten and E. H. Davidson (1985). "Introduction of cloned DNA into sea urchin egg cytoplasm: replication and persistence during embryogenesis." Dev Biol 108(2): 420-430.

Meyer, A. and Y. Van de Peer (2005). "From 2R to 3R: evidence for a fish-specific genome duplication (FSGD)." Bioessays 27(9): 937-945.

Mgomella, G. S., P. A. Venkatesh, R. J. Bosch, D. Mwakagile, W. Urassa, K. McIntosh, E. Hertzmark, G. Msamanga and W. W. Fawzi (2010). "The use of total lymphocyte count as a surrogate for low CD4+ T lymphocyte cell counts among HIV-1-infected women in Tanzania." East Afr J Public Health 7(2): 160-164.

Millott N. The photosensitivity of echinoids. Adv Mar Biol 1975;13:1-52.

Mitchell Pamela J. and Robert Tjian. “Transcriptional Regulation in Mammalian Cells by Sequence-Specific DNA Binding Proteins” (1989). Science New Series, Vol. 245, No. 4916, pp. 371-378.

Mitsui, S., S. Yamaguchi, T. Matsuo, Y. Ishida and H. Okamura (2001). "Antagonistic role of E4BP4 and PAR proteins in the circadian oscillatory mechanism." Genes Dev 15(8): 995-1006.

Moglich, A., X. Yang, R. A. Ayers and K. Moffat (2010). "Structure and function of plant photoreceptors." Annu Rev Plant Biol 61: 21-47.

Morgan E (2001) The moon and life on earth. Earth Moon Planet 85– 86:279–290.

Morin, L. P. and C. N. Allen (2006). "The circadian visual system, 2005." Brain Res Rev 51(1): 1-60.

Morioka, E., A. Matsumoto and M. Ikeda (2012). "Neuronal influence on peripheral circadian oscillators in pupal Drosophila prothoracic glands." Nat Commun 3: 909.

Moses, K., M. C. Ellis and G. M. Rubin (1989). "The glass gene encodes a zinc-finger protein required by Drosophila photoreceptor cells." Nature 340(6234): 531-536.

Moshy, J. L., H. A. Mwakyoma and M. L. Chindia (2010). "Evaluation and histological maturation characteristics of fibrous dysplasia and ossifying fibroma: a case series." East Afr Med J 87(5): 215-219.

Mracek, P., C. Santoriello, M. L. Idda, C. Pagano, Z. Ben-Moshe, Y. Gothilf, D. Vallone and N. S. Foulkes (2012). "Regulation of per and cry genes reveals a central role for the D-box enhancer in light-dependent gene expression." PLoS One 7(12): e51278.

Mrosovsky, N. (1996). "Locomotor activity and non-photic influences on circadian clocks." Biol Rev Camb Philos Soc 71(3): 343-372.

Mrosovsky, N., S. G. Reebs, G. I. Honrado and P. A. Salmon (1989). "Behavioural entrainment of circadian rhythms." Experientia 45(8): 696-702.

Nagoshi, E., C. Saini, C. Bauer, T. Laroche, F. Naef and U. Schibler (2004). "Circadian gene expression in individual fibroblasts: cell-autonomous and self-sustained oscillators pass time to daughter cells." Cell 119(5): 693-705.

Nakajima, Y. 1987. Localization of catecholaminergic nerves in larval echinoderms. Zool. Sci. 4, 293–299

Nakajima, Y., H. Kaneko, G. Murray and R. D. Burke (2004). "Divergent patterns of neural development in larval echinoids and asteroids." Evol Dev 6(2): 95-104.

Nakanishi N., E. Renfer, U. Technau, F. Rentzsch. Nervous systems of the sea anemone *Nematostella vectensis* are generated by ectoderm and endoderm and shaped by distinct mechanisms. Development, 139 (2012), pp. 347–357.

Nemer, M., E. Rondinelli, D. Infante and A. A. Infante (1991). "Polyubiquitin RNA characteristics and conditional induction in sea urchin embryos." Dev Biol 145(2): 255-265.

Naylor, E. Marine animal behaviour in relation to lunar phase (2002). Earth Moon Planets, 85-86: 291-302.

Naylor, E. Coastal animals that anticipate time and tide (2002). Ocean Challenge, 11(3): 21-26

Naylor E. Chronobiology of marine organisms (2010). Cambridge, UK: Cambridge University Press, 242.

Nielsen C. Larval and adult brains. Evol. Dev. 2005;7:483–489.

Nguyen Ba, A. N., A. Pogoutse, N. Provart and A. M. Moses (2009). "NLStradamus: a simple Hidden Markov Model for nuclear localization signal prediction." BMC Bioinformatics 10: 202.

Nybakken JW (2001) Marine biology: An ecological approach, 5th ed. Benjamin Cummings, San Francisco

Oliveri, P. and E. H. Davidson (2004). "Gene regulatory network analysis in sea urchin embryos." Methods Cell Biol 74: 775-794.

Oliveri, P., A. E. Fortunato, L. Petrone, T. Ishikawa-Fujiwara, Y. Kobayashi, T. Todo, O. Antonova, E. Arboleda, J. Zantke, K. Tessmar-Raible and A. Falciatore (2014). "The Cryptochrome/Photolyase Family in aquatic organisms." Mar Genomics 14: 23-37.

Oliveri, P., Q. Tu and E. H. Davidson (2008). "Global regulatory logic for specification of an embryonic cell lineage." Proc Natl Acad Sci U S A 105(16): 5955-5962.

Oster, H., S. Damerow, S. Kiessling, V. Jakubcakova, D. Abraham, J. Tian, M. W. Hoffmann and G. Eichele (2006). "The circadian rhythm of glucocorticoids is regulated by a gating mechanism residing in the adrenal cortical clock." Cell Metab 4(2): 163-173.

Ousley, A., K. Zafarullah, Y. Chen, M. Emerson, L. Hickman and A. Sehgal (1998). "Conserved regions of the timeless (tim) clock gene in Drosophila analyzed through phylogenetic and functional studies." Genetics 148(2): 815-825.

Ozturk, N., C. P. Selby, Y. Annayev, D. Zhong and A. Sancar (2011). "Reaction mechanism of Drosophila cryptochrome." Proc Natl Acad Sci U S A 108(2): 516-521.

Palczewski, K., K. P. Hofmann and W. Baehr (2006). "Rhodopsin--advances and perspectives." Vision Res 46(27): 4425-4426.

Paranjpe, D. A. and V. K. Sharma (2005). "Evolution of temporal order in living organisms." J Circadian Rhythms 3(1): 7.

Park JH, Helfrich-Förster C, Lee G, Liu L, Rosbash M, Hall JC (2000). “Differential regulation of circadian pacemaker output by separate clock genes in Drosophila.” Proc Natl Acad Sci U S A; 97(7):3608-13.

Partch, C. L., C. B. Green and J. S. Takahashi (2014). "Molecular architecture of the mammalian circadian clock." Trends Cell Biol 24(2): 90-99.

Pennington JT, Emlet RB (1986) Ontogenetic and diel vertical migration of a planktonic echinoid larva, Dendraster excentricus (Escholtz): Occurrence, causes and probable consequences. Exp Mar Biol Ecol 104:69–95

Peres, R., A. M. Reitzel, Y. Passamaneck, S. C. Afeche, J. Cipolla-Neto, A. C. Marques and M. Q. Martindale (2014). "Developmental and light-entrained expression of melatonin and its relationship to the circadian clock in the sea anemone Nematostella vectensis." Evodevo 5: 26.

Peschel, N., K. F. Chen, G. Szabo and R. Stanewsky (2009). "Light-dependent interactions between the Drosophila circadian clock factors cryptochrome, jetlag, and timeless." Curr Biol 19(3): 241-247.

Peschel, N. and C. Helfrich-Forster (2011). "Setting the clock--by nature: circadian rhythm in the fruitfly Drosophila melanogaster." FEBS Lett 585(10): 1435-1442.

Piggins, H. D. (2002). "Human clock genes." Ann Med 34(5): 394-400.

Pittendrigh, C. S. (1960). "Circadian rhythms and the circadian organization of living systems." Cold Spring Harb Symp Quant Biol 25: 159-184.

Plautz, J. D., M. Kaneko, J. C. Hall and S. A. Kay (1997). "Independent photoreceptive circadian clocks throughout Drosophila." Science 278(5343): 1632-1635.

Plautz, J. D., M. Kaneko, J. C. Hall and S. A. Kay (1997). "Independent photoreceptive circadian clocks throughout Drosophila." Science 278(5343): 1632-1635.

Pokorny, R., T. Klar, U. Hennecke, T. Carell, A. Batschauer and L. O. Essen (2008). "Recognition and repair of UV lesions in loop structures of duplex DNA by DASH-type cryptochrome." Proc Natl Acad Sci U S A 105(52): 21023-21027.

de Pontes B.; Engelberth R.; da Silva Nascimento E.; Cavalcante J.C.; de Oliveira Costa M.; Pinato L.; Barbosa de Toledo C.; de Souza Cavalcante J. Serotonin and circadian rhythms. (2010). Psychol. Neurosci. (Online) vol.3 no.2.

Ponting, C. P., and Aravind, L. (1997). “PAS: a multifunctional domain family comes to light.” *Curr. Biol.* 7, R674-R677.

Poustka AJ, Kühn A, Groth D, Weise V, Yaguchi S, Burke RD, Herwig R, Lehrach H, Panopoulou G. A global view of gene expression in lithium and zinc treated sea urchin embryos: new components of gene regulatory networks. Genome Biol. 2007;8(5):R85.

Raff R.A. Origins of the other metazoan body plans: the evolution of larval forms. Philos. Trans. R. Soc. London, Ser. B. 2008;363:1473–1479.

Raible, F., K. Tessmar-Raible, E. Arboleda, T. Kaller, P. Bork, D. Arendt and M. I. Arnone (2006). "Opsins and clusters of sensory G-protein-coupled receptors in the sea urchin genome." Dev Biol 300(1): 461-475.

Ramos, B. C., M. N. Moraes, M. O. Poletini, L. H. Lima and A. M. Castrucci (2014). "From blue light to clock genes in zebrafish ZEM-2S cells." PLoS One 9(9): e106252.

Reitzel, A. M., L. Behrendt and A. M. Tarrant (2010). "Light entrained rhythmic gene expression in the sea anemone Nematostella vectensis: the evolution of the animal circadian clock." PLoS One 5(9): e12805.

Reitzel, A. M., J. F. Ryan and A. M. Tarrant (2012). "Establishing a model organism: a report from the first annual Nematostella meeting." Bioessays 34(2): 158-161.

Reitzel, A. M. and A. M. Tarrant (2009). "Nuclear receptor complement of the cnidarian Nematostella vectensis: phylogenetic relationships and developmental expression patterns." BMC Evol Biol 9: 230.

Renn, S. C., J. H. Park, M. Rosbash, J. C. Hall and P. H. Taghert (1999). "A pdf neuropeptide gene mutation and ablation of PDF neurons each cause severe abnormalities of behavioral circadian rhythms in Drosophila." Cell 99(7): 791-802.

Rentzsch F., Fritzenwanker J.H., Scholz C.B., Technau U. FGF signalling controls formation of the apical sensory organ in the cnidarian *Nematostella vectensis*. Development. 2008;135:1761–1769.

Reppert, S. M. (2007). "The ancestral circadian clock of monarch butterflies: role in time-compensated sun compass orientation." Cold Spring Harb Symp Quant Biol 72: 113-118.

Reppert, S. M. and D. R. Weaver (2002). "Coordination of circadian timing in mammals." Nature 418(6901): 935-941.

Rieger, D., R. Stanewsky and C. Helfrich-Forster (2003). "Cryptochrome, compound eyes, Hofbauer-Buchner eyelets, and ocelli play different roles in the entrainment and masking pathway of the locomotor activity rhythm in the fruit fly Drosophila melanogaster." J Biol Rhythms 18(5): 377-391.

Rizzo F, Fernandez-Serra M, Squarzoni P, Archimandritis A, Arnone MI. Identification and developmental expression of the ets gene family in the sea urchin (*Strongylocentrotus purpuratus*). Dev Biol. 2006 Dec 1;300(1):35-48.

Rosato E. Circadian Rhythms: Methods and Protocols. Humana Press, 02 feb 2007.

Rosbash, M. (2009). "The implications of multiple circadian clock origins." PLoS Biol 7(3): e62.

Rowe, M. L. and M. R. Elphick (2012). "The neuropeptide transcriptome of a model echinoderm, the sea urchin Strongylocentrotus purpuratus." Gen Comp Endocrinol 179(3): 331-344.

Rozen, S. and H. Skaletsky (2000). "Primer3 on the WWW for general users and for biologist programmers." Methods Mol Biol 132: 365-386.

Rubin, E. B., Y. Shemesh, M. Cohen, S. Elgavish, H. M. Robertson and G. Bloch (2006). "Molecular and phylogenetic analyses reveal mammalian-like clockwork in the honey bee (Apis mellifera) and shed new light on the molecular evolution of the circadian clock." Genome Res 16(11): 1352-1365.

Rutila, J. E., Suri, V., Le, M., So, W. V., Rosbash, M., and Hall, J. C. (1998). “CYCLE is a second bHLH-PAS clock protein essential for circadian rhythmicity and transcription of Drosophila period and timeless.” Cell 93, 805–914).

Saez, L. and M. W. Young (1996). "Regulation of nuclear entry of the Drosophila clock proteins period and timeless." Neuron 17(5): 911-920.

Sahar, S. and P. Sassone-Corsi (2012). "Regulation of metabolism: the circadian clock dictates the time." Trends Endocrinol Metab 23(1): 1-8.

Santillo, S., P. Orlando, L. De Petrocellis, L. Cristino, V. Guglielmotti and C. Musio (2006). "Evolving visual pigments: hints from the opsin-based proteins in a phylogenetically old "eyeless" invertebrate." Biosystems 86(1-3): 3-17.

Sato, T. K., R. G. Yamada, H. Ukai, J. E. Baggs, L. J. Miraglia, T. J. Kobayashi, D. K. Welsh, S. A. Kay, H. R. Ueda and J. B. Hogenesch (2006). "Feedback repression is required for mammalian circadian clock function." Nat Genet 38(3): 312-319.

Satterlie R.A., Cameron R.A. Electrical-activity at Metamorphosis in larvae of the sea-urchin Lytechinus-pictus (Echinoidea, Echinodermata) J. Exp. Zool. 1985;235:197–204.

Schaefer MH, Wanker EE, Andrade-Navarro MA. (2012) Evolution and function of CAG/polyglutamine repeats in protein-protein interaction networks. Nucleic Acids Res. ;40(10):4273-87.

Schibler, U. (2000). "Circadian clocks. Heartfelt enlightenment." Nature 404(6773): 25, 27-28.

Schultz, J., Milpetz, F., Bork, P. & Ponting, C.P. SMART, a simple modular architecture research tool: Identification of signaling domains. PNAS 1998; 95: 5857-5864.

Sea Urchin Genome Sequencing, C., E. Sodergren, G. M. Weinstock, E. H. Davidson, R. A. Cameron, R. A. Gibbs, R. C. Angerer, L. M. Angerer, M. I. Arnone, D. R. Burgess, R. D. Burke, J. A. Coffman, M. Dean, M. R. Elphick, C. A. Ettensohn, K. R. Foltz, A. Hamdoun, R. O. Hynes, W. H. Klein, W. Marzluff, D. R. McClay, R. L. Morris, A. Mushegian, J. P. Rast, L. C. Smith, M. C. Thorndyke, V. D. Vacquier, G. M. Wessel, G. Wray, L. Zhang, C. G. Elsik, O. Ermolaeva, W. Hlavina, G. Hofmann, P. Kitts, M. J. Landrum, A. J. Mackey, D. Maglott, G. Panopoulou, A. J. Poustka, K. Pruitt, V.

Sapojnikov, X. Song, A. Souvorov, V. Solovyev, Z. Wei, C. A. Whittaker, K. Worley, K. J. Durbin, Y. Shen, O. Fedrigo, D. Garfield, R. Haygood, A. Primus, R. Satija, T. Severson, M. L. Gonzalez-Garay, A. R. Jackson, A. Milosavljevic, M. Tong, C. E. Killian, B. T. Livingston, F. H. Wilt, N. Adams, R. Belle, S. Carbonneau, R. Cheung, P. Cormier, B. Cosson, J. Croce, A. Fernandez-Guerra, A. M. Geneviere, M. Goel, H. Kelkar, J. Morales, O. Mulner-Lorillon, A. J. Robertson, J. V. Goldstone, B. Cole, D. Epel, B. Gold, M. E. Hahn, M. Howard-Ashby, M. Scally, J. J. Stegeman, E. L. Allgood, J. Cool, K. M. Judkins, S. S. McCafferty, A. M. Musante, R. A. Obar, A. P. Rawson, B. J. Rossetti, I. R. Gibbons, M. P. Hoffman, A. Leone, S. Istrail, S. C. Materna, M. P. Samanta, V. Stolc, W. Tongprasit, Q. Tu, K. F. Bergeron, B. P. Brandhorst, J. Whittle, K. Berney, D. J. Bottjer, C. Calestani, K. Peterson, E. Chow, Q. A. Yuan, E. Elhaik, D. Graur, J. T. Reese, I. Bosdet, S. Heesun, M. A. Marra, J. Schein, M. K. Anderson, V. Brockton, K. M. Buckley, A. H. Cohen, S. D. Fugmann, T. Hibino, M. Loza-Coll, A. J. Majeske, C. Messier, S. V. Nair, Z. Pancer, D. P. Terwilliger, C. Agca, E. Arboleda, N. Chen, A. M. Churcher, F. Hallbook, G. W. Humphrey, M. M. Idris, T. Kiyama, S. Liang, D. Mellott, X. Mu, G. Murray, R. P. Olinski, F. Raible, M. Rowe, J. S. Taylor, K. Tessmar-Raible, D. Wang, K. H. Wilson, S. Yaguchi, T. Gaasterland, B. E. Galindo, H. J. Gunaratne, C. Juliano, M. Kinukawa, G. W. Moy, A. T. Neill, M. Nomura, M. Raisch, A. Reade, M. M. Roux, J. L. Song, Y. H. Su, I. K. Townley, E. Voronina, J. L. Wong, G. Amore, M. Branno, E. R. Brown, V. Cavalieri, V. Duboc, L. Duloquin, C. Flytzanis, C. Gache, F. Lapraz, T. Lepage, A. Locascio, P. Martinez, G. Matassi, V. Matranga, R. Range, F. Rizzo, E. Rottinger, W. Beane, C. Bradham, C. Byrum, T. Glenn, S. Hussain, G. Manning, E. Miranda, R. Thomason, K. Walton, A. Wikramanayke, S. Y. Wu, R. Xu, C. T. Brown, L. Chen, R. F. Gray, P. Y. Lee, J. Nam, P. Oliveri, J. Smith, D. Muzny, S. Bell, J. Chacko, A. Cree, S. Curry, C. Davis, H. Dinh, S. Dugan-Rocha, J. Fowler, R. Gill, C. Hamilton, J. Hernandez, S. Hines, J. Hume, L. Jackson, A. Jolivet, C. Kovar, S. Lee, L. Lewis, G. Miner, M. Morgan, L. V. Nazareth, G. Okwuonu, D. Parker, L. L. Pu, R. Thorn and R. Wright (2006). "The genome of the sea urchin Strongylocentrotus purpuratus." Science 314(5801): 941-952.

Sehgal A. Molecular Biology of Circadian Rhythms (2004) John Wiley & Sons.

Shafer, O.T., Rosbash, M. and Truman, J.W. (2002) Sequential nuclear accumulation of the clock proteins period and timeless in the pacemaker neurons of Drosophila melanogaster. J. Neurosci. 22, 5946–5954.

Sharp DT, Gray IE (1962) Studies on factors affecting the local distribution of two sea urchins, *Arbacia punctulata* and *Lytechinus variegatus*. Ecology 43:309–313

Shichida, Y. and H. Imai (1998). "Visual pigment: G-protein-coupled receptor for light signals." Cell Mol Life Sci 54(12): 1299-1315.

Shichida, Y. and T. Matsuyama (2009). "Evolution of opsins and phototransduction." Philos Trans R Soc Lond B Biol Sci 364(1531): 2881-2895.

Shinzato, C., E. Shoguchi, T. Kawashima, M. Hamada, K. Hisata, M. Tanaka, M. Fujie, M. Fujiwara, R. Koyanagi, T. Ikuta, A. Fujiyama, D. J. Miller and N. Satoh (2011). "Using the Acropora digitifera genome to understand coral responses to environmental change." Nature 476(7360): 320-323.

Shoguchi, E., M. Tanaka, C. Shinzato, T. Kawashima and N. Satoh (2013). "A genome-wide survey of photoreceptor and circadian genes in the coral, Acropora digitifera." Gene 515(2): 426-431.

Sly B.J., Snoke M.S., Raff R.A. Who came first—larvae or adults? Origins of bilaterian metazoan larvae. Int. J. Dev. Biol. 2003;47:623–632.

Simich, L., M. Beiser, M. Stewart and E. Mwakarimba (2005). "Providing social support for immigrants and refugees in Canada: challenges and directions." J Immigr Health 7(4): 259-268.

Simons, M. J. (2009). "The evolution of the cyanobacterial posttranslational clock from a primitive "phoscillator"." J Biol Rhythms 24(3): 175-182.

Smith, M. M., L. Cruz Smith, R. A. Cameron and L. A. Urry (2008). "The larval stages of the sea urchin, Strongylocentrotus purpuratus." J Morphol 269(6): 713-733.

Spudich, J. L., C. S. Yang, K. H. Jung and E. N. Spudich (2000). "Retinylidene proteins: structures and functions from archaea to humans." Annu Rev Cell Dev Biol 16: 365-392.

Stehle, J. H., C. von Gall and H. W. Korf (2003). "Melatonin: a clock-output, a clock-input." J Neuroendocrinol 15(4): 383-389.

Stephan, F. K., J. M. Swann and C. L. Sisk (1979). "Entrainment of circadian rhythms by feeding schedules in rats with suprachiasmatic lesions." Behav Neural Biol 25(4): 545-554.

Stokkan, K. A., S. Yamazaki, H. Tei, Y. Sakaki and M. Menaker (2001). "Entrainment of the circadian clock in the liver by feeding." Science 291(5503): 490-493.

Strathmann RR. The behavior of planktotrophic echinoderm larvae: mechanisms, regulation, and rates of suspension feeding (1971). J Exp Mar Biol Ecol 6:109–60

Strathmann RR. Larval feeding in echinoderms (1975). Am Zool 15:717–30.

Sucov, H. M., B. R. Hough-Evans, R. R. Franks, R. J. Britten and E. H. Davidson (1988). "A regulatory domain that directs lineage-specific expression of a skeletal matrix protein gene in the sea urchin embryo." Genes Dev 2(10): 1238-1250.

Swalla, B. J. and A. B. Smith (2008). "Deciphering deuterostome phylogeny: molecular, morphological and palaeontological perspectives." Philos Trans R Soc Lond B Biol Sci 363(1496): 1557-1568.

Szular, J., H. Sehadova, C. Gentile, G. Szabo, W. H. Chou, S. G. Britt and R. Stanewsky (2012). "Rhodopsin 5- and Rhodopsin 6-mediated clock synchronization in Drosophila melanogaster is independent of retinal phospholipase C-beta signaling." J Biol Rhythms 27(1): 25-36.

Takahata, S., T. Ozaki, J. Mimura, Y. Kikuchi, K. Sogawa and Y. Fujii-Kuriyama (2000). "Transactivation mechanisms of mouse clock transcription factors, mClock and mArnt3." Genes Cells 5(9): 739-747.

Tamai, T. K., A. J. Carr and D. Whitmore (2005). "Zebrafish circadian clocks: cells that see light." Biochem Soc Trans 33(Pt 5): 962-966.

Tamura K, Peterson D, Peterson N, Stecher G, Nei M, Kumar S. MEGA5: molecular evolutionary genetics analysis using maximum likelihood, evolutionary distance, and maximum parsimony methods. Mol Biol Evol. 2011 Oct;28(10):2731-9.

Tanoue, S., P. Krishnan, B. Krishnan, S. E. Dryer and P. E. Hardin (2004). "Circadian clocks in antennal neurons are necessary and sufficient for olfaction rhythms in Drosophila." Curr Biol 14(8): 638-649.

Terakita, A. (2005). "The opsins." Genome Biol 6(3): 213.

Tessmar-Raible, K., F. Raible and E. Arboleda (2011). "Another place, another timer: Marine species and the rhythms of life." Bioessays 33(3): 165-172.

Toloza-Villalobos, J., J. I. Arroyo and J. C. Opazo (2015). "The circadian clock of teleost fish: a comparative analysis reveals distinct fates for duplicated genes." J Mol Evol 80(1): 57-64.

Tomioka, K. and A. Matsumoto (2010). "A comparative view of insect circadian clock systems." Cell Mol Life Sci 67(9): 1397-1406.

Tosches, M. A., D. Bucher, P. Vopalensky and D. Arendt (2014). "Melatonin signaling controls circadian swimming behavior in marine zooplankton." Cell 159(1): 46-57.

Travnickova-Bendova, Z., N. Cermakian, S. M. Reppert and P. Sassone-Corsi (2002). "Bimodal regulation of mPeriod promoters by CREB-dependent signaling and CLOCK/BMAL1 activity." Proc Natl Acad Sci U S A 99(11): 7728-7733.

Tu, Q., R. A. Cameron, K. C. Worley, R. A. Gibbs and E. H. Davidson (2012). "Gene structure in the sea urchin Strongylocentrotus purpuratus based on transcriptome analysis." Genome Res 22(10): 2079-2087.

Ugolini, A., Sonigli, S., Pasquali, V., Renzi, P., 2007. Locomotory activity rhythm and sun compass orientation in the sandhopper Talitrus saltator are related. J. Comp. Physiol. A 193, 1259–1263

Ueyama, T., K. E. Krout, X. V. Nguyen, V. Karpitskiy, A. Kollert, T. C. Mettenleiter and A. D. Loewy (1999). "Suprachiasmatic nucleus: a central autonomic clock." Nat Neurosci 2(12): 1051-1053.

Ullrich-Luter, E. M., S. D'Aniello and M. I. Arnone (2013). "C-opsin expressing photoreceptors in echinoderms." Integr Comp Biol 53(1): 27-38.

Ullrich-Luter, E. M., S. Dupont, E. Arboleda, H. Hausen and M. I. Arnone (2011). "Unique system of photoreceptors in sea urchin tube feet." Proc Natl Acad Sci U S A 108(20): 8367-8372.

Vallone, D., S. B. Gondi, D. Whitmore and N. S. Foulkes (2004). "E-box function in a period gene repressed by light." Proc Natl Acad Sci U S A 101(12): 4106-4111.

Vatine, G., D. Vallone, L. Appelbaum, P. Mracek, Z. Ben-Moshe, K. Lahiri, Y. Gothilf and N. S. Foulkes (2009). "Light directs zebrafish period2 expression via conserved D and E boxes." PLoS Biol 7(10): e1000223.

Vatine, G., D. Vallone, Y. Gothilf and N. S. Foulkes (2011). "It's time to swim! Zebrafish and the circadian clock." FEBS Lett 585(10): 1485-1494.

Velarde, R. A., C. D. Sauer, K. K. Walden, S. E. Fahrbach and H. M. Robertson (2005). "Pteropsin: a vertebrate-like non-visual opsin expressed in the honey bee brain." Insect Biochem Mol Biol 35(12): 1367-1377.

Veleri, S., D. Rieger, C. Helfrich-Forster and R. Stanewsky (2007). "Hofbauer-Buchner eyelet affects circadian photosensitivity and coordinates TIM and PER expression in Drosophila clock neurons." J Biol Rhythms 22(1): 29-42.

Veleri, S. and C. Wulbeck (2004). "Unique self-sustaining circadian oscillators within the brain of Drosophila melanogaster." Chronobiol Int 21(3): 329-342.

Vodovar, N., J. D. Clayton, R. Costa, M. Odell and C. P. Kyriacou (2002). "The Drosophila clock protein Timeless is a member of the Arm/HEAT family." Curr Biol 12(18): R610-611.

Voigt, W. P., A. S. Young, S. N. Mwaura, S. G. Nyaga, G. M. Njihia, F. N. Mwakima and S. P. Morzaria (1993). "In vitro feeding of instars of the ixodid tick Amblyomma variegatum on skin membranes and its application to the transmission of Theileria mutans and Cowdria ruminatium." Parasitology 107 (Pt 3): 257-263.

Vosko, A. M., A. Schroeder, D. H. Loh and C. S. Colwell (2007). "Vasoactive intestinal peptide and the mammalian circadian system." Gen Comp Endocrinol 152(2-3): 165-175.

Vujovic, N., A. J. Davidson and M. Menaker (2008). "Sympathetic input modulates, but does not determine, phase of peripheral circadian oscillators." Am J Physiol Regul Integr Comp Physiol 295(1): R355-360.

Wada Y, Shiraishi J, Nakamura M, Koshino Y. Role of serotonin receptor subtypes in the development of amygdaloid kindling in rats. Brain Res. 1997 Feb 7;747(2):338-42.

Waladde, S. M., A. S. Young, S. N. Mwaura, G. N. Njihia and F. N. Mwakima (1995). "Optimization of the in vitro feeding of Rhipicephalus appendiculatus nymphae for the transmission of Theileria parva." Parasitology 111 (Pt 4): 463-468.

Waladde, S. M., A. S. Young, S. A. Ochieng, S. N. Mwaura and F. N. Mwakima (1993). "Transmission of Theileria parva to cattle by Rhipicephalus appendiculatus adults fed as nymphae in vitro on infected blood through an artificial membrane." Parasitology 107 (Pt 3): 249-256.

Weber, F., D. Zorn, C. Rademacher and H. C. Hung (2011). "Post-translational timing mechanisms of the Drosophila circadian clock." FEBS Lett 585(10): 1443-1449.

Wei, Z., R. C. Angerer and L. M. Angerer (2011). "Direct development of neurons within foregut endoderm of sea urchin embryos." Proc Natl Acad Sci U S A 108(22): 9143-9147.

Welsh, D. K., J. S. Takahashi and S. A. Kay (2010). "Suprachiasmatic nucleus: cell autonomy and network properties." Annu Rev Physiol 72: 551-577.

Welsh, D. K., S. H. Yoo, A. C. Liu, J. S. Takahashi and S. A. Kay (2004). "Bioluminescence imaging of individual fibroblasts reveals persistent, independently phased circadian rhythms of clock gene expression." Curr Biol 14(24): 2289-2295.

Welsh DK, Logothetis DE, Meister M, Reppert SM. Individual neurons dissociated from rat suprachiasmatic nucleus express independently phased circadian firing rhythms. Neuron. 1995 Apr;14(4):697-706.

Westermark, P. O., D. K. Welsh, H. Okamura and H. Herzel (2009). "Quantification of circadian rhythms in single cells." PLoS Comput Biol 5(11): e1000580.

Whitmore, D., Foulkes, N.S., Strahle, U. and Sassone-Corsi, P. (1998). “Zebrafish Clock rhythmic expression reveals independent peripheral circadian oscillators.” Nat. Neurosci.1, 701–707.

Whitmore, D., N. S. Foulkes and P. Sassone-Corsi (2000). "Light acts directly on organs and cells in culture to set the vertebrate circadian clock." Nature 404(6773): 87-91.

Wijnen, H., F. Naef, C. Boothroyd, A. Claridge-Chang and M. W. Young (2006). "Control of daily transcript oscillations in Drosophila by light and the circadian clock." PLoS Genet 2(3): e39.

Wolpert L, Beddington R, Jessell T, Lawrence P, Meyerowitz E, Smith J. (2007) Principles of Development. 3th ed. London: Oxford university press.

Yaguchi, S. and H. Katow (2003). "Expression of tryptophan 5-hydroxylase gene during sea urchin neurogenesis and role of serotonergic nervous system in larval behavior." J Comp Neurol 466(2): 219-229.

Yaguchi S, Katow H. Expression of tryptophan 5-hydroxylase gene during sea urchin neurogenesis and role of serotonergic nervous system in larval behavior. (2003). J Comp Neurol Nov 10;466(2):219-29

Yaguchi S, Yaguchi J, Wei Z, Jin Y, Angerer LM, Inaba K Fez function is required to maintain the size of the animal plate in the sea urchin embryo. Development. 2011 Oct;138(19):4233-43.

Yamaguchi, S., S. Mitsui, L. Yan, K. Yagita, S. Miyake and H. Okamura (2000). "Role of DBP in the circadian oscillatory mechanism." Mol Cell Biol 20(13): 4773-4781.

Yan, J., H. Wang, Y. Liu and C. Shao (2008). "Analysis of gene regulatory networks in the mammalian circadian rhythm." PLoS Comput Biol 4(10): e1000193.

Yan, L. (2009). "Expression of clock genes in the suprachiasmatic nucleus: effect of environmental lighting conditions." Rev Endocr Metab Disord 10(4): 301-310.

Yanez, J., J. Busch, R. Anadon and H. Meissl (2009). "Pineal projections in the zebrafish (Danio rerio): overlap with retinal and cerebellar projections." Neuroscience 164(4): 1712-1720.

Ye, R., C. P. Selby, Y. Y. Chiou, I. Ozkan-Dagliyan, S. Gaddameedhi and A. Sancar (2014). "Dual modes of CLOCK:BMAL1 inhibition mediated by Cryptochrome and Period proteins in the mammalian circadian clock." Genes Dev 28(18): 1989-1998.

Yerramilli, D. and S. Johnsen (2010). "Spatial vision in the purple sea urchin Strongylocentrotus purpuratus (Echinoidea)." J Exp Biol 213(2): 249-255.

Yildiz, O., M. Doi, I. Yujnovsky, L. Cardone, A. Berndt, S. Hennig, S. Schulze, C. Urbanke, P. Sassone-Corsi and E. Wolf (2005). "Crystal structure and interactions of the PAS repeat region of the Drosophila clock protein PERIOD." Mol Cell 17(1): 69-82.

Yoo, S. H., J. A. Mohawk, S. M. Siepka, Y. Shan, S. K. Huh, H. K. Hong, I. Kornblum, V. Kumar, N. Koike, M. Xu, J. Nussbaum, X. Liu, Z. Chen, Z. J. Chen, C. B. Green and J. S. Takahashi (2013). "Competing E3 ubiquitin ligases govern circadian periodicity by degradation of CRY in nucleus and cytoplasm." Cell 152(5): 1091-1105.

Yoshida M. Photosensitivity. In: Boolootian RA, editor. Physiology of echinodermata. New York: John Wiley and Sons; 1966. p. 435-64.

Young, A. S., T. T. Dolan, S. P. Morzaria, F. N. Mwakima, R. A. Norval, J. Scott, A. Sherriff and G. Gettinby (1996). "Factors influencing infections in Rhipicephalus appendiculatus ticks fed on cattle infected with Theileria parva." Parasitology 113 (Pt 3): 255-266.

Young, A. S., T. T. Dolan, F. N. Mwakima, H. Ochanda, S. N. Mwaura, G. M. Njihia, M. W. Muthoni and R. B. Dolan (1995). "Estimation of heritability of susceptibility to infection with Theileria parva in the tick Rhipicephalus appendiculatus." Parasitology 111 (Pt 1): 31-38.

Young, M. W. and S. A. Kay (2001). "Time zones: a comparative genetics of circadian clocks." Nat Rev Genet 2(9): 702-715.

Young, M. W., K. Wager-Smith, L. Vosshall, L. Saez and M. P. Myers (1996). "Molecular anatomy of a light-sensitive circadian pacemaker in Drosophila." Cold Spring Harb Symp Quant Biol 61: 279-284.

Yu, W. and P. E. Hardin (2007). "Use of firefly luciferase activity assays to monitor circadian molecular rhythms in vivo and in vitro." Methods Mol Biol 362: 465-480.

Yuan, Q., W. J. Joiner and A. Sehgal (2006). "A sleep-promoting role for the Drosophila serotonin receptor 1A." Curr Biol 16(11): 1051-1062.

Yuan, Q., F. Lin, X. Zheng and A. Sehgal (2005). "Serotonin modulates circadian entrainment in Drosophila." Neuron 47(1): 115-127.

Yuan, Q., D. Metterville, A. D. Briscoe and S. M. Reppert (2007). "Insect cryptochromes: gene duplication and loss define diverse ways to construct insect circadian clocks." Mol Biol Evol 24(4): 948-955.

Zantke, J., T. Ishikawa-Fujiwara, E. Arboleda, C. Lohs, K. Schipany, N. Hallay, A. D. Straw, T. Todo and K. Tessmar-Raible (2013). "Circadian and circalunar clock interactions in a marine annelid." Cell Rep 5(1): 99-113.

Zhang, E. E. and S. A. Kay (2010). "Clocks not winding down: unravelling circadian networks." Nat Rev Mol Cell Biol 11(11): 764-776.

Zhang, L., M. H. Hastings, E. W. Green, E. Tauber, M. Sladek, S. G. Webster, C. P. Kyriacou and D. C. Wilcockson (2013). "Dissociation of circadian and circatidal timekeeping in the marine crustacean Eurydice pulchra." Curr Biol 23(19): 1863-1873.

Zheng, X. and A. Sehgal (2008). "Probing the relative importance of molecular oscillations in the circadian clock." Genetics 178(3): 1147-1155.

Zhu, H., Q. Yuan, A. D. Briscoe, O. Froy, A. Casselman and S. M. Reppert (2005). "The two CRYs of the butterfly." Curr Biol 15(23): R953-954.

Zoltowski, B. D., A. T. Vaidya, D. Top, J. Widom, M. W. Young and B. R. Crane (2011). "Structure of full-length Drosophila cryptochrome." Nature 480(7377): 396-399.